Gene therapy of melanoma: therapeutic and pharmaceutical investigations

Thomas, Beverley Jayne

Award date:
1997

Awarding institution:
University of Bath

Gene Therapy of Melanoma : Therapeutic and Pharmaceutical Investigations.

submitted by Beverley Jayne Thomas
for the degree of PhD.
of the University of Bath
1997

ProQuest LLC
789 East Eisenhower Parkway
P.O. Box 1346
Ann Arbor, MI 48106-1346

Summary

The diverse therapeutic applications of gene therapy are only now being realised. One major approach in the treatment of cancer involves immunostimulation. Initial studies aimed to deliver vectors containing the genes encoding MHC class II molecules, plus the costimulatory molecule B7, to murine melanoma cells, and to establish any ensuing antitumour effect. The incorporation of a melanoma-specific promoter, Trp-1, into these vectors would confer selective gene expression.

The characterisation of vectors for gene delivery requires correlation between physical stability and structure, and biological activity. This study examined the *in vitro* activity of a variety of plasmid DNA-polycation formulations and their physical attributes. The polymers examined included a variety of homopolymers, a series of lysine, alanine block co-polymers and a series of PEG-polylysine block co-polymers. Progressive exclusion of ethidium bromide was used to monitor complexation of DNA by polycations using spectrofluorimetry. The charge ratio ($^{+}$/-) at which condensation occurred was established for each polymer to be approximately 1.0.

Varying the formulation by using different polycations produced a rank order of transfection efficiency in B16 melanoma cells, although no differences were observed in the spectrofluorimetry. Transfection activity was shown to be dependent on the presence of the endosomolytic agent chloroquine. The prerequisite for chloroquine to produce transfection was shown to be a cell-specific effect. Transfection in the absence of chloroquine of formulations that produced no gene expression in B16 cells demonstrated activity in HEK293 cells.

A strategy was developed to incorporate an endosomolytic component into the polycation-DNA complex. Polymers capable of buffering the endosomal acidification process have previously been shown to enhance gene expression. A peptide was synthesised containing oligolysine for DNA binding and oligohistidine for buffering activity at the endosomal pH. No activity was observed after transfection into B16 or HEK293 cells in the absence of chloroquine.

Physical characterisation of the different formulations demonstrated that all of the systems served to protect the DNA from enzymatic degradation. Polycations were shown to exhibit reduced cellular toxicity after complexation to DNA. Analysis of complex size revealed no correlation between diameter and transfection activity, although sodium chloride was shown to affect the formation of complexes. This is believed to be a critical effect in determining the stability of the formulation. The uptake of complexes was examined at high charge ratios and in the presence of free polycation. Uptake remained unaffected under these conditions, indicating that the process was non-selective, and non saturated at these levels. Further investigations should concentrate on the processes occurring distal to the cell membrane.

Dedication

In the memory of Gwyn Thomas,

for demonstrating the ultimate

Joie de Vivre.

Acknowledgements

Many thanks must go to Dr. Colin W. Pouton for his endless optimism and enthusiasm as a supervisor throughout the course of this study. Thanks also to Dr. Steve Moss for fatherly advice on several occasions.

Additionally, this work was dependent on advice regarding FACS analysis from Dr. Graham Smith, general molecular biology techniques from Dr. Anthony Smith, Dr. Melanie Whelham and Ms. Heather Bone, and assistance with peptide synthesis from Alfred Agyeman. I am exceptionally grateful to Dr. Paul Lucas for the thoroughness of his preceding studies in this area, and for the time taken both for discussion and proof-reading of this thesis.

With thanks to the EPSRC and Pfizer Ltd. for financial assistance with this project, and to Prof. D.J. Davies for providing research facilities. I am grateful to Dr. D. Atwood for use of the laser at Manchester School of Pharmacy, and to Rupi for friendship and assistance during those dark days.

Many thanks to my parents for their support and my errant brother for demonstrating a life beyond Bath. Especially, to the occupants of Lab. 2.29 - renowned for their alternative approach to life, the universe and especially science - my heartfelt gratitude. In particular, to Plops, Rach, Boner, Niamh, Heidi, Paul, Dave and Lush for the entertaining memories. Additionally, I must thank F and G, Lionel, Klemens, Chris, Max, Rach, Hels and especially Jo Drew for making it not so short, but very sweet. Finally, I am indebted to Big Al - may convention never constrain his lifestyle.

Table of contents.

Tables

Figures

Abbreviations.

APC	antigen presenting cell
ATP	adenosine triphosphate
BSA	bovine serum albumin
cm	centimetre(s)
CMV	cytomegalovirus
Da	daltons
dAMP	deoxyadenosine-monophosphate
dCMP	deoxycytidine-monophosphate
dGMP	deoxyguanosine-monophosphate
dTMP	deoxythymidine-monophosphate
DMEM	Dulbecco's Modified Eagles Medium
DMSO	dimethyl sulphoxide
DNA	deoxyribonucleic acid
DOTAP	(N-[1-(2,3-Dioleoyloxy)propyl]-N,N,N-trimethyl ammonium methylsulfate
Dnase	deoxyribonuclease
EDTA	ethylene diamine tetra-acetic acid
FACS	fluorescence activated cell sorting
FCS	foetal calf serum
FITC	fluorescein isothiocyanate
G418	geneticin
g	acceleration due to gravity (= $9.81 ms^{-2}$)
g	gramme(s)
HBS	hepes buffered saline
HEPES	*n*-(2-hydroxyethyl)piperazine-*N*-s-ethane sulphonic acid
IL	interleukin
l	litre(s)
LB	Luria broth
M	mole(s) per litre
MHC	major histocompatibility complex
MIC	minimum inhibitory concentration
mRNA	messenger RNA
MSH	melanocyte stimulating hormone
MTT	1-[4,5-dimethylthiazol-2-yl]-3,5-diphenylformazan
µ	micro
mg	milligram(s)
ml	millilitre(s)
MUG	4-methylumbelliferyl-β-D-galactoside
nm	nanometre(s)
OD	optical density
ONPG	*o*-nitrophenyl-β-D-galactoside
PBS	phosphate buffered saline
PCR	polymerase chain reaction
PEG	polyethylene glycol

pLA	poly-L-arginine
pLL	poly-L-lysine
pLO	poly-L-ornithine
PMN	polymorphonuclear leukocyte
RNA	ribonucleic acid
rpm	revolutions per minute
RSV	rous sarcoma virus
SDS	sodium dodecyl sulphate
TE	Tris-EDTA buffer
Tris	tris (hydroxymethyl) aminomethane
Trp-1	tyrosinase-related protein-1
Tyr	tyrosinase
V	volt(s)
v/v	volume by volume
w/v	weight by volume
X-gal	5-Bromo-4-Chloro-3-Indoyl-β-D-Galactopyranoside
YE	yeast extract

CHAPTER 1. Introduction.

The understanding of the molecular biological basis of many human diseases has led to new therapeutic applications in clinical practice. This revolutionary approach arises from rapid advances in laboratory technologies and computer applications, which combine to provide a rational understanding of the basis of disease. Gene therapy provides us with the tool for treating the cause rather than the chemical or biochemical symptoms of a disease. There is the potential to treat both the immediate and the downstream effects of gene dysfunction.

Initial interest centred on the treatment of conditions resulting from single-gene defects such as cystic fibrosis (Curiel *et al.*, 1996). Subsequently, alternative approaches have evolved to allow the treatment of more complex conditions. These include attempts to down-regulate gene expression such as antigene or antisense strategies, and enhancement of the host's immune response to specific cell types, as employed in anti-tumour therapy.

This project has concentrated on the immunostimulation of melanoma cells using a murine model. The aim of this project was to alter the immunogenicity of the melanoma cells by transfection with cDNA's encoding cell surface molecules involved in the presentation of antigen and the costimulatory signal required for T cell activation.

The delivery of genes for therapeutic applications requires a high degree of specificity. This can be achieved at two levels: the physical delivery of the gene, and the cellular expression. An additional objective of this project involved the use of melanoma-specific promoters to drive the expression of the transfected genes. Also, the

formulation of non-viral vectors was studied to provide a basic understanding of the interactions between DNA and cationic polymers. Characterisation of the pharmaceutical properties of these complexes was necessary to allow the further development of more complicated and efficient targeted vectors for gene delivery.

1.1 Single gene defects.

The classical application for gene therapy was seen as the correction of a single-gene disorder by the insertion of an appropriate gene, resulting in the expression of a defective protein. Substantial interest currently centres on the disease cystic fibrosis (Crystal *et al.*, 1994). This disease is characterised by deficient electrolyte transport through epithelia due to mutations in the cystic fibrosis transmembrane conductance regulator gene (Riordan *et al.*, 1989). This gene encodes a cyclic AMP-regulated chloride ion channel (Welsh, 1990).

The major cause of mortality in cystic fibrosis is respiratory disease, due mainly to repeated opportunistic lung infection which ultimately leads to fatal inflammatory lung disease (Curiel *et al.*, 1996). Hence, the airway epithelium has been the principle target tissue for gene therapy in cystic fibrosis, and *in vitro* optimisation of the best cationic liposome for a DNA delivery vector revealed strong dependence on cell type (Caplen *et al.*, 1995b). While the initial clinical studies demonstrated an encouraging trend in the partial restoration of electrolyte transfer in the epithelium (Caplen *et al.*, 1995a), the transfection efficiency and duration of expression was shown to require enhancement.

1.2 Neoplastic disease.

Cancer is a disease where the cells are no longer responsive to the normal genetic control mechanisms. The uncontrolled cell proliferation, invasiveness and substrate independent growth characteristic of cancer is brought about by multiple mutations involving two basic routes: the production of a hyperactive stimulatory gene (the transformation of a proto-oncogene into an oncogene) or the inactivation of a tumour supressor gene (Bishop, 1991). These changes may arise from a combination of hereditary predisposition and as a response to external stimuli (Pike, 1987).

Knowledge regarding the biochemical basis of cancer has led to the application of gene therapy for the delivery of targeted cytotoxics or prodrugs to tumours (Deonarain *et al.*, 1995). Additionally, gene therapy has been used to deliver genes capable of enhancing the host's immunological response to the cancer cells (Pardoll 1993; Ostrand-Rosenberg, 1994). These approaches are intended to be more efficient and selective than existing chemotherapeutic agents or radiation (Gutierrez *et al.*, 1992), reducing the toxicity to normal cells.

Some cancers are exceptionally resistant to traditional treatment by chemotherapy and radiotherapy (Malpas, 1991). For example, the treatment of malignant melanoma is one of the least successful of all solid tumour treatments because of the rapid formation of distant metastases (Dalgleish, 1996). Attempts have been made to produce biological therapies such as the specific targeting of cytotoxic drugs to melanoma cells using melanocyte stimulating hormone (MSH). Due to the rapid degradation of the native peptide *in vivo*, D-analogues have been synthesised

which exhibit enhanced activity profiles (Sahm, 1994). This was believed to be due to a higher receptor-binding affinity plus increased resistance to degradation. Malignant melanoma was the first cancer in which gene therapy was tried in humans. This involved the treatment of patients with advanced cancer using cyclophosphamide, IL-2 and tumour infiltrating lymphocytes (Rosenberg *et al.*, 1989).

1.2.1. Malignant melanoma.

Malignant melanoma is a rapidly metastasising form of skin cancer which arises from the transformation of normal skin melanocytes to a malignant phenotype. Skin melanocytes arise from the neural crest (Boissy, 1988) and produce the pigment melanin, which they transfer to the surrounding keratinocytes in the epidermis. This helps to protect the skin from environmental ultraviolet light damage (Yaar and Gilcrest, 1991). Increasing exposure to this radiation due to changes in life-style has been linked to the current rapid increasing incidence of melanoma (Sanchez and Robinson, 1993).

Transformation of melanocyte cells results in highly migratory and invasive cells, which rapidly metastasise to major organs within the body. Additionally, this rapid and highly disseminated metastatic spread and resistance of the melanoma tumour to most chemotherapeutic regimes is problematic for treatment, resulting in poor patient prognosis (Dalgleish, 1996).

There are several predisposing factors including age, exposure to ultraviolet radiation (UVR) and the skin type (Elwood *et al.*, 1985). While older people exhibit a reduced survival rate, exposure to UVR at a young age or repeated sunburn are serious

risk factors. Fair-skinned people constitute the majority of melanoma patients, especially if they have a large number of moles (melanocytic nevi) or pronounced freckling of the upper back (Rigel *et al.*, 1985). Having more than one of these factors significantly increases the risk of developing malignant melanoma.

1.3. Enzyme pro-drug therapy.

The potential of cancer treatments based on genes which activate prodrugs within the tumour cells have been discussed in a review by Deonarain *et al.* (1995). The expression of enzymes capable of activating prodrugs in the tumour cells theoretically lends itself to the promise of gene therapy. The increased rate of proliferation of neoplastic cells is accompanied by a reduction in the level of regulation of DNA transcription. Gene therapy by enzyme-prodrug strategies is reliant on the loss of control to ensure that upregulated promoters express high levels of the enzymes capable of intracellular activation of the prodrugs. Since the enzyme is only expressed intracellularly, it does not encounter the immune system; an advantage over antibody-directed enzyme prodrug therapy. However, this advantage is offset by the delivery problems associated with the presentation of the genes and prodrugs to the intracellular compartment.

Alternative strategies for prodrug therapy have involved the generation of 5-fluorouracil from 5-fluorocytosine by the enzyme cytosine deaminase (Wallace *et al.*, 1994) and the release of doxorubicin from its prodrug by the enzyme β-glucuronidase (Svensson *et al.*, 1995). In both of these cases the delivery of the enzyme was directed specifically to the target tumour cells by fusion with antigen-specific monoclonal

antibodies. Limitations to this approach include the unpredictable toxicity seen in clinical trials, and the inability of proteins to readily diffuse into tumour cells, reflected by the small quantities of antibodies localised in tumours in human studies.

The tumour-selective expression of a prodrug-activating enzyme was first demonstrated by Harris *et al.* (1994). This group used the c-*erb*B2 promoter, which is often overexpressed in mammary tumour lines (Hollywood *et al.,* 1993), to restrict expression of the enzyme cytosine deaminase to *erb*B2-positive cell lines. This enzyme served to convert 5-fluorocytosine to 5-fluorouracil, which disrupts both DNA and RNA synthesis. Many of the mammary tumours were shown to be sensitive to treatment using this protocol.

A strategy employing the delivery of a pro-drug to malignant melanoma cells has been studied by Bonnekoh *et al.*(1995). The herpes simplex virus thymidine kinase gene was delivered to established melanomas in mice, using an adenoviral vector, sensitising the melanoma cells to subsequent administration with ganciclovir. Ganciclovir is normally non-toxic, but is converted to a DNA-synthesis inhibitor by thymidine kinase. The reduction in growth rate observed was roughly 50%, much higher than expected from a parallel *in vitro* transfection with a reporter gene. This indicated the existence of a bystander effect to the treatment. In this case, the bystander effect was reliant on the membrane translocation of the active drug between the cells, allowing access to cells neighbouring those that were transfected. The adjacent cells were then susceptible to the cytotoxic actions of the activated drug. The access is believed to be the result of passage through desmosomes between cells.

1.4. Immunotherapy.

The clinical interface between immunology and oncology has long been appreciated. Oncologists have used recently discovered information about the functional role of several cell surface molecules in attempts to enhance the endogenous immunity of tumours. Approaches to the immunostimulation of tumours have included manipulation to augment antigen presentation at the tumour cell surface (Ostrand-Rosenberg *et al*, 1990), stimulation of immunological reactivity by treatment with cytokines (Golumbek *et al.,* 1991), or by expression of a costimulatory agent necessary for the production of an immune response (Chen *et al.*, 1992).

In contrast to humoral immunity, where antibodies combat microbes in their native form in the extracellular body fluids, most of the tumour immunostimulation strategies rely on cell-mediated immunity. This involves the activation of T lymphocytes by processed antigenic proteins which are associated with the surface of a host cell. It is now widely accepted that T-cell responses are the primary target for antitumour immunisation protocols, as reviewed by Fathman (1993).

The classical cell-mediated primary immune response involves the endocytosis and processing of exogenous antigen by professional antigen presenting cells (APC's), known as dendritic cells or Langerhans cells, or presentation of antigen by macrophages. These antigenic peptides are then presented in association with a major histocompatibilty complex II (MHC II) molecule to the T cell receptor/CD3 complex on the $CD4^+$ T lymphocytes (helper T cells; T_H). This interaction produces signal 1 which primes the T cell for activation. However, additional signals are required from a variety

of cell surface adhesion molecules, cytokines and accessory costimulatory molecules to begin the cascade of communication between dendritic cells and T cells, and to activate the resting T cell (Mueller *et al.* ,1989). In the absence of costimulation the T cells may reach a state of clonal anergy (Jenkins *et al.,* 1991). Activation of the helper T cell stimulates production of the cytokine interleukin-2 (IL-2), which causes further activation and proliferation of various subsets of T and B cells. Ultimately, this results in the initiation of a cell-mediated immune response. The critical interactions between dendritic cells and T cells occur in the lymph nodes and these can result in activation of naive T cells.

A second type of MHC molecule, MHC I, is expressed by all nucleated cells. MHC I molecules directly activate $CD8^+$ T lymphocytes (cytotoxic T cells; CTL) by presentation of endogenously produced antigen. Many tumours express endogenously produced antigen, and processed viral peptides may be presented by MHC I molecules, allowing recognition by cytotoxic T cells. Cytotoxic T cells can also be activated by the production of IL-2 by helper T cells. Whereas $CD8^+$ CTL kill their targets in an antigen-specific manner, $CD4^+$ Th cells expand the immune response by releasing cytokines.

Tumour cells escape the normal host defences, in spite of many of them expressing tumour-specific antigens (Hellstrom and Hellstrom, 1991; Boon *et al.*, 1994). These antigens are derived from normal self-components, but are overexpressed and exhibit abnormal distribution in metastatic cells. A series of melanoma antigens were identified by Van der Bruggen *et al.* (1991), which were named MAGE and found to be expressed in a variety of different melanomas. This group concentrated their studies on MAGE-1, in an attempt to discern the level of expression of this antigen

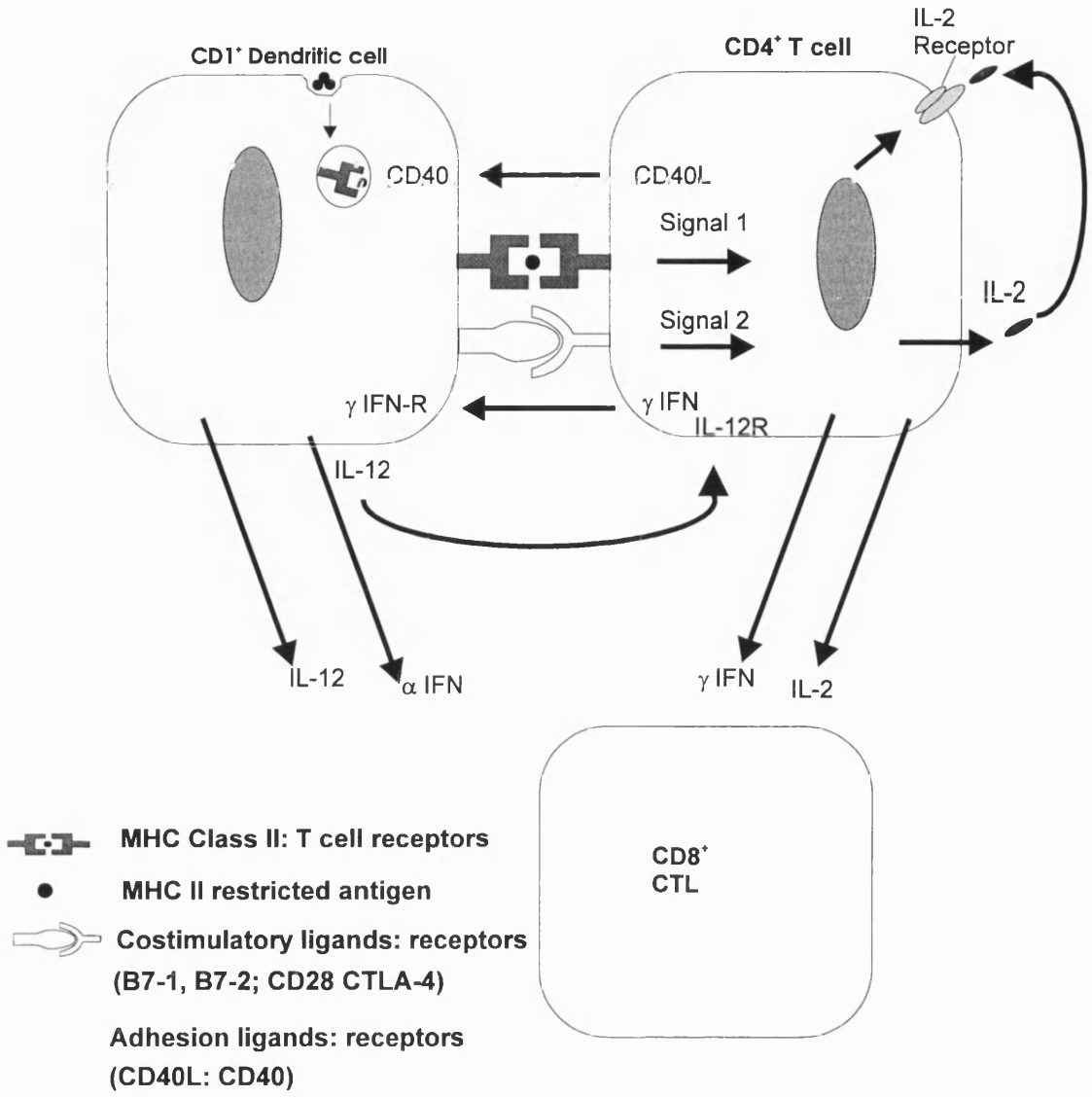

Figure 1.1. The typical interactions that occur during a cell-mediated immune response. Currently, it is postulated that there are five essential interactions during this process. An early contact is required between the CD40 ligand and its receptor on the dendritic cell. The next stage involves presentation of processed antigenic peptides in the context of MHC class II molecules, to the T cell receptor/CD3 complex. This interaction produces signal 1, which primes the T cell with the competency to respond to a potential second signal. The second signal arises after the binding of a costimulatory molecule with its receptor on the T cell. Additionally, the interaction of γ IFN at its receptor on the dendritic cell and IL-2 at its receptor on the T cell have also been demonstrated as necessary in the stimulation process. The secretion of the interferons, IL-2 and IL-12 have been shown to help expansion and stimulation of the response, and the $CD8^+$ response. In the absence of a costimulatory interaction, the T cell exhibits a state of antigen-specific anergy.

required to produce effective antigenic peptides. A review by Nossal (1993) described the capacity for immunologic tolerance that occurs during tumour progression. It was postulated that this could result from an absence of MHC II-restricted tumour antigens or from the production of a state of clonal anergy (Nossal and Pike, 1980).

1.4.1. Cancer Vaccines.

In contrast to viral vaccines, tumour vaccines involve the induction of a systemic immune response subsequent to the antigenic insult. Due to the patient-specific nature of tumour antigens, vaccines are produced using the patient's own tumour cells. This involves removal of the tumour cells from the patient, and cultivation and manipulation of the cells *ex vivo*. The transfected cells are then irradiated to render them incapable of further proliferation, before re-introduction to the patient (Morton *et al.*, 1993).

The aim of cancer vaccines is to render the tumour cells more immunogenic, and the approaches used to achieve this fall into three categories : expression of MHC-I or MHC-II antigens (Porgador *et al.*, 1989; Ostrand-Rosenberg *et al.*, 1990); expression of cytokines (Bannerji *et al.*, 1994); delivery of genes coding for costimulatory molecules (Chen *et al.*, 1992; Turcovski-Corrales *et al.*, 1995). A recent approach involved the pulsing of bone-marrow-derived dendritic cells with tumour-associated antigens, and injection into mice which were subsequently challenged with a lethal tumour burden (Mayordomo *et al.*, 1995). In more than 80% of cases, tumour regression was observed and tumour free status was maintained.

1.4.2. Major histocompatibility complex molecules.

If tumour cells could present their own peptides as antigen by the expression of MHC class II molecules, T lymphocyte activation might be enhanced. Tumour cells that have been transfected with MHC class II molecules demonstrated an increase in tumour immunogenicity (Ostrand-Rosenberg *et al.,* 1990). It has been postulated that this effect was due to the direct presentation of endogenously synthesised peptides in the context of MHC class II molecules to memory T_H cells (Topalian, 1994). This approach was based on the assumption that the effectiveness of CTL cells was dependent on sufficient help from tumour-activated $CD4^+$ T cells to amplify the immune response by the secretion of cytokines. The stimulation of $CD4^+$ T cells would also theoretically increase the likelihood of antitumour responses at distant metastatic sites. This study attempted to genetically engineer the tumour cell to act as an antigen presenting cell, as reviewed by Ostrand-Rosenberg (1994). The murine melanoma K1735 was adapted to allow presentation of endogenous tumour antigens after transfection with MHC class II genes, which activated $CD4^+$ T cells (Chen *et al.,* 1994).

Porgador *et al.* (1989) showed a reduction in the tumorigenicity of B16 melanoma after transfection with class I MHC molecules, and that this also converted high-metastatic clones into non-metastatic tumours. It was postulated by Giovanni *et al.* (1991) that this reduction in metastatic capacity was due to steric hindrance of cell association, in addition to a better interaction with the immune system of the host.

An alternative approach involved the concept of associative recognition (Kenne and Foreman, 1982). This proposed that the minor cell surface antigenic differences

occurring in cancer cells may be insufficient to induce an immune response. This may be overcome by the addition of powerful cell-surface antigens by transfection, which stimulate a response not only to the exogenous antigens, but also to the original tumour-specific antigens (Fearon *et al.,* 1988). Foreign MHC class I genes have been transfected *in vivo* into a variety of tumours in this context, inducing a cytotoxic T cell response in mice sensitised to the antigen (Plautz *et al.,* 1993). Additionally, this group demonstrated that lymphocytes from these mice were capable of stimulating an immune response against genetically unmodified tumour cells.

1.4.3. Cytokine expression.

This strategy is based on the assumption that tumour cells inherently present endogenously synthesised tumour peptides in the context of MHC class I molecules. As such, they are capable of directly stimulating class I restricted $CD8^+$ T cells, but lack sufficient immunogenicity to produce an immune response. The additional expression of cytokines that are normally secreted by Th cells or other accessory cells may enable $CD8^+$ T cells and other effector cells to be directly activated.

Several groups have analysed the immunogenicity of tumours engineered to secrete interleukin-2 (IL-2) (Foa *et al.,* 1992; Bannerji *et al.*, 1994). High levels of IL-2 expression resulted in increased tumour rejection, and the tumours were found to exhibit a massive infiltrate of lymphocytic cells. While $CD8^+$ T cells have been implicated in complete tumour eradication, initial tumour suppression was shown to be due to the local activation of natural killer cells (Hock *et al.*, 1993). A clinical trial involving the

use of IL-2 transfected allogeneic melanoma cells has been initiated to assess the anti-tumour efficacy and toxicity of this kind of treatment regimen and strategy (Osanto *et al.*, 1993).

Zatloukal *et al.* (1995) have established a receptor-mediated, adenoviral gene vector capable of stimulating a systemic anti-melanoma immune response in mice. They demonstrated that expression of IL-2 in MHC class I^+/II^- melanoma cells reduced the tumorigenicity of the cancer cells. A tumour-specific lytic activity was observed, and this was demonstrated to be due to the activation of $CD8^+$ T cells. The challenged sites of the immunised mice contained many macrophages and granulocytes, indicating that other mechanisms also contributed to the tumour destruction. A long-lasting systemic immune response was elicited in syngeneic, euthymic mice.

The majority of studies have involved IL-2, but other cytokines have also been employed to stimulate antitumour immune responses. IL-4 has shown antitumour activity in established renal cancer (Golumbek *et al.*, 1991) while interferon-γ (Hock *et al.*, 1993) and tissue necrosis factor-α (TNF-α) (Yannelli *et al.*, 1993) have shown similar activity profiles to the other cytokines.

1.4.4. Accessory molecules.

The multi-signal model for lymphocyte activation is now widely accepted (Schwartz, 1992). This describes a system where an antigen-specific signal is delivered via the antigen receptor, and an antigen non-specific or costimulatory signal is also required to determine whether engagement of the T cell receptor (TCR)/CD3 complex

causes clonal activation or anergy. Costimulation involves several cell surface molecules on APC's, which are recognised by T cell surface receptors.

The cell-surface molecule B7 (CD80) was identified as a ligand for the T cell receptors CD28 (Linsley *et al.,* 1990) and CTLA-4 (Linsley *et al.*, 1991a). Subsequently, it was shown that cells transfected with B7 provided co-stimulatory signals for activation of T cells (Gimmi *et al.*, 1991). B7 is normally expressed on professional antigen presenting cells i.e. dendritic cells (Freeman *et al.*, 1989). The co-stimulatory signal enables the generation and amplification of antigen-specific T cell responses (Linsley *et al.*, 1991b). This is as a result of the increased production of various cytokines that have autocrine and paracrine effects on the proliferation, activation and maturation of T cells to effector phenotypes. In view of the discovery of a second, functionally similar ligand B7-2 (Freeman *et al.*, 1993), the initial ligand is now referred to as B7-1. Several theories have been discussed regarding the differential functions of these two molecules, but there is currently no widely accepted mechanism described. It has recently been postulated that CTLA-4 and CD28 have opposing functions during T cell activation (Finn *et al.*, 1997).

Chen *et al.* (1992) demonstrated the capacity for tumour regression subsequent to co-transfection with a rejection antigen (associated with the human papillomavirus) and B7. Tumour cells expressing only the rejection antigen grew progressively in immunocompetent hosts. This rejection pattern has been mirrored in several different tumour types (Denfield *et al.,* 1995; Li *et al.*, 1996), and has been shown to be due to direct stimulation of $CD8^+$ T cells (Townsend and Allison, 1993; Iezzi *et al.*, 1996). In contrast to this, Li *et al.* (1994) reported that activation of $CD4^+$ Th cells was required to

amplify the tumoricidal response of $CD8^+$ T cells in the immunostimulation of the murine melanoma K1735 (Kripke, 1979). This supports the discovery by Chen *et al.* (1994) that the inherent immunogenicity of the tumour, or the immunostimulatory activity of any co-transfected antigens determines the activity profile for B7 to induce tumour immunity.

Baskar *et al.* (1995) co-transfected sarcoma cells with syngeneic MHC class II genes plus the costimulatory molecule B7. The most efficient tumour rejection occurred when both the class II and B7 molecules were co-expressed on the same tumour cell, and this response was shown to involve $CD4^+$ and $CD8^+$ T cells. This combines two of the previous strategies in an attempt to activate class II-restricted Th lymphocytes to stimulate tumour-specific immunity. A recent report by Chong *et al.* (1996) detailed studies of B7 expression in CMT93 murine colorectal tumour and K1735 murine melanoma cells. A local antitumour effect was observed in both tumours, although no significant systemic immunity was elicited in either tumour. The K1735 tumour is mildly immunogenic, but no systemic response was generated, even with co-expression of B7 and interferon-γ to produce high levels of surface MHC I expression.

1.5. Tissue-specific expression of genes.

Successful gene therapy requires the selective delivery and expression of a therapeutic gene to the target cells *in vitro* and *in vivo*. Currently available viral and non-viral vectors do not provide sufficient specificity for *in situ* use, but selective expression can be effected through manipulation of the transcriptional elements inherent to the

target cell. This approach involves the use of evolving molecular biological information about the control of eukaryotic gene expression, and the diversity of the tissue-specific control elements involved in the regulation of expression.

The majority of gene therapy vectors incorporate strong viral promoters that are indiscriminate in their cell-line related activity, and are often referred to as promiscuous promoters. In contrast, tissue-specific promoters and enhancers are preferentially active in certain cell types. Promoters are specific sequences that initiate the contact of RNA polymerase with the DNA sequence. The activity of promoters can be altered by enhancer sequences located at a distance from the start site of transcription, and these enhancers are active when placed in either orientation relative to the promoter .

Huber *et al.* (1991) demonstrated a system where tumour-specific transcriptional control elements were used to regulate expression of unrelated genes. Sikora *et al.* (1994) have shown that the promoter of the proto-oncogene c-*erb*B-2 could specifically express a prodrug in tumour cells.

1.5.1. Targeted expression to melanoma cells.

The production of melanin within mammalian cells occurs almost exclusively in melanocytes (Riley, 1977), and involves a series of chemical reactions brought about by a series of enzymes (Hearing and Tsukamato, 1991). Two promoters have been described by Jackson *et al.* (1991), which normally control expression of the proteins tyrosinase (Tyr) and tyrosinase-related protein-1 (Trp-1). Tyrosinase catalyses the conversion of tyrosine to dihydroxyphenylalanine (DOPA) and DOPA to dopaquinone

(Korner and Pawalek, 1982). Trp-1 functions as an oxidase of 5,6-dihydroxyindole-2-carboxylic acid (DHICA), producing a carboxylated indole-quinone (Kobayashi *et al.*, 1994).

Lowings *et al.* (1992) described both positive and negative elements that regulated the Trp-1 promoter, conferring melanocyte-specific gene expression. It was postulated that this control involved a highly specific interaction between the AT-rich TATA box (usually found about 30 bases upstream of the transcription start site) and a multi-component complex comprising the TATA-binding factor and multiple-associated proteins. Studies by Shibata *et al.* (1992a) demonstrated an enhancer-like activity displayed by the first intron of the Trp-1 gene, but this was demonstrated not to be a tissue-specific effect. It was concluded that this sequence was necessary for efficient transcription of the Trp-1 gene in pigment cells.

Work on the Tyr promoter has identified two possible sites for a cell-specific enhancer. Shibata *et al.* (1992b) demonstrated that a sequence located approximately 1.8 Kb upstream from the transcription start site could enhance the transient expression of a reporter gene specifically in melanoma cells. However, Ganss *et al.* (1994) discovered a 200 base pair sequence approximately 12 Kb upstream of the tyrosinase gene which displayed strong cell-specific enhancement. This group also showed, by protein binding, the presence of a melanoma-cell-specific complex that could contribute to the cell-specific activity, although the exact nature of the factor interacting with the binding motif has yet to be elucidated.

Vile and Hart (1993a) have shown that the promoters Tyr and Trp-1 are preferentially active in melanocytic cells. Further development involved the expression of the herpes simplex virus thymidine kinase under the control of the tyrosinase promoter to established murine melanomas *in vivo* (Vile and Hart, 1993b). Expression of this gene sensitises the tumour cells to subsequent administration of ganciclovir, which is phosphorylated by the kinase to an intermediate capable of disrupting DNA synthesis. Vile and Hart (1995) have also shown successful *in vitro* selective expression of cytokine genes to malignant melanoma cells using the tyrosinase promoter. The intratumoural injection of a selection of cytokines under the control of the tyrosinase promoter showed no significant reduction in tumour growth, although RNA levels demonstrated that 1% of the tumour population were expressing the exogenous genes. Chong *et al.* (1996) have developed a tissue-specific expression vector where the murine B7 gene is driven by the 5' promoter of the murine tyrosinase gene (Vile and Hart, 1993a) for expression studies in the melanoma cell line K1735.

Atruc *et al.* (1995) have performed similar work to Vile and Hart, demonstrating reporter gene upregulation in a variety of melanoma cells lines. Use of the tyrosinase promoter produced upregulation of approximately 21-fold, while a combination of the melanocyte-specific enhancer and tyrosinase promoter increased expression by up to 154-fold. Gene expression was strongly associated with the capacity for the cells to synthesise melanin.

Tissue-specific enhancers are capable of enhancing the promoter activity of an unrelated promoter, and this method has been used to enhance the weak tissue-specific expression of a gene under the control of the Tyr promoter. The Tyr enhancer has been linked to viral promoters to effect the strong expression of genes in a tissue specific manner (Dr. R. Vile, personal communication).

1.6. Gene delivery.

Pharmaceutically, the greatest challenge associated with gene therapy is the production of an efficient gene transfer vehicle. The aim is to maximise the therapeutic potential of genes, while creating a product that resembles a conventional pharmaceutical formulation in terms of composition, characterisation, safety and clinical application (Ledley, 1995). Inherent are the problems associated with the *in vivo* delivery of macromolecules and the many biological barriers that have to be overcome. In addition, immunogenicity and reticuloendothelial clearance must be considered during product development.

1.6.1. The optimal gene transfer vehicle.

The achievement of efficient *in vivo* gene delivery would dramatically increase the applications of gene therapy. A basic requirement of any such system is that the therapeutic gene must be reproducibly expressed in the target cells to produce subsequent expression of the gene in an appropriate manner (Mitani and Caskey, 1993).

The initial step of transfection of the target cell population must ultimately result in efficient gene transit across several biological barriers to the interior of the nucleus to produce functional activity. Successful transfection requires that the gene gains access to the cell population. It must then transit across the plasma membrane and cytoplasm before gaining nuclear entry (Michael and Curiel, 1994).

Davies *et al.* (1993) showed that in contrast to the belief that viral promoters acted non-specifically in cell lines, distinct differences were observed both in the levels and time over which this expression was sustained. This selectivity in promoter activity requires consideration when designing vectors to ensure optimal transcription within the target population. An ideal gene therapy delivery vector would require the inclusion of several intrinsic characteristics combining the attributes of a marketable pharmaceutical product with the desired biological activity (Michael and Curiel, 1994; Smith *et al.*, 1996):

(i) to ensure reproducible, efficient gene delivery to the target population of cells.

(ii) to include a means of target selectivity, whether through delivery or expression.

(iii) to transit several biological barriers, delivering DNA from the exterior of the cell to the nucleus.

(iv) to ideally contain no viral gene sequences, hence reducing any safety issues intrinsically associated with viruses.

(v) to be non-toxic, non-immunogenic and biodegradable.

(vi) to be pharmaceutically acceptable : to be physically,chemically and biologically stable; to be reproducibly manufactured; to be well-characterised.

1.6.2. Approaches to delivery for gene therapy.

All current vectors for gene therapy are based on either viral transduction or transfection using particulate or physical methods. Much research has focused on gene delivery using recombinant viruses, capitalising on their natural capacity to transport their genetic material into target cells. The attractiveness of non-viral systems compared with viral delivery centres around their ease of manipulation, their safety and stability on storage, which has led to the development of several non-viral approaches.

1.7. Viral vectors.

The work by Westphal *et al.* (1968) demonstrated the capacity of polyoma viruses to transfer viral DNA to the nuclei of transformed cells. Since then, many studies have involved the manipulation of this inherent property of viruses for the delivery of foreign DNA to eukaryotic cells. Successful gene delivery has been achieved with recombinant viral vectors developed using both RNA and DNA viruses, including retroviruses (Ferry *et al.*, 1991), adenoviruses (Karlsson *et al.*, 1985) and herpes simplex virus-1 (Geller and Breakefield, 1988). The majority of viral vectors for *in vivo* gene therapy are either retroviruses or adenoviruses, although a vector has recently been studied using recombinant adeno-associated virus (Mamounas *et al.*, 1995).

1.7.1. Retroviruses.

Retroviruses carry their genetic information as RNA. Retroviral infection involves internalisation of the host cells, effected by the viral envelope protein. Subsequent to infection, the RNA genome is reverse-transcribed into DNA which integrates at a random position into the host's genomic DNA. Retroviral vectors are composed of an RNA copy of the exogenous gene contained within the envelope of a replication deficient retrovirus, as detailed by Eglitis and French Anderson (1988).

This kind of delivery vector has several safety concerns associated with it (Temin, 1990). The intrinsic problems include a high rate of mutations during viral replication capable of inactivating the therapeutic gene; recombination to produce replication-competent virus; expression of viral genes with the potential to activate proto-oncogenes in the infected cells. Packaging cell lines have been developed which are replication defective (Le Gal La Salle *et al.*, 1993). The cells contain the proviral DNA of a helper virus but the signal that normally packages the viral DNA into virions has been removed. This serves to reduce the expression of inherent viral genes. Further development of such packaging cell lines has reduced the likelihood of recombinatorial events to produce wild-type virus (Miller and Buttimore, 1986).

Retroviral infection is dependent on the target cells being actively replicating at the time of infection (Miller *et al.*, 1990). This may have profound effects on transfer *in situ*, where the rate of cell division is far lower than in culture. Additionally there is a

size constraint of a maximum of 6-7 Kb (Eglitis and French Anderson, 1988) that can be packaged within the virion, which may restrict the applications for which this system is suitable.

A study by Porter *et al.* (1996) compared the efficiency of infection of different cells by a variety of retroviruses. The envelopes borne by these retroviruses were capable of recognising different receptors on human cells, and hence exhibited varying specificities for a selection of cell lines. Previously, retroviral vectors for gene therapy have used either envelopes from the murine leukaemia virus, MLV-A (Miller and Buttimore, 1986), or gibbon ape leukaemia virus, GALV (Meller *et al.*, 1991). The feline endogenous virus RD114 (Takeuchi *et al.*, 1994) was shown to be the most universally efficient system. Also, unlike other retroviruses, the RD114 envelope was shown to be stable and retain activity in serum.

Despite the safety concerns, retroviruses currently remain the most widespread delivery system utilised in gene therapy clinical trials, although many of the transduction events are carried out *ex vivo*. Retroviral vector producer cells have been used (Kun *et al.*, 1995) for the *in vivo* delivery of the HSVtk gene to malignant brain tumour cells. This trial was designed to establish the treatment load of vector producer cells required to produce successful tumour regression upon injection of the prodrug ganciclovir. An alternative use was in a gene marking study of patients with acute leukaemia carried out by Cornetta *et al.* (1996) to determine whether transplanted marrow contributed to patient relapse.

Retroviral vectors remain the most popular choice for gene therapy clinical trials because of the efficiency of delivery which they provide. It is however widely recognised that the risk of recombination of the attenuated viruses back to the wild type i.e. replication competent, is unacceptable. Hence, vector-producing cell lines require extensive testing for replication competency before use. In spite of the numerous mutations employed in the quest to produce safer retroviral vectors, it appears likely that they will eventually be replaced as *in vivo* gene therapy vectors by synthetic or particulate delivery systems.

1.7.2. Adenoviruses.

Adenoviruses are non-enveloped DNA viruses which are approximately 80-90 nm in diameter, and have a double-stranded DNA genome of 36 Kb in length. There are several serotypes of adenovirus, and types 2 and 5 have been extensively studied as a model for eukaryotic gene expression. Infection with wild-type adenovirus commonly results in upper respiratory tract infections, the 'common cold' (Straus, 1984). Only replication-defective adenoviruses are deemed suitable for gene therapy, and these are created by deletion of the E1 early transcriptional region. Adenoviral vectors are capable of accommodating 7.5 Kb foreign DNA by deletion of the E1 and the E3 region (Berkner, 1988).

In contrast to retroviruses, adenoviruses can transfect non-dividing cells, and have been shown to produce high levels of expression in hepatocytes (Jaffe *et al.*, 1992)

and terminally differentiated neurones (Le Gal La Salle, 1993). These viruses do not usually integrate into the genome of the host cell, and therefore act by producing transient expression. Therapeutically, this necessitates repeated administration, increasing the risk of stimulating an immune response against the delivery vehicle (Yei *et al.*, 1994). Further development by Bramson *et al.* (1996) has produced a double recombinant adenoviral vector capable of expressing the heterodimeric cytokine interleukin-12 *in vivo* and *in vitro.*

Adenoviruses exhibit highly promiscuous tropism, allowing widespread transduction after systemic *in vivo* delivery. Approaches to effect targeted delivery have involved extensive studies where the adenovirus has been coupled to transferrin-polylysine/DNA complexes (Wagner *et al.*, 1992a). This combined the delivery aspects of the virus with the facility to restrict uptake to cells expressing transferrin receptors, such as hepatocytes. An alternative approach has involved the production of a recombinant adenovirus vector with modified fibres (Krasnykh, 1996). These fibres contain cell recognition domains, and the production of chimeric fibres has been shown to alter the receptor recognition profile, providing a means of generating cell-specific targeting.

Adeno-associated vectors (AAV) were developed for clinical use as they are not associated with any human disease, and are able to infect a wide range of cell types (Flotte and Carter, 1995). This naturally defective, single-stranded DNA parvovirus generally requires co-infection with a helper virus for replication. In the absence of helper virus, the AAV genome integrates into the host chromosome. The lack of a

strong intrinsic promoter reduces the possibility of unwanted activation of downstream sequences. A major disadvantage was the inefficient process of vector production, but an improved titre was shown by Mamounas *et al.* (1995), involving co-infection with a 'helper' adenovirus.

1.7.3. Herpes simplex viruses.

The ability of herpes simplex virus (HSV) to infect neurones has led to initial gene therapy investigations for delivery to post-mitotic cells, as found in the nervous system, using HSV vectors. The vectors used have either been disabled to inhibit growth except in a complementing cell line, or to rely on a helper virus for replication and packaging into virus particles (Stevens, 1975). *In vitro* studies have involved delivery of a reporter gene to cultured peripheral neurones, achieving almost 100% transfection (Geller and Breakfield, 1988). Recent developments have included the delivery of HSV1 ICP34.5 deletion mutants to the nervous systems of mice (Coffin *et al.*, 1996). The infection was shown to be avirulent, yet the reporter gene was expressed close to the inoculation site. This was in contrast to wild-type infection where transgene expression was low, and found far from the inoculation site. This was an indication of the quick spread of the wild-type virus from cell to cell.

1.8. Non-viral delivery.

There are several advantages to the use of non-viral vectors over viral vectors for gene therapy. These include their resemblance to conventional pharmaceutical products

in terms of their composition, characterisation and safety, as reviewed by Ledley (1995). Non-viral vectors rely on the delivery of plasmid DNA. Plasmid DNA has exhibited activity after intramuscular injection (Wolff *et al.*, 1992) and more recently in melanoma cells after intratumoural injection (Yang and Huang, 1996). Not all tissues are capable of taking up and expressing free plasmid DNA, and hence much effort has concentrated on the generation of carrier systems. Unlike the viral vectors, there is little or no size constraint on the DNA with non-viral vectors.

The main biological challenge of non-viral gene delivery is that plasmid DNA is negatively charged. The physical properties of a particle within the body determine distribution and the extent of interaction with biological membranes. Several formulation theories and methods that were developed for controlled delivery of small-molecule drugs using particulate systems have been adapted and applied to gene delivery to cells. These systems include the use of cationic liposomes or particulate systems for the complexation of DNA expression vectors to deliver therapeutic genes *in vivo*. These systems rely on cellular mechanisms for import and nuclear transport of the DNA. Further developments of the systems currently in use will involve a greater appreciation of the fate of exogenous DNA both within the body and within the cell.

1.8.1. Liposomes.

Cationic liposomes were pioneered by Felgner *et al.* (1987) as gene delivery vectors. The variety of lipids currently available for liposome formation consist of molecules with spacers of differing lengths and a variety of positively charged head

groups (usually a single or multiple amine group), as reviewed by Gao and Huang (1995). This cationic nature allows interaction with the anionic DNA. Use of excess cation results in the formation of positively charged complexes which can interact non-specifically with the negatively charged cell surface. The DNA structure has been shown to collapse into a condensed form at charge neutralisation (Gershon *et al.*, 1993), and a further electron microscopy study of complex formation revealed a very heterogeneous population of complexes (Zabner *et al.*, 1995). Differences in structure of the liposome have been shown not to affect the type of DNA-vesicle association (Gustafsson *et al.*, 1995).

It was initially believed that uptake of liposome-DNA complexes was via fusion with the cell membrane (Zhou and Huang, 1994), but recent evidence has suggested that endocytosis is the major mechanism of entry (Zabner *et al.*, 1995 ; Friend *et al.*, 1996). The question of the fate of these complexes after internalisation has been addressed by several groups, and Friend *et al.* (1996) detailed extensive liposome-membrane interactions throughout the cytoplasm. It has been demonstrated that the complexes produced a membrane-destabilising effect, which subsequently allowed the anionic lipids present on the cytoplasmic edge of cellular membranes to displace the DNA from the liposome (Xu *et al.*, 1996).

Many studies have concentrated on the use of liposomes for gene therapy applications, as reviewed by Lasic and Templeton (1996). Initial *in vitro* transfection results produced high levels of reporter gene expression, but these levels were highly dependent on the DNA-liposome complex formulation and the cell type transfected

(Caplen *et al.*, 1995a). pH-dependent liposomes have previously demonstrated enhanced cytoplasmic delivery of macromolecules (Connor and Huang, 1986) due to the destabilisation of the liposome bilayer at acidic pH within the endosome. Legendre and Szoka (1992) showed that cationic liposomes were superior to pH-sensitive liposomes, indicating that the cationic liposomes used an alternative delivery pathway into the cell.

Clinical trials for the treatment of cystic fibrosis have used cationic liposome vectors for delivering DNA to the nasal epithelium (Caplen *et al.*, 1995b). A comparative study of the *in vitro* and *in vivo* activity of liposome-DNA complexes for cystic fibrosis gene therapy has revealed that the choice of viral promoter can enhance the levels and duration of expression (McLachlan *et al.*, 1995). Evaluation of the aerosol delivery of this vector has shown that a more stable DNA-lipid complex is required than that currently in use (Schwartz *et al.*, 1996). The use of cationic liposomes as systemic vectors *in vivo* is restricted by their lack of stability in serum and as pharmaceutical entities.

1.8.2. Polycationic polymers.

Smull and Ludwig (1962) showed that some basic proteins were capable of enhancing poliovirus RNA delivery to eukaryotic cells. Interest in the interactions between protamines and histones with DNA led to parallel studies with cationic homopolymers (Olins *et al.*, 1967; 1968). These physical and chemical studies demonstrated that the DNA was stabilised and condensed into a toroid by the interaction with polycationic polymers. Binding of DNA to the cationic polypeptides

resulted in structural phase transitions, which gave very different profiles to free DNA when analysed by electrophoretic sedimentation (Tsuboi *et al.*, 1966). The interactions were discovered to be co-operative with 1:1 stoichiometry with respect to amine and phosphate groups.

Initial adsorption and uptake studies of polycation-DNA complexes were performed by Farber *et al.* (1975). It was shown that several polycationic polymers were able to enhance the uptake of exogenous DNA into eukaryotic cells and that 95% of the DNA became nuclear-associated within 15 minutes. This rapid nuclear delivery now seems highly misleading. This group also demonstrated that optimal activity was seen when sufficient basic polymer had been added to neutralise the negative charge on the DNA.

In contrast to liposome-DNA complexes, the mechanisms of uptake of polycation-DNA systems have not been elucidated. It is generally accepted that non-specific mechanisms are used to accomplish cellular internalisation. Problems with the use of polycation-DNA complexes alone for gene therapy are associated with inefficient cellular uptake and the delivery steps distal to the cell membrane. Consequently, relatively low levels of expression are obtained compared with viral vectors. Mechanisms of overcoming these inefficiencies include the addition of a receptor ligand to provide a means of targeting the delivery to a specific cell type (Cotten *et al.*, 1993), or the use of endosomolytic agents to enhance DNA release into the cytoplasm, such as inactivated adenovirus (Curiel *et al.*, 1991) or peptides (Plank *et al.*, 1994).

The development of more elegant vectors for gene therapy, often described as self-assembly vectors, involves the combination of several moieties with different

functions: cell targeting, DNA-binding, endosomal release, nuclear delivery. Polycationic polymers have already shown their DNA-binding capacity (Olins *et al.*, 1966), and they are also capable of conferring protection to the DNA from nuclease degradation (Chiou *et al.*, 1994). Hence, the cationic polymers provide the DNA-binding moiety, and can be conjugated to molecules which will provide other functions in the resultant 'artificial viruses' for gene delivery.

This approach has been used at a basic level for cationic liposomes. The incorporation of polycations at appropriate ratios into cationic liposome-DNA mixes has been shown to alter complex formation and biological activity (Gao and Huang, 1996). Vitiello *et al.* (1996) have also shown that condensation of plasmid DNA with polylysine prior to formation of DNA-liposome complexes produced enhanced delivery and expression in muscle cells. This enhancement was found to be particularly evident for transfections performed in the presence of serum, as the polylysine served to both condense the DNA and protect it from enzymatic degradation.

1.8.3. Receptor-mediated polycationic DNA delivery.

The receptor-mediated delivery of a DNA-polycation complex was first studied by Wu and Wu (1987). The polycation acted as a DNA carrier while the covalently coupled ligand served to target the system to the receptor. Similar studies by several other groups (Wagner *et al.*, 1990, 1991; Zenke *et al.*, 1990; Gottschalk *et al.*, 1993) have shown that with a variety of ligand-receptor systems, specific receptor-mediated

uptake was maintained after covalent attachment of the DNA-polylysine complex to the ligand. Once bound to the receptor, the whole complex was internalised via receptor-mediated endocytosis (Wagner *et al.*, 1994).

Asialoorosomucoid was covalently linked to a polylysine-DNA complex and delivered to hepatoma cells expressing asialoglycoprotein receptors in a receptor-dependent manner (Wu and Wu, 1988). Successful *in vivo* delivery was achieved specifically to hepatoma cells following intravenous injection (Wu *et al.*, 1991) The majority of the exogenous gene was discovered in cytoplasmic vesicles, and seen to be DNase resistant (Chowdhury *et al.*, 1993).

Receptor-mediated gene transfer of polycation-DNA complexes has also been successfully performed using galactose (Midoux *et al.,* 1993), insulin (Rosenkranz *et al.*, 1992), an integrin-binding peptide (Hart *et al.*, 1996) and most extensively with transferrin (Wagner *et al.*, 1990). Transfection of the transferrin-polylysine-DNA complexes has further been enhanced several hundred-fold by the presence of glycerol or ethylene glycol during transfection (Zauner *et al.*, 1996). This effect is believed to arise due to the interaction of glycerol with cell membranes (Fraley *et al.*, 1981). This approach has also been applied to the cationic liposome, lipofectin. Addition of the receptor-ligand transferrin was able to enhance the transfection of HeLa cells from 4% for lipofectin alone to 98% (Cheng, 1996).

1.8.4. Enhancing endosomal release.

The majority of gene delivery methods rely on endocytosis for entry into the cell. Subsequent to endocytosis, the DNA passes into the endosome, where rapid enzymatic degradation can occur. Methods that enhance the release of the DNA before the lysosome and endosome fuse (the point at which the nucleases are introduced) would serve to enhance nuclear delivery and gene expression.

One approach involved the use of polymers that possessed a substantial buffering capacity below physiological pH, and which were potentially capable of producing membrane disruption. The main successful examples of these include the polyamidoamine cascade polymers developed by Haensler and Szoka in 1993, the interpolyelectrolyte complexes (IPEC's) produced by Kabanov and Kabanov (1995), and the organic macromolecule polyethyleneimine used by Boussif *et al.* (1995).

These polymers are all based on polycations, so retain the DNA-binding and protective properties of polylysine. Although the structures of these polymers differ, they all share the feature of residues that are protonatable at physiological pH. Their action as a network of effective 'proton sponges' allows them to disrupt the endosome (Stenseth and Thyberg, 1989). In order to ensure cellular delivery, the resulting polycation-DNA complexes required an overall positive charge, but in order to see an endosomolytic advantage, much higher polycation/DNA ratios were necessary (roughly 4-8) than for the polylysine-DNA systems. This resulted in a high density of active groups within the endosome to provide the proton sponge effect, and cause membrane disruption.

Adenoviruses have developed efficient mechanisms for host cell infection. These mechanisms have been utilised to enhance polycation-DNA complex delivery by the use of whole inactivated adenoviruses (Wagner *et al.*, 1992a) and in the development of fusogenic peptides mimicking the action of peptides involved in viral infection (Wagner *et al.*, 1992b).

Expression studies involving the enhanced delivery of transferrin-polylysine gene vectors due to co-infection with adenovirus sparked an interest in the merging of viral and non-viral vector properties (Curiel *et al.*, 1991; Cristiano *et al.*, 1993). Adenoviral particles induced endosomal lysis during the process of infection (Blumenthal *et al.*, 1986). Co-internalisation of the complexes and adenoviral particles in the endosome allowed release of the DNA after the endosome had been lysed due to the viral particles. The trans delivery of adenovirus and transferrin-polylysine/DNA complexes used transcription- and replication-defective virus, because the gene was not carried within the genome of the adenovirus particle (Cotten *et al.*, 1992). This removed the size constraint on the delivery vector, as well as enhancing the safety profile of the system.

Rapid progress by this group produced a construct where the adenovirus was coupled directly to the transferrin-polylysine/DNA (Wagner *et al.*, 1992). Transfection levels of virtually 100% were achieved in both HeLa cells and murine hepatocytes. This vehicle contains moieties to package nucleic acids (polylysine), for cell attachment and receptor-mediated endocytosis (transferrin) and an endosomolytic agent (adenovirus).

Successful *in vitro* transfection of primary canine cells and epithelial cells in haemophilia B (Lozier *et al.,* 1994), primary fibroblasts in haemophilia A (Zatloukal *et al.,* 1993), and *in vivo* transfection of airway epithelium (Gao *et al.,* 1993) have also been demonstrated.

It was only a small step to the use of specific fusogenic peptides in place of the entire virus, and initial studies involved the use of the influenza haemagglutinin HA-2 N-terminal peptide fragment (Wagner *et al.*, 1992). Approximately 10% of the HeLa cells transfected showed expression of the reporter gene after 48 hours. Although this shows a reduced efficiency compared with the complete adenovirus, this system is favoured as an *in vivo* gene therapy vector for safety reasons. Further analysis of the adenoviral cell entry mechanism by Cotten and Weber (1995) revealed that a viral protease is required for the proteolytic processing of the virus capsid to ensure effective pH 5-induced membrane disruption in the endosome. Potentially, this shows that viral particles lacking the capacity to produce the viral proteases may exhibit reduced efficiency of gene delivery compared with full adenoviral particles.

1.9. Second generation non-viral vectors.

It is widely accepted that second generation non-viral delivery vectors will need to incorporate some attributes of viral particles. While the non-viral vectors are efficient at condensing the DNA, major shortfalls in their design centre around endosomal release after internalisation and uptake into the nucleus. Information regarding viral infection mechanisms has allowed the development of fusogenic peptides capable of conferring the viral uptake profile onto non-viral vectors.

The initial studies involved the use of the HA-2 peptide (Wagner *et al.*, 1992b). This idea has been further developed by the use of synthetic endosome-disruptive peptides (Plank *et al.*, 1994). This work utilised the further knowledge gained about the fusogenic properties of the influenza haemagglutinin peptide. It was shown that the 20-N-terminal amino acids of this peptide exhibited activity only when an additional amphipathic helix was included.

Gottschalk et al. (1996) have designed and synthesised two peptides to emulate the functions of viral proteins: a DNA-condensing agent and an amphipathic, pH-dependent endosomal releasing agent. The replacement of the polylysine as the DNA-binding agent was due to the heterogeneity displayed in commercially available samples. Hence, its replacement was to ensure the production of more homogeneous and well-characterised complexes. The synthetic DNA-condensing peptide was based on the highly efficient DNA-condensing agent spermine. The number of lysine residues was varied in an attempt to discover the minimum size required for DNA binding.

The novel amphipathic peptide was designed after analysing many influenza fusion sequences and other fusion peptides, and using molecular modelling. The amphipathic peptide was a prototypic pH-dependent peptide for rupturing endosomes. The gene delivery system was created by stepwise self-assembly, and achieved high levels of gene expression in several cell lines. This system does not include a receptor ligand, and the inclusion of transferrin failed to increase expression by more than 8-fold.

Fominaya and Wels (1996) have produced a recombinant fusion protein based on the multidomain structure of the bacterial *Pseudomonas* exotoxin A. This consists of three functional domains : a single chain antibody capable of producing target cell specificity, the exotoxin domain capable of endosomolysis, and a DNA binding domain based on a yeast protein. In this case the DNA-binding domain was unable to facilitate uptake alone. The DNA required condensation and compensation of the negative charge with polylysine. The complexes that were spontaneously formed with the fusion protein were shown to be capable of transfecting cells in a ligand-specific manner *in vitro*. This demonstrates the advances currently being made towards more highly characterised and reproducible systems, where the non-viral vectors are acquiring advantageous viral attributes.

1.9.1. Nuclear localisation.

Bonner (1975a) demonstrated that certain proteins were capable of entering and accumulating in the nucleus of frog oocytes by translocation through the nuclear pores, which was attributed at the time to passive diffusion. However the fact that the nuclear protein histone is synthesised in the cytoplasm (Borun *et al.*, 1967) and then transported to the nucleus suggested the presence of a selective transport mechanism across the nuclear membrane (Bonner, 1975b). Moreland *et al.* (1987) discovered that a single amino acid substitution in the sequence of yeast histone 2B completely abolished

nuclear localisation. Additionally, it was shown that there is a large degree of conservation of this sequence in a variety of species, and that this sequence is lysine-rich.

Further studies by Breeuwer and Goldfarb (1990) demonstrated that the earlier belief that small nucleophilic proteins like histone H1 diffused into the nucleus were incorrect, as no transport occurred if the cells were chilled or energy depleted. This indicated that localisation within the nuclei occurred via a receptor-mediated process, and precluded the diffusion of proteins through the nuclear pores.

Recently, much work has been performed to elucidate the mechanisms of nuclear protein import, reviewed by Melchior and Gerace (1995). Transport across the nuclear envelope is mediated by large supramolecular structures which span the membrane, called the nuclear pore complexes. Small ions and metabolites diffuse freely through the nuclear pore complex, while most macromolecules are transported through gated channels via signal- and energy-dependent mechanisms. Nuclear localisation sequences of amino acids have been identified, and while there is no consensus sequence, they are highly enriched in basic amino acids (Dingwall and Laskey, 1991). Receptors for these nuclear localisation sequences have been identified, capable of stimulating transport of the protein into the nucleus (Adam and Gerace, 1991).

Strategies for DNA delivery have been developed incorporating this information. Histones, which naturally bind nuclear DNA, were galactosylated so as to act as asialoglycoprotein receptor-targeted DNA carriers (Chen *et al.*, 1994). The histones contain their own intrinsic nuclear localisation sequences, and galactosylated histone H1

was shown to exhibit superior transfection efficiency over other modified histone groups and non-nuclear proteins. Additionally, Conary *et al.* (1995) have shown that the use of synthetic peptides, containing a nuclear localisation signal, with liposome vectors can enhance transgene expression.

It seems clearly apparent that future developments will attempt to incorporate the viral attributes known to be advantageous to gene delivery and expression into the non-viral vectors already in use. Hence, we see development towards a synthetic virus-like delivery vector, some way between the current viral and non-viral vehicles.

1.10. Aims and Objectives.

The immunotherapeutic approach to tumour gene therapy has produced several encouraging preliminary results. Interest now centres on the production of cell-mediated immune responses, through the activation of T cells specific for both MHC class I and MHC class II restricted tumour antigens. Many of the patients presenting with cancer have immune systems that have become functionally tolerant to any tumour antigens which may be present at the tumour cell surface. Information about antigen processing, presentation and T cell regulation have allowed the use of approaches to break this tolerance by the stimulation of more potent immune responses.

Becker *et al.* (1993) demonstrated that a human melanoma cell line that expressed MHC class II induced clonal anergy in $CD4^+$ T cells. Transfection of the melanoma cells with the co-stimulatory molecule B7 stimulated IL-2 production and T

cell proliferation. Additionally, Chen and Ananthaswamy (1993) showed that the murine melanoma cell line K1735 required the expression of MHC class I antigen and either class II antigen or the presence of IL-2 to effect rejection in syngeneic mice.

The primary aim of this project was to create a tissue-specific immunotherapy for the treatment of melanoma. The approach to be used was that of co-expressing MHC class II molecules and B7-1 in the murine melanoma cell line K1735. An expression vector containing the B7-1 gene under the control of the tissue-specific promoter Trp-1 (Jackson *et al.,* 1991) was to be used to create stable transfectants. This required preliminary experiments to establish the suitability of the Trp-1 promoter for this study using the reporter gene β-galactosidase. Further experiments are described aimed at selection of stably transformed clones of K1735 expressing B7-1 and MHC class II genes. In practice, problems were encountered in producing stable expression, which are discussed in Chapter 2.

The delivery of genes for therapeutic purposes requires that the vector is safe, efficient and well-characterised. The additional objective of this project was to further the physical and biological characterisation of the interaction between polycations and DNA. The use of cationic polypeptides for condensation of DNA has been widely documented (Wagner *et al.*, 1991; Midoux *et al.*, 1993, Hart *et al.*, 1996). An understanding of the physicochemical interactions occurring will allow the development of non-viral self assembly systems, composed of several functional moieties. Each separate component will have its own function: to deliver the DNA to target cells; to bind and protect the DNA from degradation; to release the DNA from the cytoplasm; to direct uptake into the nucleus.

The characterisation of the DNA binding by cationic polypeptides in this study attempted to correlate physical attributes with biological activity. A variety of cationic polypeptide-DNA complexes were compared, both in their physicochemical properties, and their biological activities. The optimal charge-ratio ($^{+}$/-) was established for each system. A comparison of the physical properties of the optimum systems and the inefficient systems was made. Measurement of such factors as the DNA condensation capacity, particle size, protection of the DNA from degradation, and uptake and association of the complexes with cultured cell lines was carried out to clarify the interactions involved. This study will form the basis for optimisation of the DNA-binding moiety for an ultimately more complicated self-assembly system containing several other functional components.

CHAPTER 2. Tissue-specific expression of immunostimulants in melanoma cells

2.1. INTRODUCTION

The advent of gene therapy has revolutionized the approach to the treatment of various diseases, including cancer. Gene therapy allows alteration of the genotype of individual cells, hence affecting both the cell's phenotype and interaction with other cells within the organism. For cancer treatment, most interest has revolved around immunotherapies, which rely on stimulation of the host's immune system to recognise and eliminate tumour cells (as reviewed by Fathman, 1993). Several studies have involved the transformation of tumour cells with cytokines, MHC antigens or co-stimulatory molecules, so that they act as antigen-presenting cells. This serves to activate T cells in a manner similar to the classical immune response (Ostrand-Rosenberg, 1994).

Malignant melanoma is one of the more difficult cancers to treat successfully due to the rapid formation of distant metastases. Experimental studies have shown that transfection of melanoma cell lines with the co-stimulatory molecule B7 (CD80) have resulted in antitumour responses (Chen *et al.*, 1992; Townsend *et al.*, 1994; Iezzi *et al.*, 1996). However, it has recently been demonstrated that this effect may be accompanied by a reduction in systemic antitumour immunity (Chong *et al.*, 1996). An alternative protocol used MHC class I and II antigens to stimulate tumour immunity against murine melanoma (Chen and Ananthaswamy, 1993). A study by Baskar *et al.* (1995) demonstrated rejection of established sarcoma tumours after transformation with both

MHC class II plus B7 genes, and this activity was shown to be more effective than strategies using B7 alone.

This study aimed to examine the co-expression of MHC class II genes and B7 in the melanoma cell line K1735. Additionally, incorporation of a tissue-specific promoter, Trp-1 (Jackson *et al.*, 1991), upstream of the B7 gene, was planned to restrict the expression of the B7 gene to cells undergoing melanogenesis. This would serve to reduce gene expression in non-target cells, increasing the therapeutic benefit to the patient.

2.2. MATERIALS AND METHODS

2.2.1. Bacterial strains.

General cloning procedures using the vectors pRSV*lacZ*, pCEXV-3 (A^k) and pPGKPuro (Dr. M. Welham, Department of Pharmacology, University of Bath, UK) were performed using the host strain *E. coli* XL1-Blue (Stratagene). Cloning procedures using the mammalian expression vector pcDNA3 (Invitrogen, San Diego, CA, USA) were performed using the host strain *E. coli* TOP10F' (Invitrogen, San Diego, CA, USA). Amplification of the vector containing the murine B7 gene (Dr. R. Vile, ICRF, St. Thomas' Hospital, London), piLN-murB7 was performed using the host strain *E. coli* MC1061/P3 (Invitrogen, San Diego, CA, USA).

Bacterial growth media and other solutions are defined in appendix A. Growth media plates were produced by the addition of 15% Bacto Agar (Difco) to the media of choice prior to autoclaving. The solution was cooled to 55°C, and antibiotics were added (section 2.2.4) before pouring into 90 mm polystyrene petri dishes.

2.2.2. Plasmid vectors.

The melanoma-specific expression experiments were performed using the Trp-1-β-Gal vector, which was supplied by Dr. I. Hart (ICRF, St. Thomas' Hospital, London, UK). This contains 4.8 kb of the Trp-1 promoter and the first Trp intron, inserted upstream of an SV40 splice donor/ acceptor sequence, the β-galactosidase gene, and the SV40 polyadenylation sequence (Fig. 2.2).

Control expression studies were carried out using the mammalian expression vector pRSV*lacZ* (7.8 kb), kindly supplied by Dr. D. Ogilvie (Zeneca Pharmaceuticals, Alderley Edge, Cheshire, UK.). This contains the Rous sarcoma virus long terminal promoter / enhancer sequence, which drives expression of the *E. coli* β-galactosidase reporter gene (Fig. 2.1).

Initially, it was planned that the Trp-1 promoter would be inserted into the promoterless mammalian expression vector pNASSβ (Clontech). This allows cloning and testing of promoters using β-galactosidase expression. This vector contains an SV40 RNA splice site, a polyadenylation sequence and the *E. coli* β-galactosidase gene (Fig. 2.1).

The cDNA's for the α and β chains of the MHC I-A^k were a gift from Dr. S. Rosenberg (Department of Biological Sciences, University of Maryland, Baltimore, Maryland, USA). The genes were supplied as subcloned inserts at the *EcoR* I site in the mammalian expression vector pCEXV-n (Fig. 2.1; Miller and Germain, 1986). The cDNA for the α chain was 0.95 kb, while that for the β chain was 0.85 kb.

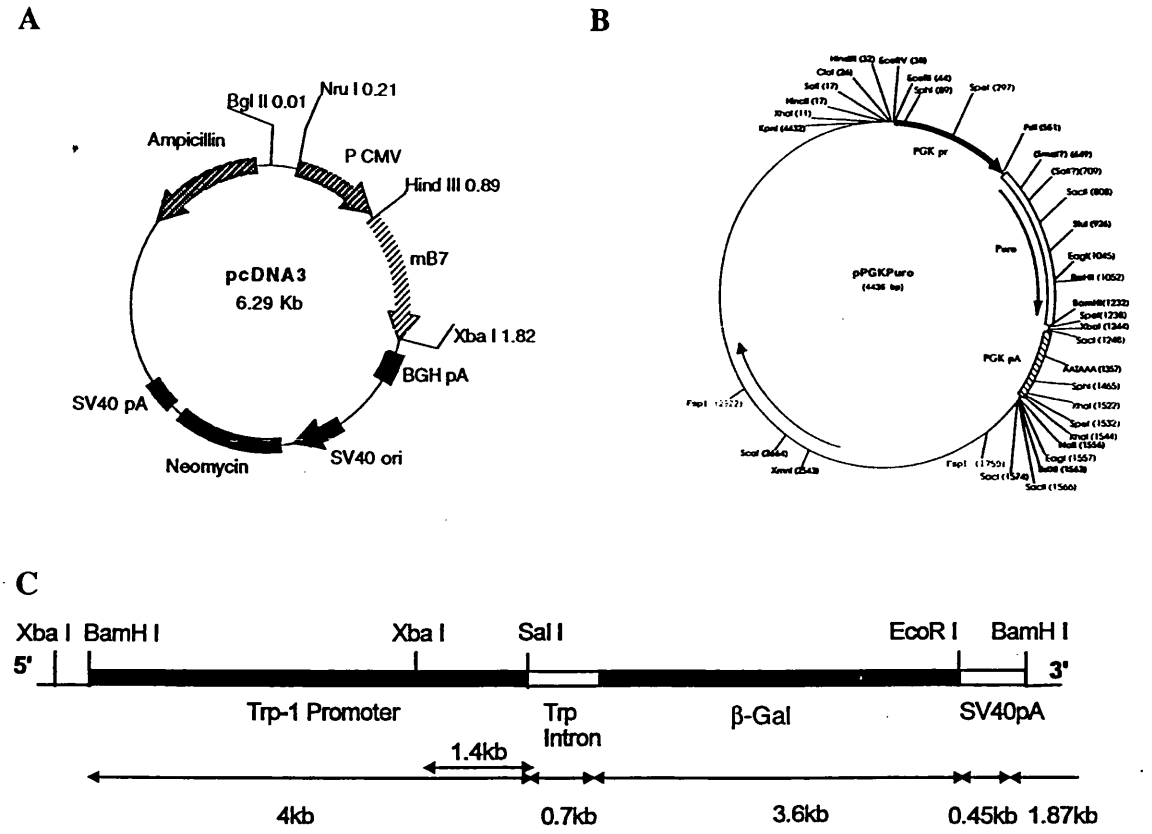

Figure 2.2. Plasmid maps of vectors. A:pcDNA3 after ligation of murine B7 gene; B: pPGKPuro; C: basic structure of construct containing the Trp-1 promoter obtained from Dr. I. Hart.

2.2.3. Preparation of electrocompetent *E. coli*.

A primary overnight culture of *E. coli* cells was diluted 1:100 in 500 ml LB medium and incubated until the OD_{600} reached 0.5 - 1.0. The cells were briefly chilled on ice then centrifuged at 4000 *g* for 10 min at 4°C using a Beckman J2-MC centrifuge. Extensive washing with water reduced the ionic strength of the cell suspension : 500 ml ice cold sterile water, 250 ml ice-cold sterile water, 10 ml sterile ice cold 10% glycerol, and finally resuspending into 1.0 ml of 10% glycerol. Electrocompetent cells were snap frozen in 40 µl aliquots in Cardice/methanol and stored at -70°C until required.

The murine B7 gene (0.93 kb) was supplied by Dr. R. Vile (ICRF, St. Thomas' Hospital, London, UK), in the vector piLN-murB7 (Fig. 2.1). This was inserted into the mammalian expression vector pcDNA3 (Invitrogen) at the *Hind* III and *Xba* I sites in the multicloning site (Fig. 2.2). The plasmid pPGKPuro (Fig. 2.2) was received as a gift from Dr. M. Welham (Bath University, Bath, UK). Both of these plasmids were used for selection of stable transformants by use of the neomycin and puromycin resistance markers respectively, as described in section 2.2.18.3.

2.2.2.1 Plasmid maps.

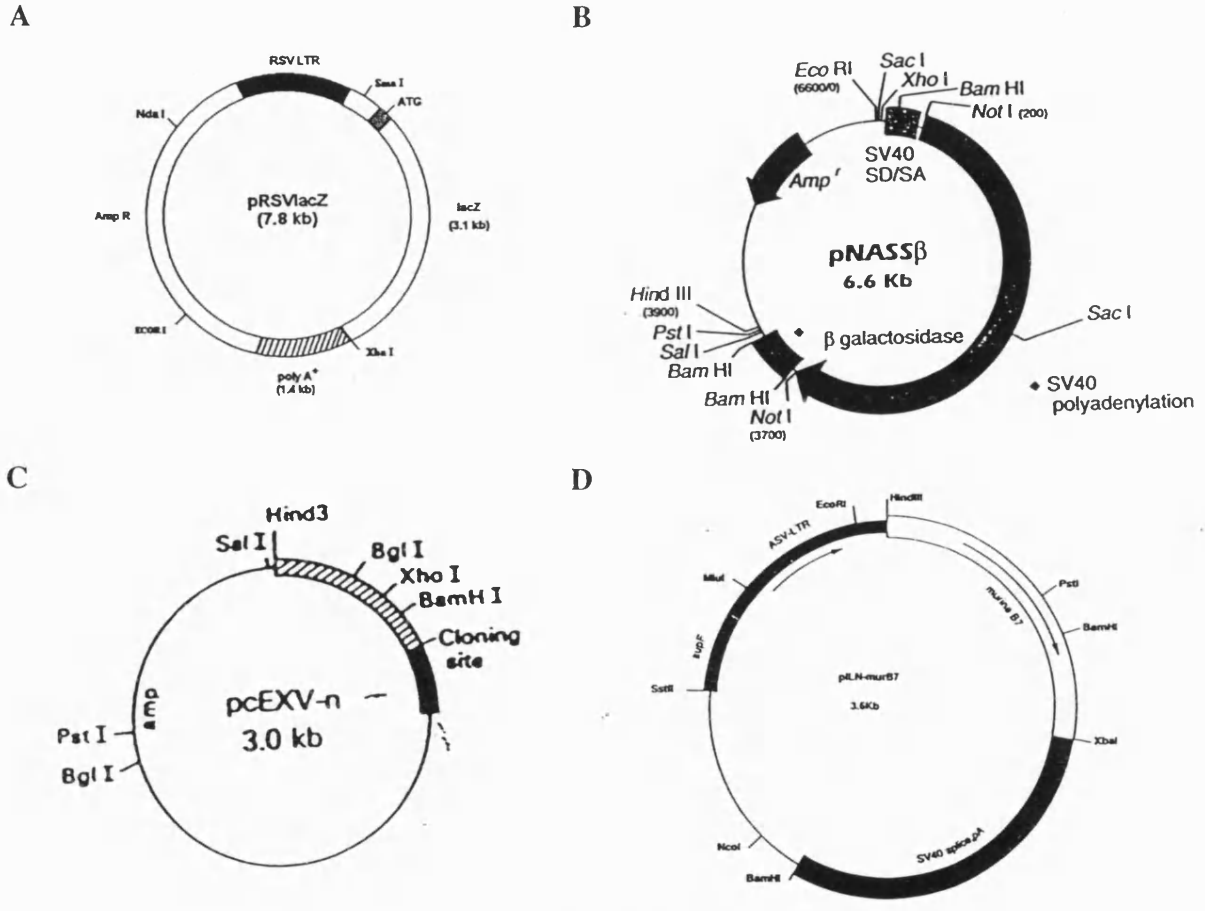

Figure 2.1. Plasmid maps of mammalian expression vectors. A: pRSVlacZ; B: pNASSβ; C: pCEXV-n; D: pILN-murB7.

2.2.4. Transformation of *E. coli* by electroporation.

Prior to transformation, the electrocompetent cells were thawed slowly on ice. Chilled plasmid DNA (up to 1 μg in water) was added, and the mixture was pipetted into a sterile pre-chilled 0.2 cm electroporation cuvette (Bio-Rad Laboratories, Richmond, CA, USA). The cuvette was placed in the chilled cuvette holder of a Bio-Rad Gene Pulser and subjected to the standard conditions of 2.5 KV, 200 Ω and 25 μFarads (Dower et al., 1988), producing a time constant of 4.8 ms. The cells were then allowed to recover in 1 ml of pre-warmed SOC medium (appendix A) at 37°C with shaking for 1 hour, allowing expression of the plasmid-coded antibiotic resistance. Transformants were selected by plating onto LB agar plates containing the antibiotics ampicillin (50 μg/ml or 30 μg/ml for MC1061/P3 cells) and tetracycline (12.5 μg/ml or 7.5 μg/ml for MC1061/P3 cells). A negative control of cells electroporated in the absence of DNA was plated in parallel onto selective media plates. Several single colonies were picked from each transformation, and grown overnight in LB broth containing antibiotics. Plasmid DNA was recovered by miniprep (section 2.2.5) and analysed by restriction endonuclease digestion.

2.2.5. Isolation and purification of plasmid.

Plasmid was initially prepared for restriction analysis by the alkaline lysis 'mini-prep' method detailed by Sambrook et al. (1989), which is adapted from that of Birnboim and Doly (1979). The DNA was routinely resuspended in 50 μl of TE buffer after drying.

2.2.6. Large scale plasmid preparation (maxipreps).

Large scale isolation was performed using Qiagen Plasmid Kits (Qiagen, Hilden, Germany). This involved a modified alkaline lysis step where 50 ml aliquots of bacterial suspension were pelleted by centrifugation at 5000 g, and the pellets resuspended in 2.5 ml buffer P1, using a sterile Pasteur pipette, before being pooled in an ultra-centrifugation tube. The composition of all buffers used in this procedure is described in appendix A. Ten millilitres of buffer P2 was added and the contents mixed by gentle inversion five times. After four minutes, 10 ml of buffer P3 was added to the cell lysate. The tube was placed on ice for 30 minutes and then centrifuged at 45,000 g at 4°C for 45 minutes in a Beckman Ti45 rotor. The supernatant was removed promptly and applied onto a single-use modified silica anion-exchange resin purification column (Qiagen) at appropriate low salt and pH conditions. The column was pre-equilibrated with 10 ml buffer QBT prior to use. The column was then washed twice with 30 ml of buffer QC, and plasmid DNA was eluted using 15 ml of buffer QF and precipitated by the addition of 10.5 ml isopropanol. The tube contents were gently mixed and centrifuged at 45,000 g for 45 minutes at 4°C. Pelleted DNA was washed with 15 ml ice-cold 70% ethanol and repelleted by centrifugation. Following aspiration of the supernatant, residual ethanol was removed from the pellet by air drying at room temperature for 10 minutes. The DNA was suspended in TE buffer containing RNAase at 20 µg/ml. Spectrophotometric analysis (section 2.2.7) showed the plasmid samples to be routinely pure enough for transfection into mammalian cells. It is possible that the addition of RNase introduced impurities to the DNA sample, and an alternative

purification procedure using a cesium chloride centrifugation gradient would reduce the contamination.

2.2.7. Spectrophotometric determination of nucleic acid concentration.

Spectrophotometric readings at 260 nm and 280 nm (Milton Roy Spectronic 601) were used to determine the quantity and purity of DNA. An OD of 1.0 at 260 nm corresponds to a solution at 50 μg/ml for double stranded DNA, 40 μg/ml for single stranded DNA and RNA (Sambrook *et al.,* 1989). Contaminating phenol and protein absorbs at 280 nm. Nucleic acid solutions with a 260 nm : 280 nm absorbance ratio of less than 1.8 were considered too impure for this method of quantification, and for subsequent transfection into eukaryotic cells.

2.2.8. Restriction endonuclease digestion of plasmid DNA.

Plasmid DNA restrictions were performed using New England Biolab (NEB) restriction enzymes and buffers, according to the manufacturers directions. Complete plasmid digestions were performed by incubation of the reaction mixtures at 37°C for 1 hour. Standard endonuclease restrictions for size analysis and cloning contained ~1 μg plasmid DNA in a total of 20 μl total reaction mix volume. Large scale restriction reactions used in the preparation of plasmids for mammalian cell transfections utilised 20 μg DNA, which was subsequently purified by phenol : chloroform extraction (section 2.2.5) before use.

2.2.9. Concentration of DNA by ethanol precipitation.

Precipitation of plasmid DNA from aqueous solutions was performed by the addition of 3 M sodium acetate (pH 5.2) to a final concentration of 0.3 M. Two volumes of ice-cold ethanol were added, and the solution mixed and incubated at -70°C for 15 minutes to precipitate. The mixture was centrifuged at 14,000 rpm for 30 minutes at 4°C in a Jouan A14 centrifuge to pellet the DNA. The washing and drying procedure was as detailed in section 2.2.5, and the DNA was finally resuspended in TE buffer.

2.2.10. Horizontal agarose gel electrophoresis.

Routinely, 1% agarose gels were produced by dissolving electrophoresis grade agarose (Gibco BRL) in 0.5x TBE buffer at 100°C. The solution was cooled to about 60°C, poured into the gel tray and allowed to set at room temperature for 45 minutes. The gels were then mounted in an electrophoresis tank (Bio-Rad mini-sub DNA cell) and submersed in 0.5x TBE. Electrophoresis was carried out at 80-200 V for sufficient time to produce full separation of the bands of interest. All gels were run with lanes of λDNA with *Hind III* and *EcoR I* digests as the marker (NBL Gene Sciences Ltd, U.K.; appendix B) and DNA samples were mixed with 0.2 volumes 5x DNA loading buffer (appendix A). The gels were stained with ethidium bromide in water at a concentration

of 0.5 μg/ml for 10 minutes. The DNA bands were visualized using a UV light box. Photographs were taken using a Polaroid MP4 camera and Polaroid 637 film.

2.2.11. Purification of DNA using Geneclean.

DNA was purified from agarose gels by adsorption of the DNA to a silica matrix using the Geneclean *II* system (Bio-101, La Jolla, CA, USA). The restriction mixture was run on an agarose gel, and the section of gel containing the fragment of interest was excised (less than 0.4 g). Three volumes of NaI solution was added to the gel, and incubated at 55°C for 5 minutes (for TBE gels, a half volume of TBE modifier and 4.5 volumes NaI were added to the agarose). The Glassmilk was resuspended by vigorous vortexing, and 5 μl was added to the agarose solution, mixed and left at room temperature for 5 minutes., mixing every 1-2 minutes. The silica matrix was pelleted by centrifugation for approximately 5 seconds, the NaI supernatant aspirated and the pellet washed three times with a wash buffer. The fragment of DNA was finally eluted from the beads into TE at 55°C for 5 minutes. Solutions of DNA were also purified by this method using 3 volumes NaI and proceeding straight to the addition of Glassmilk.

2.2.12. Ligation of DNA fragments into plasmid vectors.

The plasmid vector pcDNA3 was linearised by restriction at the *Hind III* and the *Xba I* sites within the polylinker site, as described in section 2.2.8. The enzymes were subsequently denatured by heat treatment, and 1 μg of vector was run on a horizontal agarose gel, and recovered using Geneclean as described in section 2.2.11. A fragment of approximately 900 bp was recovered from the piLN-murB7 vector and purified in a similar fashion for ligation.. The sticky end ligation was set up as detailed in Table 2.1 and incubated at 16°C for four hours. Control ligations were performed with the vector DNA alone, in the presence and absence of ligase. Purification involved the Geneclean procedure, before transformation of the host cells with a 5 μl aliquot by electroporation.

Vector: pcDNA3 (5.4 Kb)		0.5 μg
Insert: murB7 (0.9 Kb)		5.0 μg
10X Ligation Buffer (NEB)		5.0 μl
T4 DNA Ligase 400,000 U/ml (NEB)		0.5 μl
Sterile Water	to	50 μl

Table 2.1. Reaction conditions for ligation of murine B7 gene into pcDNA3.

The CMV promoter was removed from pcDNA3 by restricted at the *Nru I* and *Hind III* sites to produce a fragment of approximately 4.6 Kb. The *Hind III* site was converted to a blunt end using Klenow fragment (NEB) prior to treatment with calf intestinal alkaline phosphatase (CIAP, NEB). This treatment reduces self-ligation of the two ends of the vector in the presence of ligation enzymes, by removal of 5' phosphates.

The Trp-1 PCR product (section 2.2.13) was treated with Klenow fragment to ensure blunt ends, and the ligation was set up as detailed in Table 2.2. The reaction mixtures were purified using Geneclean before transformation of the host cell by electroporation.

Vector: pcDNA3 without CMV(4.6 Kb)		0.5 µg
Insert: Trp-1 PCR (2.1 Kb)		1.0 µg
10X Ligation Buffer (NEB)		5.0 µl
T4 DNA Ligase 400,000 U/ml (NEB)		0.5 µl
Sterile Water	to	50 µl

Table 2.2. Reaction conditions for blunt ligation of Trp-1 PCR product into pcDNA3 (no CMV).

2.2.13. Preparation of oligonucleotides.

Synthesis of oligonucleotides for PCR amplification was kindly carried out by Dr. A. Wolstenholme (School of Biochemistry, University of Bath, UK). The oligonucleotides were eluted from their synthesis columns by drawing 1 ml concentrated ammonia solution through the column in 0.2 ml aliquots at 20 minute intervals. The eluate was placed in a 1.5 ml screw-capped eppendorf and placed in a glass universal containing 0.5 ml concentrated ammonia solution. This was incubated at 55°C overnight (to remove amino-protecting groups). The ammonia solution was removed by vacuum drying in a DNA Speedvac (Savant) at room temperature in a fume cupboard. The oligonucleotide pellet resuspended in 300 µl sterile distilled water, and the DNA was precipitated using ethanol (section 2.2.9) before the dried DNA was resuspended in 1 ml sterile water. The oligonucleotide yield was determined as detailed in section 2.2.7, and diluted as necessary for the polymerase chain reaction. The typical yield was between 1-2 mg.

2.2.14. Polymerase Chain Reaction (PCR) of cDNA probes for murine Trp-1 promoter.

The cDNA of 4 kb of the Trp-1 promoter was received from Dr. I. Hart (section 2.2.2) and used as a template for PCR using the GeneAmp PCR Core Reagent Kit (Perkin Elmer Cetus, Norwalk, CT, USA) according to the setting and concentrations detailed in the manufacturers protocol. The reaction contained 10x Buffer, 10 mM dNTP's, 1 μM oligonucleotide primers (section 2.2.13) and 2.5 units Amplitaq. To this, 1-4 mM magnesium chloride and approximately 1-100 ng template cDNA was added. The reaction was exposed to cycling parameters of 94°C for 1 minute, 55°C for 1 minute and 72°C for 2 minutes, repeated for 30 cycles using a Crocodile II temperature cycler (Appligene). This protocol is based on the *Taq* DNA polymerase method described by Saiki *et al.* (1988) . The DNA fragment from this process was purified using Geneclean before further use, as detailed in section 2.2.11.

2.2.15. Mammalian cell lines.

B16 murine melanoma cells (passage 6) were donated by Dr. L.R. Kelland (Institute of Cancer Research, Sutton), and the less metastatic murine melanoma cells K1735 (passage 4) were obtained from Dr. I. Hart (ICRF, St. Thomas' Hospital, London). The murine fibroblast cell line NIH3T3 (passage 6), the human embryonal kidney line 293 (passage 50) and the SV40 transformed monkey kidney cell line were obtained from the European Collection of Animal Cell Cultures (ECACC, Porton Down, Salisbury, UK).

2.2.16. Cell culture media.

Dulbecco's Modified Eagle's Medium (DMEM) (10X concentrate) containing non essential amino acids (NEAA) was obtained containing the indicator phenol red, but without sodium bicarbonate and L-glutamine. Sterile double distilled, deionised water was used to dilute the concentrated solutions and the medium supplements L-glutamine (2 mM), penicillin (100 IU/ml) and streptomycin (100 µg/ml) (pen/strep), and the medium was buffered by the addition of 25 ml sterile 7.5% $NaHCO_3$ solution. Foetal bovine serum was supplemented (10%) in all cases. The final pH was corrected to 7.4 with sterile 1 M NaOH solution. All components were obtained from Gibco. Tissue culture flasks were obtained from Becton Dickinson Labware, USA and 6-well and 96-well plates from Nunc, Denmark.

2.2.16.1. Cell line maintenance and routine culture.

Routinely, cultures were seeded into 175 cm^2 flasks, maintained in a humidified 5% CO_2 atmosphere and incubated at 37°C in a LEEC anhydric incubator. The medium was changed on alternate days to maintain a pH of 7.2-7.4, and the cells were subcultured just prior to reaching confluence. Subculture involved washing the confluent monolayer twice with calcium and magnesium free phosphate buffered saline (PBS, Oxoid, UK) and incubating with a suitable volume of Trypsin-EDTA solution for 10 minutes at 37°C. The resulting cell suspension diluted to 10 ml with culture medium and counted. Cell numbers were established using a grid haemocytometer after staining with 0.1% trypan blue (Sigma) in PBS as described in the Sigma biochemicals catalogue

(1996, p1702-3). Cells were visualized on an M40 inverted biological microscope (Wiold Heerbrugg Ltd). Flasks were seeded at a density of $2x10^6$ cells per 175 cm^2.

2.2.16.2. Storage and freezing of cell lines.

Stocks of cells were routinely frozen for long-term storage. Cells were removed from the flasks prior to confluence, centrifuged in a MSE Micro centaur microfuge at 10000 g for 2 minutes, the medium aspirated, and washed with PBS. The cell pellet was resuspended in DMEM-FBS (10%) supplemented with 10% DMSO. The cell suspension (1.8 ml) was pipetted into polypropylene ampoules (Corning, USA) and cooled at a rate of 1°C/minute using a biological freezer unit (Union Carbide BF6). Once the cells were uniformly frozen at -70°C, they were transferred to a Union Carbide LR-40 liquid nitrogen refrigerator for long term storage at approximately -148°C.

2.2.16.3. Recovery of frozen cells.

Frozen cells were rapidly thawed in a water bath at 37°C, resuspended in 10 ml of complete pre-warmed medium. The cells were then centrifuged at 10000 g for 10 minutes to remove the cryoprotectant. The supernatant was removed, and the cells resuspended in complete medium and transferred to a 175 cm^2 flask. Cells were incubated at 37°C in 95% air / 5% CO_2.

2.2.17. Calcium phosphate mediated transfection.

B16 melanoma cells were transfected using a method adapted from that of Graham and van der Eb (1973) and Chen and Okayama (1987) of co-precipitation of the

DNA with calcium phosphate. B16 cells were harvested and seeded at a density of $1x10^5$ cells per well in 60 mm tissue culture dishes and incubated at 37°C for 24 hours prior to transfection. Separate tubes were prepared containing 500 µl aliquots of 15 µg DNA in 0.248 M calcium chloride solution, and 2x HBS. The DNA/$CaCl_2$ mixture was added dropwise to the HBS, and the reaction incubated at room temperature for 30 minutes. The calcium phosphate-DNA suspension was added dropwise to the medium in the wells along with chloroquine to a final concentration of 100 µM. The cells were incubated at standard conditions for 24 hours and the medium containing the calcium phosphate-DNA co-precipitate was removed. The cells were washed three times and overlaid with complete culture medium, and incubated for a further 24 hours at 37°C. Cell extracts were prepared (section 2.2.20.1) and the cells were assayed using the ONPG assay (section 2.2.20.2).

2.2.18. Electroporation of eukaryotic cells.

The initial expression studies using electroporation to compare promoter activity used a protocol modified from that described by Chu *et al.* (1987) and Potter (1988). This protocol involved using lower voltage and higher capacitance settings than that described in the initial electroporation studies by Neumann *et al* (1982). The cells were removed from 175 cm^2 tissue culture flasks at 70% confluence, washed three times with ice cold PBS, and resuspended at a density of $5x10^6$ cells in 500 µl PBS. These were then placed in 0.4 cm electroporation cuvettes (Bio-Rad), and 20 µg plasmid (prepared using Qiagen plasmid preparation column, section 2.2.6) added. The parameters on the Gene Pulser and the Capacitance Extender (Bio Rad) were set to those established as

optimal for the particular cell line used. Cells were then incubated for 15 minutes on ice after electroporation, before re-seeding into tissue culture flasks. Electroporated cells were incubated at 37°C and 5% CO_2 before assaying for β-galactosidase activity using the spectrophotometric ONPG assay (section 2.2.20.2).

2.2.18.1. Optimisation of electroporation parameters using FITC labelled dextran.

The optimal conditions for efficient transfection by electroporation vary for each cell line. FITC labeled dextran (Sigma, average MW 71,200) was used to establish the optimal parameters for each cell line, using a method adapted from that of Andreason and Evans (1989) and Graziadiel *et al.* (1991). An aliquot of 50 µl of FITC-dextran (10 mg/ml stock) was added to $1x10^6$ cells in a total volume of 500 µl of PBS. Electroporation was performed at a variety of capacitance and voltage values, producing a range of time constants between 4-12 msecs. They were then reseeded into tissue culture flasks, and incubated at 37°C for four hours. The cells were trypsinised, washed with PBS and resuspended into 500 µl PBS and analysed by fluorescence activated cell sorting (FACS, section 2.2.21) for fluorescence associated with uptake of the FITC-dextran. Cells were additionally labelled with 100 ng/ml propidium iodide to establish the percentage of cell death associated with each set of electroporation parameters. The parameters used for electroporation are summarised for each cell line in Table 2.3.

Cell line	No. cells	Volume	Buffer	Capacitance	Voltage
B16	$5x10^6$	500 µl	PBS	125 µF	350 V
NIH3T3	$5x10^6$	500 µl	PBS	125 µF	350 V
K1735	$2x10^7$	800 µl	Ficoll-Hepes	250 µF	400 V

Table 2.3. Summary of electroporation parameters used for each cell line.

2.2.18.2. Optimisation of electroporation parameters using a reporter gene.

Transfection of the plasmid pRSV*lacZ* (section 2.2.2) containing the reporter gene β-galactosidase in parallel to the FITC-dextran was performed. This allowed an estimation of the efficiency of gene transfer at each set of parameters. The cells were electroporated as detailed in section 2.2.17 with 20 µg of the plasmid pRSV*lacZ* and reseeded into tissue culture flasks before incubation at 37°C for 24-96 hours. Cells were washed with PBS, fixed with 1% glutaraldehyde and stained with the histochemical stain X-Gal (2.20.4) before visualisation using a Nikon Diaphot light microscope.

2.2.18.3. Production of stable transfectants.

Electroporation to produce stable transfection of K1735 melanoma cells involved a modified protocol using an adapted Hepes-buffered saline electroporation buffer containing Ficoll, supplied by Dr. M. Welham
, University of Bath (appendix A). Cells were removed from the tissue culture plates and washed twice with HBS, before resuspending at a concentration of $2x10^7$ in 0.8 ml

HBS. Cells were placed in the cuvette with 10 μg of the linearised plasmid pcDNA3mB7 (section 2.2.2) containing the selection marker geneticin (G418, Gibco). Another cuvette contained cells plus 10 μg each of the linearised plasmids pCEXV-3-A^k (α and β chains) plus 1 μg of linearised pPGKPuro containing the selection marker puromycin (Gibco). Cells were then electroporated at a capacitance of 250 μF and a voltage of 400 mV, producing time constants of 4.8 and 4.9 msecs respectively. The cells were left at room temperature for 20 minutes before reseeding into tissue culture flasks with complete culture medium. Culture medium was replaced after 48 hours with 1.5 mg/ml G418 and 1 μg/ml puromycin respectively. Selection medium was replaced every 48 hours, and colonies were plated out as a polyclonal population and grown in preparation for sorting by FACS.

2.2.19. Determination of cell number using the MTT assay.

The MTT assay as described by Mosmann (1983) was used in a modified form to establish cell number in survival and toxicity assays. Cells were plated into 96-well tissue culture plates over a range of densities. After treatment and sufficient incubation, the medium was removed by inversion and the cells washed twice with serum free DMEM. A 200 μl aliquot (1 mg/ml) of 1-[4,5-dimethylthiazol-2-yl]-3,5-diphenylformazan (MTT formazan, Sigma) was added to each well, and the plate incubated at 37°C for 3-5 hours. The MTT solution was carefully removed by gentle inversion of the plates, and the resultant crystals of formazan blue were solubilized with 200 μl DMSO and agitation on an orbital mixer for 10 minutes. Dead cells would have

detached from the plate, and been removed by the washing procedure. Cell number was established by reading the optical density of the wells (Titertek plate reader) at 540 nm, with a reference wavelength of 690 nm. The optical density in wells containing treated cells were compared with that of control wells containing untreated cells to allow the percentage viability to be established.

2.2.19.1. Optimisation of antibiotic selection of stable transfectants.

K1735 cells were seeded at a density of $3x10^3$ cells/well and allowed to adhere in complete medium for 4 hours before the addition of 0-2 mg/ml G418, or 0-40 μg/ml puromycin. Cells were then cultured for three days under standard conditions before assaying using the MTT assay as detailed in section 2.2.19 to establish the number of surviving cells. This number was calculated according to the calibration curve for cell number, displayed in appendix C.

2.2.20. Analysis of β-galactosidase expression.

The efficiency of gene transfer was determined *in vitro* using the plasmid pRSV*lacZ* (section 2.2.2). Reporter genes are routinely used to evaluate delivery efficiency, and the β-galactosidase gene is of particular use because of the diversity of assays available of varying sensitivity: histochemical, spectrophotometric, fluorimetric and FACS (MacGregor et al, 1991). The spectrophotometric assay allows the total enzyme activity in the cell extracts to be established, while the distribution of expression within the cell population can be determined by histochemical staining. Quantification

of gene expression was normalized by determining β-galactosidase activity of the samples per milligram of soluble protein.

2.2.20.1. Preparation of cell extracts.

The culture medium was removed from the cells, and the cells were washed three times with 5 ml of PBS. Each well was overlaid with 1.0 ml of PBS, and the cells removed by scraping with a cell scraper. The cell scraper was washed with 70% ethanol, rinsed with water and dried between samples. The resulting suspension was transferred to a 1.5 ml microcentrifuge tube and pelleted by centrifugation. Supernatant was aspirated and the pellet was resuspended in 250 µl of 0.1 M sodium phosphate buffer (pH 7.4). Cells were then freeze-thawed three times in a dry ice-ethanol bath, with thawing at 37°C, and centrifuged at 10,000 rpm for 2 minutes. Supernatant was then removed for immediate analysis.

2.2.20.2. Spectrophotometric assay for β-galactosidase in cell extract.

The galactoside derivative *o*-nitrophenol-β-D-galactoside (ONPG) formed the basis of the spectrophotometric assay to quantify transient β-galactosidase expression post-transfection. Cells were harvested 48-96 hours after transfection, washed, and cell extracts prepared by freeze-thawing three times in 250 µl 0.1M sodium phosphate buffer pH 7.2 (appendix A). Aliquots of the cell extract solutions were incubated at 37°C with 2X ONPG buffer (appendix A) for 30 min, and the reaction was stopped by the addition

of 1 M Sodium Carbonate. A blank reaction, containing no cell extract, was prepared in parallel. Absorbance was read at 420 nm in a Milton Roy 601 spectrophotometer.

A calibration curve was prepared for this assay using purified *E. coli* β-galactosidase (Promega), displayed in appendix C. Cell extracts were assayed for soluble protein to provide a measure of β-galactosidase expression relative to the protein content of the samples.

2.2.20.3. Quantification of soluble protein in cell extracts.

The soluble protein content of the cell extracts was quantified using the method established by Lowry *et al.* (1951). Soluble protein was assayed using a method adapted from that of Lowry *et al.* (1951). The sample was diluted to 500 µl with water and 500 µl 0.5M NaOH added. The sample was heated to 100°C for 10 minutes, then allowed to cool to room temperature. Lowry C reagent was freshly prepared by the addition of 2 ml Lowry B to 48 ml Lowry A (appendix a), and a 2.5 ml volume added to the sample, with shaking. After 10 minutes, 0.5 ml Folin and Ciocalteu's phenol Reagent (Sigma UK) was added and the solution vortexed. The sample was incubated at room temperature for 30 minutes, before determining the absorbance at 750 nm (Milton Roy Spectronic 601). A blank which contained no cell extract was also prepared in parallel. A standard curve for this assay was prepared using purified *E. coli* β-galactosidase (Promega) and is presented in appendix C.

2.2.20.4. Histochemical assay for β-galactosidase.

The efficiency of β-galactosidase expression was determined by *in situ* histochemical staining using 5-bromo-4-chloro-3-indolyl-β-D-galactosidase (X-Gal) obtained from Melford Laboratories Ltd, Ipswich, England. Cell monolayers were washed thoroughly with PBS and fixed with 1% glutaraldehyde solution (BDH Ltd, UK) at 4°C. The cells were washed again with PBS, overlaid with X-Gal solution (appendix A) and incubated at 37°C overnight. Cells expressing β-galactosidase hydrolyse the chromogenic dye to produce an insoluble indigo, which shows up as a blue colour against an unstained background. Photographs were taken using a Nikon F-301 camera attached to a Nikon Diaphot light microscope.

2.2.21. Fluorescence activated cell sorting (FACS) of cells.

2.2.21.1. *Antibodies*

R-Phycoerythrin (R-PE) conjugated hamster anti-mouse CD80 (B7-1) monoclonal antibody (IgG; 16-10A1) was obtained from Pharmingen (Sorrento Valley Road, San Diego, USA). Purified unconjugated mouse anti rat I-A antigen (IgG_1; MCA46G) was obtained from Serotec (Oxford, England). This antibody exhibits cross-reactivity with MHC class II haplotypes k and s (McMaster and Williams, 1979). Fluorescein isothiocyanate (FITC) conjugated anti-mouse polyvalent immunoglobulins (IgG, IgA, IgM; F-1010) was obtained from Sigma Immunochemicals, and used as the secondary reagent against the IgG_1 MCA46G antibody. Mouse IgG_1 isotype control was obtained from Dako (Glostrup, Denmark).

2.2.21.2. Cell labelling for FACS analysis.

Cells were removed from culture plates by trypsinisation and washed twice in ice-cold PBS. Cells were then counted and $5x10^5$ cells resuspended in 50 µl PBS with an optimal concentration of primary antibody. Generally, this involved a 1:100 dilution of the 1 mg/ml stock antibody. Samples were incubated at 4°C for 30 minutes, with periodic agitation, then washed once with PBS. Cells were then resuspended into 50 µl PBS with 0.1% BSA and incubated for 15 minutes at 4°C. One further wash with PBS was performed prior to resuspension into 50 µl PBS containing a sufficient excess of FITC-labelled secondary antibody (1 µl stock solution diluted to 50 µl). The sample was washed three times with 1 ml PBS to remove excess antibody, before analysis on a FACS Vantage analyzer (Becton Dickinson). Cell viability was estimated by the addition of propidium iodide (100 ng/ml), and samples were measured in the FL-1 emission spectrum (530 ± 15 nm) to detect fluoresceinated components, or in the FL-2 emission spectrum (575/26) for PE-derived samples.

For cell sorting, all samples were prepared and maintained in a sterile environment throughout the procedure. Generally, a population of $5x10^6$ cells were sorted into 6 ml sample tubes (Becton Dickinson) containing 500 µl DMEM. Cells were then seeded into 25 cm^2 culture flasks and maintained in G418 or puromycin-supplemented culture medium for two weeks, before subculture of the polyclonal population prior to further rounds of cell-sorting.

2.2.22. Preparation of spleen cells as positive control for MHC II genes.

Spleen cells from adult C3H-HEN (Harlan, Surrey, U.K.) mice were prepared as a positive control for the transfection of the I-A^k gene into the K1735 melanoma cells. The spleens of two mice were dissected out of freshly culled animals, and washed with 1x serum-free medium to remove the connective tissue. The spleens were emptied of the blood cells, and the cells were pelleted by centrifugation at 15000 *g* for 5 minutes. The supernatant was removed, and the pellet resuspended in 1x medium. The red blood cells were separated from the lymphocytes using pre-warmed Lymphoprep (Nycomed, Oslo, Norway), and centrifugation at 15000 *g* for 30 minutes. A lymphocyte band was carefully removed with a pipette, washed twice with 1x medium and counted, before labeling with antibody for FACS (section 2.21.1).

2.3. RESULTS

2.3.1. Transfection of B16 cells using calcium phosphate co-precipitation.

Transfection efficiency was shown to be dependent on the promoter driving gene expression (Fig. 2.3). The plasmid containing the viral promoter pRSV driving the expression of the reporter gene produced levels of activity of roughly 130 milliunits per mg of soluble protein. No detectable levels of β-galactosidase activity were observed in the cells transfected with the plasmid containing the tissue-specific promoter Trp-1. The negative control involved the treatment of cells with all of the transfection reagents except the DNA.

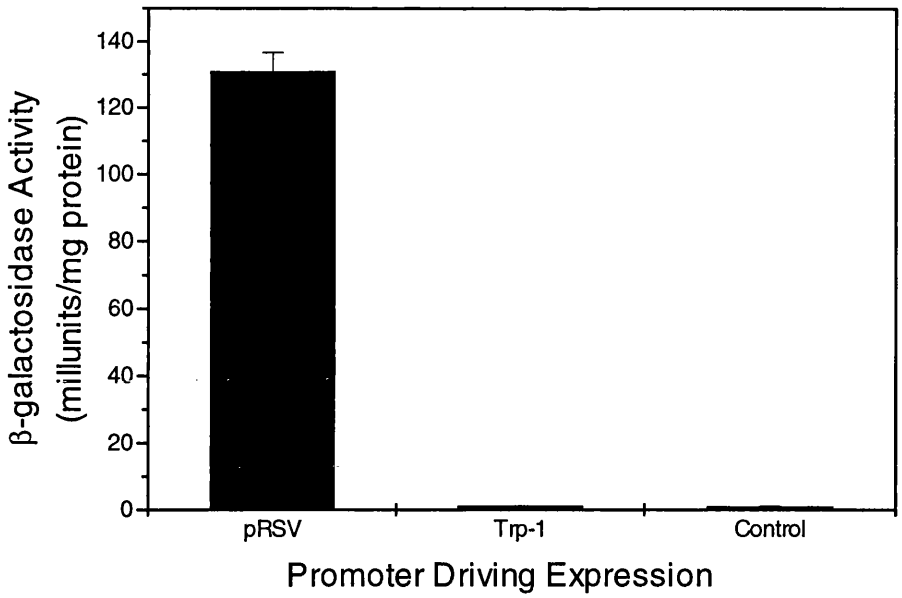

Figure 2.3. Expression of β-galactosidase activity in B16 melanoma cells, assayed 48 hours post-transfection by calcium phosphate co-precipitation. Cells were assayed using the spectrophotometric ONPG assay. Cells were transfected with 15μg pRSV*lacZ* in 0.124M $CaPO_4$ solution in HBS and chloroquine (100 μM). The control represents cells incubated with 15 μg *pRSVlacZ* without $CaPO_4$ and chloroquine. Cells were incubated with the precipitates for 24 hours, before replacement with complete culture medium, and incubation for a further 24 hours at 37°C. The data points represent the mean ± SEM (n=3).

It was decided to change the DNA delivery method to electroporation to allow optimisation of expression due to the flexibility of the parameter settings. Additionally, a larger population of cells could easily be subjected to the transfection procedure using electroporation than for co-precipitation. Prior to transfection with DNA, an optimisation procedure was performed to determine the parameter settings producing the best trade-off of cell permeability with viability. This was important to establish, as variability between cell lines can often occur.

2.3.2. Optimisation of electroporation of mammalian cells.

Establishment of the optimal conditions for electroporation required comparison of the uptake and cell viability profiles in parallel. This procedure was only carried out once, but the data (Fig. 2.4) suggested a correlation between voltage and cell death. The graphs displayed in Fig. 2.4 represent a measure of cell permeability (shown as fluorescence associated with dextran-FITC uptake) and the cell viability over a range of parameters. At the two resistance values studied, a voltage of 150 V produced relatively low levels of uptake as represented by lower cell fluorescence, but consequently higher levels of cell viability were observed. At higher voltages, for both of the resistance values, increased fluorescence levels were accompanied by large reductions in cell viability. At a capacitance of 125 μF, a linear decrease in viability (from 5%-100%) was observed above a voltage of 150 V , and this was accompanied by an increase in fluorescence to a maximum of 50%. For the voltages at a capacitance of 250 μF, the cell death reached a maximum of almost 100% at a voltage of 350 V, but this was accompanied by high levels of uptake. A representative two colour FACS analysis at the optmised parameters of 350 V and 125 μF is displayed in Figure 2.5.

The electroporation parameters 350 V and 125 μF were established as optimal from the viability and cell permeabilization experiments since these conditions provided high levels of fluorescence plus favourable levels of viability. These were used for all future transfections using B16 cells. Electroporation was carried out using pRSV*lacZ*, containing the β-galactosidase reporter gene, and the photographs in Figure 2.6 show the levels of reporter gene expression routinely obtained at these optimized electroporation conditions. Electroporation at the optimized parameters generally produced a time

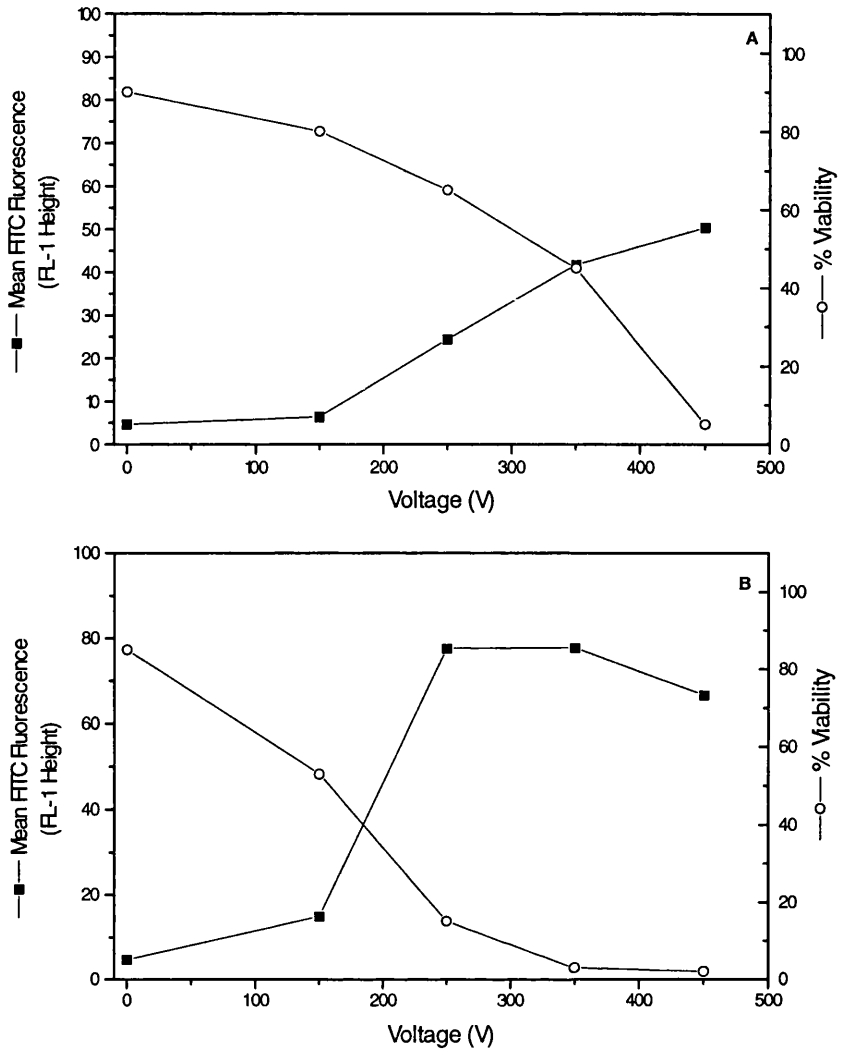

Figure 2.4. Optimisation of electroporation parameters for B16 melanoma cells. Dextran uptake was monitored in parallel to propidium iodide staining at the various combinations of voltage and capacitance. $1x10^6$ cells were electroporated with dextran-FITC (1 mg/ml) in PBS at a capacitance of 125μF (plate A) or 250μF (plate B) over a range of voltages. Propidium iodide (100 ng/ml) was added to the samples immediately prior to FACS analysis (FACS Vantage, Becton Dickinson) to establish cell viability.

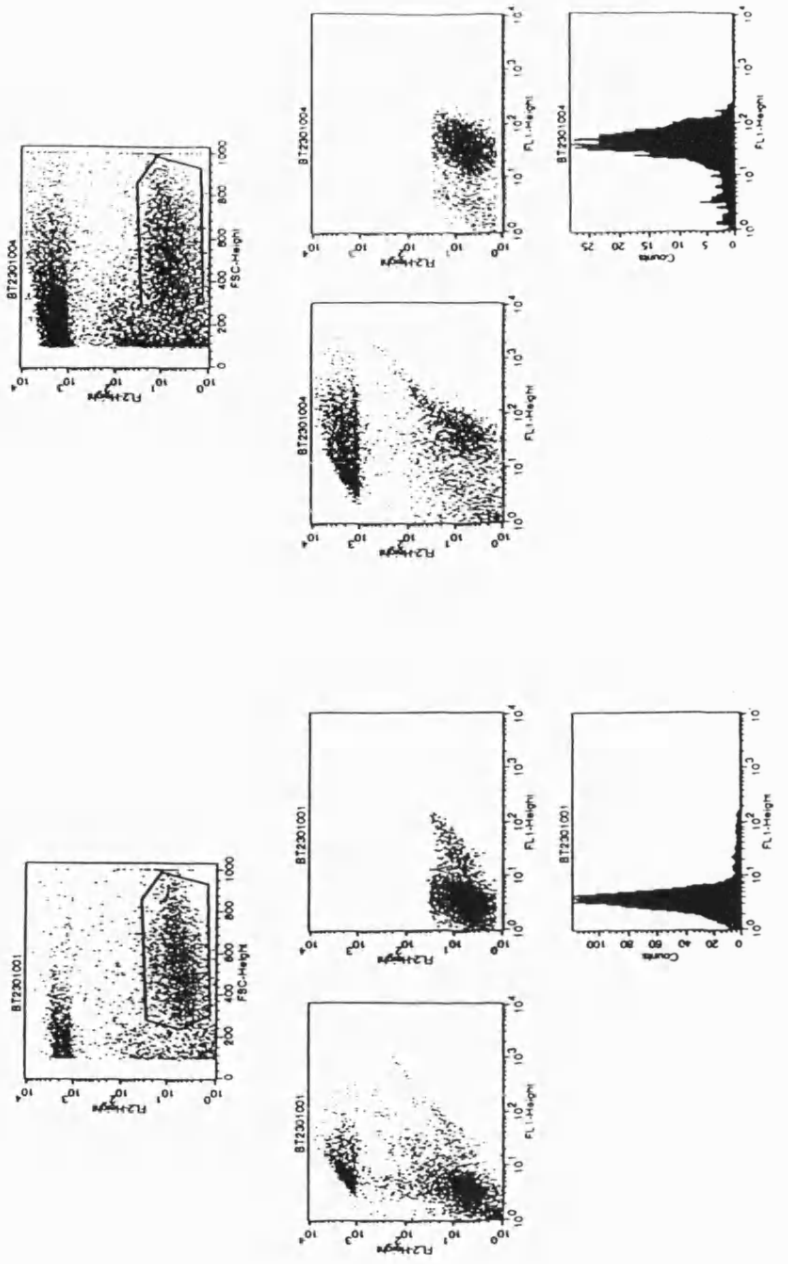

Figure 2.5. Representative two colour FACS analysis used to optimise electroporation parameters for B16 melanoma cells. Analysis was performed by monitoring dextran-FITC uptake in parallel with propidium iodide staining over a variety of voltage and capacitance settings. $1x10^6$ cells were electroporated with dextran-FITC (1 mg/ml) in PBS at over a range of voltage and capacitance. Propidium iodide (100 ng/ml) was added to the samples immediately prior to FACS analysis (FACS Vantage, Becton Dickinson) to establish cell viability. BT2301001 displays control cells exhibiting no dextran uptake; BT2301004 displays cells exhibiting dextran uptake. Live control cells were gated, and this gate was applied to the electroporated samples.

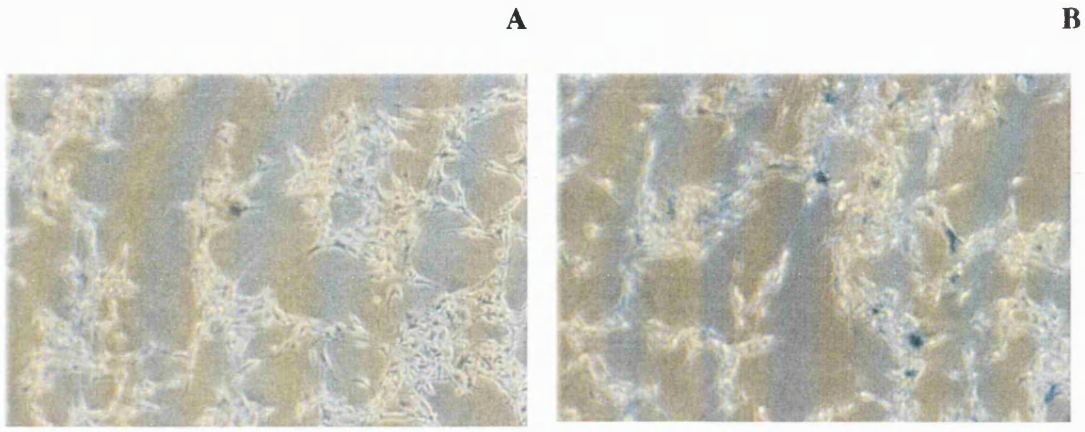

Figure 2.5. Photographs showing B16 cells fixed and treated with X-Gal solution overnight 48 hours after electroporation. Plate A shows the negative control of B16 cells electroporated in the absence of plasmid DNA, and plate B shows cells electroporated with 20 μg pRSV*lacZ*. Electroporation was performed at 350 V and 125 μF, in line with the optimized parameters for this cell line. Cells were photographed at magnification x300. Cells positive for β-galactosidase activity appear blue after X-Gal treatment.

constant of between 4-5 milliseconds, and values out of this range often gave lower levels of transfection and viability.

The optimisation procedure was repeated using the K1735 cell line over the same range of parameters as for B16 cells. A lack of ability to optimize the parameters was observed: at lower voltages, the cells showed no enhancement of fluorescence, while at the higher voltages cell viability was reduced to very low levels (data not shown). Discussion with Dr. M. Welham led to the use of a modified electroporation protocol, using a Hepes buffer containing Ficoll to reduce the osmotic shock to the cells during electroporation, and the parameters 250 μF and 400 V.

2.3.3. Control expression studies in mammalian cells post-electroporation.

The expression of β-galactosidase in mammalian cells post-electroporation was studied in two cell lines - the B16 melanoma cell line and the NIH3T3 fibroblast line. Comparative transfection efficiencies were established using the pRSV*lacZ* and the Trp-1 plasmids (section 2.2.2). The data displayed in Fig. 2.7. demonstrates that expression was observed with both the pRSV*lacZ* and the Trp-1 plasmids in the B16 melanoma cells to levels of activity of 1400 and 900 milliunits of enzyme activity per mg soluble protein respectively. The pRSV*lacZ* plasmid induced high levels of activity of about 1900 milliunits per mg soluble protein in the fibroblast cell line NIH3T3, but the Trp-1 plasmid was unable to stimulate gene expression above background levels. These levels and profiles of expression were highly unreproducible. Figure 2.6 depicts the data collected from two replicate experiments, but three further replicates demonstrated no

activity of the Trp-1 plasmid and only low levels (approximately 80 milliunits/mg protein) of the pRSV*lacZ* plasmid in the B16 melanoma cells. The negative control in this experiment involved the electroporation of cells in the absence of plasmid DNA.

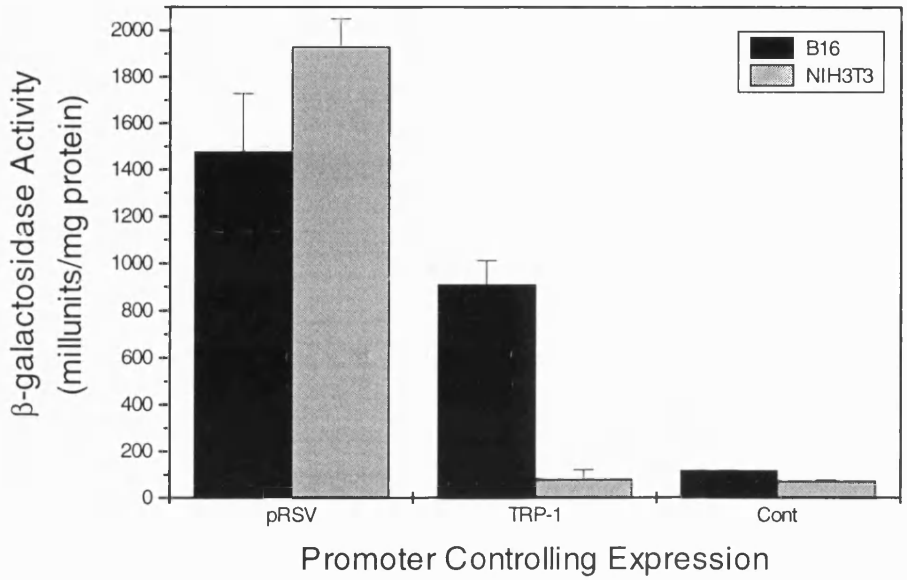

Figure 2.7. Expression of β-galactosidase in B16 melanoma cells and NIH3T3 fibroblast cells driven by the viral promoter RSV or the tissue -specific promoter Trp-1. Cells were transfected by electroporation with 20 μg plasmid DNA at 350 V, 125 μF in 500 μl PBS to produce time constants of 4-5 millisecs. Cells were assayed 48 hours post-transfection using the ONPG assay. The data points represent mean ± SD (n=2).

2.3.4. Engineering of Trp-1 promoter-B7 construct.

Initially, it was planned to engineer restriction sites into PCR primers, specific for the Trp-1 promoter, allowing ligation into the promoterless expression vector pNASSβ (section 2.2.2). A pair of PCR oligonucleotide primers were generated (section 2.2.13) using sequences generated by Jackson *et al.* (1991) and Lowings *et al.* (1992). The specific primers described below were used with a standard PCR protocol (section 2.2.14) and the Trp-1-β-Gal vector supplied by Dr. I. Hart (section 2.2.2).

Ts 5'-GGGCTCGAGATGCTGCTCTTTGCATGGAGA-3'

Ta 5'-CCCCTCGAGTTTCAGACCAGCAGACTACAA-3'

Primer Ts was designed to amplify the 1.4 Kb sequence at the 3' end of the Trp-1 promoter which has displayed tissue-selective activity (Vile and Hart, 1993a). Primer Ta was designed to incorporate the first Trp-1 intron (0.7 Kb) into the PCR fragment, as this region of the human Trp gene has previously been shown to enhance the transient expression of a reporter gene (Shibata *et al.*, 1992). Restriction sites were incorporated at the 5' ends of each oligonucleotide for the enzyme *Xho* I, which are highlighted in the sequences. This was to allow ligation into the promoterless mammalian expression vector pNASSβ. Subsequently, it was decided to change the vector to pcDNA3 to allow use of the neomycin resistance markers, allowing selection of stable transfectants in the presence of the antibiotic G418.

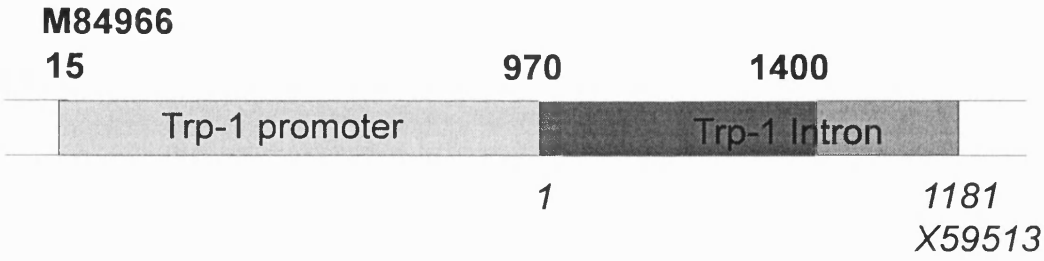

Figure 2.8. Diagrammatic representation of the overlapping sequences obtained from Genbank for the Trp-1 promoter and first intron of Trp-1 (accession numbers M84966 and X59513 respectively). PCR primers were designed specific for the region 15 bp of M84966 and 1181 bp of X59513. This allowed amplification of a 2.1 Kb fragment, incorporating 1.4 Kb of the 3' end of the Trp-1 promoter plus 0.7 Kb of the Trp-1 first intron.

This restriction of pcDNA3 with *Nru* I and *Hind* III is displayed in Figure 2.9. Lane 2 contains pcDNA3 restricted with both *Nru* I and *Hind* III. The two fragments of approximately 0.6 Kb and 4.8 Kb represent the CMV and pcDNA3 without the promoter respectively. Lane 3 represents uncut pcDNA3; lanes 4 and 5 represent pcDNA3 linearised with either *Nru* I or *Hind* III; lanes 1 and 6 contain the molecular weight marker λ *Hind* III/*EcoR* I. The fragment from lane 2 of approximately 4.8 Kb was excised from the gel and purified (section 2.2.11), the *Hind* III site blunted using Klenow and then dephosphorylated with alkaline phosphatase (section 2.2.12)

PCR using these primers with ~1 ng cDNA template and 2 mM magnesium chloride generated a single band approximately 2.1 Kb (Fig 2.10). Approximately 1 μg of the PCR fragment was removed from a 1% horizontal TBE gel using Geneclean (section 2.2.11), restricted with *Xho* I before blunting the ends using Klenow (section 2.2.12). Blunt end ligation of the PCR fragments into the phosphorylated vector was performed as detailed in section 2.2.12. The ligation was performed five times. Low levels of background were observed on the control plates, but any colonies picked from the experimental plates had no inserts. Figure 2.9 (lane 3) demonstrates that this plasmid preparation contained very little supercoiled plasmid DNA, and also contained impurities, possibly accounting for the inability to ligate the vector and insert.

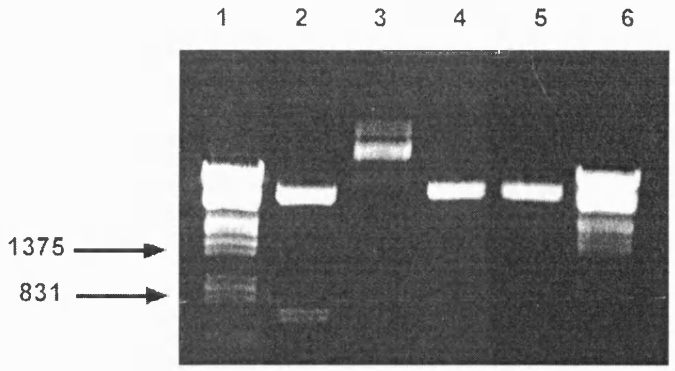

Figure 2.9. Restriction of pcDNA3 with the enzymes *Hind* III and *Nru* I to remove the CMV promoter. Lanes 1 and 6 contain the molecular weight marker λ *Hind* III/*EcoR* I; lane 2 contains pcDNA3 restricted with both *Hind* III and *Nru* I; lane 3 contains unrestricted pcDNA3; lanes 4 and 5 contain pcDNA3 restricted with *Hind* III or *Nru* I respectively. Electrophoresis was performed at 120 V for 30 minutes.

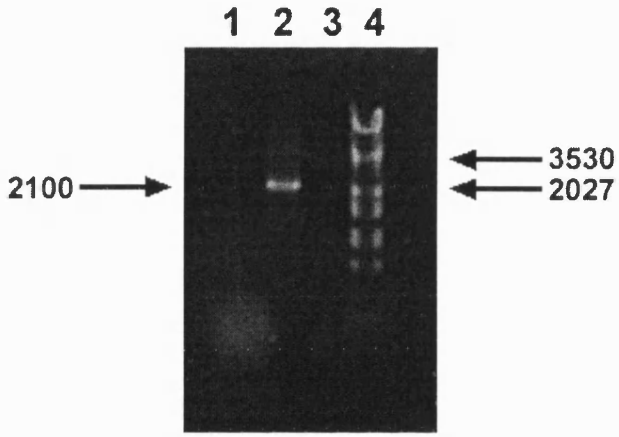

Figure 2.10. 1 % TBE agarose gel stained with 0.5 µg/ml ethidium bromide showing PCR product derived from Trp-1 promoter template and specific oligonucleotide primers (section 2.3.5). Lane 1: the control with no template; lanes 2 and 3: reactions containing 1:100 and 1:10 template dilutions respectively; lane 4: λ *Hind* III/*EcoR* I markers.

2.3.5. Analysis of the pcDNA3-B7 vector.

The murine B7 gene was removed from piLN-murN7 (section 2.2.2) by restriction with the enzymes *Hind* III and *Xba* I. The restricted sample was run on a 1%

agarose gel (as shown in Fig. 2.11), and the fragment of approximately 0.9 Kb was excised and purified (section 2.2.11). Lane 1 contains the molecular weight markers; lane 2 contains the plasmid restricted with *Hind* III and *Xba* I; lane 3 contains the uncut plasmid; lane 4 contains the plasmid linearised with *Hind* III. Lane 5 contains pcDNA3 restricted with *Hind* III and *Xba* I for ligation of the murB7 fragment.

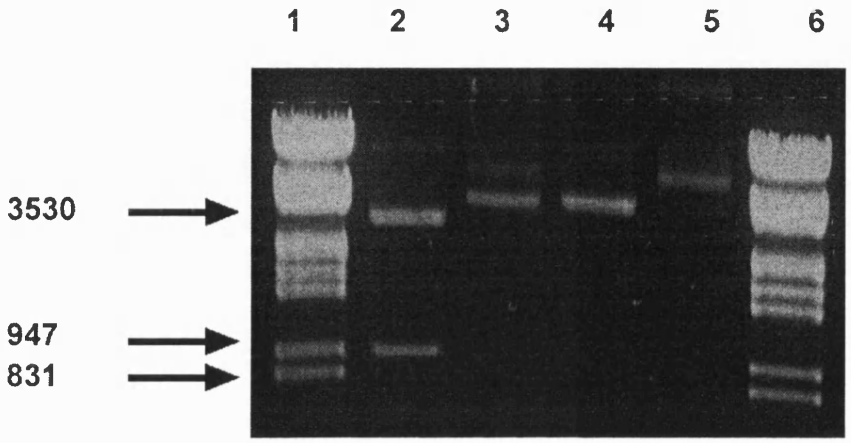

Figure 2.11. Restriction analysis of piLN-murB7 on 1% agarose gel. Lane 1 contains the molecular weight markers. Lane 2 contains the plasmid restricted with *Hind* III and *Xba* I, demonstrating two bands of approximately 0.9 Kb and 2.7 Kb. Lane 3 contains the uncut plasmid. Lane 4 contains the plasmid linearised with *Hind* III. Lane 5 contains pcDNA3 restricted with *Hind* III and *Xba* I for ligation of murB7 fragment. Electrophoresis was performed at 120 V for 30 minutes.

The vector pcDNA3 was restricted with the enzymes *Hind* III and *Xba* I, run on a 1% agarose gel, excised and purified (section 2.2.11). The two purified fragments of DNA were mixed at a ratio of 10:1 insert:vector, and ligated (section 2.2.12). An aliquot of the reaction mixture was transformed into *E. coli* TOP10F' (section 2.2.1) by electroporation, amplified and prepared by alkaline lysis (section 2.2.5). Samples were restricted with *Hind* III and *Xba* I , and run on a 1% horizontal agarose gel (Fig. 2.12). Ten colonies were picked, eight of which contained inserts of approximately 0.9 Kb. Samples of the plasmid DNA were restricted with the enzymes *Hind* III and *Xba* I

separately (lanes 3 and 4 respectively), and a double restriction was performed using both of these enzymes together (lane 5). An unrestricted sample of the plasmid DNA was run in Lane 2, and molecular weight markers were run in lanes 1 and 6.

The samples restricted with either the enzyme *Hind* III or *Xba* I have been linearised, while the sample that was restricted with both of these enzymes produced two fragments of approximately 0.9 Kb and 5 Kb.

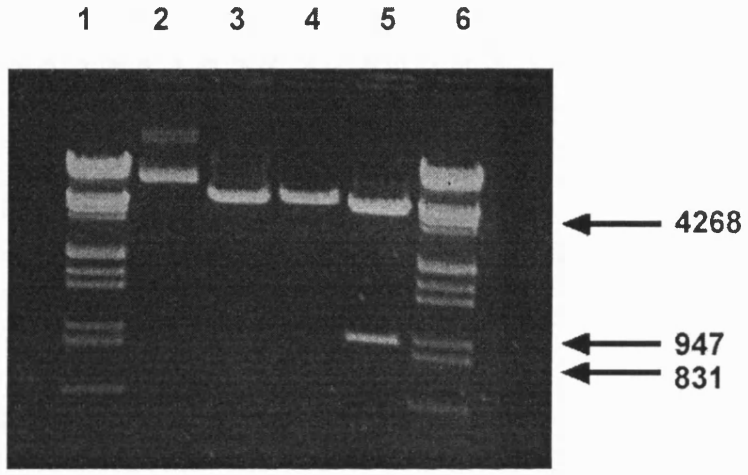

Figure 2.12. Restriction analysis of pcDNA3 on 1% agarose gel after insertion of the murine B7 gene at the Hind III and Xba I sites in the multiple cloning site. Lanes 1 and 6 contain λDNA with *Hind* III and *EcoR* I digests as the molecular weight marker. Lane 2 contains unrestricted pcDNA3. Lanes 3 and 4 contain pcDNA3-B7 singly restricted with the enzymes *Hind* III and *Xba* I respectively. Lane 5 contains the plasmid restricted with both of the enzymes *Hind* III and *Xba* I. Electrophoresis was performed at 120 V for 30 minutes.

2.3.6. Generation of control B7-expressing K1735 cells.

K1735 melanoma cells are a preferable cell line model for therapeutic applications than B16 cells because they exhibit a reduced metastatic profile. This is believed to provide a better model for comparison with the natural disease state. It was

decided to produce a line of control K1735 cells stably expressing the murine B7 gene under the control of the viral CMV promoter.

K1735 cells were electroporated, using the modified protocol (section 2.3.2), with pcDNA3-mB7. Subsequent treatment with G418 allowed selection of a resistant polyclonal population . The polyclonal population was sorted using FACS three weeks after electroporation, and the antibiotic pressure was maintained on the cells for this period.

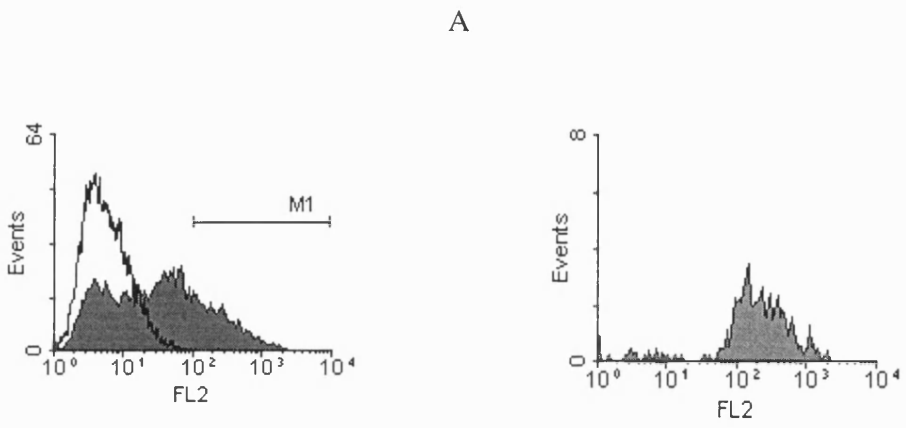

Figure 2.13. FACS data for K1735 melanoma cells transfected with pcDNA3-mB7. The transfected cells were grown in G418 for selection of stable transfectants for two weeks, then labelled with R-PE hamster anti-mouse CD80 antibody (Pharmingen, section 2.21.1) against murine B7-1. The unsorted population is displayed as shaded (A) with transfected cells labelled with a mouse IgG_1 isotype control (Dako, section 2.21.1). B shows the positive population after sorting from the gated region marked M1 in A.

Standard FACS labelling assays were used with the monoclonal antibodies described in section 2.2.21.1. The antibody was used at a concentration of 1:100 (10 µg/ml) for sorting the B7-expressing cells (shaded region, Fig. 2.13). The unshaded region represents transfected cells labelled with the mouse IgG_1 isotype control (section 2.2.21.1). Figure 2.13A represents the polyclonal population (shaded area) and the

negative control (unshaded area). The sorting parameters were gated to select the cells with the largest increase in fluorescence (about 40% population). Figure 2.13B represents the fluorescence profile associated with the sorted population, providing an indication of the efficiency of the sorting procedure.

2.3.7. Expression of MHC class II genes by K1735 melanoma cells.

Initially, the K1735 cells were transfected with the two pCEXV-3-A^k plasmids, each containing the gene for either the α or β chain of the MHC II molecule. The cells were labelled with the antibody MCA46G 48 hours post-electroporation, to test for transient expression using FACS analysis. This process was repeated three times. No expression was observed during any of these investigations.

It was decided to electroporate the K1735 cells with the same two plasmids plus pPGKpuro (all linearised) to attempt to select a polyclonal cell line with stable expression of the MHC II genes. Subsequent treatment with puromycin (1 μg/ml) produced an antibiotic-resistant population of cells, which was subcultured after two weeks, and then prepared for sorting. The cells were labelled with MCA46G followed by F-1010 (section 2.2.21.1) at 1:100 dilutions for FACS analysis. A positive control population of cells expressing MHC class II I-A^k was prepared from spleen cells of C3H HEN mice and labelled as described above. The control produced significant fluorescence in the FL1 region, represented by the shaded area (Fig. 2.14A). The unshaded area in A represents the isotype control, which is also superimposed on the population of puromycin-resistant cells shown in B. There was no significant difference

observed between the antibiotic-selected population and the isotype control, indicating that the population was not expressing the MHC II genes.

A B

Figure 2.14. FACS data for K1735 after stable selection in puromycin (1 μg/ml). Figure A shows spleen cells of C3H HEN mice (shaded area) labelled with MCA46G (IgG1; Serotec), and the FITC conjugated antibody F1010 (Sigma) as the secondary label. The unshaded region represents cells stained with the isotype control. Figure B represents the K1735 cells grown in the puromycin selection medium after transfection (shaded) and the isotype control, labelled as for the spleen cells.

2.4. DISCUSSION

2.4.1. Comparative transfection studies.

The initial priority was to determine the relative strengths and specificities exhibited by the viral promoter (RSV) and the tissue specific promoter (Trp-1). The melanoma cell line B16 formed the basis of the preliminary expression studies, with the plan to use the less invasive melanoma cell line K1735 for future stable gene expression studies. This cell line was chosen due to its less invasive nature, which is believed to provide a better model for comparison with the natural disease state.

2.4.1.1. Co-precipitation using calcium phosphate.

Transient expression studies were performed in B16 cells, using calcium phosphate co-precipitation as the method of transfection. The RSV promoter routinely produced detectable levels of β-galactosidase activity. The Trp-1 promoter however produced no detectable levels of activity, comparable with the negative control. This problem could have been due to inefficient delivery or inefficient translation. An alternative method of transfection was performed to establish whether the problem was one of delivery or not.

2.4.1.2. Transfection of mammalian cells using electroporation.

The process of electroporation was optimized for B16 cells in the studies using dextran-FITC uptake compared with cell viability over a variety of parameters. Additionally, transfections over the range of parameters were performed using the plasmid pRSV*lacZ*, and stained with the histochemical stain X-Gal (section 2.2.20.4) to determine the relative percentages of cells expressing the reporter gene under the different conditions.

The parameters established as those optimum for the melanoma B16 cells were 125 μF and 350 V. Although the level of viability was reduced to 40% under these conditions, and dextran uptake produced relative fluorescence levels of roughly 50% of the maximum under any conditions. The uptake of the FITC-dextran was closely mirrored by an increase in cell death, and these parameters were seen to create the best compromise between permeabilization and cell death. These conditions produced 30% cells expressing the reporter gene, which was seen to be the optimum from the

histochemical staining (Fig. 2.6). Viability was observed over a longer period of time during the X-Gal experiments. Recovery from the electroporation procedure was shown to be reduced with increasing voltage, in line with the short-term viability results. The results confirmed the parameters of 125 μF and 350 V as optimum for this process for longer term studies.

The permeabilization of the cells, demonstrated by the dextran uptake studies could only be used as an indication of the quantity of material taken up by the cells. It is postulated that the degree of DNA uptake under these conditions would be of similar levels to that observed with the dextran, as this is a non-selective process. The percentage of cells expressing the reporter gene were lower than the percentage of cells exhibiting fluorescence at identical parameter settings. This may have been a result of cell division without plasmid replication, causing a diluting effect of the reporter gene within the population. Alternatively, the DNA would be susceptible to enzymatic degradation and methylation in the cytoplasm of the cell. Both of these mechanisms would serve to reduce DNA delivery to the nucleus for subsequent translation.

An identical optimisation process was performed using the melanoma cell line K1735. The conditions tested proved unsuitable for transfection of this cell line, as the cells either withstood uptake of the dextran, or were fragmented completely beyond repair, by the passage of electrical current through the cell suspension. The preliminary expression studies therefore concentrated completely on the B16 cell line. The modified protocol suggested by Dr. M. Welham (Bath University) involved the use of a Hepes buffer containing Ficoll, to reduce the osmotic shock to the cells. These conditions were

not optimized due to shortness of time, but were used to electroporate the K1735 cells for selection of stable transformants.

The development of melanoma-specific promoters is necessary for the high levels of selectivity required for gene expression at target sites *in vivo*. The cell lines chosen for the tissue-selective expression studies reflected the target cell-type (melanoma cells) plus non-target cells that were likely to grow in close proximity to the melanoma cells *in vivo*. It is postulated that the initial transfection studies using the Trp-1 promoter in B16 cells may not have been carried out over a long enough time course. Several cell-type specific promoters have been shown to bind factors specific to that cell type, such as the endometrial-specific factor which binds the uteroglobin promoter (Misseyanni *et al.*, 1991). Lowings *et al.* (1992) have postulated that the Trp-1 promoter is controlled by the combination of non cell-type specific upstream factors plus cell-type specific TATA-binding protein-associated factors. These factors are likely to be present at differing levels throughout the cell cycle.

It has been suggested that the lack of reproducibility demonstrated during the comparative expression experiments in B16 and NIH3T3 cells could be due to a cell-cycle effect. The cells were always harvested prior to confluence, but it was not possible to determine the percentage of cells that had already reached stationary phase. Cells that were still rapidly dividing would be expected to recover from electroporation and resume rapid growth faster than stationary cells. Cells in log phase produce more protein than those in stationary phase. This may affect the rate of melanogenesis, and hence the production of initiation and binding factors for the Trp-1 promoter. This may explain why Vile and Hart (1993a) monitored activity 72-96 hours after transfection

when studying expression of the reporter gene β-galactosidase driven by the tyrosinase promoter in B16.F1 melanoma cells. This modification was adopted for any further expression experiments using the Trp-1 promoter.

As detailed in section (2.3.4), the initial strategy involved ligating a 2.1 Kb PCR product of the 3' end of the Trp-1 promoter plus the first intron (section 2.2.27) into the promotorless mammalian expression vector pNASSβ. Due to the requirement for selection of stable transfected cell lines, it was decided to use the vector pcDNA3 (section 2.2.2). Transfection of this vector into cells confers geneticin (G418) resistance to the cells.

It was decided to replace the viral CMV promoter inherent to pcDNA3 with the Trp-1 promoter sequence produced using PCR. This would allow assessment of the promoter activity using the reporter gene β-galactosidase. Subsequent to this, it was planned to additionally incorporate the murine B7 gene into the modified vector containing the Trp-1 promoter. The advantage of using a melanoma-specific promoter such as Trp-1 is that for gene therapy applications, it is advisable to restrict gene expression to the target cell population. This may be achieved either via selective delivery or selective expression.

Problems were encountered with the ligation of the PCR product of the Trp-1 promoter into pcDNA3. If there had been more time, it would have been sensible to redesign the PCR primers, to create restriction sites specific for those used to remove the CMV promoter. With sufficient time, expression studies would have been performed to compare the activity using the original pcDNA3 containing the CMV promoter and the modified vector with the Trp-1 promoter. These studies would have

been performed in the B16 and K1735 cell lines in parallel, to ensure that low levels of expression were not simply a cell-line specific effect. Although initial studies by Vile and Hart (1993a) involved the use of both the Trp-1 and the Tyr promoters, further work concentrated on the Tyr promoter (Vile and Hart, 1995; Chong *et al.*, 1996). Personal communication with Dr. R. Vile indicated that the Trp-1 promoter had exhibited a lack of reproducibility, leading to preferential use of the Tyr promoter for all further work.

2.4.2. Expression of genes for immunostimulation in control K1735 cells.

Problems were encountered using electroporation to transfect K1735 cells (section 2.3.2). The use of a modified buffer for electroporation containing Hepes to reduce the osmotic shock to the cells enhanced cell survival compared with the use of PBS. The initial transient transfection studies using PBS demonstrated no expression of either the B7 gene or the MHC II genes. It was decided to attempt the stable transfection of these genes separately in K1735 cells, using antibiotic selection. K1735 cells were successfully transfected with pcDNA3 containing the murine B7 gene (Fig. 2.13), a stable expressing cell line was established and frozen stocks were produced.

A population of K1735 cells were selected in antibiotic medium after transfection with the two MHC class II genes plus a puromycin selection vector. These cells did not express the class II genes, in spite of acquiring antibiotic resistance from the puromycin vector, which was transfected at a tenth of the concentration of the class II plasmids. The control spleen cells demonstrated that the antibody was active. The lack of expression could have been due to inefficient transcription or translation of the class II genes in the K1735 cells, or that the proteins were not being expressed correctly

at the cell surface. Since there was a requirement for two genes to be incorporated into the genome, it would probably have been necessary to screen many more colonies to discover a stable transformant. It would have been interesting to perform SDS-PAGE to discover whether any MHC class II proteins were present intracellularly. Unfortunately, there were no cell samples remaining to do this.

The MHC class II genes have successfully been expressed from the same vectors in the melanoma cell line K1735 by Chen *et al.* (1994) after transfection via calcium phosphate co-precipitation. It therefore seems most likely that the problem is one of delivery. Although electroporation is generally deemed a more efficient transfection method than co-precipitation, it seems that we either needed to test more clones, or maximise the efficiency of the vector and transfection method.

Widespread use of viral vectors has allowed increased efficiency of delivery to several cell lines, as reviewed by Miller and Vile (1995). Developments within the viral vector field have led to the production of retroviral vectors capable of efficiently co-expressing two genes simultaneously from the same vector, known as internal ribosome entry site (IRES) vectors (Ghattas *et al.*, 1991). This approach attempts to overcome the problems associated with multiple gene expression. These include regulated splicing of a single primary transcript to produce separate mRNAs, where one gene often produced expression at the expense of the other. Also, systems where the upstream gene was expressed from the viral promoter in the LTR while the downstream gene was expressed from an internal promoter often produced competitive interference between the promoters. The IRES vectors use the viral LTR to express a single polycistrionic transcript, from which several gene products can be translated. This avoids differential

expression of the separate genes. This technology would provide an alternative vector system for the transfection of the K1735 cells with the MHC class II genes.

2.5. SUMMARY

The lack of reproducibility of reporter gene expression driven by the tissue-specific promoter Trp-1 in B16 melanoma cells was not encouraging for its further use for restricting the expression of the costimulatory molecule B7 in melanoma cells. Efforts concentrated on establishing cell lines capable of stable expression of both the MHC class II genes and the costimulatory molecule B7. The melanoma cell line K1735 was used to produce a line exhibiting stable expression of B7, but no expression of the MHC class II genes was determined throughout the study. This meant that no immunostimulatory analysis was performed to substantiate the theory underlying the project.

CHAPTER 3. Evaluation of the transfection efficiency of poly(amino acid)-DNA complexes.

3.1. INTRODUCTION

The ability of polycationic polymers to deliver DNA to eukaryotic cells was studied by Farber *et al.* (1975) and shown to be dependent on the ratio of polycation to DNA. It is now widely accepted that cationic polypeptides form particulate systems with DNA, and early work by Olins *et al.* (1967) established that several basic polypeptides were able to stabilise DNA against thermal denaturation. More recently, Zenke *et al.* (1990) showed that chloroquine was able to elevate the gene transfer efficiency of polycation-DNA complexes *in vitro* by several orders of magnitude, and this technique has been widely used to promote transfection of cultured cells. The work presented here attempts to correlate the formation of complexes between cationic polymers and DNA with *in vitro* transfection efficiency in eukaryotic cells.

3.2. MATERIALS AND METHODS

3.2.1. Deoxyribonucleic Acid (DNA).

Plasmid pRSV*lacZ* (section 2.2.2) was used for all polycationic-DNA complexation and transfection studies. This construct contains the *Eschericia coli* β-galactosidase reporter gene under the control of the Rous sarcoma virus long terminal promoter/enhancer sequence, which allowed determination of gene transfer efficiency to eukaryotic cells. The plasmid was routinely amplified in the host strain *E. coli* XL1-Blue (Stratagene).

3.2.2. Cationic polypeptides.

All cationic polypeptides were obtained from Sigma, and their individual characteristics are described below. The cationic polypeptide solutions were prepared under clean laboratory conditions, using sterile Hepes buffered saline (HBS; appendix A). The lysine-alanine co-polymers used in this study contained different molar ratios of lysine:alanine, reflected in the abbreviations used.

Polymer	DPn	Mol. Wt. (salt)	Mol. Wt. per Unit Charge	Mw/Mn
Poly-L-lysine•HBr	219	45700	208.9	1.1
Poly-D-lysine•HBr	240	50200	208.9	1.28
Poly-L-ornithine•HBr	260	50700	194.9	1.1
Poly-L-arginine•HCl	217	41800	192.5	1.2
Poly (Lys•HBr, Ala) 1:1	355	50000	280.1	N/A
Poly (Lys•HBr, Ala) 2:1	323	52700	259.3	N/A
Poly (Lys•HBr, Ala) 3:1	178	31000	238.8	N/A

(DPn - degree of polymerisation; N/A - not available)

Table 3.1. Physical characteristics of cationic polymers. Data were supplied by the manufacturer.

poly-lysine

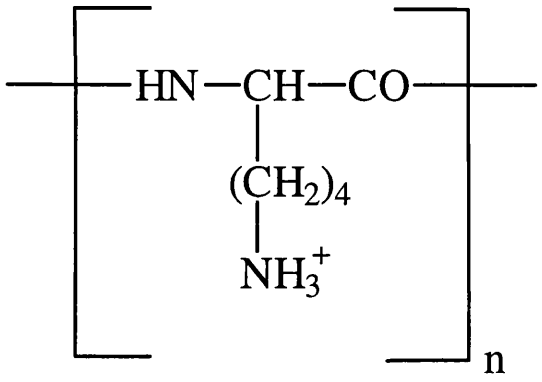

poly-ornithine

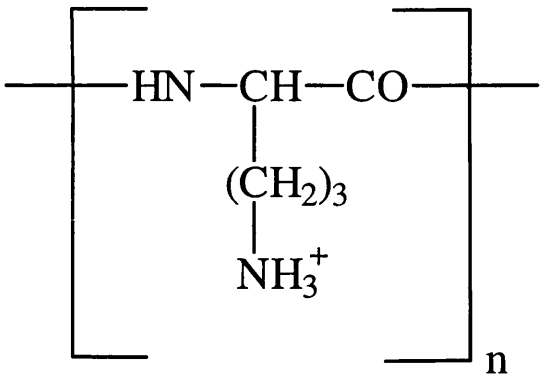

poly-arginine

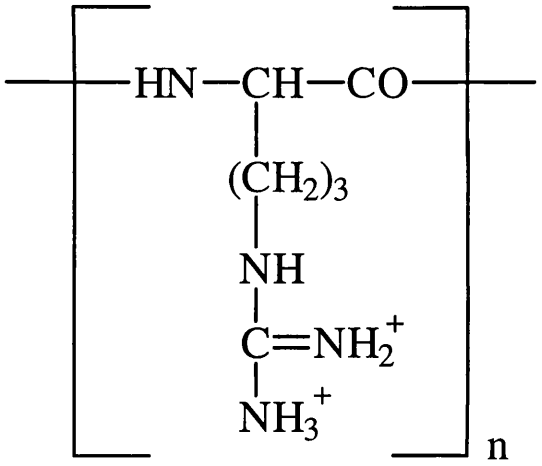

poly-(Lys), (Ala) co-polymers

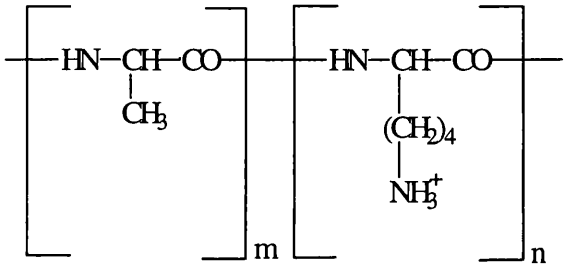

Figure 3.1. Chemical structures of the homopolymers and random co-polymers. All polymers were prepared from the corresponding N^{α}-carboxy anhydrides, providing a straight polypeptide backbone. The positive charge of polymers was the result of protonation of the amino group on the side chains at the experimental pH conditions.

3.2.3. Calculation of Polymer to DNA charge ratio.

Complexation of the plasmid pRSV*lacZ* with cationic polymers was determined as a function of both the mass of constituents and the molar charge ratio ($^{+}$/-).

$$\text{Charge Ratio } (^{+}/-) = \frac{\text{Total number of Positive charges (mols)}}{\text{Total number of Negative charges (mols)}}$$

3.2.3.1. DNA.

The calculation of negative charge provided by the DNA was determined on the basis that each nucleotide in the DNA sequence is associated with a single negative charge. A mean value of 330 was used as the molecular weight of a monophosphorylated nucleotide, as established from data given by Sambrook *et al.* (1989) for dAMP, dCMP, dGMP and dTMP.

3.2.3.2. Cationic homopolymers.

The effective molecular weight with which one positive charge is associated was calculated. Compensation was made for those polymers supplied in salt form.

3.2.3.3. Cationic co-polymers.

The molar ratio of charged to neutral polymer had to be taken into account with the co-polymers. The molecular weight associated with one charge was calculated (Table 3.1), compensating for salts or assuming complete ionisation of the side-chain amino terminal groups in those polymers not supplied as salts. Dissociation of the salts under appropriate conditions produced a protonated amino group (NH_3^+) and an anion (Br^- or Cl^-).

3.2.4. Complexation of DNA with cationic polymers.

The DNA solution comprised 6 μg of DNA in 250 μl HBS, while the polymer was prepared at the concentration of interest also in 250 μl HBS. The separate solutions were allowed to equilibrate at room temperature before adding the polymer solution to

the DNA solution. The mixture was gently mixed by inversion three times and the complexes were incubated at room temperature for 20 minutes before use.

3.2.5. Ethidium bromide as a fluorescent probe.

The intercalation of ethidium bromide (Fig. 3.2) between DNA base pairs and the resulting fluorescence of the complex has allowed it to be used as a probe for nucleic acids both in agarose gels and for quantification by spectrofluorimetry (Sharp *et al.*, 1973). Ultraviolet radiation is absorbed by the DNA and the bound dye, and the energy is re-emitted in the red-orange region of the visible spectrum (Sambrook *et al.*, 1989).

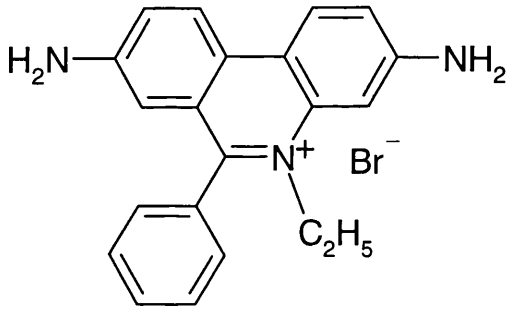

Figure 3.2. Structure of ethidium bromide : 2:7 diamino-9-phenyl-10-ethyl phenanthridinium bromide.

3.2.5.1. Fluorescence studies of polymer-DNA complexes.

The polymer-DNA complexes were prepared as described in section 3.2.4. and complexation was analysed using a method adapted from that of Gershon *et al.* (1993). The 500 µl of complex suspension was diluted to 3.0 ml with HBS and immediately prior to analysis, 3 µl of ethidium bromide was added (0.5 µg/ml). The molar ratio of ethidium to nucleotide under these conditions was 0.42. All samples were vortexed and

the fluorescence measured using a Shimadzu RF-450 spectrofluorophotometer (λ_{ex} 260 nm; λ_{em} 600 nm). A 1-cm light path cell with excitation and emission slits of 5 nm was used. The degree of complexation was measured as the percentage of the fluorescence of a control sample containing 6 μg of uncomplexed plasmid DNA. The fluorescence of the control sample was normalised to 100%. A reduction of fluorescence was seen relative to the control as the intercalation of ethidium bromide between the DNA base pairs was prevented by complexation with the cationic polymers.

3.2.6. Transfection of eukaryotic cells with polymer-DNA complexes.

Cells were seeded in 6-well plates at a density of $1x10^5$ cells per well 16-20 hours before transfection. One hour before transfection, the medium was removed and replaced with 1.5 ml complete, pre-warmed medium or the reduced-serum transfection medium opti-MEM (Gibco). The complexes were prepared as detailed in section 3.2.4, then added dropwise around the wells immediately after the addition of chloroquine at a concentration of 100 μM. The cells were incubated with the complexes at 37°C and 5% CO_2 for four hours. The transfection medium was then removed and the cells were washed twice in ice-cold complete medium, before replenishing each well with 2 ml of complete medium. The cells were then incubated for a further 44 hours at 37°C before assaying for β-galactosidase expression using the spectrophotometric ONPG assay (section 2.2.20.2).

3.3. RESULTS

3.3.1. Complexation of pRSV*lacZ* with cationic polypeptides.

The capacity for polycations to complex the DNA was initially determined using the ethidium bromide exclusion assay. The complexes were prepared over a range of charge ratios (polymer : DNA) from 0 - 3.0, which was equivalent to mass ratios between 0-1.0, and the quenching effect monitored accordingly. This assay allows determination of the ratio of polymer / DNA which is required for complexation conditions, but it does not provide an indication of the strength of interaction between the different polymers and the plasmid DNA. Additionally, conformational differences between complexes formed using the various polycations and DNA cannot be inferred from variations in the fluorescence quenching profiles of the different polymers, and exclusion of ethidium is not necessarily an indication of condensation. Thus, this assay is only of value in establishing the ratios of constituents required for complexation, but little other information can be deduced or extrapolated from the results.

3.3.1.1. Homopoly(amino acid)-DNA complexation.

Complexation exhibited by mixtures of homopoly(amino acid)s with pRSV*lacZ* were examined by ethidium bromide exclusion. Fluorescence was quenched when the DNA was complexed with polycations in agreement with Felgner *et al.* (1987).

The fluorescence intensity exhibited a linear decrease from a charge ratio of 0 - 1.0, as complex formulations with higher ratios of polymer / DNA were produced. At charge ratios greater than 1.0, a constant minimum background level was reached (Fig.

3.3a). When the complex formulations were expressed as mass ratios (Fig. 3.3b) similar profiles were observed for the fluorescence quenching since the molecular mass per unit charge was similar for these homopolymers. The decrease in fluorescence occurred between mass ratios of 0 - 0.4, above which the constant minimum background fluorescence was maintained. Poly-L-arginine appeared to deviate slightly from the profile displayed by the other homopolymers, with a slightly shallower gradient during the linear decrease, reaching the minimum at a mass ratio of 0.6. This difference was not so noticeable in the charge ratio curve.

3.3.1.2. Co-poly(amino acid)-DNA complexation.

The lysine, alanine co-polymers showed similar complexation patterns to the homopolymers with respect to the charge ratio required to provide fluorescence quenching (Fig 3.4.a). The profile exhibited was essentially the same as for the homopolymers, with a curve split into two clear regions: the initial linear decrease in fluorescence reaching a minimum at a charge ratio of 1-1.5, above which, a fairly constant minimum was maintained. The plots of fluorescence quenching versus mass ratios of the co-polymers (Fig 3.4.b) showed a shift to the right, compared with those of the homopolymers. The increased mass ratio (polymer / DNA) required to produce a similar level of fluorescence exclusion reflected the neutral component (alanine) contained within each co-polymer. An increase in the ratio of cationic lysine : neutral alanine produced a resultant decrease in the mass of co-polymer associated with each

positive charge. Consequently, a mass ratio of 1:1 for poly-lysine / DNA was equivalent to mass ratios of 1.34:1, 1.24:1 and 1.14:1 for the co-polymers lysine-alanine 1:1, 2:1 and 3:1 respectively.

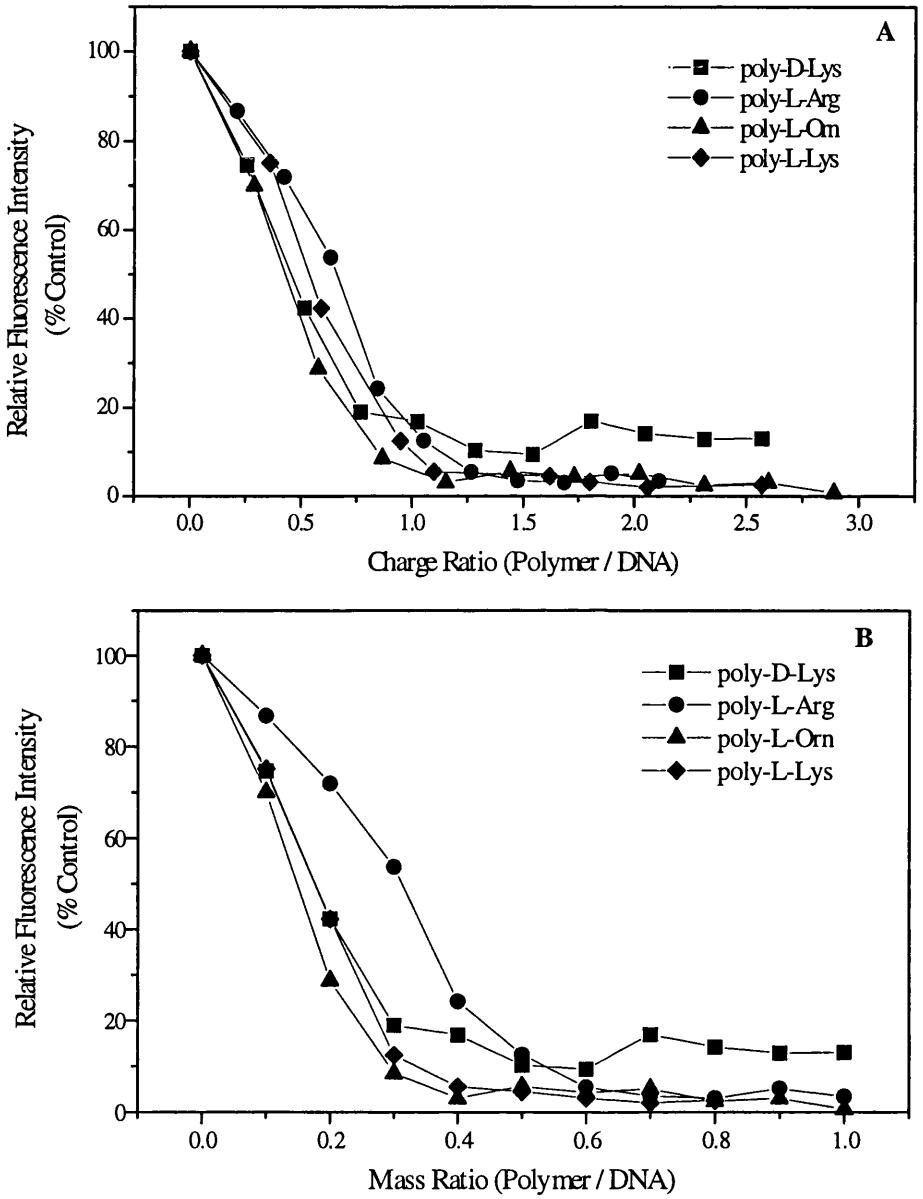

Figure 3.3. Complexation of plasmid DNA using increasing quantities of cationic homopolymers and 6 μg pRSVlacZ plasmid. After mixing, the complexes were incubated for 20 minutes at room temperature, and ethidium bromide was added (0.5 μg/ml) immediately prior to the fluorescence reading. The data is expressed in terms of the polymer:DNA charge ratio (A) and the mass ratio (B). The data points represent the mean of three replicate evaluations.

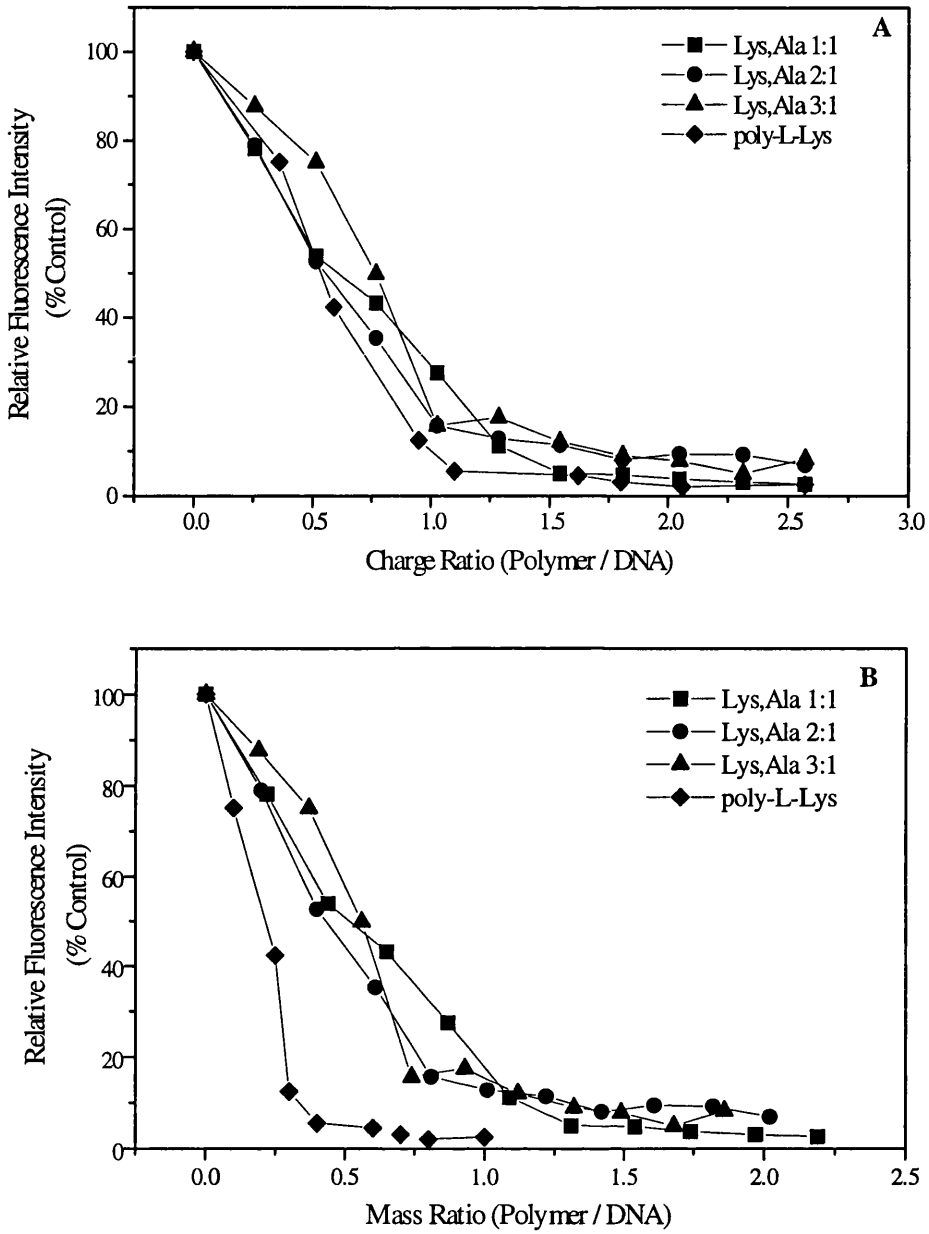

Figure 3.4. Complexation of plasmid DNA using increasing quantities of lysine-alanine co-polymers and 6 μg pRSVlacZ plasmid. Ethidium bromide (0.5 μg/ml) was added after 20 minutes incubation at room temperature, and the fluorescence measured immediately The complexation data for poly-L-lysine is also included. The data are expressed in terms of the polymer:DNA charge ratio (A) and the mass ratio (B). The data points represent the mean of three replicate evaluations.

3.3.2. Transfection of B16 murine melanoma cells.

3.3.2.1. Standardisation of transfection of B16 melanoma cells.

The activity of β-galactosidase in cell extracts assayed 48 hours post-transfection with different polymer-DNA complexes was shown to vary considerably between experiments (Fig 3.5). This problem was overcome by the introduction of a standard complex as a positive control in each experiment. The majority of transfection studies in the literature have used polylysine for complexation of DNA (Zatloukal *et al.*, 1992). The profile for transfection of B16 cells using polylysine-DNA complexes of varying charge ratios ($^{+}$/-) in the presence of 100 μM chloroquine is shown in figure 3.6. The optimum charge ratio ($^{+}$/-) for transfection was shown to be 1.5. All further transfection experiments included polylysine-DNA complexes at a charge ratio of 1.5 with chloroquine as a positive control.

3.3.2.2. Influence of polypeptide-DNA complex composition on transfection efficiency.

Initial transfection efficiency studies involved determination of the optimum polymer : DNA ratio required for the transfection of each different polymer. Complexes were prepared at increasing polymer/DNA ($^{+}$/-) ratios, and concurrent transfection with poly-L-lysine at a charge ratio of 1.5 was used as the positive control for each transfection experiment. All transfections were performed in the presence of 100 μM chloroquine.

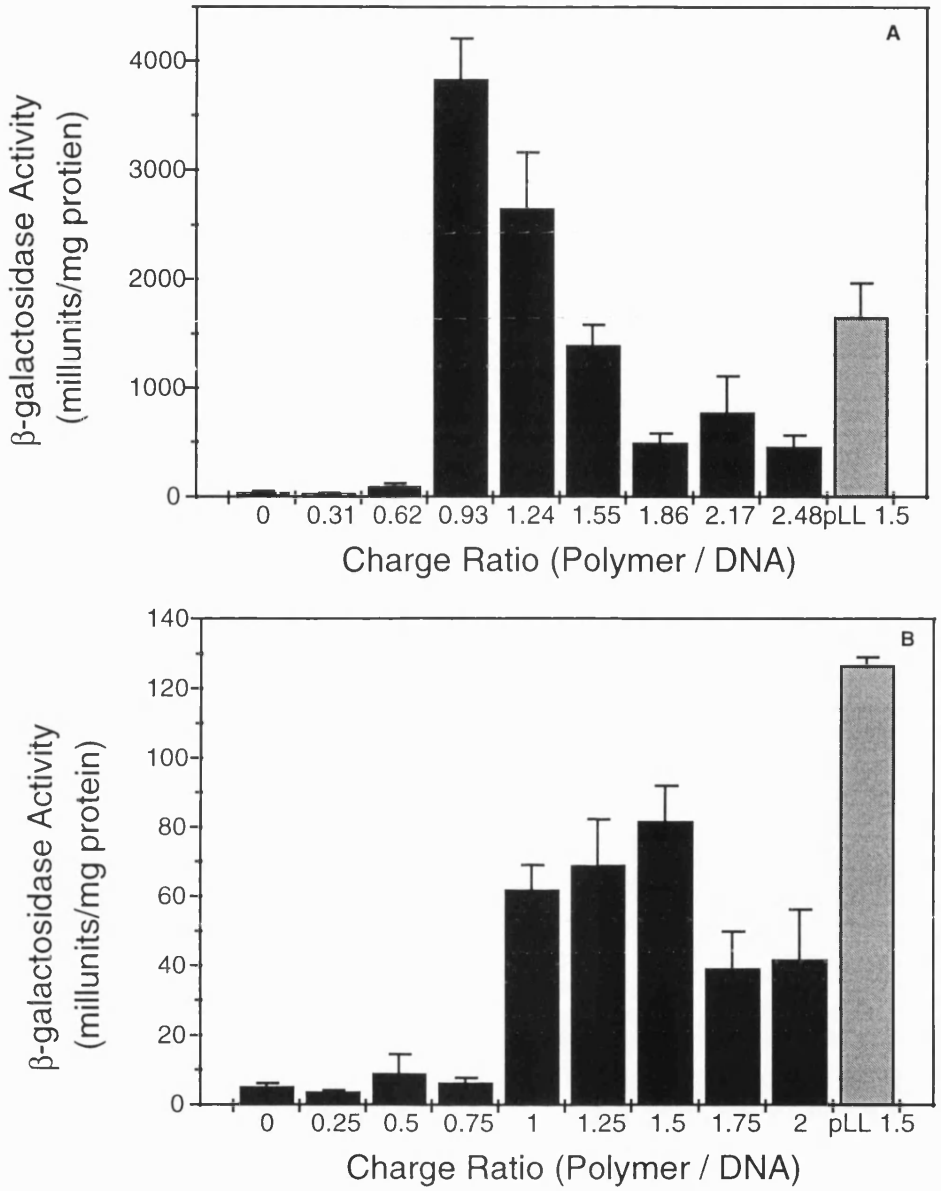

Figure 3.5. Effect of the charge ratio of poly-L-ornithine (A) and poly-L-arginine (B)-DNA complexes on the transfection efficiency into B16 melanoma cells. Transfections were performed using 6 μg pRSV*lacZ* and polymer as described in section 3.4, in the presence of 100 μM chloroquine. The cells were harvested and assayed for β-galactosidase activity 48 hours later using the ONPG assay (section 2.20.2). Transfection using complexes of poly-L-lysine and pRSV*lacZ* (■) was used as the positive control. The data presented represent the mean ± SEM (n=3).

In order to compare experiments more easily, the positive control was normalised to 100% (Figs. 3.7 and 3.8). β-galactosidase activity above basal levels was only routinely observed at or above a charge ratio of 1.0 ($^{+}$/-) for all polymer-DNA complexes, and a maximum transfection efficiency was observed near a charge ratio of 1.5. At higher charge ratios, usually a decline in transfection capacity was observed, although detectable levels of expression were still obtained within the ranges studied (generally up to a charge ratio of 2.0). It is likely that some cells were transfected at charge ratios below unity, and these could be visualised by staining with X-gal, but the ONPG assay used was insensitive unless the proportion of cells transfected was greater than approximately 0.1%. The ONPG assay required 10^9 enzyme molecules present to produce a measurable signal, compared with only 10^3 molecules for the X-gal assay (MacGregor *et al.*, 1991).

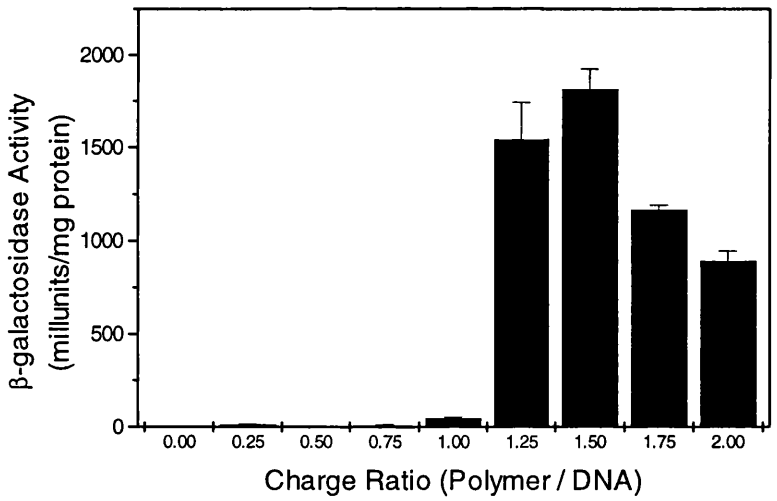

Figure 3.6. Charge-ratio ($^{+}$/-) effect of polylysine-DNA complexes on transfection efficiency in B16 melanoma cells. Transfections were performed using 6 μg pRSV*lacZ* and various quantities of polylysine (section 3.4), in the presence of 100 μM chloroquine. The cells were harvested and assayed for β-galactosidase activity 48 hours later using the ONPG assay (section 2.20.2). The data presented represent the mean ± SEM (n=3).

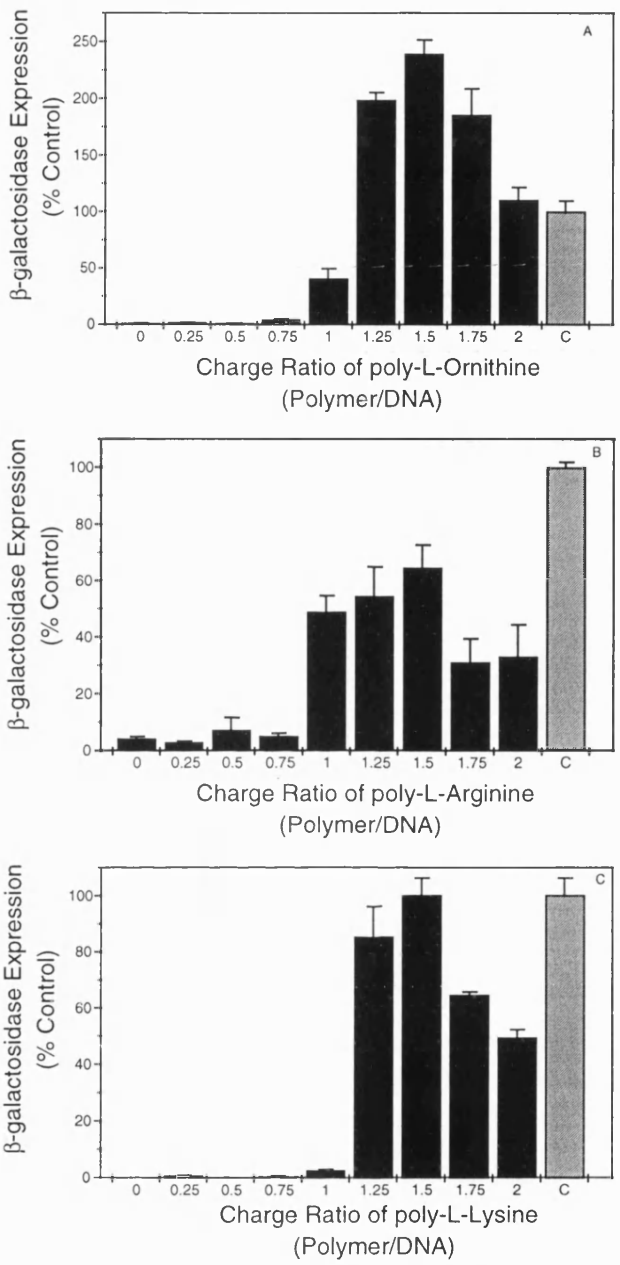

Figure 3.7. Optimisation of the polymer:DNA ratio for gene transfer. Each point represents the mean value from three replicate transfections. Complexes were formed with 6 μg plasmid DNA, and using increasing quantities of poly-L-ornithine (A), poly-L-arginine (B), and poly-L-lysine (C). All transfections utilised 100 μM chloroquine and the cells were assayed 48 hours post-transfection using the ONPG assay (section 2.20.2). Each point was calculated as a percentage of transfection using poly-L-lysine-DNA at a charge ratio of 1.5 with chloroquine (100 μM) as the positive control (■) and represent the mean ± SEM (n=3).

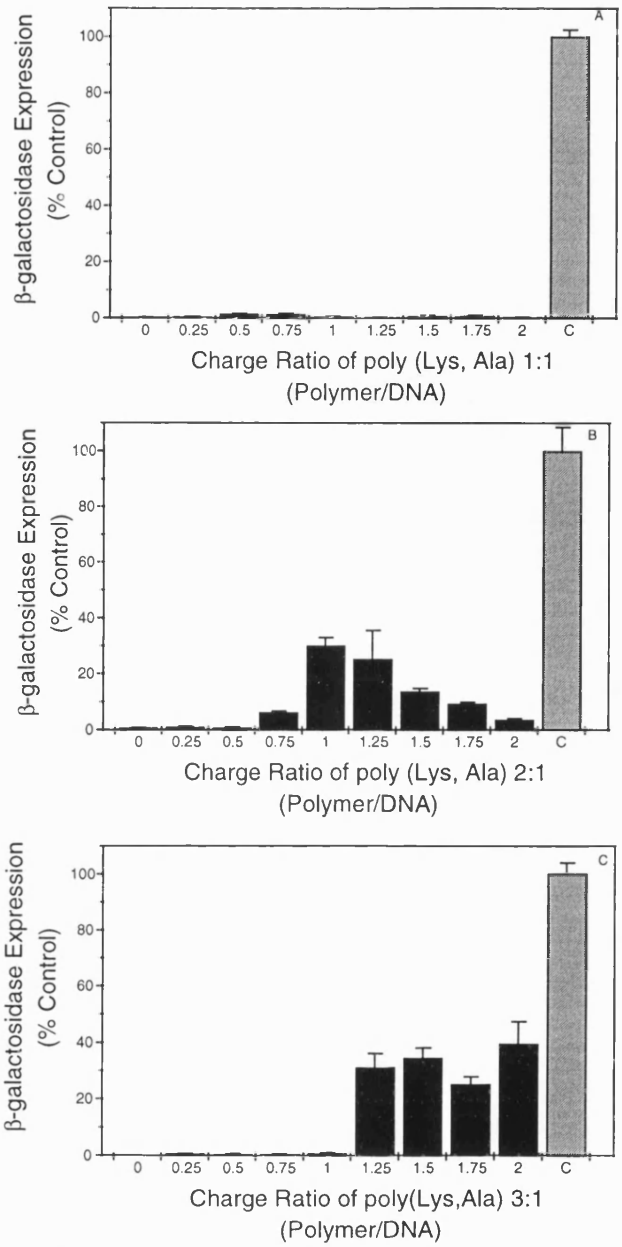

Figure 3.8. Optimisation of the co-polymer:DNA ratio for gene transfer. Each point represents the mean value from three replicate transfections. Complexes were formed with 6 μg plasmid DNA, and using increasing quantities of the lysine-alanine 1:1(L,A 1:1), 2:1 (L,A 2:1) and 3:1 (L,A 3:1) co-polymers (shown in A, B and C respectively). All transfections included 100 μM chloroquine and the cells were assayed 48 hours post-transfection by the ONPG assay (section 2.20.2). Each point was calculated as a percentage of transfection using poly-L-lysine with chloroquine (100 μM) as the positive control (■), and represent the mean ± SEM (n=3).

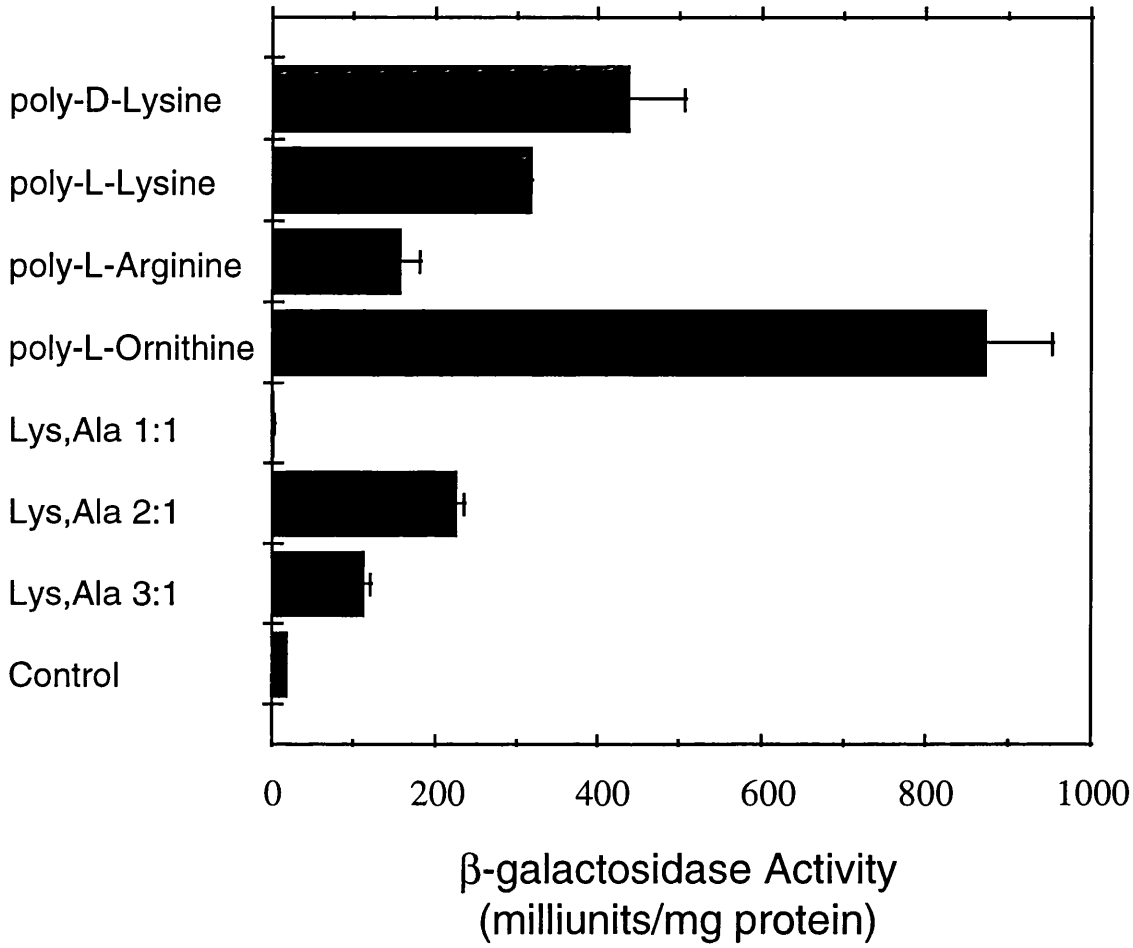

Figure 3.9. Influence of polymer used for complexation of DNA on the transfection efficiency. Complexes were formed with 6 μg pRSVlacZ at a charge ratio (+/-) of 1.5. All transfections were carried out in the presence of 100 μM chloroquine, and activity was assayed 48 hours post-transfection using the ONPG assay for β-galactosidase activity (section 2.2.20.2). Data points represent the mean ± SEM (n=3).

3.3.2.3. Comparative transfection efficiency of complexes.

A direct comparison of the transfection efficiencies for the different polymers was performed at a charge ratio of 1.5 ($^{+}$/-). This allowed a rank order for transfection efficiency to be established (Fig. 3.9) : poly-L-ornithine >> poly-D-lysine ≈ poly-L-lysine > Lys:Ala (2:1) ≈ poly-L-arginine > Lys:Ala (3:1). The co-polymer Lys:Ala (1:1), which had a lower charge density than all the other polypeptides studied, failed to increase gene expression above background levels.

The activity of the complexes was also determined *in situ* using the histochemical stain X-gal. This provided an indication of the number of cells being transfected by each complex. A by-stander effect has been observed with a pro-drug treatment of melanoma (Bonnekoh *et al.*, 1995), but the majority of gene therapy applications require that the maximum number of target cells possible should be transfected with the therapeutic gene. For this reason, delivery systems should be adapted to enhance delivery to the target cell population. There were few positively stained blue cells in all cases (1-5%). Poly Lys, Ala (1:1) showed no staining, in line with the ONPG assay results. Figure 3.10 shows representative photographs of cultured cells treated with pRSVlacZ complexed with poly-L-lysine, poly-L-ornithine, poly Lys, Ala (1:1) and poly Lys, Ala (3:1).

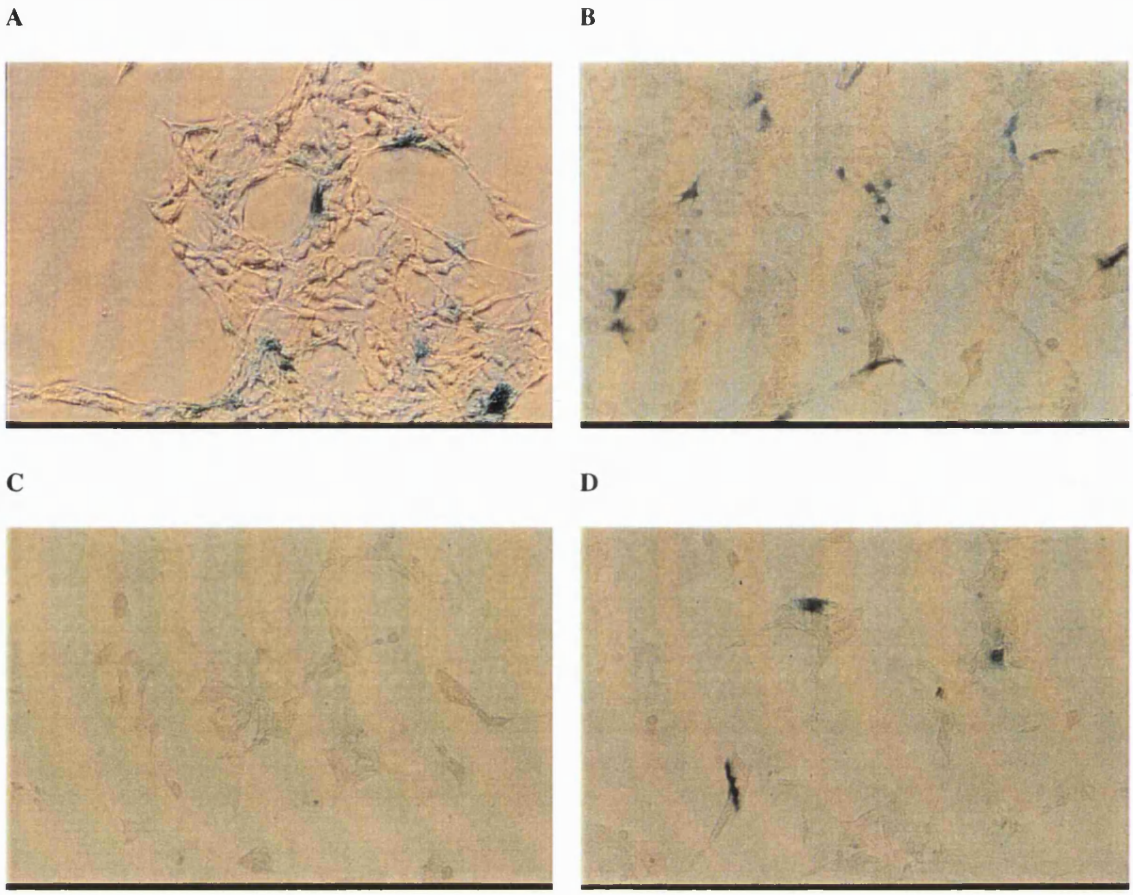

Figure 3.10. B16 melanoma cells transfected with complexes prepared with 6 μg pRSV*lacZ* plasmid and the polymers poly-L-lysine (A), poly-L-ornithine (B), poly Lys,Ala (1:1) (C) and poly Lys,Ala (3:1) (D). Transfections were performed at a charge ratio of 1.5 with 100 μM chloroquine, and the cells treated with X-Gal 48 hours post-transfection. Cells positive for β-galactosidase activity stain blue with X-Gal treatment. Cells were photographed at magnification x300. The fields shown are representative of the expression levels detected over the plates, with three wells transfected per formulation.

3.4. DISCUSSION

The association of eukaryotic nucleic DNA with cationic polypeptides such as histones and protamines stimulated investigation into the interaction of a variety of basic polymers with DNA. Physical characterisation by Olins *et al.* (1968) of complexes of linear DNA with various polycations led to the deductions that such interactions were stoichiometric and co-operative. The motivation for the present study was to determine whether this similarity between complexation of DNA and a range of polypeptide systems correlated with transfection efficiencies.

3.4.1. Complexation of plasmid-DNA using cationic polypeptides.

All of the polymers tested produced complete exclusion of ethidium bromide at electroneutrality, and for the homopolymers this equated to a polypeptide / DNA mass-ratio of approximately 0.4:1. All of the homopolymers were α-amino acids, and the positive charge was hence provided by the amino group on the side-chain. While a similar charge-ratio profile was exhibited by the co-polymers, the mass-ratio profile differed, accounting for the neutral alanine component contained within the polymer chain.

Studies by Leng and Felsenfeld (1966) demonstrated that fragments of calf thymus DNA could be partially precipitated by polylysine. This involved ultracentrifugation of systems produced under strictly controlled ionic reaction conditions. At a charge ratio of 1.0, all of the DNA was precipitated, but at any point

below this the majority of the polylysine added to the system was found in the precipitate. This indicated that under tightly regulated reaction conditions, a co-operative reaction could be produced.

The precipitation of DNA and polylysine at the charge ratio of 1.0 has also been described by Carroll (1972). It was shown in these experiments that the ionic concentration of the reaction solution could determine the characteristics of the complexes formed, consistent with the observations of Tsuboi *et al.* (1966). Additionally, Shapiro *et al.* (1969) described a selective interaction, where a well-ordered complex was produced under optimal conditions. A nucleotide selectivity for A-T-rich DNA was displayed by the polylysine, although this could be affected by altering the reaction conditions. The relatively sharp decrease in fluorescence that occurred during this assay supports the theory of a co-operative interaction during charge neutralisation of DNA molecules (Manning, 1980).

The presence of the alanine within the polymer had little effect on the complexation capacity of the charged lysine. This was a likely result of the derivatisation of the co-polymer occurring via the α-amino groups, leaving the amino groups on the side-chains to interact with the DNA. Hence, the backbone of the polymer consisted of a straight chain of amino acids, with the side-chains providing the only protrusions. Moreover, alanine residues provided little steric hindrance to the charge association, and the co-polymers exhibited similar stoichiometric behaviour to the homopolymers, with one positive unit interacting with each theoretical negative charge. Hence the stoichiometry of the interaction was apparently unaffected by the presence of the neutral alanine within the co-polymeric chain.

3.4.2. Correlation between charge ratio and transfection activity.

In contrast to the complexation data, the polymers displayed different transfection profiles, although those that successfully transfected cells all exhibited a similar pattern of activity. All of the polymers demonstrated little or no expression of the reporter gene if complexes were prepared below the critical point of charge neutralisation. This observation is at odds with the reports of a co-operative interaction between cationic polymers and DNA (section 3.4.1).

If the system was co-operative, transfection activity would have been observed at the charge ratios ($^{+}$/-) below electroneutrality. This is because during co-operative binding the initial interaction between two molecules favours further binding to the host molecule. Therefore, the population of complexes would have contained some DNA molecules that had been completely neutralised by polymer, and some that had experienced little interaction with the cationic polymer. The transfection results argue that complexes produced by 'flash'-mixing were not produced in a co-operative manner. In view of this, the fluorescence profiles could only be used to demonstrate the optimum ratios for interaction of the polymer and the DNA, and not to infer co-operativity of the reaction.

Beyond electroneutrality, there was an increase in gene expression to a maximum at a charge ratio ($^{+}$/-) around 1.5. This suggested that the complexes required an overall positive charge before they could overcome the repulsion of the DNA by the negatively charged cell surface, and interact non-specifically with it. This hypothesis was suggested by Bond and Wold (1987), who studied transfection of cell lines with polyornithine-DNA complexes. They showed that there was an optimum charge ratio for transfection, with a net overall positive charge, and that above this, the transformation efficiency decreased. Additionally, charge neutralisation is required to induce DNA collapse, producing the characteristic 'doughnut' or toroid structures (Olins *et al.*, 1971; Laemmli, 1975).

At charge ratios greater than 1.5, the transfection ability of the complexes declined. One hypothetical factor which may account for this is the structure of the complexes in the presence of excess polylysine, and whether the extra polymer continues to be incorporated into the complex. Carroll reported (1972a) that above electroneutrality, DNA-polylysine complexes produced a high level of unregulated aggregation, and a precipitation was observed at electroneutrality. At higher charge ratios ($^{+}$/-), the solubility of the complexes increased, probably due to the binding of more excess polylysine (Carroll, 1972b). The excess positive charge was believed to serve to separate the complexes by charge repulsion.

An alternative theory to account for the reduction in transfection capacity involves the belief that the excess polycation does not associate with the DNA-polymer complex. In this situation, the free polymer would be capable of competing for uptake into the cell with the complexes. Additionally, at the point of dissociation of the polycation and the DNA inside the cell, any free polymer in the vicinity would compete to bind the recently released DNA. This would theoretically provide a reduction in quantity of free DNA potentially available for transfer to the nucleus. Free polylysine would also be expected to have toxic effects on the cells in culture which could explain the lower efficiency observed at high charge ratios. This is discussed further in Chapter 6.

3.4.3. Comparative transfection activity of polymers in B16 melanoma cells.

Uptake of the complexes after association with the cell surface is believed to occur by endocytosis into lysosomes, which is supported by the prerequisite for chloroquine in the transfection medium. Luthman and Magnosson (1983) demonstrated the enhancement of transformation efficiency of polyoma cells with the use of chloroquine. Chloroquine serves as a lysomotropic agent, although its mode of action is under some discussion. The concentrations of chloroquine necessary to effect increased transfection levels are relatively high (25-100 μM), as determined by Zenke *et al.* (1990). These concentrations of chloroquine are cytotoxic, and this is a limiting factor in the transfection contact time of the complexes with the cells.

The original hypothesis for the mechanism of action of chloroquine was that as a weakly basic molecule, chloroquine was capable of increasing the pH within the lysosomes. This would serve to reduce nuclease activity and hence protect the DNA from degradation. Dean *et al.* (1984) demonstrated that a concentration of 10 μM was sufficient to inhibit nuclease activity, leading to an alternative hypothesis for the action of chloroquine in enhancing gene expression in transfected cells.

Zatloukal *et al.* (1992) postulated that accumulation of the chloroquine caused osmotic changes within the lysosome, producing membrane disruption and release of the contents into the cytosol. Studies by Sipe *et al.* (1991) demonstrated that the endosomes of K-562 cells were devoid of Na^+K^+-ATPase regulation of the pH gradient across the endosomal membrane. Hence there was no regulation of endosomal acidification observed. Therefore, chloroquine was shown to accumulate in the endosomes, and without the pH gradient regulation, the interior of the endosome became highly acidic.

There are several factors that may account for the varying transfection efficiency observed between the different polymer-DNA complexes. The complexes may exhibit a diversity in size. The postulated methods of uptake for complexes of a similar nature involve adsorptive endocytosis (Legendre and Szoka, 1992) also known as absorptive pinocytosis (Ryser and Shen, 1978). This involves the ingestion of fluid containing solutes or macromolecules via small vesicles (≤ 150 nm diameter). This is a process that most eukaryotic cells are continually performing at different rates, dependent on

cell-type (Watts and Marsh, 1992). The vesicles may endocytose molecules indiscriminately, or the more specific process of receptor-mediated endocytosis may occur via clathrin-coated pits. Cellular uptake by particles of roughly 100 nm routinely occur (Wagner *et al.*, 1991), and it can be assumed that any particles which deviate from this to a large extent may suffer selective or restricted uptake.

An alternative argument to account for the variation in transfection efficiencies of the polymers is that the polymers may be providing different stabilising effects on the DNA due to the chemical nature of the side chains. It was reported by Olins *et al.* (1967) that a decreasing order of stability towards melting was exhibited by poly-L-ornithine > poly-L-lysine > poly-L-arginine, which corresponds to the rank order of efficiency of transfection for the homopolymers shown in these studies. This would indicate that the complexes with reduced transfection efficiency are likely to be less stable in the transfection medium.

The release from the endosome of all the complexes is primarily a result of the presence of chloroquine, as determined by the inability of cells transfected without chloroquine to express the reporter gene. Distal to this process, differences in transfection effectiveness may be introduced by variations in the dissociation of the DNA from the polymer, transfer to the nucleus, and uptake and transcription within the nucleus. Transcription has been shown to be reduced by methylation of the DNA and additionally affected by the local concentration of histone H1 (Johnson *et al.*, 1995). Different expression efficiencies may be related to the degree of protection of the DNA from methylation conferred by the various polymers.

3.4.4. Histochemical staining of transfected cells.

The histochemical staining revealed very little difference in the percentage of cells within the population that expressed the reporter gene (1-5%). This was in contrast to the spectrophotometric assay, where the levels of expression were shown to vary within orders of magnitude from one polymer to another. This suggests that individual positively stained cells transfected with one system were expressing higher levels than similar cells which had been transfected with a different polymer-DNA complex.

3.5. SUMMARY

The complexation of plasmid DNA by a variety of polycationic polymers was demonstrated using spectrofluorimetry. All of the polymers appeared to bind the DNA in a similar manner, such that the DNA was completely complexed at a 1:1 ratio of positive / negative units. A co-operative reaction has been reported for such complexes, although this contrasted with the transfection activity profile, where no expression was observed below electroneutrality. The polymer-DNA systems exhibited an optimum of expression between a charge ratio of 1-1.5, and different transfection abilities were observed with the selection of polycations. The rank order of efficacy was poly-L-ornithine >> poly-D-lysine ≈ poly-L-lysine > Lys:Ala (2:1) ≈ poly-L-arginine > Lys:Ala (3:1). The co-polymer Lys,Ala (1:1) did not transfect B16 melanoma cells. Histochemical staining with X-Gal did not reflect the variation seen with the spectrophotometric assay.

CHAPTER 4. Characterisation and biological activity of complexes formed by DNA and polyethylene glycol-poly-L-lysine block co-polymers.

4.1. INTRODUCTION

Polymer conjugation has been used extensively to alter the biodistribution, elimination and rate of metabolism of covalently bound drugs. Conjugation of polymers to biologically active protein drugs has been used as a method to increase efficacy and reduce toxicity. Polymers have also been utilised in the design of polymer-drug conjugates to facilitate controlled release and targeting of low molecular weight drugs.

Hydrophilic polymer-protein conjugates can exhibit increased solubility and stability, reduced proteolytic degradation, lower immunogenicity, and a prolonged protein plasma elimination half-life. For these reasons, a variety of polymers have been utilised as drug carriers, including poly(hydroxyethylglutamate) (PHEG; De Marre *et al.*, 1994), hydroxypropylmethacrylamide (HPMA; Kopecek *et* al., 1987) and polyethylene glycol (PEG; Abuchowski and Davis, 1979).

PEG has been used extensively for the modification of therapeutic proteins, conferring a decrease in the toxicity and immunogenicity of the protein, whilst both increasing the water solubility and plasma half-life (Katre, 1993; Fuertges and Abuchowski, 1990). PEG is believed to alter the properties of the conjugated protein due to the formation of a PEG mantle around the protein molecule (Lee *et al.*, 1981).

It has been postulated that PEG sterically hinders reaction with cells of the immune system (Tomiya et al, 1985), and PEG itself has been shown to be non-immunogenic (Abuchowski *et al.*, 1977). PEG-protein conjugates exhibit varying degrees of reduced immunogenicity which differ for each protein and with the amount of PEG attached to the protein surface (Ashihara *et al.*, 1978). PEG also protects the conjugated moiety from proteolytic degradation (Wieder et al, 1979) and reduces the biological activity of the protein. This loss of activity is more than offset by the concomitant increase in plasma circulation, which is often augmented from a few minutes to several hours or even days.

A similar strategy could be utilised to modify the properties of condensed DNA particles. In this study this has been investigated using PEG-polylysine co-polymers. The core of such a complex would consist of the polylysine-DNA complex, and the PEG chains would be expected to extend into the aqueous solution (Fig. 4.1). PEG is an extremely hydrophilic polymer, and the establishment of a water shell around the peptide core would be expected to result in a colloid with enhanced lyophilic character.

PEG has been used to modify the surface properties of other colloidal systems. PEG has been used to coat the surface of liposomes (Woodle and Lasic, 1992), producing an increase in hydrophilicity. Liposomes are normally cleared from the circulation by the reticuloendothelial system (RES), and circulation time is related to vesicle size and phospholipid or cholesterol content (Senior, 1987). The RES constitutes mononuclear phagocytes which engulf 'foreign' macromolecules, and they are particularly concentrated in the lung, in the liver (as the Kuppfer cells) and in the spleen (Poste, 1983). PEG coating of these liposomes reduces the rate of RES-mediated

clearance, a phenomenon which has also been observed when polystyrene particles were coated with polymeric glycols (Illum *et al.*, 1986). This phenomenon is thought to be due to the polymers on the liposome surface exerting a long-range mutual repulsion between adjacent bilayers, inhibiting the interaction of macromolecules and cellular surfaces in the blood with the PEG-coated liposomes (Wu *et al.*, 1993).

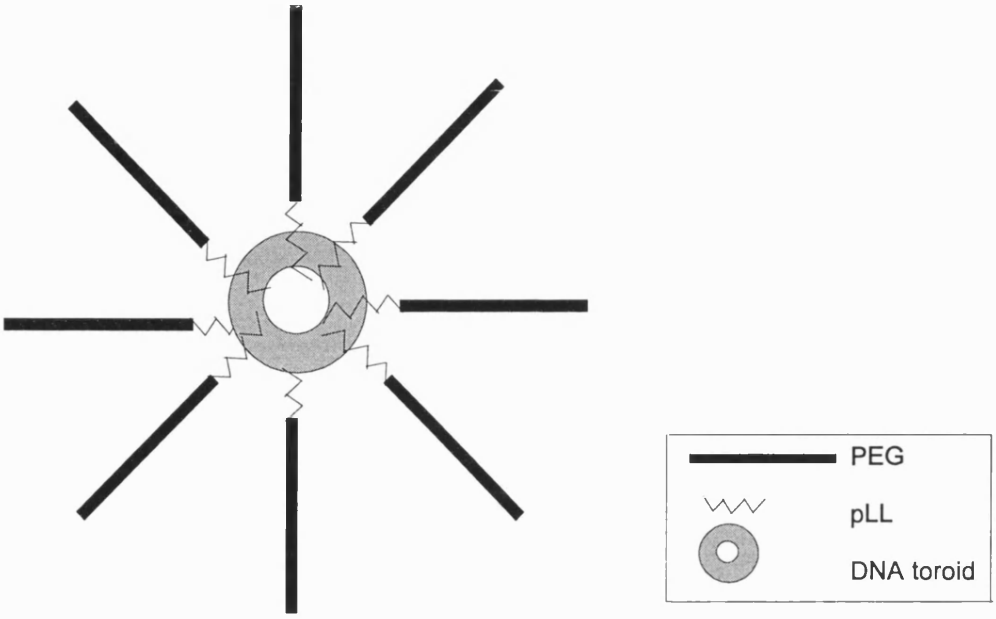

Figure 4.1. Schematic diagram of the putative structure of PEG-pLL-DNA complexes in aqueous systems, showing the PEG mantle expected to form around the hydrophobic core of complexed pLL-DNA.

PEG-coated liposomes have become known as 'stealth' liposomes, and have been demonstrated to preferentially accumulate in tumours (Gabizon and Papahadjopoulos, 1988). The rationale for the use of these vehicles to deliver anthracycline anticancer agents preferentially to tumours was due to the belief that this characteristic resulted from the increased circulating time (Gabizon, 1992). However, Wu *et al.* (1993) demonstrated that a higher intrinsic vascular permeability of PEG-coated liposomes helped to effect preferential accumulation in tumours.

Traditional gene therapy vectors require development for future *in vivo* applications. This will involve alteration of the current vectors to overcome the problems related to toxicity, degradation and inefficient DNA delivery. The rationale for the production of a polylysine-PEG co-polymer for DNA delivery is to attempt to utilise the beneficial properties of PEG-protein conjugates, which result in reduced toxicity, reduced immunogenicity and reduced degradation of the drug. The polylysine moiety is necessary for DNA-binding, while the PEG could serve to enhance the performance of the system as a viable delivery vector for gene therapy. Studies on block co-polymers of this nature by Katayose and Kataoka (1996) have demonstrated that complexes of different polylysine chain length exhibited different stoichiometry of interaction. This group has also shown that the complexed DNA could be displaced from the co-polymers by excess poly-aspartic acid. This indicated that under appropriate conditions, the complexed DNA could be released from the vector to ultimately produce gene expression.

This chapter describes the investigation of complexation properties and transfection efficiencies of a selection of synthesized co-polymers. The synthesis of these block co-polymers was strictly controlled, so that accurate mass ratios of poly-lysine : PEG were established. The co-polymers have well-defined structures, with little polydispersity. These studies attempt to determine how the co-polymers compare with the poly(amino acid)s investigated in Chapter 3, and whether the presence of PEG in the structure affects the interaction with DNA and the efficiency of gene delivery and expression.

4.2. MATERIALS AND METHODS.

4.2.1. Structure of block co-polymers.

All of the polyethylene glycol-poly-L-lysine (PEG-pLL) co-polymers were kindly donated by Professor E. Schacht (University of Gent, Belgium). The block co-polymers were formed by linkage via the alpha amino group, and their general structure is depicted in Figure 4.2. The ratio of components in each co-polymer is shown in Table 4.1.

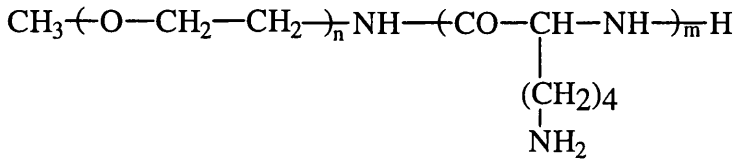

Figure 4.2. General structure of co-polymers.

Polymer	Mol. Wt. (PEG : pLL)	Mol. Wt. : per unit charge	Effective molar ratio (PEG : pLL)
96-7	5,000:5,000	322.58	3:1
96-8	5,000:10,000	192.31	1.5:1
96-9	5,000:20,000	160.26	0.7:1
96-10	12,000:5,000	548.39	7:1
96-11	12,000:10,000	282.05	3.5:1
96-12	12,000:20,000	205.13	1.7:1
96-13	20,000:5,000	806.45	12:1
96-14	20,000:10,000	384.62	6:1
96-15	20,000:20,000	256.41	3:1

Table 4.1. Mass and molar ratios of co-polymers. (pLL - polylysine)

4.2.2. Calculation of charge ratios for complexation.

The mass ratios of charged lysine to neutral PEG were documented by the supplier for each co-polymer. The effective molecular weight for each charged and uncharged monomer unit was calculated, and the ratio of charged-to-neutral component calculated for each polymer. The effective mass of polymer associated with one positive charge was calculated (Table 4.1). Complete ionisation of the lysine side-chain amino group was assumed at the experimental pH of 7.4.

The liposome DOTAP (N-[1-(2,3-Dioleoyloxy)propyl]-N,N,N-trimethyl ammonium methylsulfate; Boehringer Mannheim, Germany) was used as a positive control in transfection experiments. The effective mass associated with one mole of positive charge was 774.21 g, and complexes were routinely prepared at a charge ratio of 2.5, according to the manufacturers' directions. This charge ratio has been established as optimum for the B16 cell line (A. Uduehi, personal communication).

4.2.3. Ethidium bromide exclusion assay.

Complexes were formed using increasing masses of PEG-pLL and 6 μg pRSV*lacZ* to produce the charge range 0 - 2.5 ($^{+}$/-), as detailed in section 3.4. DNA complexation was analysed using a spectrofluorimeter (section 3.2.5.1).

4.2.4. Fluorometric assay for β-galactosidase.

In cases where expression of β-galactosidase was low, a more sensitive assay using 4-methylumbelliferyl-β-D-galactoside (MUG) as the substrate for the enzyme was used (Macgregor *et al.*, 1991). Cells were removed from the culture plates by gentle

scraping, and cell extracts were prepared by freeze-thawing three times in 250 µl Z buffer (appendix A).

An aliquot of cell extract supernatant (10-105 µl) was added to the well of a microtitre dish (Nunc). The volume was made up to 150 µl with 30 µl of 3 mM MUG and the remainder with Z buffer. The plate was incubated at 37°C for 90 minutes, then 75µl of STOP buffer (app. A) was added. Fluorescence was measured using a Fluoroskan II (λ_{ex} 350 nm; λ_{em} 450 nm), and the results calculated relative to the soluble protein content of the samples.

4.2.5. Protein assay of cell extracts.

Cell extracts were prepared in 250 µl Z buffer, and a 50 µl aliquot used for protein quantification. The soluble protein was assayed as detailed in section 2.2.20.3, and the standard curve for the assay is presented in appendix C.

4.3. RESULTS

4.3.1. Complexation studies using the ethidium bromide exclusion assay.

The fluorescence exclusion profiles of the various co-polymers are displayed in Figures 4.3, 4.4 and 4.5. The maximum exclusion for all of the co-polymers was reached at a charge ratio of approximately 1.25. These profiles were similar to those exhibited by the homopolymers and lysine-alanine co-polymers studied in Chapter 3. The linear decrease up to a charge ratio of 1.25 exhibited very little displacement from

that observed with polylysine. At charge ratios above this, no further quenching occurred and a minimum background level of fluorescence was maintained.

As expected the profiles for the mass ratio-related fluorescence quenching exhibited distinct translocation from the polylysine exclusion profile. Within each series of co-polymers, where the mass of PEG remained constant, and an increasing mass of polylysine was present a trend was observed. As the quantity of polylysine was increased, the profile shifted left, towards that of the polylysine. Hence, the co-polymer within each series containing the lowest charge density was displaced furthest to the right, and the co-polymer with the highest charge density the furthest to the left (i.e. closest to the polylysine profile). This was useful verification of the composition of the co-polymers.

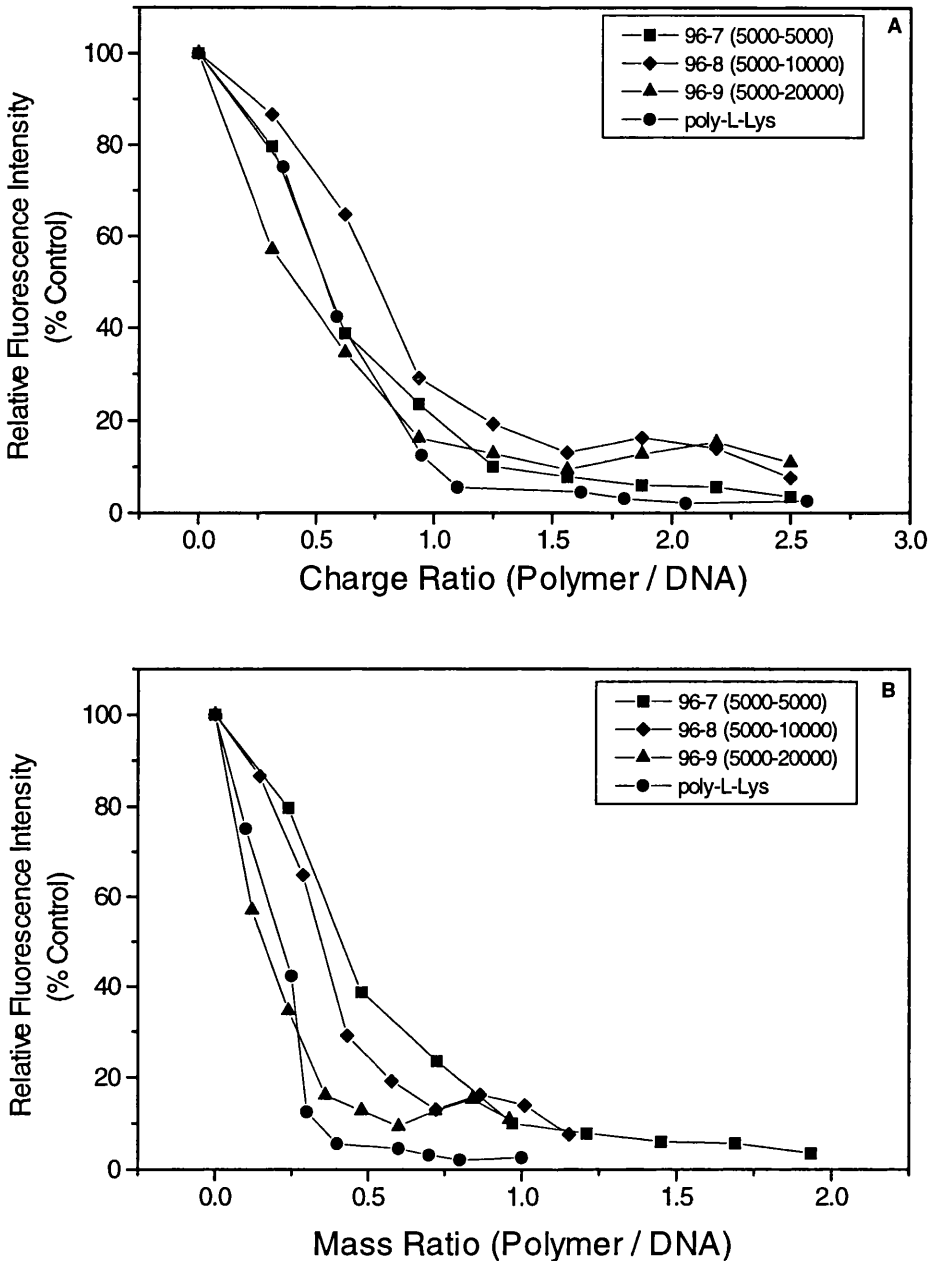

Figure 4.3. Ethidium bromide exclusion assay for PEG-pLL co-polymers. The complexes were prepared using 6 μg plasmid DNA and increasing quantities of each co-polymer to produce the required charge ratio. Ethidium bromide (0.5 μg/ml) was added immediately prior to the measurement of the fluorescence. This series of co-polymers contains a constant quantity of PEG (5000), with varying ratios of polylysine (5000, 10000 and 20000). The exclusion profile for polylysine is also shown for comparison. The data points are expressed in terms of the polymer / DNA charge ratio (A) and the mass ratio (B). All data points are calculated as a percentage of a control containing 6 μg plasmid DNA, and represent the mean of three replicate evaluations.

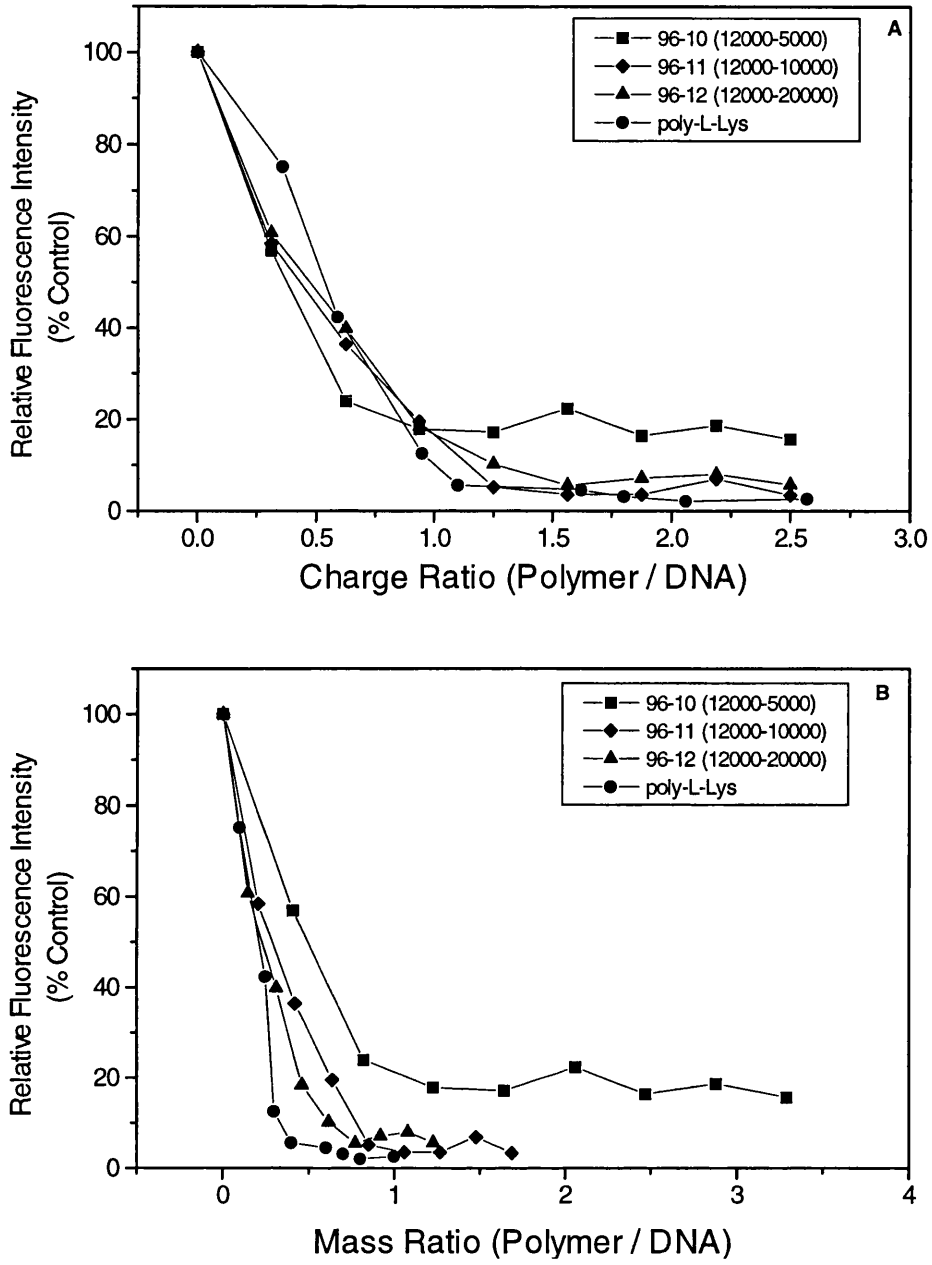

Figure 4.4. Ethidium bromide exclusion assay for PEG-pLL co-polymers. The complexes were prepared using 6 μg plasmid DNA and increasing quantities of each co-polymer to produce the required charge ratio. Ethidium bromide (0.5 μg/ml) was added immediately prior to the measurement of the fluorescence. This series of co-polymers contains a constant quantity of PEG (12000), with varying ratios of polylysine (5000, 10000 and 20000). The exclusion profile for polylysine is also shown for comparison. The data points are expressed in terms of the polymer / DNA charge ratio (A) and the mass ratio (B). All data points are calculated as a percentage of a control containing 6 μg plasmid DNA, and represent the mean of three replicate evaluations.

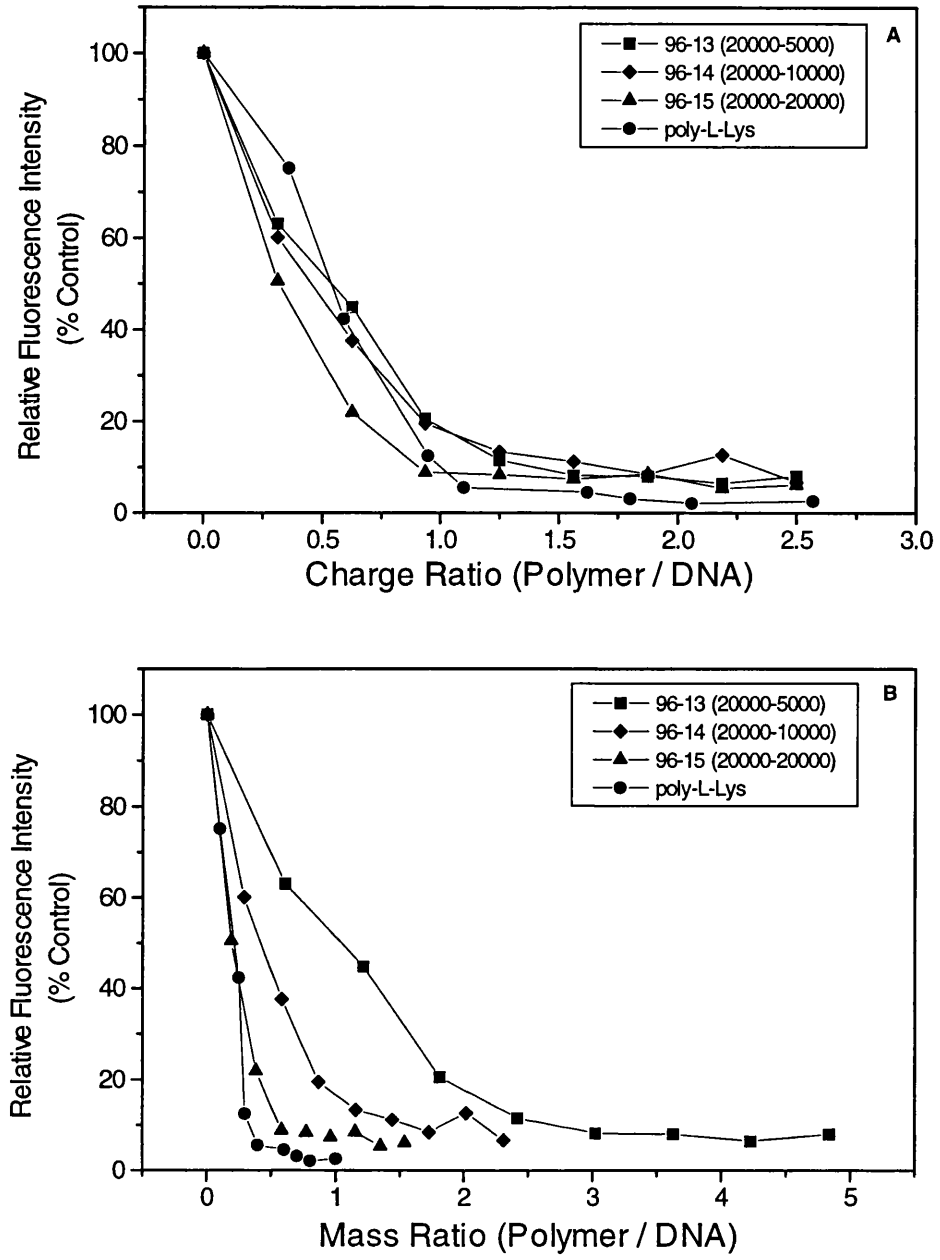

Figure 4.5. Ethidium bromide exclusion assay for PEG-pLL co-polymers. The complexes were prepared using 6 μg plasmid DNA and increasing quantities of each co-polymer to produce the required charge ratio. Ethidium bromide (0.5 μg/ml) was added immediately prior to the measurement of the fluorescence. This series of co-polymers contains a constant quantity of PEG (20000), with varying ratios of polylysine (5000, 10000 and 20000). The exclusion profile for polylysine is also shown for comparison. The data points are expressed in terms of the polymer / DNA charge ratio (A) and the mass ratio (B). All data points are calculated as a percentage of a control containing 6 μg plasmid DNA, and represent the mean of three replicate evaluations.

4.3.2. Comparative transfection capacities in B16 melanoma cells.

The various co-polymers form three subsets, where for one subset the amount of PEG is maintained at 5000, and the mass of polylysine conjugated to it increased from 5000 to 10000 to 20000. This pattern is repeated for other subsets prepared with PEG masses of 12000 and 20000. All of the co-polymers exhibited the capacity to generate reporter gene expression levels above the background levels in B16 melanoma cells, when transfection was carried out in the presence of chloroquine (Fig. 4.6A). Transfections were performed at a charge ratio of 1.5, assuming that the co-polymers demonstrated similar charge-related transfection profiles to the homopolymers and lysine-alanine co-polymers. The levels of β-galactosidase activity were determined using the fluorescence-based MUG assay (section 4.2.4).

The dependency of the co-polymer-DNA complexes on chloroquine to produce effective transfection is shown in Figure 4.5B. Co-polymer complexes were active in the presence of chloroquine but produced no expression in B16 melanoma cells in the absence of chloroquine. At best, the co-polymers in the presence of chloroquine produced one third of the activity of polylysine-DNA complexes. The co-polymers containing a high PEG:polylysine ratio produced the lowest levels of expression. The co-polymers containing the most polylysine in all three subgroups exhibited slightly greater activity than the other co-polymers in the subset.

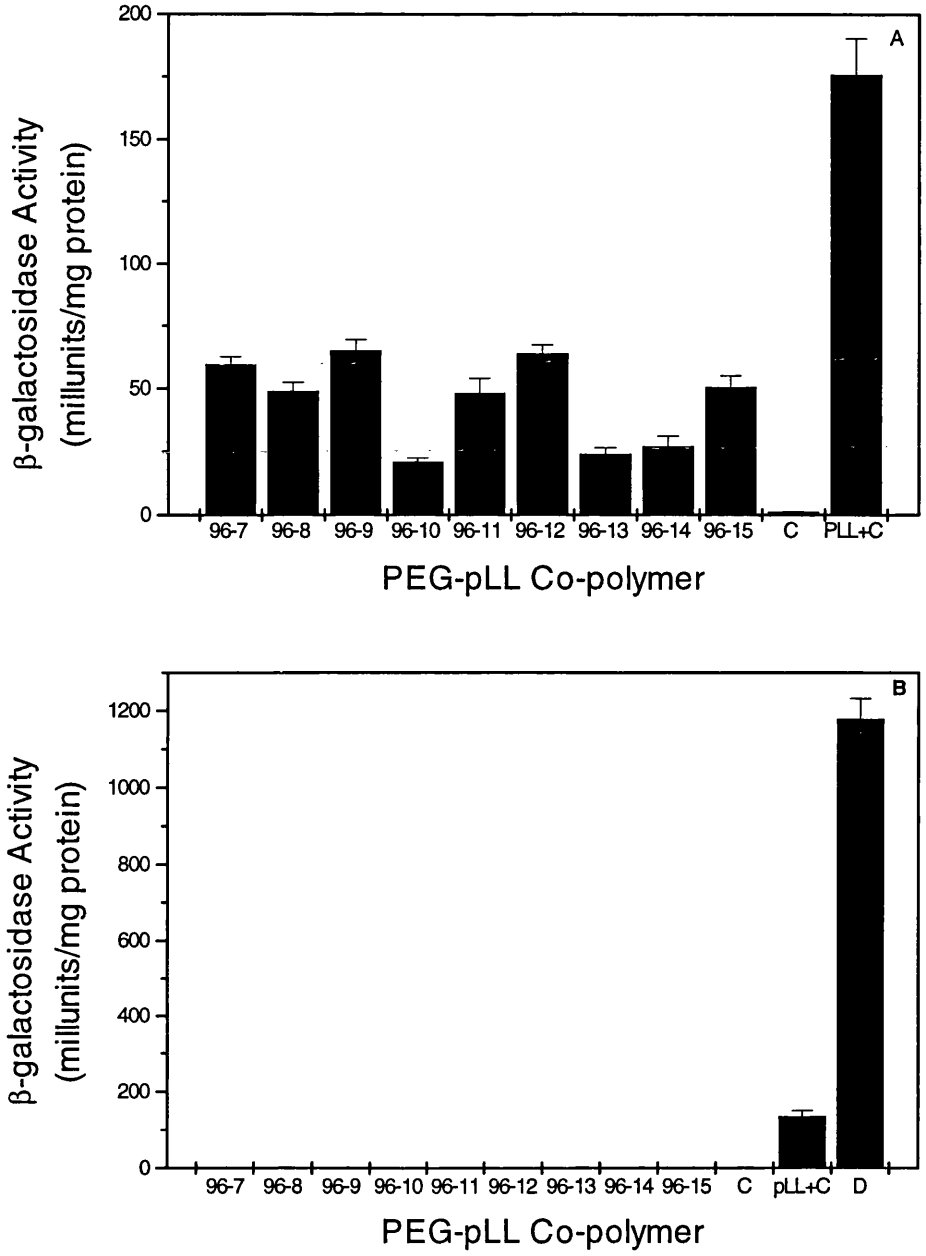

Figure 4.6. Comparison of transfection efficiency of PEG-pLL-DNA complexes using B16 melanoma cells. All complexes contained 6 μg pRSV*lacZ* plasmid and were prepared at a charge ratio of 1.5. Chloroquine (100μM) was added to the transfection medium in A, but was excluded in B. The positive control in A and B consisted of poly-L-lysine-DNA plus chloroquine (pLL+C). DOTAP (D) was included as a positive control in B, as an agent that successfully transfects cells without chloroquine. The negative control (C) in both cases consisted of free DNA added to the transfection medium. The cells were assayed after 48 hours using the MUG assay. Each point represents the mean ± SEM (n=3).

4.3.3. Comparative expression studies in HEK293 cells.

Encouraging reports from Dr. L. Seymour (personal communication) regarding the transfection efficiency of particulate complexes in HEK293 cells resulted in the use of this cell line for comparative transfection studies in parallel to B16 cells. The PEG-pLL co-polymers were all shown to produce gene expression above background levels in HEK293 cells, both with and without chloroquine. Transfections were performed at a polymer / DNA charge ratio ($^{+}$/-) of 1.5 for comparative purposes, and the levels of β-galactosidase activity determined using the fluorescence-based MUG assay (section 4.2.4). The three subsets of co-polymers, containing three masses of PEG, each with three different quantities of polylysine exhibited no trend in transfection efficiency.

The efficiency of transfection produced in the presence of chloroquine (Fig. 4.7A) was higher than the efficiency of polylysine and chloroquine in all but one case (polymer 96-7, containing PEG:pLL 5000:5000). In several cases, the efficiency was comparable to that of the liposome DOTAP without chloroquine. It was difficult to assign any trend relating efficiency with increasing PEG or polylysine content.

Transfection of HEK293 cells with the various complexes of co-polymers and plasmid DNA in the absence of chloroquine was shown to be successful in all cases. The positive controls within this experiment were complexes of plasmid DNA with the liposome DOTAP or polylysine, both without chloroquine. DOTAP routinely generated levels of β-galactosidase expression around 1500 millunits/mg protein, whilst polylysine in the absence of chloroquine resulted in levels around 50 milliunits/mg protein. The co-polymers all exhibited greater activity than polylysine alone, although the optimum formulation produced approximately 14% of the levels of gene expression observed

with DOTAP. Once again, there appeared to be little trend relating efficiency with increasing PEG or polylysine content.

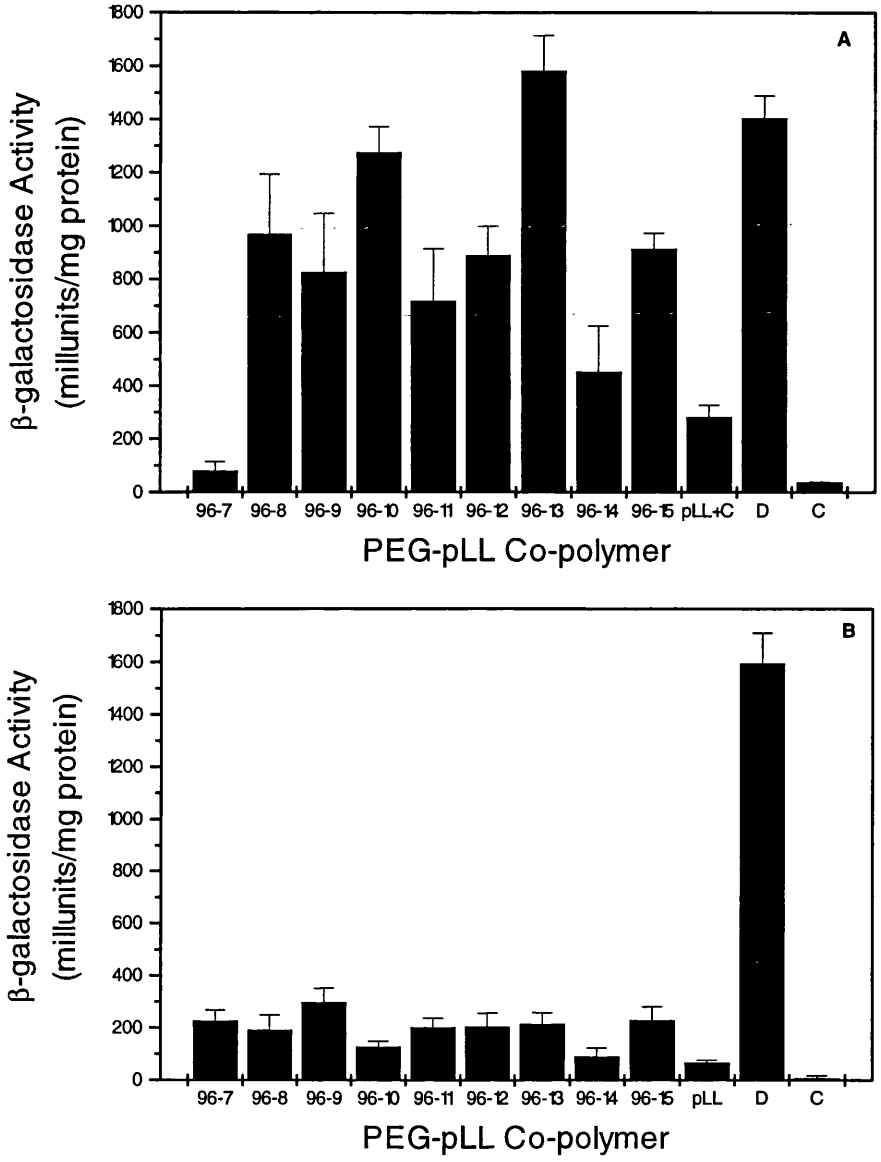

Figure 4.7. Transfection of HEK293 cells with PEG-pLL complexes. Complexes were prepared with 6 μg pRSV*lacZ* and the corresponding mass of polymer to provide a charge ratio (polymer / DNA) of 1.5. Transfection was performed with 100 μM chloroquine (A), and without chloroquine (B). The cells were incubated in complete medium for 48 hours post-transfection, before assaying for β-galactosidase activity using the MUG assay (section 4.4). Expression was measured per milligram of protein to account for cell number, and compared with the liposome DOTAP as a positive control. Each point represents the mean ± SEM (n=3).

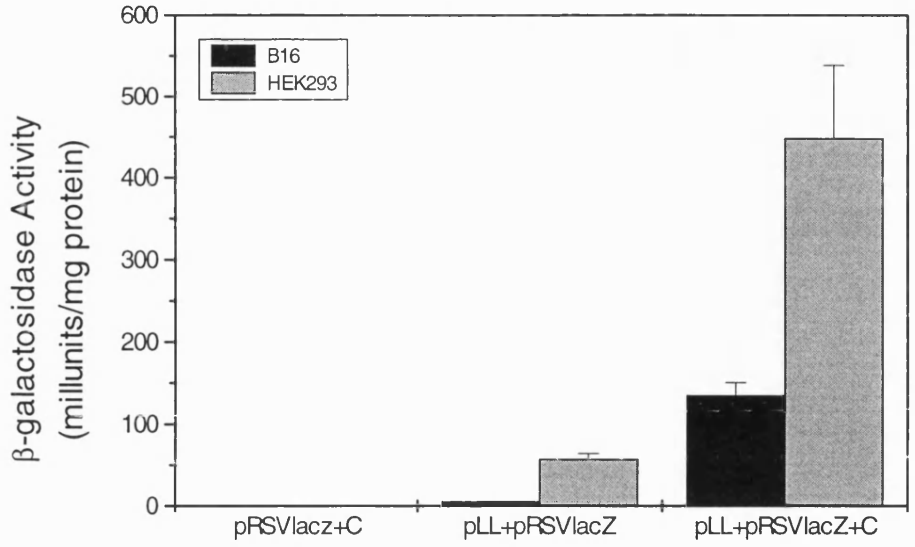

Figure 4.8. Comparative transfection efficiencies of plasmid DNA and chloroquine, DNA-polylysine and DNA-polylysine complexes with chloroquine. The transfections were performed in the two cell lines : HEK293 and B16 melanoma cells All systems contained 6 μg pRSV*lacZ*, and complexes were prepared at a charge ratio of 1.5. Where necessary, chloroquine was present in the transfection medium at a concentration of 100 μM. The data points represent the mean activity ± SEM (n=3).

4.3.4. Requirement of chloroquine for transfections.

The transfection efficiency for polylysine-DNA complexes with and without chloroquine were compared in the two cell lines used for the co-polymer complex transfections i.e. HEK293 and B16 melanoma cells (Fig. 4.8). Transfection of both cell lines with free plasmid DNA alone produced no activity, while transfection of the cells with polylysine-DNA complexes in the presence of chloroquine produced measurable levels of activity in both cases. The activity in the HEK293 cells was approximately five times greater than that observed in the B16 melanoma cells. Transfection of cells using polylysine-DNA complexes in the absence of chloroquine produced no measurable levels of activity in the B16 cell line. In the HEK293 cells, levels of β-

galactosidase expression in transfections without chloroquine were about 10% of those seen with transfections in the presence of chloroquine. Hence it is clear that the prerequisite for chloroquine to effect transfection is a cell-line dependent parameter.

4.4. DISCUSSION

4.4.1. Ethidium bromide exclusion by PEG-pLL co-polymers.

Co-polymers containing polylysine conjugated to PEG retained the capacity for inhibiting the intercalation of ethidium bromide into plasmid DNA. This indicated that all of the polymers were capable of interaction with the negatively charged DNA. The relationships between exclusion profiles and charge ratio were similar to those of the homopolymers and lysine-alanine co-polymers examined in Chapter 3. The maximum ethidium exclusion was reached at charge ratios near electroequivalence. This suggested that the presence of the PEG component within the co-polymer presented little steric hindrance to the interaction between the cationic polylysine and the anionic DNA molecules.

The co-polymer was prepared by conjugation via the α-amino group, and hence the side-chain amino groups would remain available for interaction with the nucleotides of the DNA molecules. It would appear that the neutral PEG component of the co-polymer did not prevent the positively charged amines from interacting with the plasmid DNA with a similar stoichiometry to that observed with polylysine (Tsuboi *et al.*, 1966).

The profiles relating ethidium exclusion to the mass ratios of co-polymer / DNA showed differences between the co-polymers in accordance with expectation. The co-polymer containing the highest PEG : pLL ratio in each subgroup produced a profile shifted furthest to the right away from that of polylysine. As the ratio of PEG : pLL decreased, so the profile shifted to the left, approaching that of polylysine more when the PEG content was lowest. This phenomenon was clearly a function of the mass associated with each unit charge, which varied according to the ratio of neutral / cationic components within each co-polymer.

The minimum molecular weight of a repeating unit of polylysine contained in any of the co-polymers was 5000, which was equivalent to 38 lysine units. This chain length appeared to be sufficient to condense the DNA. Studies with various chain lengths of polylysine by Lucas (1995) indicated that for a short chain length polymer (DPn = 13), the interaction no longer exhibited a 1:1 stoichiometry; much higher lyine / phosphate ratios were required to produce maximum ethidium exclusion. Leng and Felsenfeld (1966) established that the interaction of polylysine with DNA was affected by the size of the polylysine used, but that between chain lengths of 7-200 the observed interactions appeared fairly uniform. This is at odds with the data reported by Lucas (1995) although the material used by Lucas (1995) was not sufficiently well characterised to allow firm conclusions to be drawn.

4.4.2. Transfection of B16 melanoma cells.

The prerequisite for chloroquine to effect transfection of co-polymer-DNA complexes in B16 melanoma cells suggested similar mechanisms of uptake and eventual expression to those used by polylysine / DNA complexes. The levels of expression were lower for the complexes produced using the co-polymers than for polylysine systems, which may be a result of the PEG component. The PEG mantle may serve to reduce the interaction of the positively charged core of polylysine-DNA with the negatively charged cell membrane.

As discussed in section 4.4.1, the ethidium exclusion profiles for the co-polymers were not significantly displaced from that of polylysine, indicating little steric hindrance of the polycation-DNA interaction. The differences in transfection efficiencies may therefore have been the result of the co-polymers forming complexes of a different size to the polylysine-DNA complexes, which would modify the rate of absorptive endocytosis. Polylysine has been shown to condense DNA, forming toroid-like structures with a diameter of about 80-100 nm (Wagner *et al.*, 1991) which are small enough to be contained in endocytic vesicles of $\leq$ 150 nm (Watts and Marsh, 1992). Recently, Wolfert and Seymour (1996) have shown that the complex size and polydispersity is determined by the molecular weight of the cationic polylysine used for complexation of the DNA. It was demonstrated that lower molecular weight polylysine molecules produced smaller more homogeneous complexes with DNA.

It has been demonstrated by Chiou *et al.* (1994) that complexation of plasmid DNA with polylysine confers resistance to nuclease degradation compared with the

rapid degradation of uncomplexed DNA. Hence, the DNA could be protected from nuclease degradation to a lesser degree by complexation with different polymers. Alternatively, the complex components could be interacting more strongly, hence reducing release of the DNA from the co-polymer inside the cell.

4.4.3. Transfection of HEK293 cells.

The levels of β-galactosidase expression after transfection with many of the co-polymer-DNA complexes in the presence of chloroquine were comparable to that obtained with DOTAP. In all but one case, the transfection efficiency observed was greater than for polylysine-DNA complexes in the presence of chloroquine. This indicated that the presence of PEG either served to enhance endosomal release in this cell line, or conferred a greater degree of protection on the DNA from enzymatic degradation.

A study by Maggio *et al.* (1976) demonstrated that poly(ethylene glycol) was capable of reducing the surface potential of phospholipid monolayers, and that lower concentrations of polymer reduced the surface potential as the molecular weight increased. This would theoretically encourage the passage of PEG-polylysine-DNA complexes across the plasma membrane and their release from the endosomes. If this was the sole reason for the activity seen with these co-polymers, increased levels of activity would have been observed as the PEG content increased from 5000 to 12000 to 20000. One practical use of the reduction in phospholipid surface potential caused by polyethylene glycol was described by Okada and Rechsteiner (1982), who delivered macromolecules to mammalian cells by the osmotic lysis of pinocytic vesicles. It is

possible that certain cells are more susceptible than other cell lines to the osmotic effects of polyethylene glycol, which would account for the different activity profiles observed in the two cell lines. Enhancement of transfection by chloroquine could be explained if the polyethylene glycol operated by a different mechanism of action than chloroquine. Alternatively, it is possibly that there was a threshold concentration of osmotically active component, and that the chloroquine and PEG had an additive osmotic effect on the membranes.

Another hypothesis which would account for this activity profile is that the presence of the PEG could result in complexes with different morphologies to those produced with polylysine alone. This could allow the polymer and DNA to be separated inside the cell more easily, making the process of nuclear delivery, and hence expression, more efficient. This is not supported by the data for transfection of B16 cells in the presence of chloroquine.

The co-polymers 96-10 (5000:10000) and 96-13 (5000:20000) were the most efficient in their sub-groups at transfection with chloroquine. This may be as a result of two interacting factors: the compactness of the polylysine-DNA complex; the formation of a complete PEG-mantle around the DNA-polylysine complex. Wolfert and Seymour (1996) observed that polylysine-DNA complexes of increasing size were formed as the polylysine chain length increased. Hence, the complexes formed by polymers with a polylysine mass of 5000 would have formed smaller complexes. This would make it easier for a complete PEG mantle to form around the DNA-polylysine complex, hence better protecting the DNA from nuclease degradation than polylysine alone.

The complexes formed with co-polymers with a small mass of polylysine would be expected to form the most compact structures. The activity of the complexes formed by polymers with a polylysine mass of 5000 fall into two categories: either they produced the highest levels of expression in the sub-groups (96-10, 96-13), or the lowest levels (96-7). If enhanced activity was due to the protective effect of a complete PEG mantle in addition to good complexation of the DNA with polylysine, then this may explain the low levels of expression observed with co-polymer 96-7. This is a dangerous assumption since other PEG (5000) polymers produced high levels of transfection.

4.4.4. Transfection activity without chloroquine.

Comparative transfections of polylysine complexes in B16 melanoma cells and HEK293 cells showed that the HEK293 cells exhibited greater activity than B16 cells, both with and without chloroquine. The fact that activity was observed in the HEK293 cells for polylysine-DNA complexes in the absence of chloroquine indicated that there is a difference in the integrity of the endosome of the HEK293 cells compared with the B16 cells. Release of active DNA from the endosome did not rely on the activity of chloroquine, although the inclusion of chloroquine for transfections with the HEK293 cells showed a further increase in expression levels. This showed that although there was some reason why endosomal release was achieved easier in HEK293 cells than in B16 cells, the endosome was still sensitive to the actions of chloroquine, which further

enhanced gene expression. It has been demonstrated that certain cell lines exhibit anomalous endosomal characteristics, such as the erythroleukaemic cell line K-562, which lacks the normal regulation over endosomal acidifcation observed in other cells. The unexpected transfection activities observed in the HEK293 cells may be due to a similar abnormal characteristic.

4.5. SUMMARY

The experimental data presented in this chapter show primarily that *in vitro* transfection studies are highly cell line specific. The activity of complexes formed from PEG-polylysine complexes all exhibited activity in B16 melanoma cells and HEK293 cells, although no trend was observed relating the structure of the co-polymer to biological activity. The co-polymer complexes exhibited lower activity than polylysine complexes in the B16 cells, but this was reversed in the HEK293 cell. Additionally, all of the complexes produced gene expression in HEK293 cells when the transfections were performed in the absence of chloroquine, a phenomenon that was not repeated in B16 cells. Fluorescence quenching studies showed little difference between the behaviour of all of the co-polymers during complex formation.

CHAPTER 5. Adaptation of polycations to allow endosomal release.

5.1. INTRODUCTION

The adaptation of polymers to facilitate the release of complexed DNA from endosomes is not a new concept. Non-linear polycationic polymers (polyamidoamines) have been developed which are capable of binding DNA and also of disrupting the endosome in a manner commonly observed with weak bases (Stenseth and Thyberg, 1989). Polyamidoamines were shown to mediate high levels of reporter gene transfection in a variety of cell lines and this efficiency could be further enhanced by the covalent attachment of an amphipathic peptide to the polymer (Haensler and Szoka, 1993). Studies using the cationic polymer polyethyleneimine (PEI) for gene delivery were based on a similar premise of endosomolysis combined with a DNA-binding capacity at neutral pH (Boussif *et al.*, 1995).

The polymers discussed above all contain residues which are protonated at the acidic pH found within the endosomes (Maxfield, 1932). It is this capacity that appears to explain their endosomolytic action. The branched polymeric network of PEI contains a secondary or tertiary amino group every third atom of the polymeric chain, producing what has been described as a proton sponge. This buffering capacity is believed to protect the DNA from nuclease degradation, and to stimulate lysosomal swelling and membrane rupture, consequently allowing release of the complexed DNA from the lysosome.

The approach taken in the present study involved the synthesis of a block co-polymer containing a cationic element plus an element capable of protonation at lysosomal pH. It was proposed that this would produce a more controlled condensation of DNA than in PEI/DNA complexes. The cationic component of the co-polymer was provided by polylysine and polyhistidine provided the amino groups capable of protonation at the pH within the lysosome. The pKa's of the ionising side chain for lysine and histidine are 10.53 and 6.0 respectively. Initial attempts to construct such a block co-polymer involved carbodiimide coupling of polylysine and polyhistidine. This proved to be a difficult coupling due to the paucity of carboxyl groups available for coupling. After several unsuccessful attempts to purify a co-polymer product, a solid phase synthetic strategy was adopted. This allowed the synthesis of a pure polypeptide $H_{20}K_{25}$.

5.2. MATERIALS AND METHODS

5.2.1. Peptide synthesis.

A Millipore 9050 pepSynthesizer (Millipore corp., Milford, MA, USA) was used for peptide assembly using solid phase synthesis (Atherton-Sheppard, 1989). The solid support resin used was polyethylene-glycol-polystyrene (PEG-PS) (Perspective Biosystems UK Ltd., Hertford, UK), which was pre-derivatised with a linker group and the first amino acid residue of the desired peptide sequence to be synthesized. Amino acids, protected at the primary end with N-(9-fluorenyl)methoxycarbonyl (Fmoc) and activated as O-pentafluorophenyl (Opfp) esters (Perspective Biosystems), were used in coupling reactions for 30 minutes *in situ* using 0.3 M 1-hydroxybenzotriazole (HOBT)

(Aldrich, Dorset, UK) in N,N, Dimethylformamide (DMF, Peptide synthesis grade; Rathburn Ltd, UK). The side chain protection group for both of the amino acids was Boc. Deprotection of the α-amino groups resulted from washing the resin with 20% piperidine in DMF for 5 minutes, then rinsing away the piperidine with DMF for 10 minutes, prior to each coupling step. After the final coupling and deprotection step, the resin was washed with DMF, then dichloromethane (DCM), and finally with diethylether, before drying with nitrogen gas. The peptides were cleaved from the resin and the side chain protecting groups were removed by treating 1 g of the resin with 5 ml Trifluoroacetic acid (TFA)/thioanisole/ethanedithiol/anisole (90:5:3:2) for 4-6 hours. The TFA was evaporated under vacuum, and the peptides were precipitated by the gentle addition of three 20 ml aliquots of ether and the liquid was decanted to remove the thioanisole/ethanedithiol/ anisole. The crude peptide was dissolved in distilled water and lyophilised

5.2.2. Peptide purification.

Peptides were purified using reverse phase high performance liquid chromatography (HPLC). The crude peptide mixture was dissolved in 0.1% acetic acid, 5% acetonitrile, distilled water to 100%, and the pH adjusted to 9.6 with ammonia solution. This was then applied to a self-packed 2.5 x 25 cm POROS column (Perspective Biosystems), and eluted with a linear gradient between 0.1% trifluoroacetic acid, 5% acetonitrile, distilled water to 100% (pH 9.6), and 0.1% trifluoroacetic acid, 5% distilled water and acetonitrile to 100% (pH 9.6). The POROS columns are polymer based, and are suitable for pH ranges between 2-12.

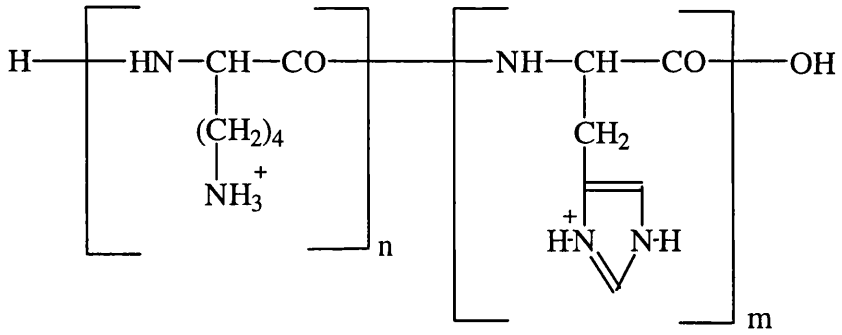

Figure 5.1. Chemical structure of the peptide synthesised by solid phase methods (section 5.1). This co-polymer contained 20 histidine residues (m = 20) and 25 lysine residues (n = 25) . The pKa of the side-chain amino group was 10.53 and 6.0 for lysine and histidine respectively.

5.2.3. Cationic polymers.

The peptide (L-His)$_{20}$-(L-Lys)$_{25}$ ($H_{20}K_{25}$) was synthesised as described in section 5.1. Polyethyleneimine was obtained as a 50% ($^{w}/_{v}$) solution (Fluka) and used to prepare a 10 mM aqueous solution (with respect to the monomer) for complexation studies. Polyhistidine was obtained as the hydrochloride salt (MW 18400) from Sigma.

5.2.4. Complexation of DNA with synthetic peptide, polyhistidine and PEI.

Complexes were prepared with 6 μg of plasmid DNA and polyhistidine (Sigma), $H_{20}K_{25}$ and PEI at the concentrations of interest, to produce a range of charge ratios from 0 - 3.0 (section 3.4). A stock solution of 10 mM monomer PEI was prepared as described by Boussif *et al.* (1995). Briefly, 9 mg of the commercial PEI solution (50% $^{w}/_{v}$) was diluted to 10 ml with water, neutralised with hydrochloric acid, and filter sterilised (0.2 μm filter). This stock solution contained 10 nmol of amine nitrogen per microlitre of solution.

The charge ratio was calculated using the cationic lysine residues, assuming that the histidine residues did not contribute any charge at the pH of preparation (pH 7.4). The complexes were prepared in a total volume of 500 µl of HBS, and incubated for 20 minutes at room temperature after mixing.

The polyhistidine complexes were prepared in a series of citrate-phosphate buffers at pH 4, 5, 6, 7 and 8 (appendix A). The same mass ratios (polymer / DNA) were prepared at each pH.

5.2.5. Ethidium bromide exclusion assay.

DNA complexation by polyhistidine was studied over the mass ratio range 0 - 1.5, in the pH range 4 - 8. The changes were investigated using the ethidium exclusion spectrofluorimetic technique (section 3.2.5.1). The exclusion of ethidium bromide was also monitored for complexes of DNA with $H_{20}K_{25}$ and PEI over the charge ratio ($^{+}$/-) range 0 - 2.5.

5.2.6. Transfection studies in eukaryotic cells.

Complexes were prepared in a total volume of 500 µl HBS as detailed in section 3.2.4. The complexes were incubated at room temperature for 20 minutes, and then added to the culture medium for four hours, either in the presence or absence of 100 µM chloroquine (section 3.2.6). The transfection medium was then replaced with complete

culture medium, and the cells incubated for a further 44 hours before assaying for β-galactosidase expression, using the MUG assay (section 4.2.4). The total protein content was also determined (section 4.2.5).

5.3. RESULTS

5.3.1. Ethidium exclusion assay.

5.3.1.1. The effects of pH on polyhistidine.

The effect of pH on the ionisation of the side-chain amino group of histidine was examined using the ethidium bromide exclusion assay. The interaction between plasmid DNA and the ionised side-chain served to exclude ethidium as more polymer became associated with the DNA. The profile for ethidium exclusion at pH 4 was similar to that observed with polymers that were completely ionised at the experimental pH (section 3.3.1). There was a decrease in fluorescence up to a mass ratio of 1.0, beyond which low background levels were maintained. Increase in pH to 5.0 produced a profile that was displaced to the right, indicating lower availability of protonated amines. At pH 6,7 and 8 very small degrees of exclusion were observed. Even at pH 6, 80% fluorescence was preserved at a mass ratio of 1.5.

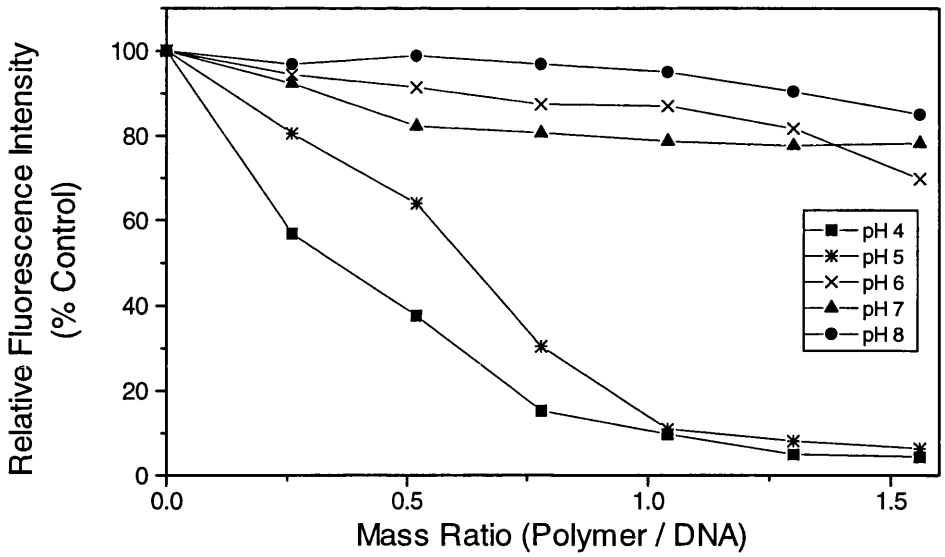

Figure 5.2. Ethidium bromide exclusion assay with poly-histidine-pRSV*lacz* complexes over the pH range 4-8. Complexes were prepared from 6 μg pRSV*lacZ* and varying quantities of polyhistidine, flash mixed and incubated at room temperature for 20 minutes. Ethidium bromide (0.5 μg/ml) was added immediately prior to the measurement of fluorescence. All data points are calculated as a percentage of a control containing 6 μg plasmid DNA, and each point represents the mean (n=3).

5.3.1.2. Polycation-DNA interactions.

DNA complexation by each of $H_{20}K_{25}$, PEI and polylysine was established using the ethidium bromide exclusion assay. The charge ratio for the synthetic peptide $H_{20}K_{25}$ was calculated using only the polylysine component, assuming that the polyhistidine was completely unionised at the experimental pH of 7.4. The profile for $H_{20}K_{25}$ was almost identical to that exhibited by polylysine, with an initial linear decrease to a charge ratio of 1.0, beyond which a minimum background fluorescence level was maintained. The profile for PEI displayed a translocation to the right, reaching a minimum at a charge ratio of approximately 2.0.

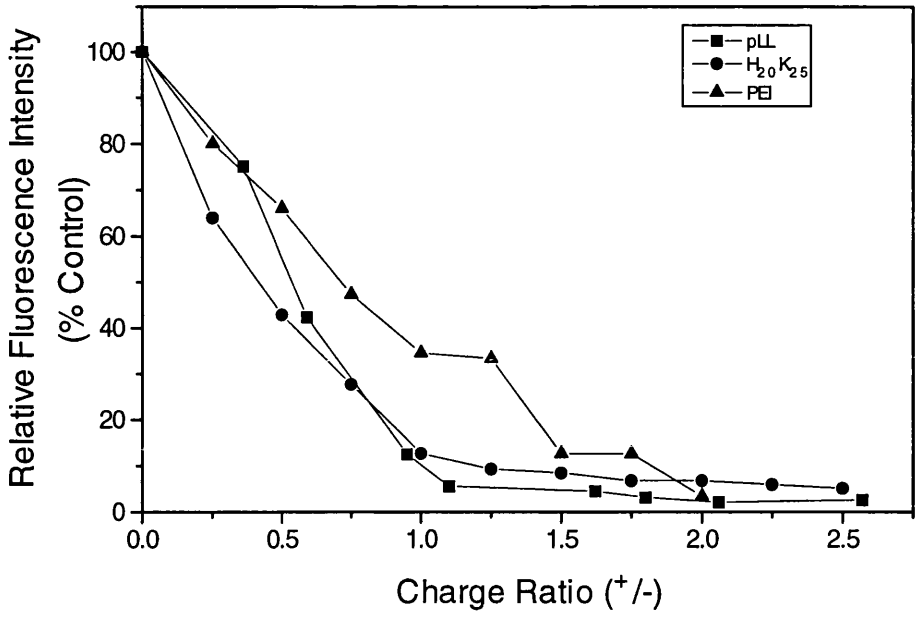

Figure 5.3. Ethidium bromide exclusion assay for complexes formed with plasmid DNA using $H_{20}K_{25}$, PEI or polylysine. The complexes were prepared using 6 μg pRSV*lacZ* and increasing quantities of the respective polymer, to create the required charge ratio (+/-). Ethidium bromide (0.5 μg/ml) was added immediately prior to measurement of the fluorescence. The exclusion for polylysine is shown for comparison. The data points were calculated as a percentage of a control containing 6 μg plasmid DNA, and each point represents the mean (n=3).

5.3.2. Transfection with PEI-DNA complexes.

B16 melanoma cells were transfected with PEI-DNA complexes both in the absence and the presence of the endosomolytic agent chloroquine at a concentration of 100μM (Figs. 5.4 and 5.5 respectively). The charge ratios used for the transfections were high relative to those used for previous polymers for two reasons. Firstly, the ethidium exclusion assay had indicated that charge ratios of approximately 2.0 were required to produce similar exclusion levels to polylysine at a charge ratio of 1.0. Additionally, the proposed mechanism of endosomal release for PEI-DNA complexes

relies on a high charge density accumulating within the endosome to allow the proton sponge activity.

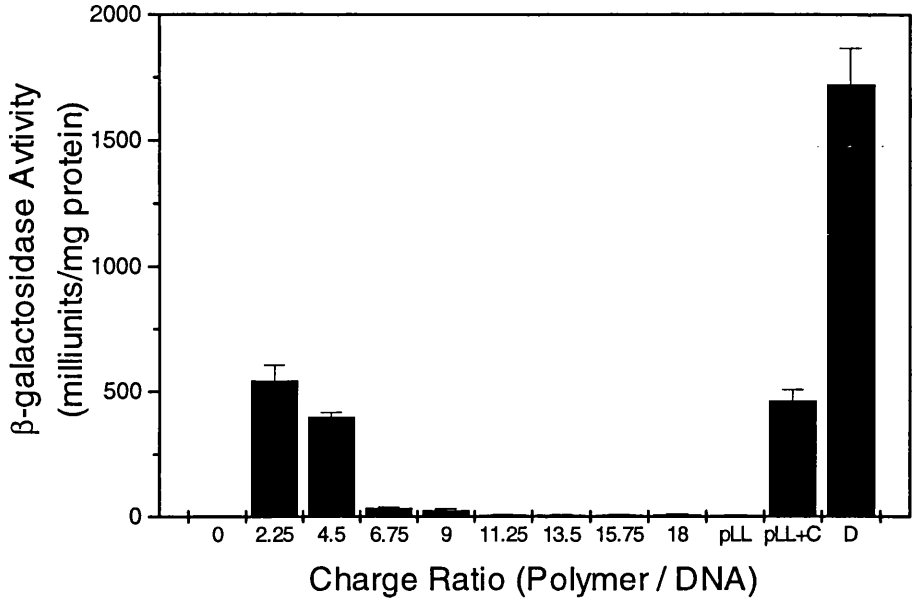

Figure 5.4. Transfection of B16 melanoma cells with PEI-DNA complexes. The complexes were prepared with 6μg pRSV*lacZ* and varying quantities of the PEI polymer, to produce a range of charge ratios ($^{+}$/-). All transfections were carried out in the absence of chloroquine. The cells were assayed after 48 hours for β-galactosidase activity using the fluorescence-based MUG assay. The data were standardised per mg protein. Two positive controls were included: polylysine/DNA with chloroquine, and the liposome DOTAP/DNA complexes without chloroquine, as systems routinely used for successful transfection of B16 melanoma cells. Background levels were established with polylysine without chloroquine. All data points represent the mean ± SEM (n=3).

The transfection activity of PEI-DNA complexes in B16 cells without chloroquine were comparable at charge ratios of 2.25 and 4.5 with the activity of polylysine-DNA complexes in the presence of chloroquine. The other charge ratios studied showed little or no elevation of activity above the background levels seen for polylysine-DNA complexes without chloroquine. An additional positive control of DNA-DOTAP ($^{+}$/- = 2.5) complexes was included as a liposome system known to be

capable of transfection of B16 melanoma cells without chloroquine. The maximum activity for PEI-DNA complexes reached levels of 25% that observed with the liposome system.

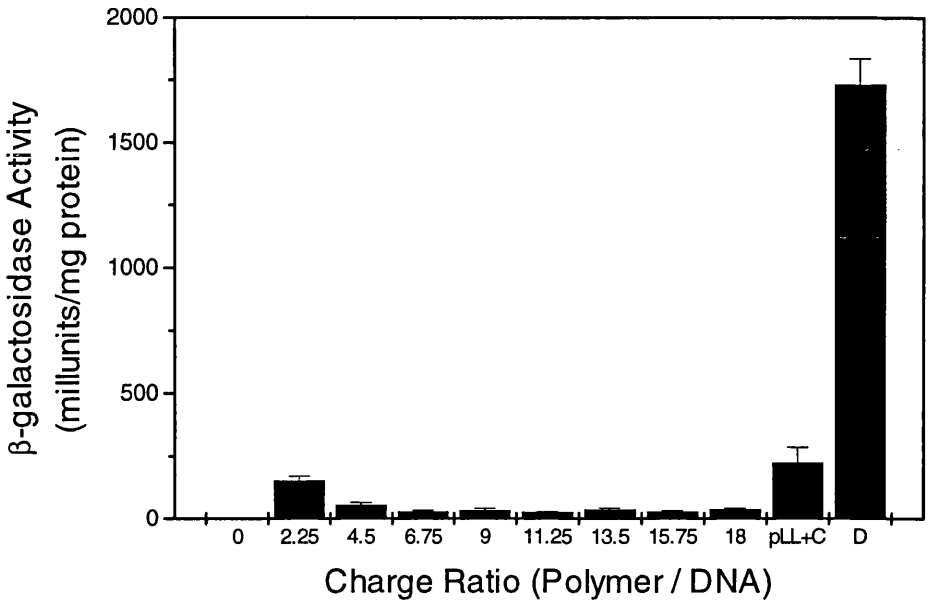

Figure 5.5. Transfection of B16 melanoma cells with PEI-pRSV*lacZ* complexes. The complexes were prepared with 6μg DNA and varying amounts of the cationic polymer, to produce the required range of charge ratios. Transfections were performed in the presence of 100 μM chloroquine. Cell extracts were prepared 48 hours post-transfection, and assayed for β-galactosidase activity using the MUG assay. The protein content of the samples was determined, and the levels of expression calculated per unit mass of protein. Data points represent the mean ± the SEM, (n=3).

The activity profile for transfections using PEI-DNA complexes in the presence of 100 μM chloroquine showed significant expression levels only at a charge ratio of 2.25 (Fig. 5.5). All of the other charge ratios tested showed levels that were similar to control levels. The control levels were established by transfection of plasmid DNA with chloroquine, and this is labeled as a charge ratio of zero on the diagram. The activity of the complexes at a charge ratio of 2.25 was equivalent to approximately 60% the

activity of the polylysine-DNA with chloroquine, and approximately 10% of the activity produced by DOTAP.

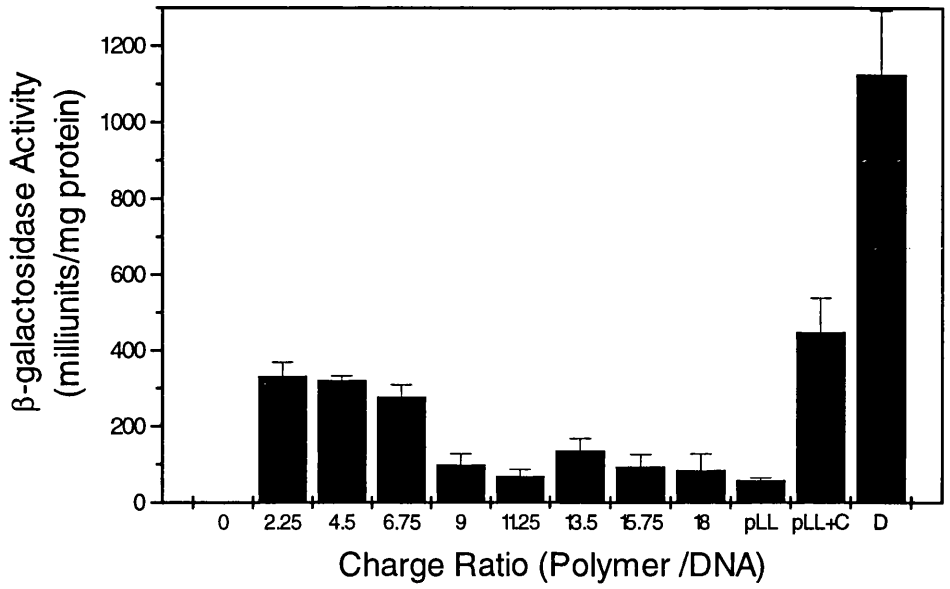

Figure 5.6. Transfection of HEK293 cells with PEI-DNA complexes. Varying quantities of the cationic polymer were mixed with 6 μg pRSV*lacZ* plasmid, to produce the range of charge ratios. Transfections were performed in the absence of chloroquine. Positive controls included polylysine-DNA complexes in the presence of chloroquine and DOTAP/DNA (+/- 2.5). The cells were assayed 48 hours after the transfection using the MUG assay, for detection of β-galactosidase activity. Data points represent the mean ± SEM (n=3).

PEI-DNA complexes were also tested in HEK293 cells in the absence of chloroquine (Fig. 5.6). The profile showed activity over a wider range of charge ratios than observed in the B16 cells, either with or without the inclusion of chloroquine. The highest levels of activity were produced at charge ratios of 2.25 and 4.5, which were approximately 75% of the levels seen with polylysine and chloroquine, and 25% of the activity with DOTAP-DNA complexes. All of the PEI-DNA complexes at different charge ratios produced activity levels greater than those observed with polylysine in the

absence of chloroquine. The polylysine system produced activity levels approximately 10% of those observed for polylysine with chloroquine.

5.3.4. Transfection using the synthetic peptide $H_{20}K_{25}$.

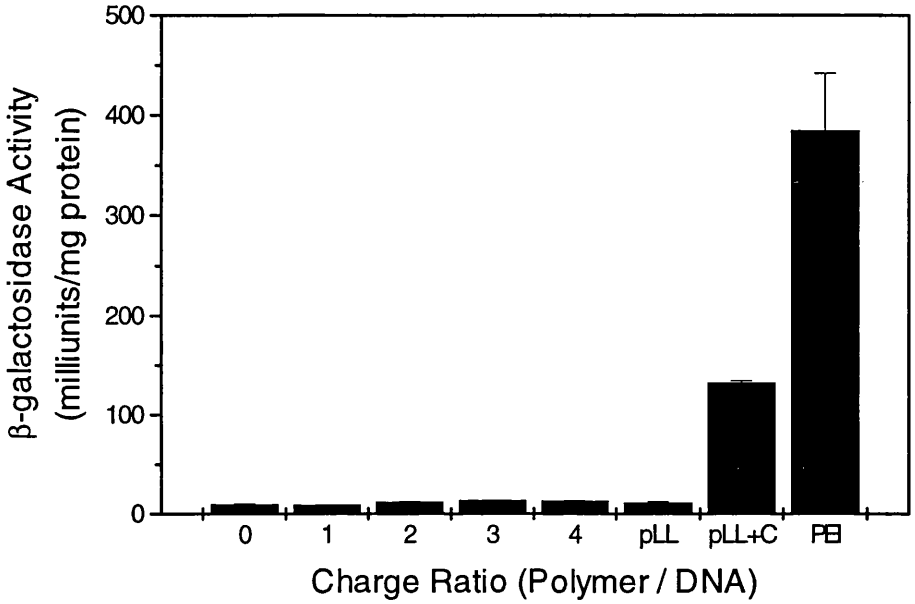

Figure 5.7. Transfection of B16 melanoma cells with complexes of $H_{20}K_{25}$ with DNA. Various quantities of the peptide were mixed with 6 μg pRSV*lacZ* plasmid, to produce the range of charge ratios. Transfections were performed in the absence of chloroquine. Positive controls used for comparison included polylysine-DNA complexes (charge ratio 1.5) plus chloroquine and PEI-DNA complexes (charge ratio 2.25) in the absence of chloroquine. The cells were assayed for β-galactosidase activity 48 hours post-transfection using the MUG assay. Data points represent the mean ± SEM (n=3).

Transfections were performed using complexes formed over a range of charge ratios using $H_{20}K_{25}$ and plasmid DNA. The activity levels were tested in both B16 and HEK293 cell lines, and transfections were performed in the absence of chloroquine in both cases. The positive controls used in the experiments included polylysine-DNA complexes at a charge ratio of 1.5 in the presence of chloroquine, and PEI-DNA complexes at a charge ratio of 2.25 without chloroquine. Polylysine-DNA complexes

(charge ratio 1.5) were also used in the absence of chloroquine as a marker for background activity levels.

The β-galactosidase activity levels observed in the B16 melanoma cells (Fig. 5.7) were comparable with the background levels observed with plasmid DNA alone, or polylysine-DNA complexes in the absence of chloroquine. The expression levels detected in the HEK293 cells after transfection with $H_{20}K_{25}$-DNA complexes in the absence of chloroquine (Fig. 5.8) showed a little enhancement over background levels, producing only 36% activity compared with polylysine-DNA complexes alone. This was equivalent to 10% of the activity of polylysine-DNA complexes plus chloroquine, and only 4% of the activity of PEI-DNA complexes.

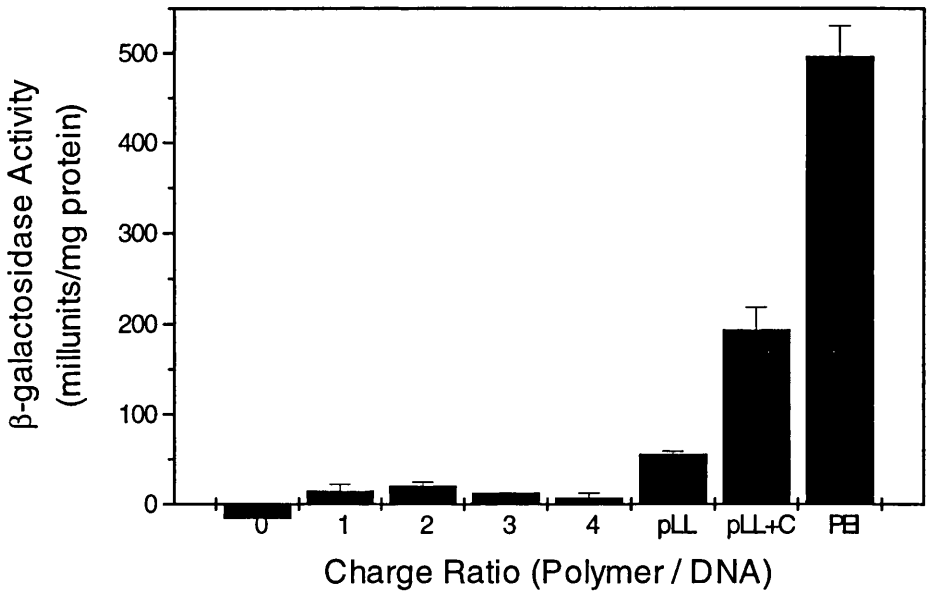

Figure 5.8. Transfection of HEK293 cells with complexes of the $H_{20}K_{25}$ with DNA. Various quantities of $H_{20}K_{25}$ were mixed with 6 μg pRSV*lacZ* plasmid, to produce the range of charge ratios. Transfections were performed in the absence of chloroquine. Positive controls used for comparison included polylysine-DNA complexes (charge ratio 1.5) plus chloroquine and PEI-DNA complexes (charge ratio 2.25) without chloroquine. The cells were assayed for β-galactosidase activity 48 hours post-transfection using the MUG assay. Data points represent the mean ± SEM (n=3).

5.4. DISCUSSION

The development of more efficient non-viral vectors for gene therapy is reliant on improving the transport of the DNA from the extracellular matrix to the nucleus of the target cell. Oligonucleotides have been shown to enter cells by endocytosis (Akhtar and Juliano, 1992), and most have been shown to pass through the endosome (Shoji, 1991). The use of chloroquine to enhance plasmid DNA delivery and resultant expression (Zatloukal *et al.* 1992) is routine for polycation-DNA delivery systems *in vitro*. Alternative approaches to overcome the use of chloroquine for development of *in vivo* vectors have included the use of synthetic viral fusogenic peptides which have endosomolytic activity (Gottschalk *et al.*, 1996), or the use of amphipathic polyamidoamines (Kukowska-Latallo *et al.*, 1996). These polymers are postulated to buffer the pH change in the lysosome, hence reducing the nuclease activity. The buffering activity is also believed to enhance lysosomal swelling and membrane rupture because of osmotic effects. The approach used here involved the synthesis of a polypeptide combining a DNA-binding moiety (oligolysine), and a component capable of buffering the pH of the endosome (oligohistidine). For comparison the studies involved evaluation of the transfection capacity of polyethyleneimine, a polymer with reported lysosomal buffering capacity (Boussif *et al.*, 1995).

5.4.1. Ethidium exclusion assays.

The exclusion assay was initially used to establish the effect of pH on the ionisation of the side-chain amino group of the polyhistidine. The pKa of this side-chain amino group is 6.0, and hence at pH 4.0, 99% of the amino groups would theoretically have been ionised. This was reflected by the similarity of the ethidium exclusion profile for polyhistidine compared with the polylysine profile. As the pH was increased from 4 to 5, 6, 7 and 8, the theoretical degree of ionisation at the side chains were reduced to values of 90%, 50%, 10% and 0.99% respectively. This was reflected by a reduction in the capacity of the polyhistidine to exclude the ethidium from interaction with the plasmid DNA, as observed by the maintenance of high levels of fluorescence with increasing mass ratios of polymer : DNA. This test demonstrated that the polyhistidine would not complex DNA at pH 7.4, but would be capable of a buffering action at acidic pH values, as found within the endosomes (Maxfield, 1982).

The exclusion assay for the synthetic peptide $H_{20}K_{25}$ showed that if it was assumed that only the lysine residues would be charged at pH 7.4, the exclusion profiles for $H_{20}K_{25}$ and polylysine were very similar. Precise estimation of the degree of polyhistidine ionisation showed that 3.8% of the histidine residues would be ionised at pH 7.4, indicating that there was a very slight underestimation of the positive charge within the system. This was not expected to cause a significant problem in the interpretation of data.

The profile for PEI displayed some irregularity compared with the exclusion patterns seen with polycations such as polylysine. Although there was a reduction in fluorescence associated with an increase in charge ratio ($^{+}$/-), the decline was not of the characteristic sharpness, nor was a minimum background level reached and maintained until a charge ratio of 2.0 was used. This was likely to be due to the actual mass ratios of the polymer / DNA present in the mixing environment. A charge ratio ($^{+}$/-) of 1.0 was equivalent to mass ratios of 0.44, 0.72 and 0.13 for polylysine, $H_{20}K_{25}$ and PEI respectively. The PEI molecule would have a high charge density, which could possibly cause steric problems for the interaction of the negatively charged nucleotides. Twice as much charge was required to reach the background fluorescence levels observed for polylysine. The charge ratio was calculated from the amine nitrogen content of the PEI. At pH 7.4, only half of the nitrogen atoms would be expected to be protonated, in line with the capacity for PEI to accept protons as the pH decreased.

5.4.2. Transfection with PEI-DNA complexes.

The comparative activities of the various PEI-DNA formulations after transfection into B16 cells both in the presence and absence of chloroquine demonstrated distinct differences to the polylysine-DNA complex activity profile. Since the levels of activity were higher than the positive controls in the absence of chloroquine, it was possible that the chloroquine was destabilising the PEI/DNA complexes. Alternatively, the PEI could have effected endosomal release by the same

mechanism as the chloroquine, and this process may have already been maximised so that no further increase in DNA release could be produced. The optimum charge ratio for transfection of PEI/DNA complexes without chloroquine using B16 cells was established. These conditions were used as a positive control when examining complexes believed to facilitate endosomal release by buffering endosomal acidity, a similar mechanism to PEI.

PEI-DNA complexes were transfected into HEK293 cells without chloroquine. The experiment was not repeated with chloroquine since HEK293 cells have previously shown that they are capable of detectable expression levels in the absence of chloroquine for polylysine-DNA complexes. These cells demonstrated activity comparable with polylysine and chloroquine at the optimal charge ratios of PEI/DNA of 2.25 and 4.5. For the majority of charge ratios studied, the PEI-DNA complexes exhibited greater activity than polylysine-DNA complexes in the absence of chloroquine, demonstrating some advantage due to the formulation. It can be postulated that this is due to increased sensitivity to a buffering action of the polymer within the endosome. The theory that the integrity of the endosomes in the HEK293 cells exhibits distinct differences to the endosomes found in B16 cells has already been discussed (section 4.4.4).

5.4.3. Transfection with $H_{20}K_{25}$.

Transfection of complexes using $H_{20}K_{25}$ and plasmid DNA produced no detectable levels of activity in B16 cells, and very low levels of expression in the HEK293 cells. At the optimum formulation, 36% of the level of activity of transfection observed with polylysine-DNA complexes in the absence of chloroquine was obtained. This demonstrated no enhancement over polylysine for complexation and delivery of the DNA.

A possible explanation for this is that the mass of unprotonated amine delivered to the endosome was too low to disrupt the endosomal membrane. PEI is often used at higher charge density, which may be necessary to promote escape of the plasmid. Also, the early endosome maintains an internal environment at pH 6.2, and these conditions would induce ionisation of approximately 39% of the histidine side-chain amino groups. At the pH in the lysosomes (5.2), roughly 86% of the histidine residues would be ionised, and although this provides more buffering capacity to effect the escape mechanism, DNA would be exposed to lysosomal enzymes to some extent. This process has been studied by Hughes *et al.* (1996) who compared the fate of a lipid that becomes fusogenic at the pH within the early endosome with a pH sensitive polymer that had previously shown membrane activity with phospholipid vesicles (Tirrell *et al.*, 1985).

An alternative theory to explain the lack of enhancement using this system for DNA delivery is that the decrease in pH as the complex enters the endosome and possibly the lysosome affects the polyhistidine amino groups. Since the pKa of the polyhistidine amino groups is 6.0, more of the groups become ionised as the pH becomes more acidic. These ionised amino groups are then able to contribute to the cationic charge supplied by the co-polymer in the system. This factor would affect the overall cation / anion ratio, hence affecting the interaction of the polymer with the DNA. It has previously been demonstrated that above a threshold charge ratio, the activity profile decreases (section 3.3.2.2), so the endosomal environment may be altering the charge ratio of the complexes to more cationic systems than has been calculated. This could theoretically produce a system where the complexes were more strongly held together, and the reduced activity profile may be due to less of the DNA being released from association with the co-polymer after release from the endosome. This would serve to reduce nuclear delivery and hence resultant transcription and expression.

Due to time limitations, no transfections using $H_{20}K_{25}$-DNA complexes were performed in the presence of chloroquine. Enhancement of activity with the use of chloroquine would have confirmed that the polyhistidine component was incapable of effecting endosomal release of the DNA. Alternatively, if the chloroquine produced no increases in activity, it would have indicated that the polyhistidine was capable of causing endosomal release, but that the DNA was not reaching the nucleus for subsequent transcription, or that transcription itself was being inhibited.

5.5. SUMMARY

Plasmid DNA can be complexed using polycations, even if they contain endosomolytic components. Polymers with a very high charge density appear to require larger quantities of polymer to completely complex DNA, as determined by the ethidium exclusion assay. Polymers with extensive buffering capacity in acidic pH conditions can enhance endosomal escape mechanisms for DNA. Polyhistidine acts as a buffer at low pH values, and conjugation of polyhistidine to polylysine did not appear to affect the DNA-binding capacity. Detectable levels of β-galactosidase activity were not observed in either B16 or HEK293 cells after transfection with peptide $H_{20}K_{25}$-DNA complexes in the absence of chloroquine.

CHAPTER 6. Physical characterisation of polycation-DNA complexes.

6.1. INTRODUCTION

The previous chapters have concentrated on characterisation of the interaction of polycations and plasmid DNA using the ethidium exclusion assay combined with *in vitro* biological transfection data. The combination of these two experimental procedures has revealed basic information about the attributes of complexes which rendered them active for transfection, but a more detailed study into the physical characteristics of each complex was deemed necessary. The stability of these complexes in different environments was also an important issue with a view to production of a pharmaceutical product. A clearer understanding of the uptake mechanisms associated with each complex, and the affect of the physical composition and structure of the complexes on gene delivery and expression were other areas identified as crucial to the development of non-viral vectors for *in vivo* use.

6.1.1 Particle sizing by photon correlation spectroscopy.

Photon correlation spectroscopy (PCS) is a technique used for measuring the dynamic changes in light scattering associated with macromolecular and colloidal systems. Particles in solution undergo the random movement of Brownian motion, which occurs due to collisions with the smaller molecules of the continuous phase. The suspended particles are constantly in a state of motion, and hence undergo diffusion. Diffusion is governed by the average distance of travel before collision

with another molecule, which causes a diversion from the original path of motion. When a solution of macromolecules is illuminated, the light is scattered by the particles in Brownian motion, and the intensity of this light yields information regarding the molecular weight.

PCS analyses the constantly changing patterns of laser light scattered or diffracted by particles in solution, exhibiting Brownian motion. The rate of change of the scattered light during diffusion is monitored. The scattered light displays a spectrum of frequencies due to the Doppler effect. Fluctuations in the intensity arise because the centres of light scattering are constantly moving, producing different extents of interference. An autocorrelation function allows the intensity fluctuations to be characterised. The intensities are measured at short time intervals (5-10 μs) over a longer time period of several minutes, and recorded digitally.

PCS allows estimation of the translational diffusion coefficient (D). D is related to the equivalent hydrodynamic radius of the particle by the Stokes-Einstein equation:

$$D = \frac{k_B T}{6\pi\eta r_h}$$

where k_B is the Boltzman constant, T is the absolute temperature (Kelvin), η is the viscosity of the solvent and r_h is the hydrodynamic radius.

6.1.1.1. Analysis.

CONTIN analysis was used to fit the experimental intensity decay curve with a curve calculated assuming a distribution of decay rates. This method extracts a smoothed or regularised size distribution by matrix techniques. Larger particles produce a greater intensity of scattered light, and this may interfere with the intensity from smaller species. In extreme cases, the intensity of light scattered from small particles may be masked by the interference and intensity from only a tiny percentage of large particles within the population.

Solutions which contain more than one species require correction for the intensity interference problems. The correlation function contains the same number of terms as species in the sample, but each term is weighted by the intensity of light scattered from each species. The output from CONTIN analysis includes information about weight and number distribution within the sample.

6.1.2. Isothermal titration calorimetry.

Isothermal titration calorimetry measures the energetics of biochemical or molecular reactions, such as ligand-binding phenomena, at constant temperature. A heat change is an almost universal property of binding reactions, and the sensitivity of the equipment enables measurements to be made from nanomole quantities of reactants (Wiseman *et al.*, 1989). This method allows the generation of a binding isotherm, which allows the binding saturation of the ligand to be determined. The experimental method involves titration of a reactant into the sample solution containing the other reactant. After the addition of each aliquot, the heat changes are monitored by the isothermal titration calorimeter.

6.2. MATERIALS AND METHODS

6.2.1. Stability of polymer-DNA complexes in serum.

Complexes were prepared using 6 μg of the plasmid pRSV*lacZ*, and sufficient polymer to produce a charge ratio ($^{+}$/-) of 1.5, in a volume of 500 μl HBS (section 3.4). The complexes were incubated at room temperature for 20 minutes before adding to 1.5 ml complete culture medium. This was incubated at 37°C for 4 hours, before removing a 40 μl aliquot, adding 10 μl of 5x loading buffer and mixing. A 15 μl aliquot was loaded onto a 1% horizontal agarose gel, which was run at a constant voltage (80V) for one hour. The gels contained ethidium bromide (0.5 μg/ml), allowing visualisation of the DNA. The gels were then viewed and photographed over a UV light box, as described in section 2.10.

6.2.2. Toxicity of free polymer or DNA-polymer complexes.

Toxicity studies were performed on the polymers supplied by Sigma (Table 3.1) using the MTT assay (section 2.19). B16 melanoma cells were seeded at 3000 cells per well, and allowed to adhere in complete medium under standard incubation conditions for one hour. Free polymer toxicity was determined by the addition of aliquots of polymer stock solutions (0.05 μg/ml) to the wells over the concentration range 0 - 10 μg/ml. The cells were incubated under standard conditions for 4 hours, the supernatant removed, and MTT (1 mg/ml) in serum free medium added to each well. The remainder of the assay was performed as detailed in section 2.19, and the percentage of cell survival was determined compared to a control, to which no polymer had been added.

The poly-L-lysine-DNA complex was assessed for toxicity in a similar manner. Complexes at a charge ratio ($^{+}$/-) of 1.5 were produced using 6 μg plasmid DNA and the appropriate mass of polymer. The complex was incubated at room temperature for 20 minutes, before adding aliquots of the mixture to the wells, producing a concentration range of poly-L-lysine from 0 - 6 μg/ml. The incubation procedure and MTT assay were identical to that for the free polymers. A toxicity profile was prepared in parallel for free poly-L-lysine over the same range of concentrations for direct comparison between free and complexed poly-L-lysine.

6.2.3. Size analysis of polymer-DNA complexes.

Polymer-DNA complexes were sized by the method of photon correlation spectroscopy (section 6.1). Complexes were prepared as detailed in section 3.4 in water not HBS, using 6 μg plasmid DNA and varying quantities of polymer, to produce a variety of charge ratios ($^{+}$/-). The complexes were incubated for 20 minutes at room temperature, then 1.5 ml distilled milliQ water was added, and then placed in sample bottles in the water-bath of a PCS 100SM (Malvern, UK) with a Coherent Innova 90 laser. This was connected to a B1-9000 AT digital correlator (Brookhaven Instruments), which performed CONTIN analysis on the collected data.

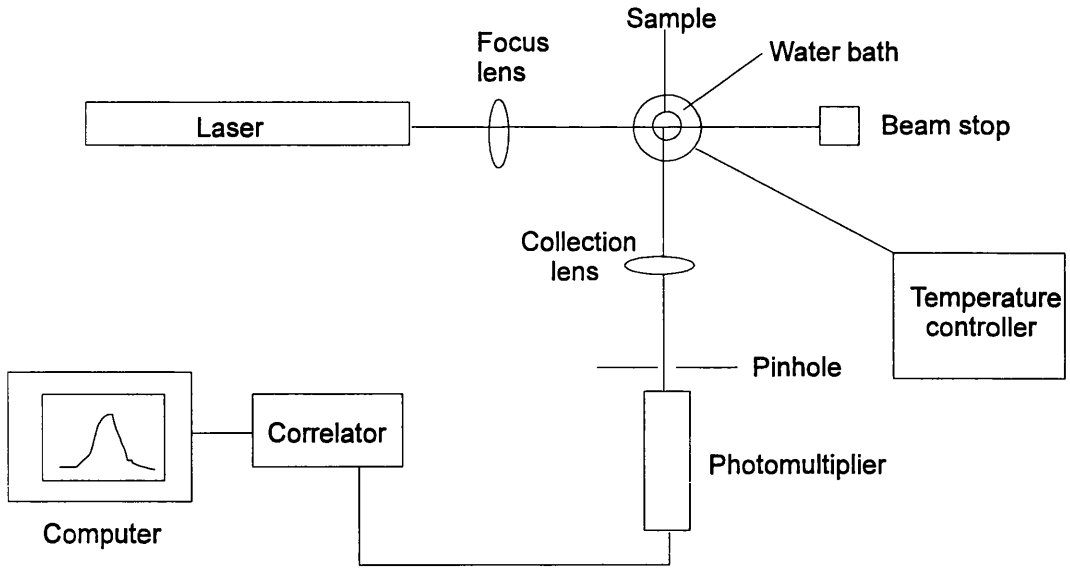

Figure 6.1. Schematic diagram of photon correlation spectroscopy system.

6.2.4. Thermometric activity monitoring .

A solution containing 0.5 mg DNA in 2.5 ml HBS was prepared and placed into the stainless steel ampoule of a 4 ml titration unit (Thermometric, Sweden), the ampoule was sealed and lowered in stages into the ThermoMetric 2277 Thermal Activity Monitor. A solution containing 10 mg/ml polylysine (Sigma. U.K.) in HBS was used to fill a 200 µl graduated glass syringe linked to a canula, which was then inserted into the titration shaft. The polylysine solution was titrated into the DNA solution in 4 µl aliquots at 15 minute intervals, while stirring at a rate of 10 rpm. This process was continued until a total volume of 200 µl polylysine solution had been dispensed. A control was performed to calculate the heat associated with dilution of the DNA solution by the addition of 4 µl aliquots of HBS for a total of 200 µl.

6.2.5. Uptake of polypeptide-DNA complexes by B16 melanoma cells.

The uptake of DNA-polypeptide complexes by B16 melanoma cells was analysed using flow cytometry. FITC-labelled poly-L-lysine (Sigma, MW 11800) and standard poly-L-lysine (Sigma, MW 45700) were mixed with plasmid DNA to produce complexes according to the normal protocol (section 3.4). Complexes were prepared at charge ratios ($^{+}$/-) of 1.5, 2.0, 2.5, and 5.0. The FITC-polylysine component was kept constant while increasing the standard polylysine constituent. Cells were plated onto 6-well plates 18-20 hours prior to transfection and the positively charged complexes were incubated with the cells for four hours (section 3.6). The transfection medium was removed, and the cells were washed three times with ice-cold PBS. The adherent cells were removed from the plates with Trypsin-EDTA, and collected by centrifugation in a 1.5 ml microcentrifuge tube. The cells were washed two more times, before resuspension in 1.0 ml of PBS.

The fluorescence intensity of each sample was measured relative to a control population of cells using a FACS Vantage analyser (Becton Dickinson). The viability stain propidium iodide (100 ng/ml; Dako Ltd., U.K.) was added to each sample immediately prior to analysis, and the data collection (FL-1 emission spectrum) was gated for the live cells only. A minimum of 5000 cells were analysed per sample, and this was increased to 10000 where cell viability was sufficiently high to allow for this. Comparative transfection studies by D. Milroy at 4°C and 37°C (unpublished results) have shown that there was little complex remaining adsorbed to the cell surface after the washing procedure.

6.2.6. Effect of free polylysine on complex uptake by B16 melanoma cells.

The effect of free polylysine on the uptake of polylysine-DNA complexes by B16 melanoma cells was analysed using flow cytometry. Complexes were prepared from FITC-polylysine and plasmid DNA at a charge ratio of 1.5 (section 3.4). The complexes were added to the transfection medium of B16 cells in 6-well plates, and unlabelled polylysine was added to the medium to produce an effective charge ratio of 2.5, 5.0, 7.5, and 10.0. The cells were incubated with these systems for four hours, before washing with PBS and collecting the cells for FACS analysis as detailed in section 6.7. The cells were stained with propidium iodide (100 ng/ml) and the data collection was gated to analyse only the live cells in the population.

6.3. RESULTS

6.3.1. Stability of polycation-DNA complexes in serum.

Representative electrophoretic gels displaying the stability of complexes prepared from the various polycations and plasmid DNA are shown in Figures 6.2 and 6.3. The complexes were prepared at a charge ratio of 1.5 ($^{+}$/-), as it was assumed that the plasmid DNA would be completely complexed by the polycations at this charge ratio. Figure 6.2 shows the homopolymers and co-polymers supplied from Sigma, as detailed in section 3.2.2. These included poly-L-lysine, poly-D-lysine, polyornithine, polyarginine, lysine-alanine (1:1), lysine-alanine (2:1) and lysine-alanine (3:1) in lanes 5 - 11 respectively. Additionally, plasmid DNA incubated in HBS, serum alone and plasmid DNA incubated in serum are shown in lanes 2 - 4 respectively. Lanes 1 and 12 contain the molecular weight marker λ DNA with *Hind* III and *EcoR* I digests.

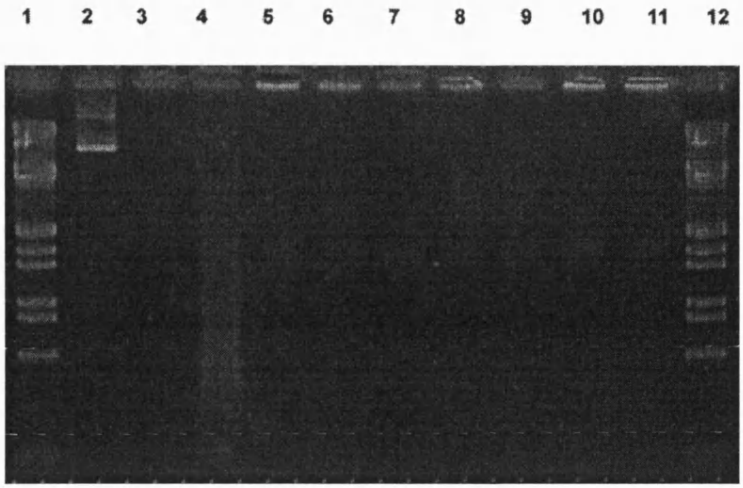

Figure 6.2. Agarose gel displaying stability of complexes prepared using plasmid DNA and the homopolymers and co-polymers supplied by Sigma (section 3.2.2). The complexes were prepared in HBS as detailed in section 3.2.4, incubated in DMEM supplemented with 10% serum for 4 hours before loading onto a 1% agarose gel and running at 80V for one hour. Complexes prepared using poly-L-lysine, poly-D-lysine, polyornithine, polyarginine, lysine,alanine (1:1), lysine,alanine (2:1) and lysine,alanine (3:1) were loaded into lanes 5 - 11 respectively. Lanes 2 - 4 contain plasmid DNA in HBS, serum, and plasmid DNA incubated in serum respectively. Lanes 1 and 12 contain the molecular weight marker λ DNA with *Hind* III and *EcoR* I digests.

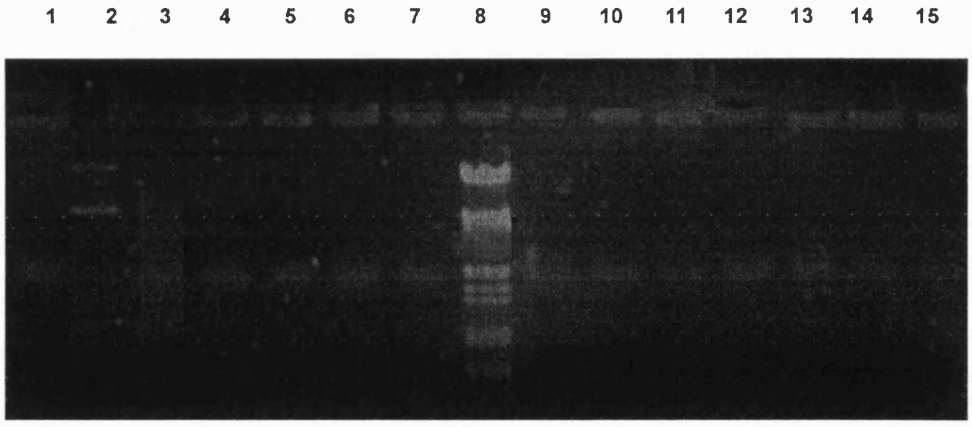

Figure 6.3. Agarose gel displaying stability of complexes prepared using plasmid DNA and PEG-pLL (section 4.1), $H_{20}K_{25}$ and PEI (section 5.3). The complexes were prepared in HBS as detailed in section 3.2.4, incubated in DMEM supplemented with 10% serum for 4 hours before loading onto a 1% agarose gel and running at 80V for one hour. Complexes prepared using PEI and $H_{20}K_{25}$ were loaded into lanes 4 and 5, while complexes prepared using PEG-pLL 96-7 through to 96-15 were loaded in lanes 6 - 15 respectively. Lanes 1 - 3 contain serum, plasmid DNA in HBS, and plasmid DNA incubated in serum respectively. Lane 8 contains the molecular weight marker λ DNA with *Hind* III and *EcoR* I digests.

All of the plasmid-DNA complexes remained in the wells during electrophoresis and no DNA smearing was observed, indicating that these systems were stable to the degradative nature of the serum enzymes. The plasmid DNA incubated in HBS (lane 2) exhibited no degradation, and the bands represent, from the bottom of the gel to the top, supercoiled and open circular conformations respectively. The free plasmid DNA incubated in serum was degraded, as indicated by the small fragments observed migrating rapidly through the gel causing smearing (lane 4). Lane 3 contained serum alone, to demonstrate any background fluorescence due to the presence of various proteins contained in the serum.

A similar profile was observed when the stabilities of the PEG/pLL/DNA (section 4.1), $H_{20}K_{25}$/DNA and PEI/DNA (section 5.3) complexes were examined (Fig. 6.3). Serum was run in lane 1, plasmid DNA in HBS and plasmid DNA in serum were loaded into lanes 2 and 3 respectively. Complexes formed using PEI, $H_{20}K_{25}$ and the PEG-pLL polymers were loaded into lanes 4 to 15, with lane 8 containing the molecular weight marker λ DNA with *Hind* III and *EcoR* I digests. The PEG-pLL co-polymers 96-7 through to 96-15 were in lanes 6 - 15 respectively (except lane 8).

All of the DNA-polycation complexes were prepared at a charge ratio of 1.5 ($^{+}$/-) and remained in the wells of the gel. This indicated that the DNA was fully complexed with the polycations in each case, and the lack of smearing in the lanes showed that the DNA was protected from enzymatic degradation under the incubation conditions. The plasmid DNA incubated in serum (lane 3) showed the degraded fragments of DNA migrating at different rates through the gel, causing the

characteristic smear. Lane 2 contained plasmid DNA in HBS, and the two bands represent open circular and supercoiled conformations moving from the well respectively. Lane 1 contained serum alone, and the fluorescence in this lane indicated any non-specific interaction of serum components with the ethidium bromide, for comparison with all of the other samples.

6.3.2. Polymer toxicity studies.

The comparative toxicities of the uncomplexed polycations were determined using the MTT assay (section 2.2.19) over the concentration range 0 - 10 μg/ml). The cationic homopolymers exhibited similar toxicities (Fig. 6.4A), each having an EC50 of approximately 3 μg/ml. The poly (lysine, alanine) co-polymers exhibited varying degrees of toxicity, which correlated with the ratio of alanine to lysine (Fig. 6.4B). The co-polymer containing the ratio of lysine : alanine 1:1 was considerably more toxic than either the 2:1 or 3:1 co-polymer. The lys,ala (1:1) co-polymer had a similar toxicity profile to that of polylysine, whereas the remaining two co-polymers were less toxic than polylysine at all of the concentrations studied.

The toxicity of the free polylysine was compared with that of polylysine complexed to plasmid DNA (Figure 6.5). At all of the concentrations examined (0 - 6 μg/ml) the complexed polylysine was less toxic to B16 cells. The profiles exhibited a similar shape, but the curve for the complexed polylysine appeared to be displaced to the right of the curve for the free polylysine. No significant toxicity was observed for complexes at concentrations below 2 μg/ml. The estimated EC50 for the complexed polylysine was 4.5 μg/ml, compared with 2.75 μg/ml for the free polylysine.

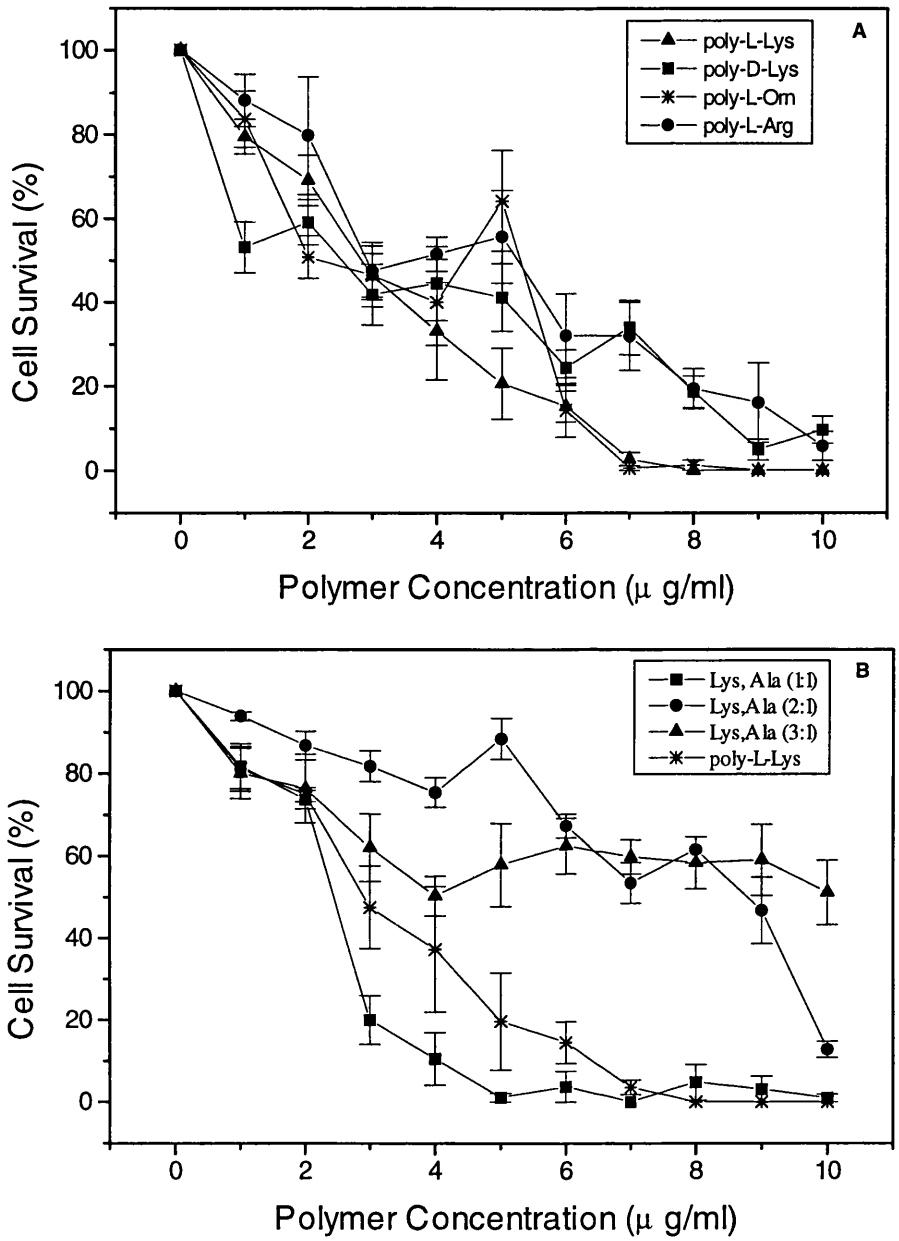

Figure 6.4. Toxicity of free polymers as determined using B16 melanoma cells. B16 cells were seeded at a concentration of 3000 cells per well of a 96-well plate, and allowed to adhere in complete medium for 1 hour. Stock solutions of the polymers (0.05μg/ml) were prepared, and aliquots added to the wells to produce concentrations in the range 0 - 10 μg/ml. The cells were incubated under standard conditions for 4 hours, washed twice with serum free medium, and assayed using the MTT assay (section 2.19). Cell survival was determined by comparison with a control population of cells, which had been incubated in medium alone, using the cell number standard curve (appendix C). Data points represent mean ± SEM (n=4).

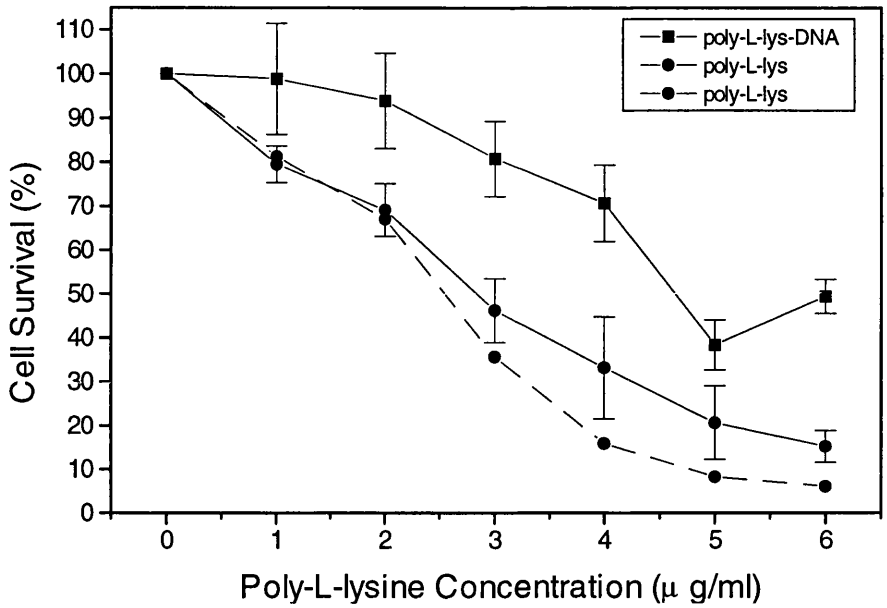

Figure 6.5. Toxicity of free poly-L-lysine on B16 melanoma cells compared with the toxicity of poly-L-lysine-DNA complexes, as determined by MTT assay (section 2.19). B16 melanoma cells were seeded at 3000 cells per well in a 96-well plate, and incubated for one hour in complete medium to allow cell adherence. Poly-L-lysine-DNA complexes were prepared at a charge ratio of 1.5, using 6 μg DNA and the required mass of polymer, and incubated at room temperature for 20 minutes. Aliquots of this mixture were added to the wells, to provide concentrations of poly-L-lysine in the range of 0-6 μg/ml. Free poly-L-lysine was added to wells to provide a similar range of poly-L-lysine concentrations. Cell survival was determined by comparison with a control population of cells, which had been incubated in medium alone, using the cell number standard curve (appendix C). The broken line represents the mean viability of B16 cells in a replicate MTT for poly-L-lysine. Data points represent mean ± SEM (n=4).

6.3.3. Size analysis of polycation-DNA complexes.

6.3.3.1. Size analysis in water.

A representative histogram of the size distribution exhibited by polylysine-DNA complexes at a charge ratio of 1.0 is shown in Fig. 6.6, indicating that the size distribution was narrow. In general complexes were compared using the median diameter and the span of the distribution. The mean of the median diameter for three

replicate experiments with polylysine-DNA complexes at the charge ratio 1.0 ($^{+}$/-) was 86 nm (S.D.of the median = 8.19).

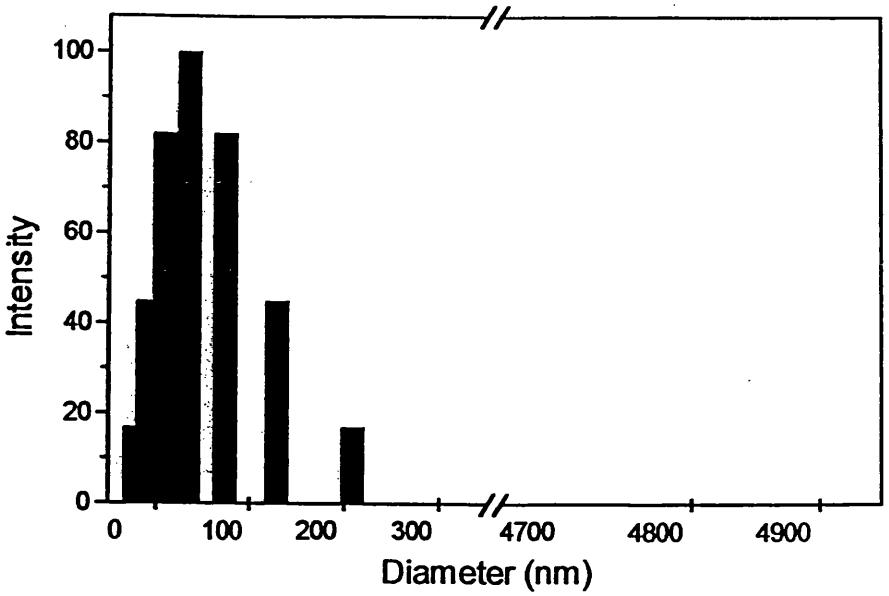

Figure 6.6. Representative histogram of size distribution of polylysine-DNA complexes, as determined by PCS. Complexes were prepared using 6 µg pRSV*lacZ* and polylysine at a charge ratio of 1.0 in a total volume of 0.5 ml water. After incubation for 20 minutes at room temperature, the volume was made up to 2.0 ml with water, and the samples analysed immediately (section 6.2.3).

Table 6.1 shows the size of polylysine-DNA complexes prepared over the range of charge ratios ($^{+}$/-) from 0 to 3.0. The complexes were incubated at room temperature for twenty minutes immediately after mixing, and were then diluted to 2.0 ml in water (section 6.2.3). The complexes maintained a similar size of approximately 100 nm over the range of charge ratios examined. The span of sizes exhibited at each charge ratio was usually seen to be between 40 - 250 nm.

Charge Ratio (+/-)	0.2	0.4	0.6	0.8	1.0	1.5	2.0	2.5	3.0
Diameter (nm)	77	105	132	83	83	88	119	92	117
Span (nm)	55-128	79-140	66-264	41-165	45-173	43-258	86-228	45-270	85-224

Table 6.1. Size analysis of polylysine-DNA complexes, as determined by PCS. Complexes were prepared using 6 μg pRSV*lacZ* and varying quantities of polylysine to produce a range of charge ratios, in a total volume of 0.5 ml water. After incubation for 20 minutes at room temperature, the volume was made up to 2.0 ml with water and the samples analysed immediately (section 6.2.3). Data are representative of three replicate experiments.

The homopolymers and co-polymers supplied from Sigma (section 3.2) were used to prepare complexes at a charge ratio of 1.5, and sized in water. The effective diameters and the span of sizes measured within each population are displayed in Table 6.2. The diameters quoted were the medians, and for all of the systems tested except poly-D-lysine the sizes were approximately 100 - 150 nm, with spans routinely between 70 and 200 nm. The poly-D-lysine apparently produced complexes that were greater than 200 nm, and the span observed in the population was wider than for the other polymers tested (69 - 307 nm).

Sample	PLL	PDL	PLO	PLA	L,A 1:1	L,A 2:1	L,A 3:1
Diameter(nm)	95	231	145	93	145	139	101
Span (nm)	71-127	69-307	109-193	70-124	40-193	104-185	76-135

Table 6.2. Diameter (nm) of complexes formed at a charge ratio of 1.5 between the various polymers and 6μg of the plasmid pRSV*lacZ*. The complexes were initially formed in 0.5 ml water, incubated at room temperature for 20 minutes, and the volume was made up to 2.0 ml with water. The complexes were immediately analysed using PCS (section 6.2.3) to establish the particle diameter.

Median Diameter and Span (nm)			
pLL → PEG ↓	5000	10000	20000
5000	230 173-307	195 102-209	252 218-291
12000	N/A	126 63-251	118 84-333
20000	N/A	197 147-262	133 70-184

(N/A - not available)

Table 6.3. Diameter and span of complexes formed at a charge ratio of 1.5 using the various PEG-pLL co-polymers (Table 4.1) and 6μg pRSV*lacZ*. The complexes were initially formed in 0.5 ml water, incubated at room temperature for 20 minutes, and the volume was made up to 2.0 ml with water. The complexes were immediately analysed using PCS (section 6.2.3) to establish the particle diameter.

Complexes prepared from the PEG-pLL co-polymers (section 4.1) and plasmid DNA at a charge ratio of 1.5 ($^{+}$/-) were analysed in water, and the diameters are displayed in Table 6.4. The complexes had diameters of between 110 to 250 nm, and the spans observed ranged from 60 to 330 nm. The co-polymers with a high PEG:pLL ratio could not be sized using this method for reasons which were not established. No trend was observed with an increase in polylysine content within the co-polymers.

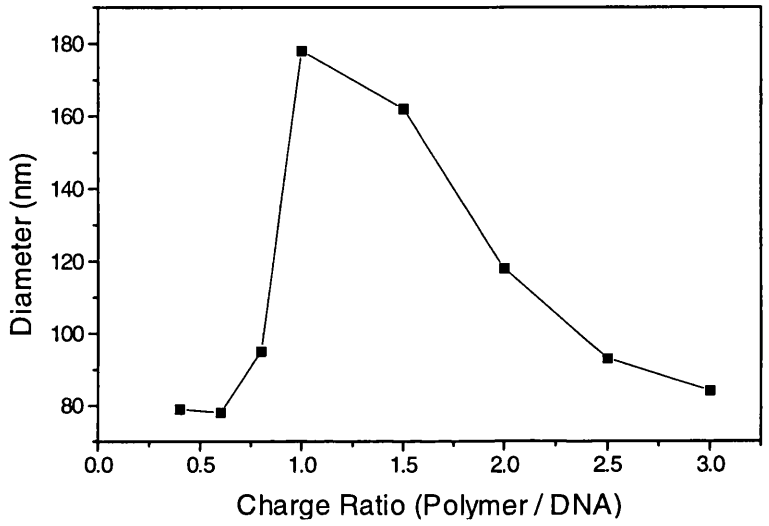

Figure 6.7. Relationship between $H_{20}K_{25}$-DNA complex diameter and charge ratio (+/-). Complexes were prepared using 6 μg pRSV*lacZ* and various quantities of $H_{20}K_{25}$ (section 5.2). The complexes were initially formed in 0.5 ml water, incubated at room temperature for 20 minutes, and the volume was made up to 2.0 ml with water. The complexes were immediately analysed using PCS (section 6.2.3) to establish the particle diameter.

PCS was used to size complexes formed using $H_{20}K_{25}$ and DNA in water over a range of charge ratios ($^{+}$/-) up to 3.0 (Fig. 6.7). The complexes were not able to be sized below a charge ratio of 0.4, but above this there was a rapid increase in size from 80 nm to 180 nm with charge ratio up to 1.0. Above this charge ratio, the size decreased back to approximately 80 nm at a charge ratio of 3.0. The span of size

distributions observed within the populations ranged from 40 nm to 280 nm (Table 6.4), except at a charge ratio of 1.0, where the smallest particles within the population has a diameter of 130 nm. Above a charge ratio of 1.0, the largest particles within each population had diameters of approximately 250 nm.

Charge Ratio	**0.4**	**0.6**	**0.8**	**1.0**	**1.5**	**2**	**2.5**	**3.0**
Diameter (nm)	79	78	95	178	162	118	93	84
Span (nm)	40-159	55-219	59-127	129-341	81-236	84-236	30-281	41-247

Table 6.4. The diameter and span of complexes prepared using 6μg pRSV*lacZ* and various quantities of $H_{20}K_{25}$ (section 5.3). The complexes were initially formed in 0.5 ml water, incubated at room temperature for 20 minutes, and the volume was made up to 2.0 ml with water. The complexes were immediately analysed using PCS (section 6.2.3) to establish the particle diameter.

6.3.3.2. Size analysis in buffers.

Complexes were prepared from polylysine and plasmid DNA in 0.5 ml water over the range of charge ratios 0 - 3.0. They were then incubated at room temperature for 20 minutes before dilution to 2.0 ml with either water or the buffer opti-MEM. The particles were then immediately sized using PCS, and the comparative diameters are shown in Figure 6.8. The complexes formed in water maintained a constant size around 100 nm over the range of charge ratios examined, but this pattern was not exhibited by the complexes diluted in opti-MEM. The size of these complexes rapidly increased from 100 nm at a charge ratio ($^{+}$/-) of 0.4 to approximately 700 nm at a charge ratio of 1.0. This instability was less pronounced when the charge ratio was increased to 2 or above.

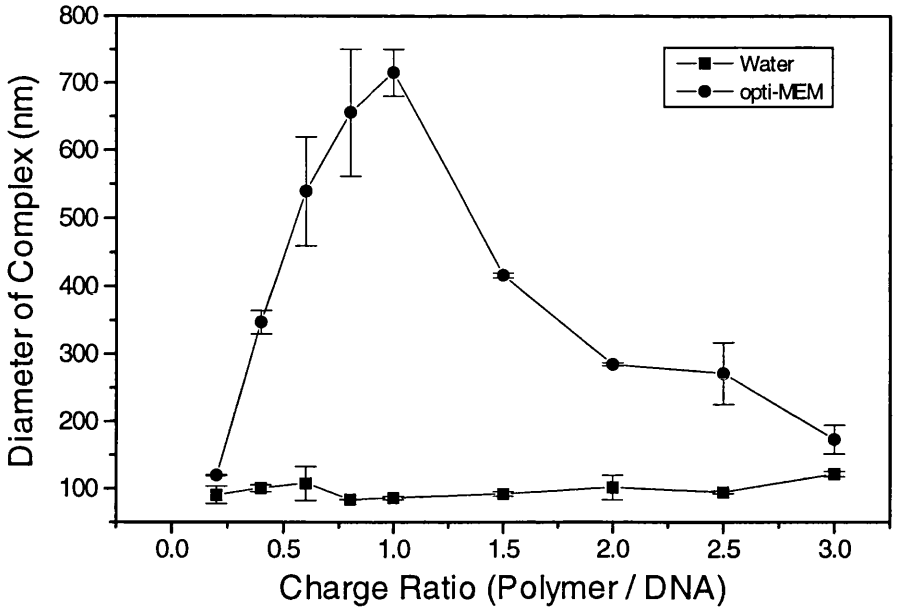

Figure 6.8. Size analysis of polylysine-DNA complexes, as determined by PCS. Complexes were prepared using 6 μg pRSV*lacZ* and varying quantities of polylysine to produce a range of charge ratios, in a total volume of 0.5 ml water. After incubation for 20 minutes at room temperature, the volume was made up to 2.0 ml with water or opti-MEM, and the samples analysed immediately (section 6.2.3) (n=2).

HEPES concentration (mM)	Diameter (nm)	Span (nm)
10	97	51-134
20	71	54-95
30	93	70-124
40	125	66-173
50	82	41-164

Table 6.5. Diameter of polylysine-DNA complexes prepared in increasing concentrations of Hepes buffer. The complexes were prepared at a charge ratio of 1.0 using 6 μg DNA and the necessary mass of polylysine in 500 μl water containing the increasing concentrations of Hepes. The complexes were incubated at room temperature for twenty minutes before diluting to 2.0 ml in the respective Hepes solutions. The samples were analysed immediately using PCS to establish the particle diameter.

The effect of hepes buffer on the formation of polylysine-DNA complexes and their resultant size was examined over the concentration range of 10 - 50 mM Hepes. The complexes were prepared in the various concentrations of buffer, and the results are displayed in Table 6.5. The diameter of the complexes remained close to 100 nm for all of the buffer concentrations, and the range of sizes within each population was between 40 to 170 nm.

NaCl Concentration (M)	Diameter (nm)	Span (nm)
0.01	1512	154-274; 791-2090
0.025	790	269-1623
0.05	1111	541-1795
0.075	335	251-447
0.1	283	305-541
0.125	1155	100-178; 1155-1778
0.15	257	140-846

Table 6.6. Effect of NaCl on $H_{20}K_{25}$-DNA complex size. Complexes were prepared using 6 μg DNA and sufficient mass of $H_{20}K_{25}$ to produce a charge ratio of 1.0 ($^{+}$/-). The complexes were initially prepared in 500 μl NaCl solution of the appropriate concentration, incubated at room temperature for twenty minutes, before dilution to 2.0 ml with NaCl solution. The complexes were analysed immediately using PCS to establish the particle diameter.

The effect of sodium chloride (NaCl) on the formation and size of the complexes formed was investigated using polylysine-DNA and $H_{20}K_{25}$/DNA complexes at a charge ratio of 1.0 ($^{+}$/-), which were formed in NaCl solutions of increasing concentrations from 0.01 to 0.15 M. The polylysine system was unable to be analysed due to large fluctuations in the counts detected, indicating a large degree of interference. The median diameters of the $H_{20}K_{25}$/DNA complexes at the different

NaCl concentrations fluctuated from 280 nm to 1512 nm, but followed no pattern with increase in NaCl concentration (Table 6.6). The range of particle sizes observed at each NaCl concentration was much wider than that observed for the complexes formed in water (129 nm - 341 nm, Table 6.4). In two cases, at 0.01 M and 0.125 M, two distinct populations were observed within the system. This indicated that the NaCl was affecting the complex formation, producing a more heterogeneous system than that produced when the complexes were formed in water.

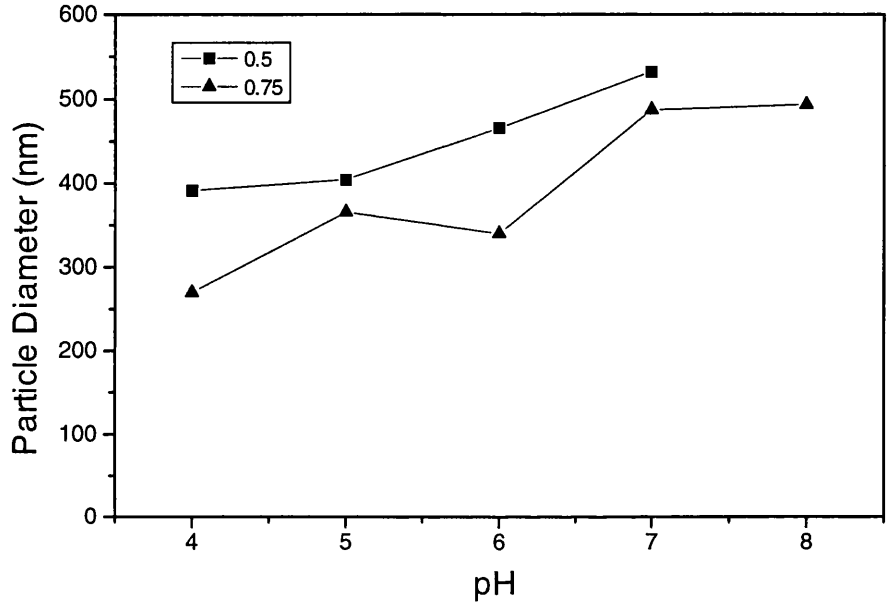

Figure 6.9. Effect of pH on particle size of complexes containing $H_{20}K_{25}$ and DNA at charge ratios ($^{+}$/-) of 0.5 and 0.75. The complexes were prepared using 6 μg DNA and the necessary mass of $H_{20}K_{25}$ to produce the required charge ratio in 500 μl phosphate-citrate buffer at the different pH values. The complexes were incubated at room temperature for twenty minutes before diluting to 2.0 ml in the appropriate buffer. Samples were analysed immediately using PCS to establish the particle diameter.

The effect of pH on the formation of complexes by $H_{20}K_{25}$ and plasmid DNA was examined using PCS, and the results are represented in Figure 6.9. The complexes were prepared at theoretical charge ratios ($^{+}$/-) of 0.5, 0.75 and 1.0 in phosphate-citrate buffers at pH values of 4, 5, 6, 7 and 8 and analysed immediately.

The pattern for the complexes prepared at charge ratios of 0.5 and 0.75 showed a steady increase in size as the pH increased from 4 to 8. The range of sizes within the populations observed were broad for the complexes at charge ratio 0.5, and were generally in the range 200 nm to 1000 nm. These complexes could not be sized at a pH of 8.

The complexes at charge ratio 0.75 exhibited narrower ranges of particle sizes, but there was a shift towards larger particles as the pH was increased. At pH 4, particle sizes ranged from 91 - 552 nm, and at pH 8 the range was from 369 - 657 nm. Complexes prepared at a charge ratio of 1.0 could only be sized at a pH of 8, and the median diameter was established as 482 nm.

6.3.4 Isothermal titration calorimetry.

The graphs shown in Fig. 6.10 represent the traces obtained from the thermometric analysis of the titration of polylysine (10 mg/ml) into a solution of 250 μg/ml pRSV*lacZ*. The control trace for the titration of HBS into the plasmid solution exhibited a very similar profile. Peaks from the corrected profiles were integrated automatically, providing energy values corresponding with the titration processes. There were problems encountered with precipitation inside the ampoule, and this was observed even at points where the charge ratio was as low as 0.4. Variation of the DNA concentration, the aliquot volume and the mixing speed had no effect on the precipitation problem. This indicated that this method of mixing and thermometric analysis was unsuitable for the interactions occurring in this system.

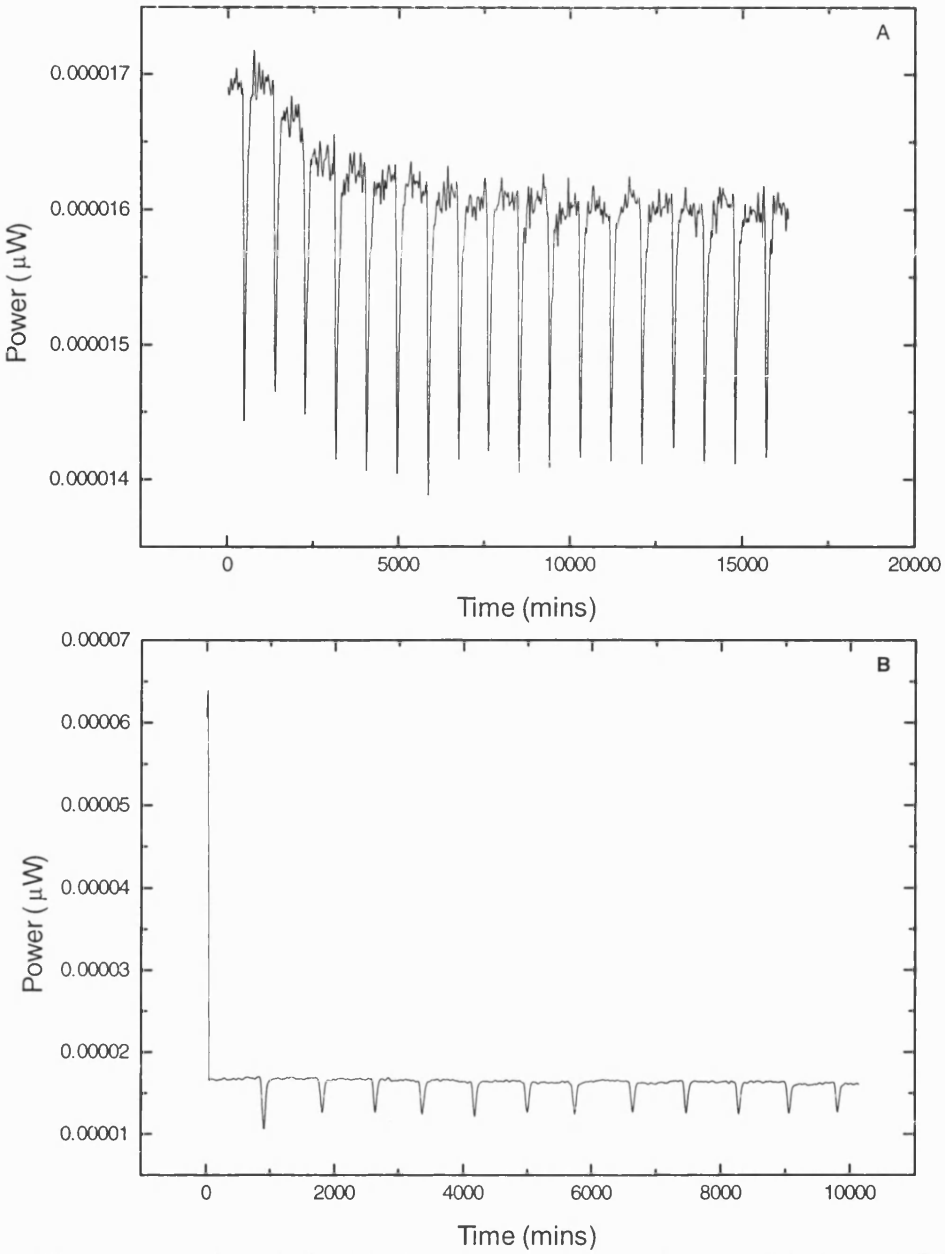

Figure 6.10. Thermometric analysis of the formation of complexes from poly-L-lysine and pRSV*lacZ*. A polylysine solution (10 mg/ml) was titrated into a DNA solution (250 µg/ml pRSV*lacZ*) contained in a 4 ml stainless steel titration ampoule. Aliquots of 4 µl of polylysine solution were titrated into the DNA at 15 minute intervals, while stirring at 10 rpm, until a total volume of 200 µl had been dispensed. A control was performed where HBS solution was titrated into the DNA solution to calculate the heat of dilution associated with the DNA. All measurements were performed using a Thermometric 2277 Thermal Activity Monitor. Figure A shows the raw trace produced by the titration process, while B shows the corrected data, accounting for the lag time of the transfer of thermometric measurements by the system compared with the actual temperature fluctuations. This was done automatically using the correction program supplied as part of the system.

6.3.5. Uptake studies of polylysine-DNA complexes.

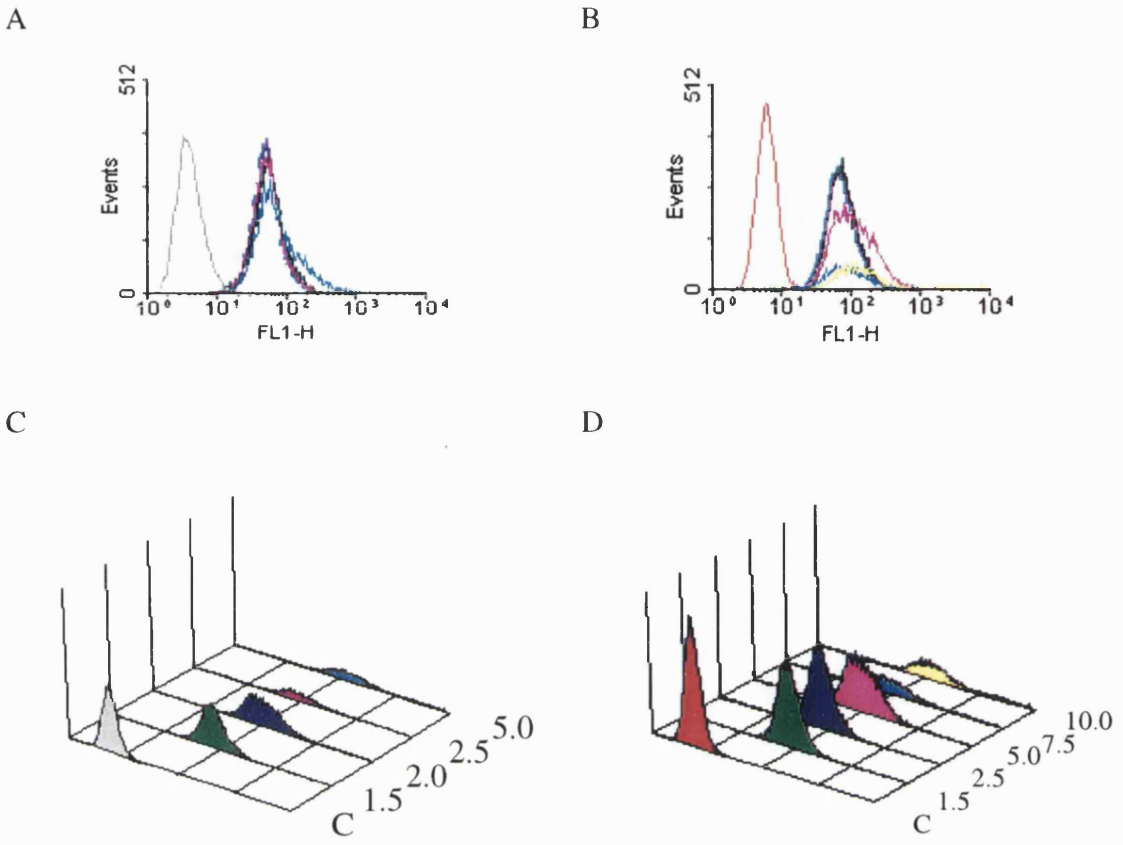

Figure 6.11. Uptake studies of polylysine-DNA complexes in B16 melanoma cells. Complexes were prepared over the range of charge ratios (+/-) 1.5, 2.0, 2.5, and 5.0 using 6 µg pRSV*lacZ*, and a constant mass of FITC-polylysine and various quantities of standard polylysine to produce the desired charge ratios (A). The complexes were incubated with the cells for 4 hours at standard conditions, before analysis with FACS. Alternatively, complexes were prepared from 6 µg pRSV*lacZ* and FITC-polylysine at a charge ratio of 1.5, and added to the culture medium. Standard uncomplexed polylysine was then added to the transfection medium to produce effective charge ratios of 2.5, 5.0, 7.5 and 10.0 (B). The cells were incubated for four hours at standard conditions before FACS analysis. Figures C and D depict 3-D representations of Figs. A and B respectively. The profiles are representative of two replicate experiments.

The uptake of polylysine-DNA complexes in B16 melanoma cells was examined using FITC-labelled polylysine and FACS. Initially, the uptake of polylysine-DNA complexes of charge ratios ($^{+}$/-) on the range 1.5 - 5.0 was examined (Figure 6.11, plates A and C). Cell viability was also determined by staining with propidium iodide immediately prior to FACS analysis. The grey line represented the negative control sample of cells which had not been incubated with any complex. The green, navy, pink and pale blue lines represent cells incubated with complexes at charge ratios of 1.5, 2.0, 2.5, and 5.0 respectively. The profiles for the different charge ratios were almost completely overlaid, but the 3-D histogram showed that the cell viability decreased with increasing charge ratio of the complexes.

Additional studies into the effect on complex uptake by free polylysine involved transfection using complexes of charge ratio 1.5, and the addition of free polylysine into the culture medium to produce an effective charge ratio in the medium of 2.5, 5.0, 7.5 and 10.0. Similar ranges of fluorescence were observed in all of the samples (Plates B and D), and the toxicity increased as the cationic charge and quantity of free polylysine in the medium was increased. Comparative cell viability of the polylysine-DNA complex at a charge ratio ($^{+}$/-) of 5.0 and 1.5 with free polylysine up to a theoretical charge ratio of 5.0 were 76% and 44% respectively.

6.4. DISCUSSION

6.4.1. Stability of complexes in serum.

The production of pharmaceutical products requires assessment of the stability of the formulation. A major limitation to the therapeutic application of gene therapy is the presence of nucleases *in vivo* and *in vitro* which can rapidly digest DNA. Complexation of DNA with polycations has been shown to enhance stability towards melting (Olins *et al.,* 1967), and chemical modification of oligonucleotides to produce phosphorothioates has also been shown to confer protection on the DNA from enzymatic degradation (Zobel *et al.*, 1996). The assay used here was developed to establish the comparative stability of the complexes of various formulations to enzymatic degradation in serum. The polycation-DNA stability studies relied on the resolution of the complexes on agarose gels for visualisation of any degradation that had occurred. Electrophoresis of DNA requires that the molecules are negatively charged to effect migration. Beyond the point of charge neutralisation by complexation with polylysine, P. Lucas (1995) demonstrated that plasmid DNA remained in the well during electrophoresis. This method allowed DNA samples that had been degraded by the nucleases in serum to be identified, as non-degraded samples would remain in the wells, but smaller degraded fragments would migrate towards the cathode during electrophoresis.

All of the complexes were prepared at a charge ratio of 1.5, as this was the ratio used for transfection studies. The complexes were then incubated in the presence of complete tissue culture medium with 10% foetal calf serum for four hours, to mimic the conditions of the transfection procedure. None of the complexes

prepared from any of the polymers exhibited any degree of DNA degradation. There were no differences observed between all of the homopolymers, or the lysine,alanine co-polymers. Additionally, the PEG-pLL co-polymers all protected DNA to the same degree, as did $H_{20}K_{25}$ and PEI. Internal controls were included in the experiments and these behaved as expected, with uncomplexed DNA suffering degradation in serum but not in HBS. The serum alone revealed a band of fluorescence due to interaction of some of the proteins with the ethidium bromide, and this was observed in all of the samples. This band ran faster than the undegraded DNA, so did not interfere with the interpretation of the gel.

This assay demonstrated that the polymers all conferred a similar level of protection from degradation to the DNA. This assay does not allow quantification of the DNA, which could be done in parallel using radiolabelled DNA, as performed by Chiou *et al.* (1994). These results demonstrated that despite the observations of Olins *et al.* (1967)that different side-chains conferred varying degrees of stability on complexed DNA towards melting, all of the polycations were capable of protecting the DNA from nuclease degradation. Hence, these results illustrate that differences in transfection efficiencies of complexes prepared with the various polycations are unlikely to be due to degradation in the transfection medium. This indicates that the differences are either due to differential uptake or processes occurring distal to the cell membrane.

6.4.2. Toxicity studies of the polycations.

The cellular toxicity exhibited by the polymers studied would primarily be as a result of the concentration of cationic charge. All of the homopolymers demonstrated similar toxicity profiles, as would be expected from their similar molecular weight/charge ratios (Table 3.1). For all the homopolymers, at a concentration of 4 μg/ml, the cells were subjected to a cationic charge of $2x10^{-5}$ M. Hence it would appear that all of the homopolymers exerted cellular toxicity due to their cationic nature, and that the degree of toxicity was similar in all cases.

The lysine, alanine co-polymers produced a less homogeneous pattern of toxicity. The charge density of the co-polymers differed from each other and polylysine, and for lysine, alanine ratios of 1:1, 2:1, 3:1 and polylysine, the respective molar concentrations of lysine at 4 μg/ml were $1.43x10^{-5}$, $1.63x10^{-5}$, $1.72x10^{-5}$ and $2x10^{-5}$. If the cellular toxicity was solely due to the cationic charge then the decreasing order of toxicity of the polycation would be polylysine, then the co-polymers of molar ratio 3:1, 2:1 and 1:1.

The lysine, alanine (1:1) co-polymer with the lowest charge density was the most toxic studied, followed by polylysine, then the 3:1 and the 2:1 co-polymers. The order of charge density-related toxicity was observed for polylysine, the co-polymers (3:1) and (2:1), but the (1:1) co-polymer did not fit into this pattern. This implies that there is another factor contributing to cellular toxicity with lysine, alanine (1:1). The

neutral alanine component could be toxic to cells above a threshold concentration, and below this concentration the toxicity could be primarily due to the cationic charge effects. The molar concentrations of alanine in the co-polymers 1:1, 2:1 and 3:1 at 4 μg/ml were $1.43x10^{-5}$, $8.18x10^{-6}$ and $5.73x10^{-6}$ respectively.

A molecular weight influence on toxicity has been reported by Wolfert and Seymour (1996), although they showed that higher molecular weights exerted greater toxicity. This is in contrast to the results presented here, as the lysine, alanine (3:1) co-polymer had a molecular weight of 31,000, whereas the other two lysine,alanine co-polymers, (1:1) and (2:1),had molecular weights of 50,000 and polylysine was 45,000.

Reduced toxicity was observed with DNA-polylysine complexes compared with free polylysine. If the cellular toxicity was due directly to the concentration of cationic charge, then complexation of the polycation with anionic DNA would serve to reduce this toxicity. The complexes routinely used for transfection had a charge ratio ($^{+}$/-) of 1.5, so although they maintained an overall positive charge, interaction with the anionic DNA served to reduce the cellular toxicity. There may have been free polylysine available for interaction with the cells, as it could not be removed from the preparations before toxicity testing. In spite of this possibility, at the concentration used for transfection with polylysine-DNA complexes of 3.5 μg/ml, the free polylysine produced approximately 40% viability compared with 75% for the polylysine-DNA complexes.

6.4.3. Size analysis of complexes.

The variation of *in vitro* transfection efficiencies observed between complexes formed with the different cationic polymers, and at different charge ratios have been shown in an earlier part of this study (section 6.2.3). One postulation to account for this was that the complexes formed were of different sizes, which would result in differential uptake into cells. The size analysis of complexes formed from DNA and a variety of polycations, at a range of charge ratios and in different conditions was performed to investigate this possibility.

The size analysis studies of the polycation-DNA complexes demonstrated that all of the complexes were between 100 - 150 nm diameter when prepared in water. The experiment required that the equipment was very clean from contaminating particles. This was because even one large particle could sway the mean considerably, due to intensity interference. To reduce the effect of this, the median diameter was taken for comparison, as this was a measure of the diameter of the majority of particles within the population. An idea of the range of sizes was also included (the span) for comparative purposes. The reproducibility of the measurements was initially demonstrated using the polylysine-DNA system at a charge ratio of 1.0 in triplicate. Due to severe time restrictions using the equipment, many of the subsequent measurements were performed either once or in duplicate.

6.4.3.1. PCS of complexes in water.

The polylysine-DNA complexes were all shown to be about 100 nm if formed in water at charge ratios ($^{+}$/-) of between 0 - 3.0. Analysis was initially attempted in HBS, but there was considerable interference with the light scattering pattern, and the

correlation program was unable to interpret the data. The complexes were then prepared in water, which allowed analysis to be performed, but clearly these conditions did not mimic the normal procedure for complex preparation, or the environment during transfection.

Sizing of complexes prepared from the various cationic polymers did not demonstrate any differences between them which correlated with the pattern of transfection efficiency. The system did not mimic the normal transfection procedure conditions very strongly, so further size analysis focused on the properties of complexes prepared in electrolyte solutions, to identify any differences due to constituents of the buffer system used.

The PEG-pLL complexes were sized in water as between 110 - 250 nm, with spans ranging from 60 to 330 nm. The complexes formed from the co-polymers with a high PEG : pLL ratio were unable to be sized. This could be due to the large mass of PEG relative to the polylysine causing a heterogeneity in the conformation of the complexes. If the PEG was producing a mantle enclosing a hydrophobic core in a controlled manner, then the particles would be quite likely to have a spherical shape. In cases where the PEG : pLL ratio was high, the particles could be less spherical, causing variable light scattering patterns, which the computer programme would have difficulty interpreting.

Analysis of $H_{20}K_{25}$-DNA complexes in water demonstrated a maximum size of 180 nm at a charge ratio of 1.0. Below this charge ratio the complexes were close to 80 nm, and above 1.0, particle size fell gradually back to approximately 80 nm at a charge ratio of 3.0. The range of sizes observed within the populations was shown to

increase above a charge ratio of 1.0. The maximum size at electroneutrality can be accounted for due to the complexes at this point exhibiting no overall charge. Hence, no electrostatic repulsion would be expected to occur between the complex molecules, and particle aggregation could occur.

6.4.3.2.. PCS of complexes in buffers.

The size of polylysine-DNA complexes over the range of charge ratios ($^{+}$/-) from 0 - 3.0 showed no differences in water, but in the buffer system opti-MEM (pH 7.4), a peak of 700 nm was observed at 1.0, beyond which the size fell once again to 150 nm. This indicated that components contained in opti-MEM were affecting the complex formation, as the complexes were much larger when formed in this system than in water. Also, the change in size with alteration of the charge ratio, with a maximum at the charge neutralisation point, demonstrated aggregation of the complexes at this point due to reduced repulsion between the individual particles. This pattern was not mimicked in water as the system was probably very sensitive to the mixing method.

The polylysine-DNA complexes were sized at a charge ratio ($^{+}$/-) of 1.0 in Hepes buffer at concentrations in the range 10-50 mM to try to explain the differences observed between complex formation in water and opti-MEM. The complexes all sized at roughly 100 nm, with a narrow range of size distributions at each Hepes concentration. It was concluded that the Hepes was not the component in the buffer system that was altering the complex formation compared with the water system.

Complex formation was affected considerably by the presence of NaCl. Polylysine-DNA complexes could not be analysed when formed at any of the NaCl concentrations studied. The controlled formation of co-operative complexes has previously been shown to be dependent upon the NaCl concentration (Leng and Felsenfeld, 1966; Shapiro *et al.*. 1969). The mixing process used by these groups involved a more controlled process than the flash mixing used for complex formation throughout this study. The ionic concentration of the solvent is likely to affect the electrostatic interaction between the anionic DNA and the polycations. The stability of the polycation-DNA complexes is an important consideration in the production of these systems as pharmaceutical products, and the effect of NaCl on the various formulations will require attention in the future. Some means of stabilisation will be required if these systems are to be used *in vivo*.

The $H_{20}K_{25}$-DNA complexes were sized in various concentrations of NaCl. There was considerable fluctuation in size and a wide span of sizes within each population, although no pattern emerged relating complex size to the ionic concentration of the solvent. At some charge ratios, more than one population of particles with distinct size distributions were observed. This indicated that the complex formation was being affected by the presence of the NaCl. The process appeared to produce a more heterogeneous population of particles when the complexes were formed in NaCl solution. The susceptibility of complexes to the effects of NaCl over time would provide an indication of the comparative stability of

each system, and this could have been monitored using PCS to detect size distribution fluctuations within populations of particles. The main limitation within the present study was the availability of a laser with sufficient power to allow sizing of DNA particles at 10 μg/ml DNA.

6.4.3.3. pH effects on $H_{20}K_{25}$-DNA complexes.

The effect of pH variation on the complexes formed between plasmid DNA and $H_{20}K_{25}$ were examined because of the proposed pH-dependent DNA release mechanism from the endosome (section 5.1.1). The charge ratio at each pH was calculated assuming that only the polylysine component was contributing to the cationic effect and a constant mass of polymer was used at each pH. However, at the lowest pH of 4.0; approximately 99% of the polyhistidine would also have been positively charged; at a pH of 8.0, approximately 0.99% of the polyhistidine would have been protonated. Therefore, at the theoretical charge ratio of 0.5 the actual charge ratios at pH 4, 5, 6, 7 and 8 would have been 0.9, 0.86, 0.7, 0.53 and 0.5 respectively. Similarly, at the theoretical charge ratio of 0.75 the actual charge ratios at pH 4, 5, 6, 7 and 8 would have been 1.34, 1.29, 1.05, 0.81 and 0.76.

A size increase was observed with rise in pH, which could now be attributed to a charge ratio effect. The presence of a neutral component within the block co-polymer would provide steric hindrance to the formation of a highly compact species. A situation similar to the formation of a PEG mantle (section 4.1.1) could exist. As the percentage of protonation of the neutral polymer increased, the particle

morphology would be affected. The increase in heterogeneity observed within populations as the degree of polymer ionisation decreased supported the hypothesis that more disorganised systems were formed when the polyhistidine remained unprotonated.

6.4.4. Isothermal titration calorimetry.

The technique of titration calorimetry has been shown to be highly sensitive, allowing binding constants and heats of binding to be established for enzyme-substrate systems (Wiseman *et al.*, 1989). The enthalpy for binding of repressors to DNA operator sites have also been established using calorimetry (Merabet and Ackers, 1995). This method was chosen to establish comparative binding enthalpies for the different cationic polymers with DNA. This information might have been expected to provide an indication of the relative strengths of association between polymer and DNA for the complexes. Systems with high binding enthalpies would be more stable but also more resistant to dissociation inside the cell. This would possibly affect the availability of the DNA for uptake into the nucleus and subsequent transcription and expression.

There were several drawbacks to the use of this technique for analysis of polycation/DNA complexes. The mixing process during titration of small aliquots of highly concentrated polylysine (10 mg/ml) into a concentrated DNA solution (250 μg/ml) bore little resemblance to the flash mixing of the two dilute solutions (15 μg/ml and 6 μg/ml for polylysine and DNA respectively). The concentrations of both components had to be increased to produce measurable enthalpy changes, and the

aliquots were small so that the titrant was still thermostatically controlled. An alternative model of the calorimeter has two chambers which contain the two reactants. The reactants are mixed by removal of the dividing partition, and the enthalpy of the whole association can be established (batch calorimetry). This would have been a better system for measuring and comparing the different polycation-DNA interactions. Unfortunately there was no accessibility to the batch calorimeter for this study, and this work was therefore terminated since the titration calorimeter was not an appropriate instrument.

6.4.5. Uptake studies in B16 melanoma cells.

Basic polyamino-acids have been demonstrated to enhance the uptake of protein molecules (Ryser, 1967) and DNA (Farber *et al.*, 1975) into certain cell lines. It would appear that a mechanism exists for the association of these complexes with the cell membrane, leading to internalisation. It was postulated in section 3.12 that the differences observed in transfection efficiency between complexes prepared at different charge ratios were due to selective or differential uptake. It has been demonstrated that the complex diameter does not correlate with transfection efficiency (section 6.3.3), so another characteristic appears to govern the activity. The lack of transfection activity below a charge ratio ($^{+}$/-) of 1.0 was attributed to the necessity for association with the negatively charged cell membrane. It was postulated that observation of peak efficiency at charge ratio 1.5, and subsequent decrease in expression with increase in charge ratios, was due to uncomplexed polylysine inhibiting either complex uptake or dissociation inside the cell (section 3.12).

The uptake of polylysine-DNA complexes of charge ratios from 1.5 to 5.0 were examined to assess any correlation between uptake and the optimum transfection charge ratio of 1.5. The lack of difference observed in uptake profiles demonstrated that the peak in transfection activity was not related to a differential uptake profile. The similarity in fluorescence levels observed at the different charge ratios implied that the complexes incorporated all of the polylysine into their structure on formation. If this was not the case, then as more non-fluoresceinated polylysine was used for mixing with the constant mass of FITC-polylysine, the relative proportion of FITC-polylysine incorporated into the complex would be decreased. This would produce a resultant decrease in fluorescence associated with the complex. The washing procedure has been shown to successfully remove any complexes not internalised (D. Milroy, personal communication), so that the fluorescence observed provided an accurate indication of complex uptake. This showed that the uptake mechanism was non-selective for complexes with different overall positive charges.

The competition of free polylysine for either uptake or dissociation after internalisation was studied by the addition of uncomplexed polylysine to transfection medium already containing polylysine-DNA complexes of charge ratio ($^{+}$/-) 1.5. If the uptake mechanism had been saturated, a reduction in fluoresceinated complex uptake would be observed as the quantity of free polylysine increased. No difference in uptake profiles was observed, although the levels of cellular toxicity observed in the experiments with free polylysine were considerably higher than with the complexes alone (44% and 76% viability respectively). The toxicities observed were similar to

those seen with the MTT assay comparing polylysine with DNA-polylysine complexes (section 6.3.2). These results demonstrated that for complexes of charge ratios ($^{+}$/-) greater than 1.5, the excess polylysine appeared to be associated with the complex, and did not remain uncomplexed.

These results therefore disprove the theory that the polylysine used to form complexes at high charge ratios ($^{+}$/-) did not all associate with the complexes, inhibiting complex uptake or dissociation within the cell. It appeared that the differences observed with *in vitro* transfection activities both for complexes formed at different charge ratios and using various polycations were due to characteristics which affected the processes distal to cellular uptake.

6.6. SUMMARY

The physical characteristics of delivery systems require investigation prior to optimisation and development into a pharmaceutical product. Preliminary studies have revealed that all of the cationic polymers used for plasmid DNA complexation conferred similar levels of protection on the DNA from the enzymatic degradation of nucleases present in serum. Polylysine-DNA complexes were shown to be less toxic to B16 melanoma cells than free polylysine. No correlation was observed between complex size and the transfection efficiency, and sodium chloride was shown to affect complex formation considerably, compared with complex production in water. This appeared to be a critical effect for establishing the stability of the complexes. The uptake of positively charged complexes was unaffected by increases in charge or the presence of free polylysine, indicating that the mechanism of uptake was non-selective

and not saturated at the levels tested. The toxicity of the complexes increased with positive charge, but remained lower than the toxicity due to free polylysine. Further investigations should include electron microscopy attempting to visualise the uptake and transport processes distal to the cell membrane. Other aspects of importance include determination of the relative dissociation of the various complexes, and whether this process must occur prior to nuclear localisation.

CHAPTER 7. Concluding discussion.

The therapeutic applications of gene therapy are reliant on both identification of the genetic causes of a disease and ways of overcoming them, plus efficient delivery of the gene into the target cells. It has rapidly been realised that gene therapy can be used not only for replacement of genetically defective genes as in cystic fibrosis, but also for multifactorial diseases such as cancer and inflammatory disorders. Ideally, gene expression would be restricted to the target cell population, whether achieved via selective delivery or transcription, courtesy of tissue-specific promoters. Additionally, the gene must access the nucleus once inside the cell, ultimately allowing gene expression.

Despite the lack of progress exhibited with the immunotherapeutic approach detailed in this study, many investigations are currently concentrating on the generation of tumour-specific immunity. The potential for targeting exogenous antigen into the phagocytic pathway, resulting in presentation by MHC class I molecules, has been investigated by Falo *et al.* (1995). *In vivo* studies confirmed the generation of tumour rejection and protection from subsequent challenge both with tumours presenting the antigen previously used, plus other antigens expressed by the tumour. Alternatively, several of the MAGE antigens (restricted to melanoma cells) have been transfected into tumours, subsequently eliciting anti-tumour immunity via both $CD4^+$ and $CD8^+$ T cells (H. Bueler, personal communication). Co-expression of GM-CSF or B7-1 enhanced this anti-tumour effect during *in vivo* murine studies.

The lack of reliability demonstrated by the Trp-1 promoter system in these studies has also been observed in other investigations (Dr. R. Vile, personal communication). Current interest on melanoma-specific promoter activity centres on the tyrosinase promoter (section 1.4.1). This has been used to induce melanoma-specific expression of B7, resulting in an *in vivo* antitumour effect in immunocompetent mice (Chong *et al.*, 1996). Substitution of the Trp-1 promoter with the tyrosinase promoter would therefore seem natural in the progression of this study.

Optimisation of delivery vectors for gene therapy involves characterisation of the interactions of the DNA with the vector. It is desirable that pharmaceutical products are well-characterised and reproducible in their effects. While much interest has centred on the use of attenuated viruses for clinical trials, it is widely accepted that these will ultimately be replaced with safer, non-viral vectors. The use of cationic polypeptides for binding DNA has been widely acknowledged, but more efficient vectors require additional characteristics to ensure transport of the DNA from outside the cell membrane to the nucleus.

The particulate nature of polycation-DNA complexes has been well documented by Olins *et al.* (1967). In the present study, modification of the chemical nature of the polycation was shown to have little effect on the 1:1 stoichiometry for DNA condensation with respect to charge ratio. The charge density of the various cations affected the mass ratio of interaction, which was most noticeable with the co-polymers containing neutral components.

The relationship between overall ionic charge of the complexes and *in vitro* biological activity initially described for polylysine by Lucas (1996) was demonstrated to apply to complexes formed using a variety of cationic polymers and co-polymers. Reporter gene expression was effected after non-specific uptake in these studies, and this was observed only when the complexes were positively charged. The lack of *in vitro* biological activity observed below a charge ratio ($^{+}$/-) of 1.0 indicated that the particulate systems formed by the flash mixing method used in this study were not co-operative. This was in contrast to observations by Manning (1980) where the conditions for mixing and complex preparation were very closely regulated. The lack of activity below charge ratio ($^{+}$/-)1.0 suggested that no active complexes were formed below this ratio. Hence, the flash mixing appears to cause even distribution of the polycations throughout the population of DNA molecules. A co-operative interaction would infer that the initial interaction between a DNA molecule and a cation would favour further binding of cations to the same DNA molecule. This would result in a heterogeneous population of DNA molecules, each associated with various numbers of cations.

The complexes prepared using co-polymers containing a neutral component to reduce toxicity exhibited reduced transfection efficiency compared with polylysine. This was believed to result from differences in complex stability, uptake or endosomal release. Recently, Mislick and Baldeschwieler (1996) have reported that polycation-DNA complexes achieve cell-entry via interaction of the cation with anionic sulfated proteoglycans, found in basement membranes and the extracellular matrix. Restriction

of direct interaction of the cations with the proteoglycans would serve to reduce uptake. This may account for the reduced activity profile observed for complexes prepared from PEG-polylysine co-polymers and DNA, due to the formation of a PEG mantle around the core containing the polycation and DNA.

The cell-specific prerequisite for chloroquine to effect transfection using polycation-DNA complexes demonstrated that these systems are unsuitable for delivery *in vivo*. One theory to account for the differences observed between the B16 and the 293 cells suggested that endosomes in different cell lines may exhibit variation in membrane integrity or internal endosome conditions. The erythroleukaemic cell line K-562 has been shown to exhibit increased transfection after treatment with chloroquine far in excess of that observed with other cell lines. This was established to be due to the presence of an unregulated acidified endosomal environment (Wagner *et al.*, 1992).

Production of a co-polymer containing polylysine and polyhistidine attempted to combine DNA-binding with the capacity for protonation within the endosome. This 'proton sponge' effect has been attributed to a lysosomotropic action (Stenseth and Thyberg, 1989). The lack of transfection activity with this system indicated that a greater membrane-disruption activity was required. High levels of activity have been produced from the use of synthetic peptides similar to those used by viruses for cell-entry (Gottschalk et al., 1996; Fominaya and Wels 1996). Wilke *et al.* (1996) have demonstrated gene delivery using a similar multifunctional vector. This group established the necessity for a mitotic event, in addition to efficient delivery, to produce high levels of transfection *in vitro*.

These studies established no difference in uptake of polylysine-DNA complexes of increasing charge ratio ($^{+}$/-). This profile contrasted with the decrease observed in gene expression above a charge ratio ($^{+}$/-) of 1.5, indicating that the uptake of complexes was not the limiting step for *in* vitro biological activity. No differences were observed in the stability of complexes to the enzymatic degradation associated with incubation in serum. These results infer that the differential expression observed with the various formulations of complexes occur due to processes distal to cellular uptake.

There has been considerable interest in the cell-specific activity profiles observed by the various vectors currently used for gene therapy. Several reports have indicated that free plasmid DNA can transfect several tissues *in vivo* (Wolff *et al.*, 1992; Yang and Huang, 1996), which are profiles not mimicked *in vitro*. Due to the lack of correlation observed between *in vitro* and *in vivo* activity profiles, there is currently a move away from the use of *in vitro* transfection data in the evaluation of gene therapy vectors.

Since these systems were colloidal in nature, properties including the particle size and physical stability were assessed. Precipitation of complexes at the bottom of the cell culture wells has been suggested as a reason for the unsuitability of *in vitro* uptake and expression studies. This would cause localised high concentrations of complexes, altering the distribution patterns within the transfection medium, and hence affecting the cellular uptake patterns. The particles were initially sized in water and shown to be between 100 - 250 nm. Further analysis in buffers mimicking those used

for transfection established that electrolytes increased both the particle size and heterogeneity of the population of particles. The electrical properties of the complexes will induce the formation of an electrical double layer in the presence of positive and negative ions in aqueous solution. The presence of these ions during the formation of the complexes will affect the interaction between the DNA and the polycations. These studies also showed that addition of ions after complex formation in water generated larger particles with a less homogeneous population. There was no direct correlation observed between complex size and transfection efficiency, although the effect of ions on complex preparation is recognised as a critical factor in the physical stability of these systems.

Further work.

Further work involving the therapeutic aspects of this study would involve the use of the tyrosinase promoter for the restricted expression of genes capable of enhancing the immune response towards cancer cells. The development of an *in vivo* murine model to establish the degree of immunostimulation achieved with different systems would provide a closer correlation between the experimental outcome and the therapeutic profile. Ultimately, the therapeutic study would also involve the use of an optimised non-viral vector for the gene delivery.

This study has demonstrated the need for further investigations into the stability of the polycation-DNA complexes, both over prolonged time periods, and in biological buffers. It would appear that these profiles could be affected by the formulation and the method of preparation. The degree of flocculation observed within the systems would

be likely to affect both the stability and the efficiency of cellular uptake, and hence expression.

The physico-chemical properties of the complexes require optimisation for cellular uptake. The mechanisms of DNA transport to the nucleus have yet to be fully elucidated. Gold labeling of the DNA would allow visualisation using electron microscopy during the cellular processing, after internalisation. Parallel labeling of the polycation would enable the point of dissociation to be established.

The importance of multifunctional peptides, capable of binding the DNA and membrane disruption is becoming more apparent. The design and synthesis of peptides incorporating these characteristics plus a nuclear localisation sequence would provide invaluable evidence about vector optimisation.

A crucial factor for consideration of the development of gene therapy vectors is that many of the effects observed thus far exhibit a large degree of cell-specificity. Additionally, a great divide exists between the activity profiles observed *in vitro* compared with *in vivo.* While, the expense and difficulty of performing mechanistic *in vivo* studies are very large, future work should attempt to concentrate, or at least attempt to correlate these two profiles more closely.

References.

Abuchowski A., and Davis F.F. (1979) Preparation and properties of polyethylene glycol-trypsin adducts. Biochim.Biphys.Acta. **578**, 41-46.

Abuchowski A., Van Es T., Palczuk N.C., and Davis F.F. (1977) Alteration of immunological properties of bovine serum albumin by covalent attachment of polyethylene glycol. J.Biol.Chem., **11**, 3578-3581.

Adam S.A. and Gerace L. (1991) Cytosolic proteins that specifically bind nuclear localisation signals are receptors for nuclear import. Cell, **66**, 837-847.

Akhtar S., and Juliano R.L. (1992) Cellular uptake and intracellular fate of AS oligonucleotides. Trends in Cell Biol., **2**, 139-144.

Andreason G.L., and Evans G.A. (1989) Optimization of electroporation for transfection of mammalian cell lines. Anal.Biochem., **180**, 269-275.

Artuc M., Nurnberg W., Czarnetzki B.M., and Schadendorf D. (1995) Characterisation of gene regulatory elements for selective gene expression in human melanoma cells. Biochem.Biophys.Res.Comm., **2**, 699-705.

Ashihara Y., Kono T., Yamazaki S., and Inada Y. (1978) Modification of *E. coli* asparaginase with polyethylene glycol: disappearance of binding ability to anti- asparaginase serum. Biochem.Biophys.Res.Comm. ., **83**, 385-391.

Atherton E., and Sheppard R.C. (1989) in Solid phase peptide synthesis - a practical approach.

Bannerji R., Arroyo C.D., Cordon-Cardo C., and Gilboa E. (1994) The role of IL-2 secreted from genetically modified tumour cells in the establishment of antitumour immunity. J.Immunol., **152**, 2324-2332.

Baskar S., Glimcher L., Nabavi N., Jones R.T., and Ostrand-Rosenberg S. (1995) Major histocompatibility complex class II^+ $B7\text{-}1^+$ tumour cells are potent vaccines for stimulating tumour rejection in tumour-bearing mice. J.Exp.Med., **181**, 619-629.

Becker J.C., Brabletz T., Czerny C., Termeer C., and Brocker E.B. (1993) Tumour escape mechanisms from immunosurveillance: induction of unresponsiveness in a specific MHC-restricted $CD4^+$ T cell clone by the autologous MHC class II^+ melanoma. International Immunol., **5**, 1501-1508.

Berkner K.L. (1988) Development of adenovirus vectors for the expression of heterologous genes. Biotechniques, **6**, 616-629.

Birnboim H.C., and Doly J. (1979) A rapid alkaline extraction procedure for screening recombinant plasmid DNA. Nucl. Acids Res., **7**, 1513-1523.

Bishop J.M., (1991) Molecular themes in oncogenesis. Cell, **64**, 235-248.

Blumenthal R., Seth P., Willingham M.C., and Pastan I. (1986) pH-dependent lysis of liposomes by adenovirus. Biochemistry, **25**, 2231-2237.

Boissy R.E. (1988) The melanocyte - its structure, function and subpopulations in skin, eyes and hair. Dermatol.Clin., **6**, 161-173.

Bond V.C., and Wold B. (1987) Poly-L-ornithine-mediated transformation of mammalian cells. Mol.Cell.Biol., **7**, 2286-2293.

Bonnekoh B., Greenhalgh D.A., Bundman D.S., Eckhardt J.N., Longley M.A., Chen S-H., Woo S.L.C., and Roop D.R. (1995) Inhibition of melanoma growth by adenoviral-mediated HSV thymidine kinase gene transfer *in vivo*. J.Invest.Dermatol., **104**, 313-317.

Bonner W.M. (1975a) Protein migration into nuclei. I. Frog oocyte nuclei accumulate a class of microinjected histones, allow entry of small proteins, and exclude large proteins. J.Cell Biol., **64**, 421-430.

Bonner W.M. (1975b) Protein migration into nuclei. II. Frog oocyte nuclei accumulate a class of microinjected oocyte nuclear proteins and exclude a class of microinjected oocyte cytoplasmic proteins. J.Cell.Biol.,**64**, 431-437.

Boon T., Cerottini J-C., Van den Eynde B., Van der Bruggen P., and Van Pel A. (1994) Tumour antigens recognised by lymphocytes. Annu.Rev.Immunol., **12**, 337-365.

Borun T.W., Scharff M., and Robbin E. (1967) Rapidly labeled, polysome associated RNA having the properties of a histone messenger. Proc.Natl.Acad.Sci.U.S.A., **58**, 1977-1983.

Boussif O., Lezoualc'h F., Zanta M.A., Mergny M.D., Scherman D., Demeneix B., and Behr J-P. (1995) A versatile vector for gene and oligonucleotide, transfer into cells in culture and *in vivo*: polyethyleneimine. Proc.Natl.Acad.Sci.U.S.A., **92**, 7297-7301.

Bramson J., Hitt M., Gallichan W.S., Rosenthal K.L., Gauldie J, and Graham F.L. (1996) Construction of a double recombinant adenovirus vector expressing a heterodimeric cytokine: *in vitro* and *in vivo* production of biologically active Interleukin-12. Human Gene Therapy, **7**, 333-342.

Breeuwer M., and Goldfarb D.S. (1990) Facilitated nuclear transport of histone H1 and other small nucleophilic proteins. Cell, **60**, 999-1008.

Caplen N.J., Kinrade E., Sorgi F., Gao X., Gruenert D., Geddes D., Coutelle C., Huang L., Alton E.W.F.W., and Williamson R. (1995a) In vitro liposome-mediated DNA transfection of epithelial cell lines using the cationic liposome DC-Chol/DOPE. Gene Therapy, **2**, 603-613.

Caplen N.J., Alton E.W.F.W., Middleton P.G., Dorin J.R., Stevenson B.J., Gao X., Durham S.R. *et al*, (1995b) Liposome-mediated CFTR gene transfer to the nasal epithelium of patients with cystic fibrosis. Nature Medicine, **1**, 39-46.

Carroll D. (1972a) Optical properties of deoxyribonucleic acid-polylysine complexes. Biochemistry, **11**, 421-426.

Carroll D. (1972b) Complexes of polylysine with polyuridylic acid and other polynucleotides. Biochemistry, **11**, 426-433.

Chen C., and Okayama H. (1987) High-efficiency transformation of mammalian cells by plasmid DNA. Mol.Cell.Biol., **7**, 2745-2752.

Chen J., Stickles R.J., and Daichendt K.A. (1994) Galactosylated histone-mediated gene transfer and expression. Human Gene Therapy, **5**, 429-435.

Chen L., Ashe S., Bray W.A., Hellstrom I., Hellstrom E., Ledbetter J.A., Mcgowan P., and Linsley P.S. (1992) Costimulation of antitumour immunity by the B7 counterreceptor for the T lymphocyte molecules CD28 and CTLA-4. Cell, **71**, 1093-1102.

Chen L., Mcgowan P., Ashe S., Johnston J., Li Y., Hellstrom I., and Hellstrom K.E. (1994) Tumour immunogenicity determines the effect of B7 costimulation on T-cell mediated tumour immunity. J.Exp.Med., **179**, 523-532.

Chen P.W., and Ananthaswamy H.N. (1993) Rejection of K1735 murine melanoma in syngeneic hosts requires expression of MHC class I antigens and either class II antigens or IL-2. J.Immunol., **151**, 244-255.

Chen P.W., Ullrich S.E., and Ananthaswamy H.N. (1994) Presentation of endogenous tumour antigens to $CD4^+$ T lymphocytes by murine melanoma cells transfected with major histocompatibility complex class II genes. J.Leukocyte Biology, **56**, 469-474.

Cheng P. (1996) Receptor-ligand-facilitated gene transfer: enhancement of liposome-mediated gene transfer and expression by transferrin. Human Gene Therapy, **7**, 275-282.

Chiou H.C., Tangco M.V., Levine S.M., Robertson D., Kormis K., Wu C.H. and Wu G.Y. (1994) Enhanced resistance to nuclease degradation of nucleic acids to asialoglycoprotein-polylysine carriers. Nucleic Acids Res., **22**, 5439-5446.

Chong H., Hutchinson G., Hart I.R., and Vile R.G. (1996) Expression of co-stimulatory molecules by tumour cells decreases tumourigenicity but may also reduce systemic antitumour immunity. Human Gene Therapy, **7**, 1771-1779.

Chowdhury N.R., Wu C.H., Wu G.Y., Ternemi P.C., Bommineni V.R., and Chowdhury J.R. (1993) Fate of DNA targeted to the liver by asialoglycoprotein receptor-mediated endocytosis *in vivo*. J.Biol.Chem., **268**, 11265-11271.

Chu G., Hayakawa H., and Berg P. (1987) Electroporation for the efficient transfection of mammalian cells with DNA. Nucleic Acids Res., **15**, 1311-1326.

Coffin R.S., MacLean A.R., Latchman D.S., and Brown S.M. (1996) Gene delivery to the central and peripheral nervous systems of mice using HSV1 ICP34.5 deletion mutant vectors. Gene Therapy, **3**, 886-891.

Conary J.T., Faulks R.D., Gagne L., Price P., Kon V., Canonico A.E., Christman B.W., Erdos G., Brigham K.L. and Schreier H. (1995) Use of synthetic peptides to enhance transgene expression. Proceed.Intern.Symp.Control.Rel.Bioact.Mater., **22**, 435-437.

Connor J., and Huang L. (1986) pH-sensitive immunoliposomes as an efficient and target-specific carrier for antitumour drugs. Cancer Res., **46**, 3431-3435.

Cornetta K., Srour E.F., Moore A., Davidson A., Broun E.R., Hromes R., Moen R.C., Morgan R.A., Rubin L., Anderson W.F., Hoffman R., and Tricot G. (1996) Retroviral gene transfer in autologous bone marrow transplantation for adult acute leukaemia. Human Gene Therapy, **1**, 1323-1330.

Cotten M., Wagner E., Zatloukal K., Phillips S., Curiel D.T., and Birnstiel M.L. (1992) High-efficiency receptor-mediated delivery of small and large (48 kilobase gene constructs) using the endosome-disruption activity of defective or chemically inactivated adenovirus particles. Proc.Natl.Acad.Sci.U.S.A., **89**, 6094-6098.

Cotten M., Wagner E., and Birnstiel M.L. (1993) Receptor-mediated transport of DNA into eukaryotic cells. Methods in Enzymology, **27**, 618-644.

Cotten M., and Weber J.M. (1995) The adenovirus protease is required for virus entry into host cells. Virology, **213**, 494-502.

Cristiano R.J., Smith L.C., and Woo S.L. (1993) Hepatic gene therapy: adenovirus enhancement of receptor-mediated gene delivery and expression in primary hepatocytes. Proc.Natl.Acad.Sci.U.S.A, **90**, 2122-2126.

Crystal R.G., McElvaney N.G., Rosenfeld M.A., Chu C.S., Mastrangeli A., Hay J.G., Brody S.L., Jaffe H.A., and Danel C. (1994) Administration of an adenovirus containing the human CFTR cDNA to the respiratory tract of individuals with cystic fibrosis. Nature Genet., **5**, 397-402.

Curiel D.T., Agarwal S., Wagner E., and Cotten M. (1991) Adenovirus enhancement of transferrin-polylysine-mediated gene delivery. Proc.Natl.Acad.Sci.U.S.A, **88**, 8850-8854.

Curiel D.T., Pilewski J.M., and Albelda S.M. (1996) Gene therapy approaches for inherited and acquired lung diseases. Am.J. Respiratory Cell and Molecular Biology, **14**, 1-18.

Dalgleish A. (1996) The case for therapeutic vaccines. Melanoma Res., **6**, 5-10.

Davis H.L., Whalon R.G., and Demeneix B.A. (1993) Direct gene transfer into skeletal muscle *in vivo*: factors affecting efficiency of transfer and stability of expression. Human Gene Therapy, **1**, 114-121.

Dean R.T., Jessup W., and Roberts C.R. (1984) Effects of exogenous amines on mammalian cells, with particular reference to membrane flow. **217**, 27-40.

De Giovanni C., Palmeri G., Nicoletti G., Landuzzi L., Scotlandi K., Bontadini A., Tazzari P-L., Sensi M., Santoni A., Nanni P., and Lollini P-L. (1991) Immunological and non-immunological influence of H-2K^b gene transfection on the metastatic ability of B16 melanoma cells. Int.J.Cancer, **48**, 270-276.

Demarre A., Seymour L.W., and Schacht, E. (1994) Evaluation of the hydrolytic and enzymatic stability of macromolecular mitomycin-c derivatives. J.Controlled Release, **31**, 89-97.

Denfield R.W., Dietrich A., Wuttig C., Tanczos E., Weiss J.M., Vanscheidt W., Schopf E., and Simon J.C. (1995) *In situ* expression of B7 and CD28 receptor families in human malignant melanoma: relevance for t-cell-mediated anti-tumour activity. Int.J.Cancer, **62**, 259-265.

Deonarain M.P., Spooner R.A., and Epenetos A.A. (1995) Genetic delivery of enzymes for cancer therapy. Gene Therapy, **2**, 235-244.

Dingwall C., and Laskey R. (1991) Nuclear targeting sequences - a consensus? Trends Biochem. Sci., **16**, 478-481.

Dower W.J., Miller J.F., and Ragsdale C.W. (1988) High efficiency transformation of *E. coli* by high voltage electroporation. Nucleic Acids Res., **16**, 6127-6145.

Eglitis M.A., and French Anderson W.(1988) Retroviral vectors for introduction of genes into mammalian cells. Biotechniques, **6**, 608-614.

Elwood J.M., Gallagher R.P., Hill G.B., and Pearson J.C.G. (1985) Cutaneous melanoma in relation to intermittent and constant sun exposure - the western Canada melanoma study. Int.J.Cancer. **35**, 427-433.

Falo L.D., Kovacsovics-Bankowski M., Thompson K., and Rock K.L. (1995) Targeting antigen into the phagocytic pathway *in vivo* induces protective tumour immunity. Nature Medicine, **1**, 649-653.

Farber F.E., Melnick J.L., and Butel J.S. (1975) Optimal conditions for uptake of exogenous DNA by Chinese hamster lung cells deficient in hypoxanthine-guanine phosphoribosyltransferase. Biochim. Biophys. Acta, **390**, 298-311.

Fathman C.G. (1993) Stimulating the lymphocytes. Current Biology, **3**, 558-559.

Fearon E.R., Itaya B., Hunt B., Vogelstein B., and Frost P. (1988) Induction in a murine tumour of immunogenic tumour variants by transfection with a foreign gene. Cancer Res., **48**, 2975-2980.

Felgner P.L., Gadek T.R., Holm M., Roman R., Chan H.W., Wenz M., Northrop J.P., Ringold G.M., and Danielsen M. (1987) Lipofection: a highly efficient, lipid-mediated DNA transfection procedure. Proc.Natl.Acad.Sci.U.S.A, **84**, 8850-8854.

Ferry N., Dupleiss O., Houssin O., Danos O., and Heard J. (1991) Retroviral-mediated gene transfer into hepatocytes *in vivo*. Proc.Natl.Acad.Sci.U.S.A, **88**, 8377-8381.

Finn P.W., He H.Z., Wang Y.S., Wang Z.M., Guan G.M., Listman J., Perkins D.L. (1997) Synergistic induction of CTLA-4 expression by costimulation with TCR plus CD28 signals mediated by increased transcription and messenger ribonucleic acid stability. J.Immunol., **158**, 4074-4081.

Flotte T.R., and Carter B.J. (1995) Adeno-associated virus vectors for gene therapy. Gene Therapy, **2**, 357-362.

Foa R., Guarini A., and Gansbacher B. (1992) IL-2 treatment for cancer: from biology to gene therapy. Br.J.Cancer, **66**, 992-998.

Fominya J. and Wels W.(1996) Target cell-specific DNA transfer mediated by a chimeric multidomain protein. J.Cell.Biol., **271**, 10560-10568.

Fraley R., Straubinger R.M., Rule G., Springer E.L., and Papahadjopoulos D. (1981) Liposome-mediated delivery of deoxyribonucleic acid to cells: enhanced efficiency of delivery related to lipid composition and incubation conditions. Biochem., **20**, 6978-6987.

Freeman G.J., Freedman A.S., Segil J.M., Lee G., Whitman J.F., and Nadler L.M. (1989) B7, a new member of the Ig superfamily with unique expression on activated and neoplastic B cells. J.Immunol., **143**, 2714-2722.

Freeman G.J., Borriello F., Hodes R.J., Reiser H., Gribben J.G., Ng J.W., Kim J., Goldberg J.M., Hathcock K., Laszlo G., Lombard L.A., Wang S., Gray G.S., Nadler L., and Sharpe A.H. (1993) Murine B7-2, an alternative CTLA4 counter-receptor that costimulates T cell proliferation and interleukin 2 production. J.Exp.Med., **178**, 2185-2192.

Friend D.S., Papahadjopoulos D., and Debs R.J. (1996) Endocytosis and intracellular processing accompanying transfection mediated by cationic liposomes. Biochim.Biophys.Acta, **1278**, 41-50.

Fuertges F., and Abuchowski A. (1990) The clinical efficacy of poly(ethyleneglycol)-modified proteins. J.Controlled Release, **11**, 139-148.

Gabizon A. (1992) Selective tumour localisation and improved therapeutic index of anthracyclines encapsulated in long-circulating liposomes. Cancer Res., **52**, 891-896.

Gabizon A., and Papahadjopoulos D. (1988) Liposome formulations with prolonged circulation time in blood and enhanced uptake by tumours. Proc.Natl.Acad.Sci.U.S.A., **85**, 6949-6953.

Ganss R., Montoliu L., Monaghan A.P., and Schutz G. (1994) A cell-specific enhancer far upstream of the mouse tyrosinase gene confers high level and copy number-related expression in transgenic mice. EMBO J., **13**, 3083-3093.

Gao X., and Huang L. (1995) Cationic liposome-mediated gene transfer. Gene Therapy, **2**, 710-712.

Gao X., and Huang L. (1996) Potentiation of cationic liposome-mediated gene delivery by polycations. Biochemistry, **35**, 1027-1036.

Gao L., Wagner E., Cotten M., Agarwal S., Harris C., Romer M., Miler L., Hu P.C., and Curiel D. (1993) Direct *in vivo* gene transfer to airway epithelium employing adenovirus-polylysine-DNA complexes. Human Gene Therapy, **4**, 14-24.

Geller A.I., and Breakefield X.O. (1988) A defective HSV-1 vector expresses *Eschericia coli* β-galactosidase in cultured peripheral neurons. Science, **241**, 1667-1669.

Gershon H., Ghirlando R., Guttman S.B., and Minsky A. (1993) Mode of formation and structural features of DNA-cationic liposome complexes used for transfection. Biochemistry, **32**, 7143-7151.

Ghattas I.R., Sanes J.R., and Majors J.E. (1991) The encephalomyocarditis virus internal ribosome entry site allows efficient coexpression of two genes from a recombinant provirus in cultured cells and in embryos. Mol.Cell.Biol., **11**, 5848-5859.

Gimmi C.D., Freeman G.J., Gribben J.G., Sugiti K., Freedman A.S., Morimoto C., and Nadler L.M. (1991) B cell surface antigen B7 provides a costimulatory signal that induces T cells to proliferate and secrete interleukin 2. Proc.Natl.Acad.Sci.U.S.A., **88**, 6575-6579.

Gluzman Y. (1981) SV40-transformed simian cells support the replication of early SV40 mutants. Cell, **23**, 175-182.

Golumbek P., Lazenby A., Levitsky H., Jaffee E., Karasuyama H., Baker M., and Pardoll D. (1991) Treatment of established renal cancer by tumour cells engineered to secrete interleukin-4. Science, **254**, 713-716.

Gottschalk S., Cristiano R.J., Smith L.C., and Woo S.L.C. (1993) Folate receptor mediated DNA delivery into tumour cells: potosomal disruption results in enhanced gene expression. Gene Therapy, **1**, 185-191.

Gottschalk S., Sparrow J.T., Hauer J., Mims M.P., Leland F.E., Woo S.L.C., and Smith L.C. (1996) A novel DNA-peptide complex for efficient gene transfer and expression in mammalian cells. Gene Therapy, **3**, 448-457.

Graham F.L., and van der Eb A.J. (1973) A new technique for the assay of the infectivity of human adenovirus 5 DNA. Virology, **52**, 456-467.

Graziadei L., Burfeind P., and Bar-Sagi D. (1991) Introduction of unlabelled proteins into living cells by electroporation and isolation of viable protein-loaded cells using dextran-fluorescein isothiocyanate as a marker for protein uptake. Anal.Biochem., **194**, 198-203.

Gustafsson J., Arvidson G., Karlsson G., and Almgren M.(1995) Complexes between cationic liposomes and DNA visualized by cryo-TEM. Biochim. Biophys. Acta, **1235**, 305-312.

Gutierrez A.A., Lemoine N.R., and Sikora K. (1992) Gene therapy for cancer. Lancet, **339**, 715-721.

Haensler J., and Szoka F.C. (1993) Polyamidoamine cascade polymers mediate efficient transfection of cells in culture. Bioconjugate Chem., **4**, 372-379.

Harris J.D., Gutierrez A.A., Hurst H.C., Sikora K., and Lemoine N.R. Gene therapy for cancer using tumour-specific prodrug activation. Gene Therapy, **1**, 170-175.

Hart S.L., Harbottle R.P., Cooper R., Miller A., Williamson R., and Coutelle C. (1996) Gene delivery and expression mediated by an integrin-binding peptide. Gene Therapy, **2**, 552-554.

Hearing V.J., and Tsukamato K. (1991) Enzymatic control of pigmentation at the molecular level. FASEB J., **5**, 2902-2909.

Hellstrom K.E., and Hellstrom I. (1991) Principles of tumour immunity: tumour antigens. *In* The Biologic Therapy of Cancer. V.T. De Vita, Jr., S. Hellman, and S.A. Rosenberg, editors. J.B. Lippincott Co., Philadelphia. 35-52.

Hock H., Dorsch M., Kunzendorf U., Qin Z., Diamantstein T., and Blankenstein T. (1993) Mechanisms of rejection induced by tumour cell-targeted gene transfer of interleukin 2, interleukin 4, interleukin 7, tumour necrosis factor, or interferon γ. Proc.Natl.Acad.Sci.U.S.A., **90**, 2774-2778.

Hollywood D., and Hurst H.C. (1993) A novel transcription factor, OB2-1 is required for overexpression of the proto-oncogene c-*erb*B2 in mammary tumour lines. EMBO J., **12**, 2369-2375.

Huber B.E., Richards C.A., and Krenitsky T.A. (1991) Retroviral-mediated gene therapy for the treatment of hepatocellular carcinoma: an innovative approach for cancer gene therapy. Proc.Natl.Acad.Sci.U.S.A., **88**, 8039-8043.

Hughes J.A., Aronsohn A.I., Avrutskaya A.V., and Juliano R.L. (1996) Evaluation of adjuvants that enhance the effectiveness of antisense oligodeoxynucleotides. Pharm.Res., **13**, 404-410.

Iezzi G., Pria Protti M., Rugarli C., and Bellone M. (1996) B7.1 expression on tumour cells circumvents the need of professional antigen presentation for *in vitro* propagation of cytotoxic T cell lines. Cancer Research, **56**, 11-15.

Illum L., Hunneyball I.M., and Davis S.S. (1986) The effect of hydrophilic coating on the uptake of colloidal particles by the liver and by peritoneal macrophages. Int.J.Pharm., **29**, 53-65.

Jackson I.J., Chambers D.M., Budd P.S., and Johnson R. (1991) The tyrosinase-related protein-1 gene has a structure and promoter sequence very different from tyrosinase. Nucleic Acids Res., **19**, 3799-3804.

Jaffe H.A., Danel C., Longenecker G., Metzger M., Setoguchi Y., Rosenfeld M.A., Gant T.W., Thorgeirsson S.S., Stratford-Perricaudet L.D., Pavirani, A., Lecocq J.-P., and Crystal R.G. (1992) Adenovirus-mediated *in* vivo gene transfer and expression in normal rat-liver. Nature Genetics, **1**, 372-378.

Jenkins M.K., Taylor P.S., Norton S.D., and Urdahl K.B. (1991) CD28 delivers a costimulatory signal involved in antigen-specific IL-2 production by human T-cells. J.Immunol., **147**, 2461-2466.

Johnson C.A., Goddard J.P., and Adams L.P. (1995) The effect of histone H1 and DNA methylation on transcription. Biochem.J., **305**, 791-798.

Kabanov A.V., and Kabanov V.A. (1995) DNA complexes with polycations for the delivery of genetic material into cells. Bioconjugate Chem., **6**, 7-20.

Karlsson S., Humphries R.K., Gluzman Y., and Nienhuis A.W. (1985) Transfer of genes into hematopoietic cells using recombinant DNA viruses. Proc.Natl.Acad.Sci.U.S.A, **82**, 158-162.

Katayose S. and Kataoka K. (1996) Water soluble polyion complex between DNA and PEG-Poly(L-Lysine) block copolymers for novel gene vector. Proceed.Intern.Symp.Contrl. Rel.Bioact.Mater., **23**, 899-900.

Katre N.V. (1993) The conjugation of proteins with polyethylene glycol and other polymers, Adv.Drug Deliv.Rev., **10**, 91-114.

Kenne J.A., and Foreman J., (1982) Helper activity is required for the *in vivo* generation of cytotoxic T lymphocytes. J.Exp.Med., **155**, 768-782.

Krasnykh V.N., Mikheeva G.V., Douglas J.T., and Curiel D.T. (1996) Generation of recombinant adenovirus vectors with modified fibres for altering viral tropism. J.Virol., **70**, 6839-6846.

Kripke M.L. (1979) Speculations on the role of ultraviolet radiation in the development of malignant melanoma. J.Natl.Cancer.Inst., **63**, 541-545.

Kobayashi T., Urabe K., Winder A., Jimenez-Cervantes C., Imokawa G., Brewington T., Solano F., Garcia-Borron J.C., and Hearing V. (1994) Tyrosinase related protein 1 (TRP1) functions as a DHICA oxidase in melanin biosynthesis. EMBO J., **13**, 5818-5825.

Kopecek J., and Duncan R., in Illum L, Davis S.S., eds. (1987) Polymers in Controlled Drug Delivery, Wright, Bristol, U.K.

Korner A.M., and Pawalek J.M. (1982) Mammalian tyrosinase catalyses 3 reactions in the biosynthesis of melanin. Science, **217**, 1163-1165.

Kuchroo V.K., Das M.P., Brown J.A., Ranger A.M., Zamvil S.S., Sobel R.A., Weiner H.L., and Glimcher L.H. (1995) B7-1 and B7-2 costimulatory molecules activate differentially the TH1/TH2 development pathways - application to autoimmune-disease therapy. Cell, **80**, 707-718.

Kukowska-Latallo J.F., Bielinska A.U., Johnson J., Spindler R., Tomalia D.A., and Baker J.R. (1996) Efficient transfer of genetic material into mammalian cells using Starburst polyamidoamines. Proc.Natl.Acad.Sci.U.S.A, **93**, 4897-4902.

Kun L.E., Gajjar A., and Muhlbauer M. (1995) Stereotactic injection of Herpes Simplex thymidine kinase vector producer cells (PA317-G1Tk1SvNa.7) and intravenous ganciclovir for the treatment of progressive or recurrent primary pediatric malignant brain tumours. Human Gene Therapy, **6**, 1231-1255.

Laemmli U.K., (1975) Characterisation of DNA condensates induced by poly(ethylene oxide) and polylysine. Proc.Natl.Acad.Sci.U.S.A, **72**, 4288-4292.

Lasic D.D., and Templeton N.S. (1996) Liposomes in gene therapy. Adv. Drug Del. Rev., **20**, 221-266.

El Gal La Sal G., Robert J.J., Bernard S., Radix V., Stratford-Perricaudet LAD., Perricaudet M., and Mallet J. (1993) An adenovirus vector for gene transfer into neurons and glib in the brain. Science, **259**, 988-990.

Ledley F.D. (1995) Nonviral gene therapy: the promise of genes as pharmaceutical products. Human Gene Therapy, **6**, 1129-1144.

Lee W.Y, Sheen A.S.H., and Aberblom E. (1981) Suppression of reaginic antibodies with modified allergens. IV. Induction of suppressor T cells by conjugates of polyethylene glycol (PEG) and mono-methoxy PEG with ovalbumin. Int.Arch.Allergy Appl.Immunol., **64**, 100-114.

Legendre J.Y., and Szoka F.C. (1992) Delivery of plasmid DNA into mammalian cell lines using pH-sensitive liposomes: comparison with cationic liposomes. Pharm.Res., **9**, 1235-1242.

Leng M., and Felsenfeld G. (1966) The preferential interactions of polylysine and polyarginine with specific base sequences in DNA. Proc.Natl.Acad.Sci.U.S.A., **56**, 1325-1332.

Li Y., Hellstrom K.E., Ashe Newby S., and Chen L. (1996) Costimulation by CD28 and B7-1 induces immunity against poorly immunogenic tumours. J.Exp.Med., **183**, 639-644.

Li Y., McGowan P., Hellstrom I., Hellstrom K.E., and Chen L. (1994) Costimulation of tumour-reactive $CD4^+$ and $CD8^+$ T lymphocytes by B7, a natural ligand for CD28, can be used to treat established mouse melanoma. J.Immunol., **153**, 421-428.

Linsley P.S., Clark E.A., and Ledbetter J.A. (1990) T cell antigen CD28 mediates adhesion with B cells by interacting with activation antigen B7/BB1. Proc.Natl.Acad.Sci.U.S.A., **87**, 5031-5035.

Linsley P.S., Brady W., Urnes M., Grosmaire L., Damle N.K., and Ledbetter J.A.(1991a) CTLA-4 is a second receptor for the B cell activation antigen B7. J.Exp.Med., **174**, 561-569.

Linsley P.S., Brady W., Grosmaire L., Aruffo A., Damle N.K., and Ledbetter J.A.(1991b) Binding of the B cell activation antigen B7 to CD28 costimulates T cell proliferation and interleukin 2 mRNA accumulation. J.Exp.Med., **173**, 721-730.

Lowings P., Yavuzer U., and Goding C.R. (1992) Positive and negative elements regulate a melanocyte-specific promoter. Mol.Cell.Biol., **12**, 3653-3662.

Lowry O.H., Rosebrough N.J., Farr A.L., and Randall R.J. (1951) Protein measurement with the Folin phenol reagent. J.Biol.Chem., **193**, 265-275.

Lozier J.N., Thompson A.R., Hu P.C., Read M., Brinkhous K.M., High K.A., and Curiel D.T. (1994) Efficient transfection of primary cells in a canine Hemophilia B model using adenovirus-polylysine-DNA complexes. Human Gene Therapy, **5**, 313-322.

Lucas P. (1995) Cationic polypeptides for gene delivery to eukaryotic cells. Ph.D. thesis, University of Bath.

Lugtenberg B., Meifers J., Peters R., Van der Hoek P., and Van Alphen L (1975) Eletrophoretic resolution of the major outer membrane protein of *E. coli* K12 into four bands. FEBS Lett., **58**, 254-258.

Luthman H., and Magnosson G. (1983) High efficiency polyoma DNA transfection of chloroquine treated cells. Nucleic Acids Res., **11**, 1295-1308.

MacGregor G.R., Nolan G.P., Fiering S., Roederer M., and Herzenberg L.A. (1991) Use of E. coli *lacZ* (β-galactosidase) as a reporter gene. Methods Mol. Biol., **7**, 217-235.

Maggio B., Ahkong Q.F., and Lucy J.A. (1976) Poly(ethylene glycol), surface potential and cell fusion. Biochem.J., **158**, 647-650.

Malpas J. (1987) Chemotherapy. In Introduction to the cellular and molecular biology of cancer. (L.M. Franks, N.M. Teich, eds), 2nd ed., p63-92, Oxford, U.K. Oxford University Press.

Mamounas M., Leavitt M., Yu M., and Wong-Staal F. (1995) Increased titer of recombinant AAV vectors by gene transfer with adenovirus coupled to DNA-polylysine complexes. Gene Therapy, **2**, 429-432.

Manning G.S. (1981) The possibility of intrinsic local curvature in DNA toroids. Biopolymers, **20**, 1261-1270.

Maxfield F.R. (1982) Weak bases and ionophores rapidly and reversibly raise the pH of endocytic vesicles in cultured mouse fibroblasts. J.Cell.Biol., **95**, 676-681.

Mayordomo J.I., Zorina T., Storkus W.J., Zitvogel L., Celluzzi C., Falo L.D., Melief C.J., Ildstad S.T., Kast W.M., Deleo A.B., and Lotze M.T. (1995) Bone-marrow-derived dendritic cells pulsed with synthetic tumour peptides elicit protective and therapeutic antitumour immunity. Nature Medicine, **1**, 1297-1302.

McLachlan G., Davidson D.J., Stevenson B.J., Dickinson P., Davidson-Smith H., Dorin J.R., and Porteus D.J. (1995) Evaluation *in vitro* and *in vivo* of cationic liposome-expression construct complexes for cystic fibrosis gene therapy. Gene Therapy, **2**, 614-622.

McMaster W.R., and Williams A.F. (1979) Identification of Ig glycoproteins in rat thymus and purification from rat spleen. Eur.J.Immunol., **9**, 426-433.

Melchior F., and Gerace L. (1996) Mechanisms of nuclear protein import. Curr.Opin.Cell Biol., **7**, 310-318.

Merabet E., and Ackers G.K. (1995) Calorimetric analysis of λ cI repressor binding to DNA operator sites. Biochem., **34**, 8554-8563.

Michael S.I., and Curiel D.T. (1994) Strategies to achieve targeted gene delivery via the receptor-mediated endocytosis pathway. Gene Therapy, **1**, 223-232.

Midoux P., Mendes C., Legrand A., Raimond J., Mayer R., Monsigny M., and Claude Roche A. (1993) Specific gene transfer mediated by lactosylated poly-L-lysine into hepatoma cells. Nucleic Acids Res., **21**, 871-878.

Miller A.D., and Buttimore C. (1986) Redesign of retrovirus packaging cell lines to avoid recombination leading to helper virus production. Mol.Cell Biol., **6**, 2895-2902.

Miller A.D., Garcia J.V., Suhr N.V., Lynch C.M., Wilson C., and Eiden M.V. (1991) Construction and properties of retrovirus packaging cells based on gibbon ape leukaemia virus. J.Virol., **65**, 2220-2224.

Miller D.G., Mohammed A.A., and Miller A.D. (1990) Gene transfer by retrovirus vectors occurs only in cells that are actively replicating at the time of infection. Mol.Cell Biol., **10**, 4239-4242.

Miller J., and Germain R.N. (1986) Efficient cell surface expression of class II MHC molecules in the absence of associated invariant chain. J.Exp.Med., **164**, 1478-1489.

Mislick K.A., and Baldeschwieler J.D. (1986) Evidence for the role of proteoglycans in action-mediated gene transfer. Proc.Natl.Acad.Sci.U.S.A., **93**, 12349-12354.

Misseyanni A., Klug J., Suske G., and Beato M. (1991) Novel upstream elements and the TATA-box region mediate preferential transcription from the uteroglobin promoter in endometrial cells. Nucleic Acids Res., **19**, 2849-2859.

Mitani K., and Caskey C.T. (1993) Delivering therapeutic genes - matching approach and application. Trends in Biotechnology, **11**, 162-166.

Moreland R.B., Langevin G.L., Singer R.H., Garcea R.L., and Hereford L.M. (1987) Amino acid sequences that determine the nuclear localisation of yeast histone 2B. Mol.Cell.Biol., **7**, 4048-4057.

Morton D.L., Hoon D.S.B., Nizze J.A., Foshag L.J., Famatiga E., Wanek L.A., Chang C., Irie R.F., Gupta R.K., and Elashoff R. (1993) Polyvalent melanoma vaccine improves survival of patients with metastatic melanoma. Annals of the New York Academy of Sciences, **690**, 120-134.

Mosmann T. (1983) Rapid colorimetric assay for cellular growth and survival: application to proliferation and cytotoxicity assays. J. Immunological Methods, **65**, 55-63.

Mueller D.L., Jenkins M.K., and Schwartz R.H. (1989) Clonal expression vs functional inactivation: a costimulatory pathway determines the outcome of T-cell receptor occupancy. Ann.Rev.Immunol., **7**, 445-480.

Neumann E., Schaeferridder M., Wang Y. and Hofschneider P.H. (1982) Gene-transfer into mouse lyoma cells by electroporation in high electric-fields. EMBO J. 1(7): 841-845.

Nossal G.J.V., and Pike B.L. (1980) Clonal anergy: persistence in tolerant mice of antigen-binding B lymphocytes incapable of responding to antigen or mitogen. Proc.Natl.Acad.Sci.USA., **77**, 1602-1606.

Nossal G.J.V., (1993) Tolerance and ways to break it. Annals of the New York Academy of Sciences. **690**, 34-41.

Okada C.Y., and Rechsteiner M. (1982) Introduction of macromolecules into cultured mammalian cells by osmotic lysis of pinocytic vesicles. Cell, **29**, 33-41.

Olins D.E., Olins A.L., and von Hippel P. (1967) Model nucleoprotein complexes: Studies on the interaction of cationic homopolypeptides with DNA. J.Mol.Biol., **24**, 157-176.

Olins D.E., Olins A.L., and von Hippel P. (1968) On the structure and stability of DNA-protamine and DNA-polypeptide complexes. J.Mol.Biol., **33**, 265-281.

Olins D.E., and Olins A.L. (1971) Model nucleohistones: The interaction of F1 and F2a1 histones with native T7 DNA. J.Mol.Biol., **57**, 437-455.

Osanto S., Brouwenstyn N., Naessen N., Figdor C.G., Melief C.J.M., Schrier P.I. (1993) Immunization with interleukin-2 transfected melanoma cells. A phase I-II study in patients with metastatic melanoma. Human Gene Therapy, **4**, 323-330.

Ostrand-Rosenberg S., Thakur A., and Clements V. (1990) Rejection of mouse sarcoma cells after transfection of MHC class II genes. J. Immunol., **144**, 4068-4071.

Ostrand-Rosenberg S., (1994) Tumour immunotherapy: the tumour cell as an antigen-presenting cell. Curr.Opin.Immunol., **6**, 722-727.

Pardoll D.M. (1993) Cancer vaccines.TiPS, **14**, 202-208.

Pike M.C. (1987) Epidemiology of cancer. In Introduction to the cellular and molecular biology of cancer. (L.M. Franks, N.M. Teich, eds), 2nd ed., p63-92, Oxford, U.K. Oxford University Press.

Plank C., Oberhausen B., Mechtler K., Kock C., and Wagner E. (1994) The influence of endosome-disruptive peptides on gene transfer using synthetic virus-like gene transfer systems. J.Biol.Chem., **269**, 12918-12924.

Plautz G.E., Yang Z., Wu B., Gao X., Huang L., and Nabel G.J. (1993) Immunotherapy of malignancy by *in vivo* gene transfer into tumours. Proc.Natl.Acad.Sci.U.S.A., **90**, 4645-4649.

Porgador A., Feldman M., and Eisenbach L. (1989) H-2K^b transfection of B16 melanoma cells results in reduced tumourigenicity and metastatic competence. J.Immunogen., **16**, 291-303.

Porter C.D., Collins M.K.L., Taylor C.S., Parkar M.H., Cosset F-L., Weiss R.A., and Takeuchi Y. (1996) Comparison of efficiency of infection of human gene therapy cells *via* four different retroviral receptors. Human Gene Therapy, **7**, 913-919.

Poste G. (1983) Liposome targeting *in vivo* - problems and opportunities. Biol.Cell, **47**, 19-38.

Potter H. (1988) Application of electroporation in recombinant DNA technology. Methods in Enzymology, **217**, 461-478.

Rigel D.S., Friedman R.J., and Rogers G.S. (1985) Prognostic factors in melanoma. Dermatol.Clin., **3**, 305.

Riley P.A. (1977) The mechanism of melanogenesis. Symp. Zoo. Soc. Lond., **39**, 77-95.

Riordan J.R., Rommens J.M., Kerem B-S., Alon N., Rozmahel R., Grzelchak Z., Zielenski J., *et al.* (1989) Identification of the cystic fibrosis gene: cloning and characterisation of complementary DNA. Science, **245**, 1066-1073.

Rosenberg S.A., Packard B.S., and Aebersold P.M. (1989) Use of tumour-infiltrating lymphocytes and interleukin-2 in the immunotherapy of patients with metastatic melanoma. N.Engl.J.Med., **319**, 1676-1680.

Rosenkranz A.A., Yachmenev S.V., Jans D.A., Serebryakova N.V., Murav'ev V.I., Peters R., and Sobolev A.S. (1992) Receptor-mediated endocytosis and nuclear transport of a transfecting DNA construct. Exp.Cell Res., **199**, 323-329.

Ryser H.J-P. (1967) A membrane effect of basic polymers dependent on molecular size. Nature, **215**, 934-936.

Ryser H.J-P., and Shen W-C., (1978) Conjugation of methotrexate to poly (L-lysine) increases drug transport and overcomes drug resistance in cultured cells. Proc.Natl.Acad.Sci.U.S.A, **75**, 3867-3870.

Sahm U.S. (1994) Interaction of naturally occurring and synthetic MSH peptides with peripheral and CNS melanocortin receptors. Ph.D. thesis, University of Bath.

Saiki R.K., Gelfland D.H., Stoffel S., Scharf S.J., Higuchi R., Horn G.T., Mullis K.B. and Erlich H.A. (1988) Primer-directed enzymatic amplification of DNA with a thermostable DNA polymerase. Science 239: 487-491.

Sanchez J.A., and Robinson W.A. (1993) Malignant melanoma. Annu.Rev.Med., **44**, 335-342.

Sambrook J., Fritsch E.F., and Manniatis T. (1989) Molecular Cloning. A laboratory manual. 2nd edition, Cold Spring Harbor, New York: Cold Spring Harbor Laboratory Press.

Schreier H. (1994) The new frontier: gene and oligonucleotide therapy. Pharm.Acta.Helv., **68**, 145-159.

Schwartz L.A., Johnson J.L., Black M., Cheng S.H., Hogan M.E., and Waldrep J.C. (1996) Delivery of DNA-cationic liposome complexes by small-particle aerosol. Human Gene Therapy, **7**, 731-741.

Schwartz R.H. (1990) A cell culture model for T lymphocyte clonal anergy. Science, **248**, 1349-1356.

Schwartz R.H. (1992) Costimulation of T-lymphocytes - the role of CD28, CTLA-4, and B7/BB1 in interleukin-2 production and immunotherapy. Cell, **71**, 1065-1068.

Senior J.H. (1987) Fate and behaviour of liposomes *in vivo*: A review of controlling factors. CRC Crit.Rev.Ther.Drug Carrier Syst., **3**, 123-193.

Shapiro J.T., Leng M., and Felsenfeld G. (1969) Deoxyribonucleic acid-polylysine complexes. Structure and nucleotide specificity. Biochemistry, **8**, 3219-3232.

Shibata K., Takeda K., Tomita Y., Tagami H., and Shibahara S. (1992) Downstream region of the human tyrosinase-related protein gene enhances its promoter activity. Biochem.Biophys.Res.Comm., **2**, 568-575.

Shoji Y., Akhtar S., Periasamy A., Herman B., and Juliano R.L. (1991) Mechanisms of cellular uptake of modified oligodeoxynucleotides containing methylphosphonate linkages. Nucl.Acids Res., **19**, 5543-5550.

Sikora K., Harris J., Hurst H., and Lemoine N. (1994) Therapeutic strategies using c-*erb*B-2 promoter controlled drug activation. Annals of the New York Academy of Sciences, **716**, 115-125.

Sipe D.M., Jesurum A., and Murphy R.F. (1991) Absence of Na^+,K^+-ATPase regulation of endosomal acidification in K-562 erythroleukaemia cells. J.Biol.Chem., **266**, 3469-3474.

Smith K.T., Shepherd A.J., Boyd J.E., and Lees G.M. (1996) Gene delivery systems for use in gene therapy: an overview of quality assurance and safety issues. Gene Therapy, **3**, 190-200.

Smull C.E. and Ludwig E.H. (1962) Enhancement of the plaque-forming capacity of poliovirus ribonucleic acid with basic proteins. J.Bacteriol., **84**, 1035-1040.

Stenseth K., and Thyberg J. (1989) Monensin and chloroquine inhibit transfer to lysosomes of endocytosed macromolecules in cultures mouse peritoneal macrophages. Eur.J.Cell.Biol., **49**, 326-333.

Stevens J.G. (1975) Reactivation of latent herpes simplex virus after pneumococcal pneumonia in mice. Infectious Immunology, **11**, 635-639.

Shoji Y., Akhtar S., Periasamy A., Herman B., and Juliano R.L. (1991) Mechanism of cellular uptake of modified oligodeoxynucleotides containing methylphosphonate linkages. Nucleic Acids Res., **19**, 5543-5550.

Straus S.E. (1984) Adenovirus infection in humans. In The adenoviruses. (H.S. Ginsberg, ed.) p451-496, Plenum Press, New York.

Svensson H.P., Vrudhula V.M., Emswiler J.E., MacMaster J.F., Cosand W.L., Senter P.D., Wallace, P.M. (1995) *In vitro* and *in vivo* activities of a doxorubicin prodrug in combination with monoclonal antibody β-lactamase conjugates. Cancer Res., **55**, 2357-2365.

Takeuchi Y., Cosset F.L., Lachmann P.J., Okada H., Weiss R.A. and Collins M.K.L. (1994) Type C retrovirus inactivation by human complement is determined by both the viral genome and producer cell line. J.Virol., **68**, 8001-8007.

Temin H.M. (1990) Safety considerations in somatic gene therapy of human disease with retrovirus. Human Gene Therapy, **1**, 111-123.

Tirrell D.A., Takigawa D.Y., and Seki K. (1985) pH sensitization of phospholipid vesicles via complexation with synthetic poly(carboxylic acid)s. Annal.New York Acad. Sci., **446**, 237-247.

Tomiya N., Watanabe K., Awaya J., Kurono M., and Fujii S. (1985) Modification of acyl-plasminstreptokinase complex with polyethylene-glycol - reduction of sensitivity to neutralizing antibody. FEBS Letters, **193**, 44-48.

Topalian S.L. (1994) MHC class II restricted tumour antigens and the role of $CD4^+$ T cells in cancer immunotherapy. Curr.Opin.Immunol., **6**, 741-745.

Towbin H., Staehelin T., Gordon J. (1979) Electrophoretic transfer of proteins from polyacrylamide gels to nitrocellulose sheets: Procedure and some applications. Proc.Natl.Acad.Sci.U.S.A., **76**, 4350-4354.

Townsend S.E., and Allison, J.P. (1993) Tumour rejection after direct costimulation of $CD8^+$ T cells by B7-transfected melanoma cells. Science, **259**, 368-370.

Townsend S.E., Su F.W., Atherton J.M., and Allison J.P. (1994) Specificity and longevity of antitumour immune responses induced by B7-transfected tumours. Cancer Research, **54**, 6477-6483.

Tsuboi M., Matsuo K., and T'so P.O.P. (1966) Interaction of poly-L-lysine and nucleic acids. J.Mol.Biol., **15**, 256-267.

Turcovski-Corrales S.M., Fenton R.G., Peltz G., and Taub D.D. (1995) CD28:B7 interactions promote T cell adhesion. Eur.J.Immunol., **25**, 3087-3093.

Van der Bruggen P., Traversari C., Chomez P., Lurquin C., De Plaen E., Van den Eynde B., Knuth, A., and Boon T. (1991) A gene encoding an antigen recognized by cytolytic T lymphocytes on a human melanoma. Science, **254**, 1643-1647.

Vile R.G., and Hart I.R. (1993a) *In vitro* and *in vivo* targeting of gene expression to melanoma cells. Cancer Res., **53**, 962-967.

Vile R.G., and Hart I.R. (1993b) Use of tissue-specific expression of herpes simplex virus thymidine kinase gene to inhibit growth of established murine melanomas following direct intratumoural infection of DNA. Cancer Res., **53**, 3860-3864.

Vile R.G., and Hart I.R. (1995) Targeting of cytokine gene expression to malignant melanoma cells using tissue specific promoter sequences. Annals of Oncology, **5**, 59-65.

Vitiello L., Chonn A., Wasserman J.D., Duff C., and Worton R.G. (1996) Condensation of plasmid DNA with polylysine improves liposome-mediated gene transfer into established and primary muscle cells. Gene Therapy, **3**, 396-404.

Wagner E., Zenke M., Cotten M., Beug H. and Birnstiel M.L. (1990) Transferrin-polycation conjugates as carriers for DNA uptake into cells. Proc.Natl.Acad.Sci.U.S.A, **87**, 3410-3414.

Wagner E., Cotten M., Foisner R., and Birnstiel M.L. (1991) Transferrin-polycation-DNA complexes: the effect of polycations on the structure of the complex and DNA delivery to cells. Proc.Natl.Acad.Sci.U.S.A., **88**, 4255-4259.

Wagner E., Zatloukal K., Cotten M., Kirlappos K., Mechtler K., Curiel D.T., and Birnstiel M.L. (1992a) Coupling of adenovirus to transferrin-polylysine/DNA complexes greatly enhances receptor-mediated gene delivery and expression of transfected genes. Proc.Natl.Acad.Sci.U.S.A, **89**, 6099-6103.

Wagner E., Plank C., Zatloukal K., Cotten M., and Birnstiel M.L. (1992b) Influenza virus haemagglutinin HA-2 N-terminal fusogenic peptides augment gene transfer by transferrin-polylysine-DNA complexes: toward a synthetic virus-like gene-transfer vehicle. Proc.Natl.Acad.Sci.U.S.A, **89**, 7934-7938.

Wagner E., Curiel D., and Cotten M. (1994) Delivery of drugs, proteins and genes into cells using transferrin as a ligand for receptor-mediated endocytosis. Adv.Drug Del.Rev., **14**, 11-135.

Wallace P.M., MacMaster J.F., Smith V.F., Kerr D.E., Senter P.D., and Cosand W.L. (1994) Intratumoral generation of 5-fluorouracil mediated by an antibody-cytosine deaminase conjugate in combination with 5-fluorocytosine. Cancer Res., **54**, 2719-2723.

Watts C., and Marsh M. (1992) Endocytosis: what goes in and how?. J.Cell.Sci., **103**, 1-8.

Welsh M.J. (1990) Abnormal regulation of ion channels in cystic fibrosis epithelia. FASEB J., **4**, 2718-2725.

Westphal H., and Dulbecco R. (1968) Viral DNA in polyoma- and SV40- transformed cell lines. Proc.Natl.Acad.Sci.U.S.A, **59**, 1158-1165.

Wieder K.J., Palczuk N.C., Van Es T., and Davis F.F. (1981) Some properties of polyethylene glycol:phenylalanine ammonia lyase adducts. J.Biol.Chem., **254**, 12579-12587.

Wilke M., Fortunati E., van den Broek M., Hoogereen A.T., and Scholte B.J. (1996) Efficacy of a peptide-based gene delivery system depends on mitotic activity. Gene Therapy, **3**, 1133-1142.

Wiseman T., Williston S., Brandts J.F., and Lin L-N. (1989) Rapid measurement of binding constants and heats of binding using a new titration calorimeter. Anal.Biochem., **179**, 131-137.

Wolfert M.A., and Seymour L.W. (1996) Atomic force microscopic analysis of the influence of the molecular weight of poly(L)lysine on the size of polyelectrolyte complexes formed with DNA. Gene Therapy, **3**, 269-273.

Wolff J.A., Ludtke J.J., Ascadi G., Williams P., and Jani A. (1992) Long-term persistence of plasmid DNA and foreign gene expression in mouse muscle. Human Molecular Genetics, **1**, 363-369.

Woodle M.C., and Lasic D.D. (1992) Sterically stabilized liposomes. Biochim.Biophys.Acta., **1113**, 171-199.

Wu G.Y., and Wu C.H. (1987) Receptor-mediated *in vitro* gene transformation by a soluble DNA carrier system. J.Biol.Chem., **262**, 4429-4432.

Wu G.Y., and Wu C.H. (1988) Evidence for targeted gene delivery to HepG2 hepatoma cells *in vitro*. Biochemistry, **27**, 887-892.

Wu G.Y., Wilson J.M., Shalaby F., Grossman M., Shafritz, D.A. and Wu C.H. (1991) Receptor-mediated gene delivery *in vivo*. J.Biol.Chem., **266**, 14338-14342.

Wu N.Z., Da D., Rudoll T.L., Needham D., Whorton A.R., and Dewhirst M.W. (1993) Increased microvascular permeability contributes to preferential accumulation of Stealth liposomes in tumour tissue. Cancer Res., **53**, 3765-3770.

Xu Y., and Szoka F.C. (1996) Mechanism of DNA release from cationic liposome/DNA complexes used in cell transfection. Biochemistry, **35**, 5616-5623.

Yaar M. and Gilcrest B.A. (1991) Human melanocyte growth and differentiation: a decade of new data. J. Invest. Dermatol. 97 (4): 611-617

Yanelli J.R., Hyatt C., Johnson S., Hwu P., and Rosenberg S.A. (1993) Characterisation of human tumour cell lines transduced with the cDNA encoding either tumour necrosis factor α (TNF-α) or interleukin-2 (IL-2). J.Immunolog.Methods, **161**, 77-90.

Yang J-P., and Huang L. (1996) Direct gene transfer to mouse melanoma by intratumoral injection of free DNA. Gene Therapy, **3**, 542-548.

Yei S., Mittereder N., Tang K., O'sullivan C., and Trapnell B.C. (1994) Adenovirus-mediated gene transfer for cystic fibrosis: quantitative evaluation of repeated *in vivo* vector administration to the lung. Gene Therapy, **1**, 192-200.

Zabner J., Fasbender A.J., Moninger T., Poellinger K.A., and Welsh M.J. (1995) Cellular and molecular barriers to gene transfer by a cationic lipid. J.Biol.Chem., **270**, 18997-19007.

Zatloukal K., Wagner E., Cotten M., Phillips S., Plank C., Steinlein P., Curiel D.T., and Birnstiel M.L. (1992) Transferrinfection: A highly efficient way to express gene constructs in eukaryotic cells. Ann.N.Y.Acad.Sci., **660**, 136-153.

Zatloukal K., Cotten M., Berger M., Schmidt W., Wagner E., and Birnstiel M.L. (1994) *In vivo* production of human factor VIII in mice after intrasplenic implantation of primary fibroblasts transfected by receptor-mediated, adenovirus-augmented gene delivery. Proc.Natl.Acad.Sci.U.S.A, **91**, 5148-5152.

Zatloukal K., Schneeberger A., Berger M., Schmidt W., Koszik F., Kutil R., Cotten M., Wagner E., Buschle M., Maass G., Payer E., Stingl G., and Birnstiel M.L. (1995) Elicitation of a systemic and protective anti-melanoma immune response by an IL-2 based vaccine. J.Immunol., **154,** 3406-3419.

Zauner W., Kichler A., Schmidt W., Sinski A., and Wagner E. (1996) Glycerol enhancement of ligand-polylysine /DNA transfection. Biotechniques, **20**, 905-913.

Zenke M., Steinlein P., Wagner E., Cotten M., Beug H., and Birnstiel M.L. (1990) Receptor-mediated endocytosis of transferrin-polycation conjugates: An efficient way to introduce DNA into hematopoietic cells. Proc.Natl.Acad.Sci.U.S.A, **87**, 3655-3659.

Zhou X., and Huang L. (1994) DNA transfection mediated by cationic liposomes containing lipopolylysine: characterization and mechanism of action. Biochim.Biophys.Acta, **1189**, 195-203.

Zobel H-P., Kreuter J., Werner D., Atmaca-Abdel-Azis S., Noe C.R., and Zimmer A. (1996) Protection of antisense-oligonucleotides from enzymatic degradation by adsorption to colloidal drug carriers. Pharm.Res., **13**, S-388.

Appendix A. Media and Solutions.

Where appropriate, media and solutions were sterilised by autoclaving for 20 minutes at 15 lbs/sq. inch (121°C) on a liquid cycle. Unless specified, all reagents were obtained from Sigma Biochemicals.

Buffer P1: 100 µg/ml RNase A, 50 mM Tris-HCl, 10 mM EDTA, pH 8.0.

Buffer P2: 200 mM NaOH, 1% ^{w}/v SDS.

Buffer P3: 3.0 Potassium acetate, pH 5.5.

Buffer QBT: 750 mM NaCl, 50 mM MOPS, 15% ^{v}/v ethanol, 0.15% ^{v}/v Triton X-100.

Buffer QC: 1.0 M NaCl, 50 mM MOPS, 15% ^{v}/v ethanol.

Buffer QF: 1.25 M NaCl, 50 mM Tris-HCl, 15% ^{v}/v ethanol.

Chloroform:isoamyl alcohol: Chloroform mixed with isoamyl alcohol 24:1 (Amresco).

Citrate-Phosphate buffer: 0.1 M citric acid, 0.2 M disodium phosphate. Ratios varied according to pH, as detailed in Table A.1. The pH was adjusted as necessary with HCl or NaOH.

pH	Volume 0.1M citric acid (ml)	Volume 0.2M disodium phosphate (ml)
4	61.45	38.55
5	48.5	51.5
6	36.85	63.15
7	18.15	81.85
8	2.75	97.25

DNA loading buffer: 50 mM EDTA, 0.2% SDS, 0.05% ^{w}/v bromophenol blue, 50% glycerol.

Electroporation buffer: 25 mM Hepes, 140 mM KCl, 10 mM NaCl, 2 mM $MgCl_2$. 0.5% Ficoll. Filter sterilise using 0.2 µM filter.

Ethidium Bromide: 1 mg/ml in double distilled water.

Hepes Buffered Saline (HBS): 20 mM Hepes, 150 mM NaCl, pH 7.4.

LB medium (Luria-Bertani medium): (per litre) 10g Bacto tryptone (Difco), 5g Bacto yeast extract (Difco) and 10g NaCl, pH adjusted to 7.0 with NaOH. LB plates were prepared from 1 litre of LB medium plus 20g agar (Difco).

Lowry A: 5% ^{w}/v Na_2CO_3 in double distilled water.

Lowry B: 0.5% ^{w}/v $CuSO_4.5H_2O$ / 1% NaK tartrate solution.

ONPG (2X) assay buffer: 1.35 mg/ml o-nitrophenylgalactopyranoside, 2 mM $MgCl_2$, 100 mM 2-mercaptoethanol, 200 mM sodium phosphate, pH 7.3).

PBS: 15 mM sodium phosphate, 150 mM sodium chloride (pH 7.3).

Penol/chloroform: Tris Phenol : Chloroform : Isoamyl alcohol 25:24:1 (Amresco).

SOC: 2% Bacto tryptone (Difco), 0.5% Bacto yeast extract (Difco), 10 mM NaCl, 2.5 mM KCl, 10 mM $MgSO_4$, 20 mM glucose.

Sodium Phosphate buffer (pH 7.4): 77.4 ml 1M Na_2HPO_4 solution , 22.6 ml 1M NaH_2PO_4 solution.

Solution I (minipreps): 50 mM glucose, 25 mM Tris, 10 mM EDTA.

Solution II (minipreps): 0.2 N NaOH, 1% SDS; freshly prepared aseptically from 10 N NaOH and 10% SDS stocks.

Solution III (minipreps): (per 100 ml) 60 ml 5 M potassium acetate, 11.5 ml glacial acetic acid, ddH_2O 28.5 ml.

STOP Buffer: 300 mM glycine, 15 mM EDTA, pH 11.2.

TBE (1x): 10.8g Tris base, 5.5g boric acid, 0.93g Na_2 EDTA.H_2O pH 8.3.

TBS: 150 mM NaCl, 20 mM Tris HCl. pH 7.5.

TE: 10 mM Tris-HCl, 1 mM EDTA pH 7.0.

X-Gal solution: 0.2% X-Gal (Melford laboratories), 1 mM $MgCl_2$, 150 mM NaCl, 3.3 mM $K_4Fe(CN)_6$, 3.3 mM $K_3Fe(CN)_6$.

Z Buffer: 100 mM sodium phosphate, 10 mM KCl, 1 mM $MgCl_2$, pH 7.0.

Appendix B. Molecular Weight Markers.

For agarose gel electrophoresis, markers consisted of *Eco*R1/*Hind*III-cut lanbda DNA (Northumbria Biologicals). The digest consists of DNA fragments of the following sizes (base pairs):

1:	21226	8:	1584
2:	5148	9:	1375
3:	4973	10:	947
4:	4268	11:	831
5:	3530	12:	564
6:	2027	13:	125
7:	1904		

Appendix C: Calibration curves for quantitative assays.

C.1. MTT assay for K1735 cell number.

Cells were plated at densities ranging from $2.5x10^3$ to $40x10^3$ into 96-well plates. The cells were allowed to adhere for 1 hour before assay using the standard MTT protocol. A linear Beer-Lambert plot for absorbance (540 nm - 690 nm) was obtained (Fig. C.1) with the following linear regression analysis:

Slope = $2.06x10^{-2}$ Intercept = $8.64x10^{-2}$ r = 0.996

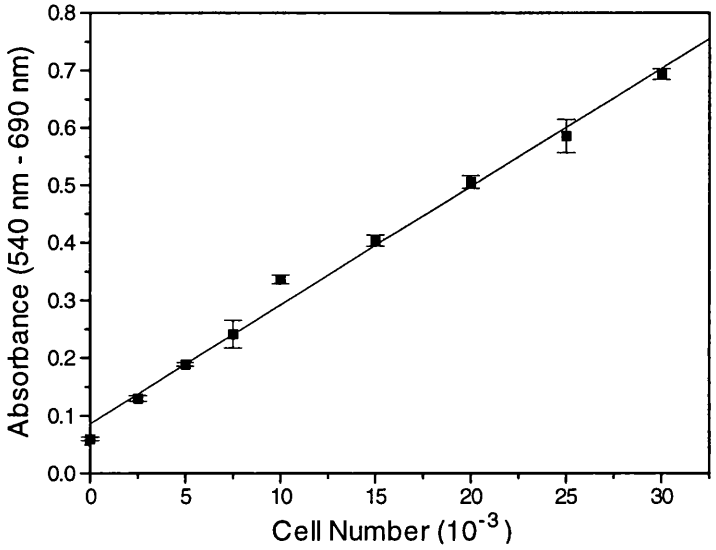

Figure C.1. Calibration curve for the MTT assay for K1735 cell number. Each point represents mean absorbance value (540 nm - 690 nm) ± SEM (n=8). The data are representative of two experiments.

C.2. MTT assay for viability of K1735 cells.

The K1735 cells were seeded at a density of $3x10^3$ cells/well and allowed to adhere in complete medium for 4 hours before the addition of 0-5 mg/ml G418, or 0-40 μg/ml puromycin. The cells were assayed after 3 days to establish viability using

the MTT assay, and the cell number determined using the MTT calibration curve for K1735 cells (section C.1). The minimum concentration to inhibit cell growth was 1.5 mg/ml for G418 and 1 μg/ml for puromycin respectively.

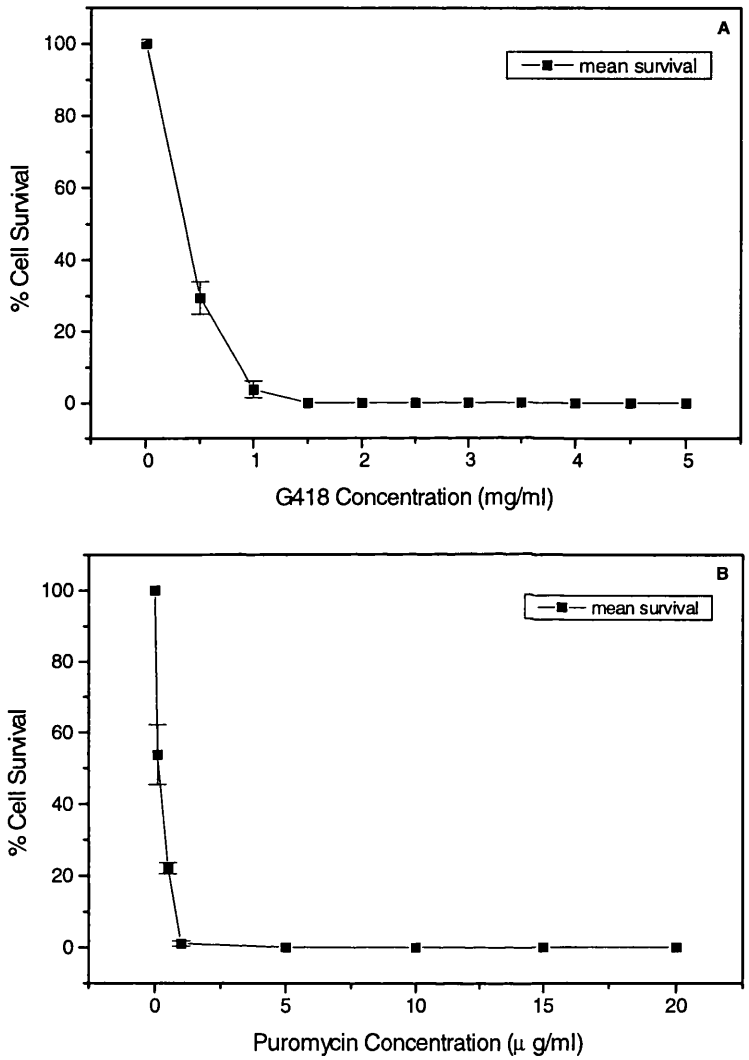

Figure C.2. Kill curves for the treatment of K1735 melanoma cells with the antibiotics G418 (A) and puromycin (B), to establish concentrations required for selection of stable transfectants.

C.3. MTT assay for B16 cell number.

Cells were plated at densities ranging from $2.5x10^3$ to $40x10^3$ into 96-well plates. The cells were allowed to adhere for 1 hour before assay using the standard MTT protocol. A linear Beer-Lambert plot for absorbance (540 nm - 690 nm) was obtained (Fig. C.3) with the following linear regression analysis:

Slope =0.0468 Intercept = 0.04803 r = 0.987

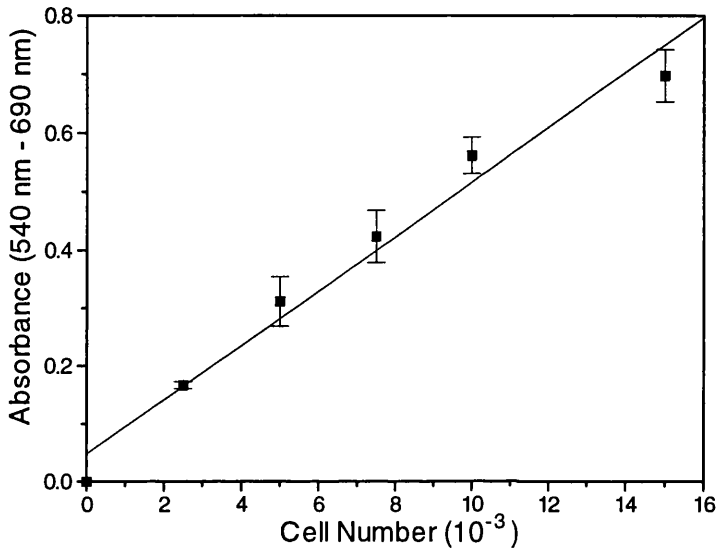

Figure C.3. Calibration curve for the MTT assay for B16 cell number. Each point represents mean absorbance value (540 nm - 690 nm) ± SEM (n=8). This data is representative of three experiments.

C.4. Lowry protein assay for cell extracts for ONPG analysis.

A series of BSA solutions in 0.1 M sodium phosphate buffer were prepared over the range 0-1.2 mg/ml. The samples were then assayed by the method described in section 2.2.20.3. A linear Beer-Lambert plot was obtained for absorbance at 750 nm (Fig. C.4) with the following linear regression analysis.

Slope =0.37185 Intercept = 0.02646 r = 0.995

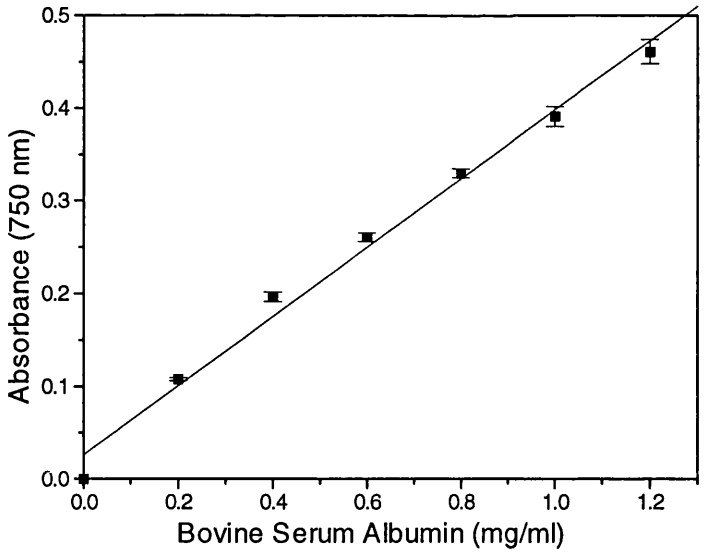

Figure C.4. Standard curve for Lowry protein assay. Calibration was performed using bovine serum albumin in 0.1 M sodium phosphate buffer at increasing concentrations and measuring the absorbance at 750 nm (section 2.2.20.3).

C.5. ONPG assay for β-galactosidase activity in cell extracts.

A series of β-galactosidase solutions were prepared in 0.1 M sodium phosphate buffer over the range 0-12 milliunits of activity. The stock solution contained 1.06 units/ml). The samples were assayed as detailed in section 2.2.20.2. A linear Beer-Lambert plot was obtained for absorbance at 420 nm (Fig. C.5) with the following linear regression analysis.

Slope = 0.0409 Intercept = 0.00128 r = 0.999

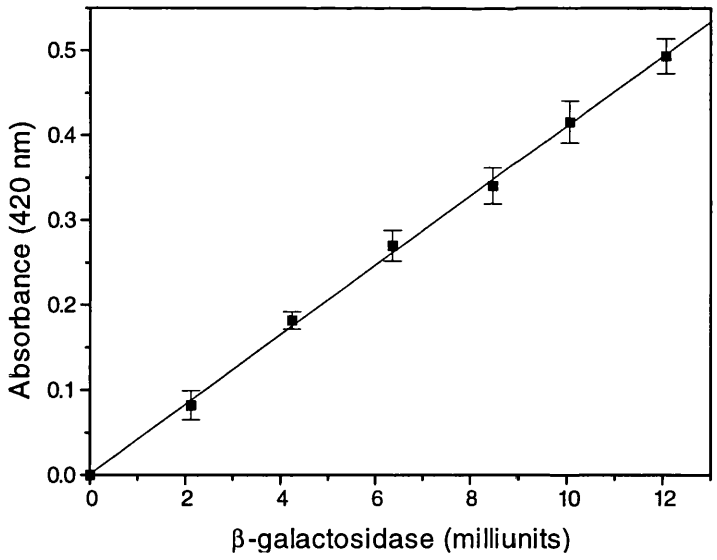

Figure C.5. Calibration curve for absorbance at 420 nm versus β-galactosidase activity. The ONPG assay reagent (appendix A) was incubated with increasing quantities of β-galactosidase enzyme (section 2.2.20.2). Absorbance was measured after 30 minutes.

C.6. Lowry protein assay for cell extracts for MUG analysis.

A series of BSA solutions in Z buffer (appendix A) were prepared over the range 0-1.2 mg/ml. The samples were then assayed by the method described in section 2.2.20.3. A linear Beer-Lambert plot was obtained for absorbance at 750 nm (Fig. C.4) with the following linear regression analysis.

Slope = 0.2194 Intercept = 0.0324 r = 0.995

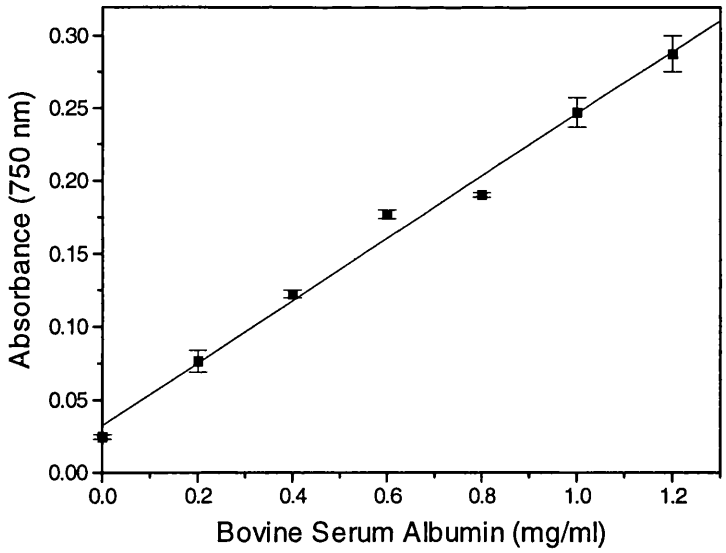

Figure C.6. Standard curve for Lowry protein assay. Calibration was performed using bovine serum albumin in Z buffer at increasing concentrations and measuring the absorbance at 750 nm (section 4.2.5).

C.7. MUG assay for β-galactosidase activity in cell extracts.

A series of β-galactosidase solutions were prepared in Z buffer over the range 0-100 milliunits of activity. The stock solution contained 1.06 units/ml. The samples were assayed as detailed in section 4.2.4. A linear Beer-Lambert plot was obtained for fluorescence over the range 0-70 milliunits of activity (λ_{ex} 350 nm, λ_{em} 450 nm; Fig. C.7) with the following linear regression analysis.

Slope = 69.919 Intercept = 246.42 r = 0.994

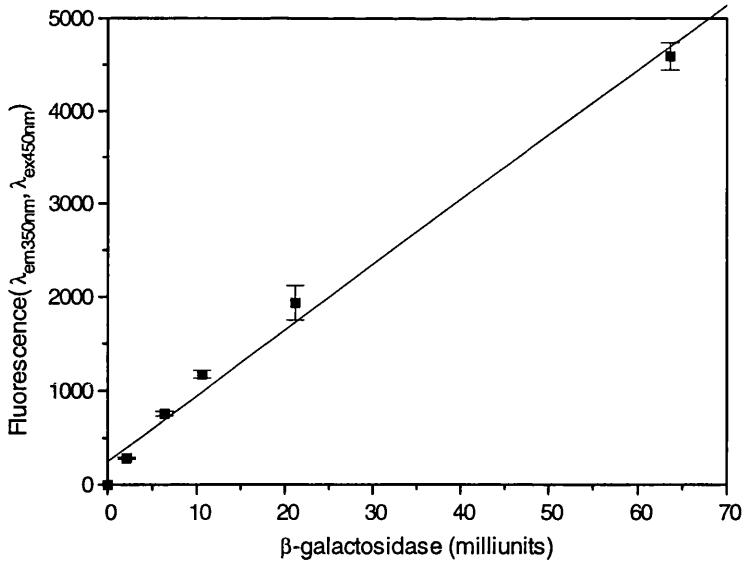

Figure C.7. Fluorescence associated with β-galactosidase activity (λ_{em} 350 nm, λ_{ex} 450 nm). Increasing concentrations of β-galactosidase enzyme (1.06 units/ml) were incubated with a 30 µl aliquot of 3 mM MUG assay reagent, as described in section 4.2.4. The fluorescence was measured after incubation at 37°C for 90 minutes.

Appendix D. Amino acids.

Amino acid. (hydrophilicity).	Abbreviation.	Code Letter.	Mass.	Properties
Alanine	Ala	A	89.09	Neutral, (-0.5)
Arginine	Arg	R	174.2	Basic, (3.0)
Asparagine	Asn	N	132.1	Neutral, (0.2)
Aspartic acid	Asp	D	133.1	Acidic, (3.0)
Cysteine	Cys	C	121.12	Neutral, (-1.0)
Glutamic acid	Glu	E	147.13	Acidic, (3.0)
Glutamine	Gln	Q	146.15	Neutral, (0.2)
Glycine	Gly	G	75.07	Neutral, (0.0)
Histidine	His	H	155.16	Basic, (-0.5)
Isoleucine	Ile	I	131.17	Neutral, (-1.8)
Leucine	Leu	L	131.17	Neutral, (-1.8)
Lysine	Lys	K	146.19	Basic, (3.0)
Methionine	Met	M	149.21	Neutral, (-1.3)
Phenylalanine	Phe	F	165.19	Neutral, (-2.5)
Proline	Pro	P	115.13	Neutral, (0.0)
Serine	Ser	S	105.09	Neutral, (0.3)
Threonine	Thr	T	119.12	Neutral, (-0.4)
Tryptophan	Trp	W	204.22	Neutral, (-3.4)
Tyrosine	Tyr	Y	181.19	Neutral, (-2.3)
Valine	Val	V	117.15	Neutral, (-1.5)

Hydrophilicity value according to Hopp and Woods (1981)